Identification Of Effective New Drugs Combinations Exploiting The Ability Of trabectedin To Modulate Transcription

Thesis

ABSTRACT

Ewing's sarcoma (ES) is the second most common malignant bone tumor of childhood. The hallmark of this disease is the characteristic chromosomal translocation involving the EWS and FLI1 genes. The fusion of these two genes generate the chimeric protein EWS-FLI1, that alters the transcription of different genes. The five-year overall survival of patients with localized disease is approximately 70%; unfortunately the majority of patients with a metastatic disease have a poor prognosis with a five-year overall survival around the 30%. Among the recently registered drugs for the therapy of sarcomas, trabectedin could be of potential great interest as it seems very active in some "translocated sarcomas".

Trabectedin exerts its antitumor activity with different mechanisms of action.

One of the most important is related to its ability to interfere with DNA repair mechanisms (NER and HR), that cause cell cycle perturbations.

Furthermore trabectedin is able to displace the oncogenic EWS-FLI1 chimera from its target promoters, modulating the transcription of these genes, in ES cells.

Although trabectedin has shown some activity against ES, the overall clinical results indicated only a marginally activity of trabectedin given as single agent in ES.

The thesis is aimed at using the available knowledge on trabectedin mechanism of action to identify some effective combinations.

Since trabectedin induces cell cycle perturbations I speculated that its activity could be increased by checkpoint inhibitors. The studies performed on the combination of trabectedin and the WEE1 inhibitor, AZD-1775, have shown that the inhibition of WEE1 enhances the trabectedin activity, thus the combination is synergic.

Since trabectedin affects the transcription of several genes, I have developed a new approach based on the use of silencing RNA (siRNA) libraries to identify whether the downregulation of some genes was synthetically lethal when ES cells were pretreated with trabectedin. An important part of the thesis was the development, validation and initial application of this approach.

AKNOWLEDGEMENTS

The work in this thesis was performed under the supervision of Dr. Maurizio D'Incalci, head of the Department of Oncology at the IRCCS- Istituto di Ricerche Farmacologiche "Mario Negri" – Milan.

I would like to thank Prof. Silvio Garattini that gave me the possibility to work in his Institute for 10 beautiful years.

I am extremely grateful to the Dr. Maurizio D'Incalci, who has been a constant source of guidance and support.

A thank to Dr. John Hartley for the help that he gave me.

I would like to thank Dr. Laura Carrassa and Dr. Giovanna Damia for the support in the development of the siRNA screening.

Dr. Paolo Ubezio and Francesca Falcetta for the isobolograms and analysis of the siRNA screening, respectively.

I would like to thank all my colleagues of the Department of Oncology for the support and the special years together.

I would like to thank Dr. Eugenio Erba, one of the most important person in my life: my mentor and my guide.

A special thank for a very important person in my life: Giovanna Balconi.

I would like to thank my special friends Michela Romano, Benedetta Colmegna, Francesca Bizzaro and Francesca Ricci: the crazy girls that were always able to support me in so many ways. You are the best friend that I could hope. Always in my heart.

A thanks to Nicolò Panini; no words could describe this fantastic person: a friend.

A very big thanks to Marzia, Emanuele and Giovanni. You are the example of what life has given me: precious gifts. Yesterday, today and tomorrow together.

A thank to my friends Andrea, Giovanna and Fabio: the oddest group that I've never had. Life without you would not be so beautiful and funny.

A big thank to my family: my life, my power my big love. Thanks to my parents (Luigi and Licia) and my sisters (Paola e Viviana) that are always my support and my first “supporters”.

Last but not the least, a thank to my husband Gennaro. I believe in you as much as you believe in me. Never give up.

Non sai mai quanto sei forte, finchè essere forte è l’unica scelta che hai - You never know how strong you are until being strong is the only choice you have -

INTRODUCTION

1. CANCER

Cancer (tumor) is probably the major disease that affects the modern society, in all age groups. It is important to distinguish from benign and malignant tumors because this distinction is crucial in determining the appropriate treatment and prognosis. The features that differentiate a malignant from a benign tumor are:

1) malignant tumors invade and destroy adjacent normal tissue; benign tumors grow by expansion but are normally encapsulated and do not invade surrounding tissue.
2) Malignant tumors metastasize through lymphatic channels or blood vessels to lymph nodes and other tissues in the body. Benign tumors remain localized and do not metastasize.
3) Malignant tumor cells are normally “anaplastic” or less well differentiated a normal cell of the tissue in which they arise. Benign tumors usually resemble normal tissue more closely than malignant tumors do.

The rapidly expanding medical technology has produced significant progress in diagnostic testing improving dramatically the oncologist’s ability to obtain tissues for examination and to identify small, potentially cancerous lesions in previously inaccessible sites in the body.

Tumors are generally classified with the following criterium:

1) Anatomic site of primary tumor and metastasis
2) Tissue type and histologic classification
3) Histologic grade of malignancy
4) Extent of tumor progression (size and degree of invasion and metastatic spread).

The correct classification of a neoplasm is crucial to determine the patient’s prognosis, the type, intensity and duration of the therapy (Ruddon R.W.,2007). The cancer disease is generically characterized by a multi-step process involving genetic damage and by rapid, abnormal and uncontrolled specific cell division with increased rate of DNA synthesis and very fast metabolism that requires a high rate of glycolysis (Ganapathy *et al*, 2009).

Genetic changes that cause cancer can be inherited from the parents or they can arise during a person's lifetime, as a result of accumulation of errors in dividing cells or because of damage to DNA, caused by different environmental exposures. These environmental causes include substances (such as the chemicals in tobacco smoke) and radiation (such as ultraviolet rays from the sun). The tumor that affects a person is characterized by a unique combination of genetic changes. As the cancer continues to grow, additional changes will occur. Even within the same tumor, different cells may have different genetic changes.

The genetic changes that contribute to cancer tend to affect three main types of genes:

1) proto-oncogenes
2) tumor suppressor genes
3) DNA repair genes

These changes are sometimes called "drivers" of cancer.

Proto-oncogenes are involved in normal cell growth and division but when these genes are altered in certain ways or are more active than normal, they may become cancer-causing genes (or oncogenes), allowing cells to grow and survive when they should not.

Tumor suppressor genes are also involved in controlling cell growth and division. Cells with certain alterations in tumor suppressor genes may divide in an uncontrolled manner. Cells with mutations in these genes tend to develop additional mutations in other genes. Together, these mutations may cause the cells to become cancerous. Certain specific mutations commonly occur in many types of cancer. Because of this, cancers are sometimes characterized by the types of genetic alterations that are believed to be driving them, not just by where they develop in the body and how the cancer cells look under the microscope.

The diffusion of cancer cells from the place where they start to grow to another place in the body is called "metastatic cancer" and the process by which the cells spread to other parts of the body is called metastasis.

During the metastatic process cancer cells break away from where they first formed (**primary cancer**), travel through the blood or lymph system, and form new tumors (**metastatic tumors**) in other parts of the body. The metastatic tumor is the same type of cancer as the primary tumor. For example, breast cancer that spreads to and forms a metastatic lesion in the lung is metastatic breast cancer, not lung cancer.

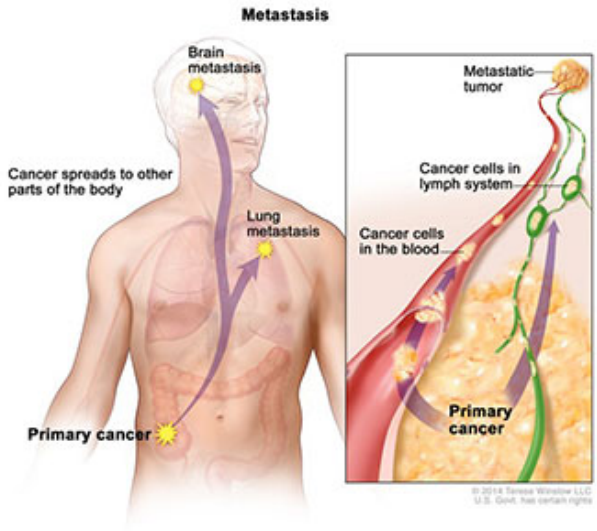

Figure 1: the metastatic process. Cancer cells leave the primary site of cancer and invade other parts of the body, using the blood or lymph system.

Picture from "National Cancer Institute" website (*https://www.cancer.gov/about-cancer/understanding/what-is-cancer*).

In general the primary goal of treatments of metastatic cancer is to control the growth of the cancer or to relieve symptoms caused by it.

There are more than 100 types of cancer, usually named for the organs or tissues where they originate from.

Some important and frequent categories of cancers are reported here:

1) **Carcinoma** is the most common cancer, formed by the many types of epithelial cells (the cells that cover the inside and outside surfaces of the body), which often have a column-like shape when viewed under a microscope.

The different epithelial cells can originate different type of carcinomas:

a) Adenocarcinoma: cancer that forms in epithelial cells that produce fluids or mucus. Most cancers of the breast, colon, and prostate are adenocarcinomas.
b) Basal cell carcinoma: a cancer that begins in the lower or basal layer of the epidermis, the external layer of the skin.
c) Squamous cell carcinoma: a cancer that forms in squamous cells, which are epithelial cells located below the epidermis. Squamous cells also line many other organs, including the stomach, intestines, lungs, bladder, and kidneys. Squamous cells look flat, like fish scales, when viewed under a microscope. Squamous cell carcinomas are sometimes called epidermoid carcinomas.
d) Transitional cell carcinoma: a cancer that forms in a type of epithelial tissue called transitional epithelium (or urothelium), made up of many layers of epithelial cells that can get bigger and smaller; it is found in the linings of the bladder, ureters, and part of the kidneys (renal pelvis), and a few other organs.

2) **Sarcoma** is a neoplastic disease that form in bone and soft tissues, including muscle, fat, blood vessels, lymph vessels, and fibrous tissue (such as tendons and ligaments). Osteosarcoma is the most common cancer of bone. The most common types of soft tissue sarcoma are leiomyosarcoma, malignant fibrous histiocytoma, liposarcoma, and dermatofibrosarcoma protuberans.

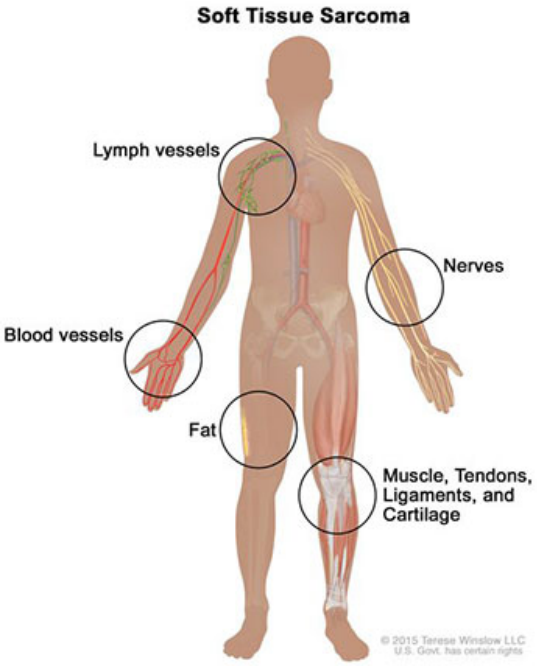

Figure 2: Possible localization of soft tissue sarcomas: the soft tissues of the body, including muscle, tendons, fat, blood vessels, lymph vessels, nerves, and tissue around joints.

Picture from "National Cancer Institute" website (*https://www.cancer.gov/about-cancer/understanding/what-is-cancer*).

3) **Leukemias:** neoplastic disease that begin in the blood-forming tissue of the bone marrow and do not form solid tumors. Instead, large numbers of abnormal white blood cells (leukemia cells and leukemic blast cells) build up in the blood and bone marrow, crowding out normal blood cells. The low level of normal blood cells cause a serious difficulty for the body to get oxygen to its tissues, control bleeding, or fight infections. There are four common types of leukemia, which are grouped based on how quickly the disease gets worse (acute or chronic) and on the type of blood cell the cancer starts in (lymphoid or myeloid).

4) **Lymphomas**: are neoplastic disease related to the transformation of lymphocytes (T cells or B cells). In this tumor abnormal lymphocytes build up in lymph nodes and lymph vessels, as well as in other organs of the body. There are two main types of lymphoma:

Hodgkin lymphoma – People with this disease have abnormal lymphocytes that are called Reed-Sternberg cells. These cells usually form from B cells.

Non-Hodgkin lymphoma – This is a large group of cancers that start in lymphocytes. The cancers can grow quickly or slowly and can form from B cells or T cells.

5) **Multiple myeloma:** a cancer that begins in plasma cells, another type of immune cells. The abnormal plasma cells, called myeloma cells, build up in the bone marrow and form tumors in bones all through the body. Multiple myeloma is also called “plasma cell myeloma” and “Kahler disease”.

6) **Melanoma:** this cancer begins in cells that become melanocytes, which are specialized cells that make melanin (the pigment that gives skin its color). Most melanomas form on the skin, but melanomas can also form in other pigmented tissues, such as the eye.

7) **Brain and Spinal Cord Tumors:** these tumors are named based on the type of cell in which they formed and where the tumor first formed in the central nervous system. For example, an astrocytic tumor begins in star-shaped brain cells called astrocytes, which help keep nerve cells healthy. Brain tumors can be benign (not cancer) or malignant (cancer).

8) Other Types of Tumors like **Germ Cell Tumors** (begins in the cells that give rise to sperm or eggs), **Neuroendocrine Tumors** (form from cells that release hormones into the blood in response to a signal from the nervous system) or **Carcinoid Tumors** (a type of neuroendocrine tumor that grow slowly and are usually found in the gastrointestinal system).

2. SARCOMAS

Soft-tissue sarcomas are a rare and heterogeneous group of tumors of mesenchymal origin that includes 70 different histologic subtypes, with approximately 12,000 new diagnoses per year.

These tumors can occur anywhere in the body, especially in the extremities and retroperitoneum. A macroscopically complete resection with negative microscopic margins remains the standard of care for localized soft-tissue sarcomas as the only potentially curative treatment. However, the location of the tumor can make this very difficult to achieve, and even in the event of a complete resection, local recurrence rates range from 22% to 84%. In extremity sarcomas, emphasis is placed on function-preserving limb conservation in addition to negative resection margins. Retroperitoneal sarcomas provide a challenge to clinicians because of their typically late presentation and subsequent large size at time of presentation. They frequently involve multiple organs and can occur in close proximity to vital neurovascular structures.

2.1 Ewing's Sarcoma (ES)

The Ewing's sarcoma family of tumours (ESFT) is an aggressive form of childhood cancer. This rare disease is the second most common primary bone tumour that can occurs at any age but rarely in adults over the age of 30; its incidence is higher in white populations (rare in black populations) and in men (Parkin *et al*, 1993). About a quarter of ES arise in soft tissues rather than bone, and about a quarter of patients have detectable metastases at diagnosis. The lungs are the most common site for metastases (50%), followed by bone (25%) and bone marrow (20%) (Grier, 1997). Many illnesses can cause the same symptoms as ES and is sometimes missed in its early stages. Pain or swelling in an arm or leg, chest, back, or pelvis are the most common symptoms; normally the pain gets progressively worse.

In addition to these symptoms fever with no known reasons and the breaks of a bone with no apparent cause could represent the "alarm symptoms" for this disease.

The first step in the assessment phase should be imaging of the suspected tumour, preferably by MRI, encompassing the entire involved bone or compartment. ES often have extensive necrosis, and there must be sufficient tissue for immunohistochemical and molecular diagnostic techniques. Following pathological confirmation of an ES a complete staging assessment is needed including a CT scan of the chest to detect the pulmonary metastases, bone scintigraphy to detect the bone metastases and, sometimes, bone marrow aspirate and biopsy (Balamuth & Womer, 2010).

The ES is characterized by a high grade of heterogeneity with the presence of non random chromosomal translocations involving the Ewing sarcoma breakpoint region 1 (EWSR1, or commonly named EWS) and one of the several members of the ETS transcription factor genes, which ultimately originates a chimeric fusion protein.

The translocation t(11;22)(q24;q12) is the most common and is associated to 90% of cases.

This translocation fuses the EWSR1 gene on chromosome 22 to the FLI1 gene on chromosome 11 and encodes the EWS/FLI1 fusion protein (Delattre *et al*, 1992). In this chimeric protein a strong transcriptional activation domain is contributed by EWS and an ETS-type DNA binding domain is contributed by FLI1 (Delattre *et al*, 1992; Lessnick *et al*, 1995; May *et al*, 1993a). Both of these domains are required for the oncogenic function of EWS/FLI1, supporting the notion that the fusion acts as an aberrant transcription factor (May *et al*, 1993a; May *et al*, 1993b). In Ewing's sarcoma cases lacking the EWS/FLI1 are normally present other fusion proteins characterized by the constant presence of EWS gene fused with other members of ETS family proteins, including ERG, ETV1, ETV4 and FEV (Jeon *et al*, 1995; Sorensen *et al*, 1994), which mimic EWS/FLI1.

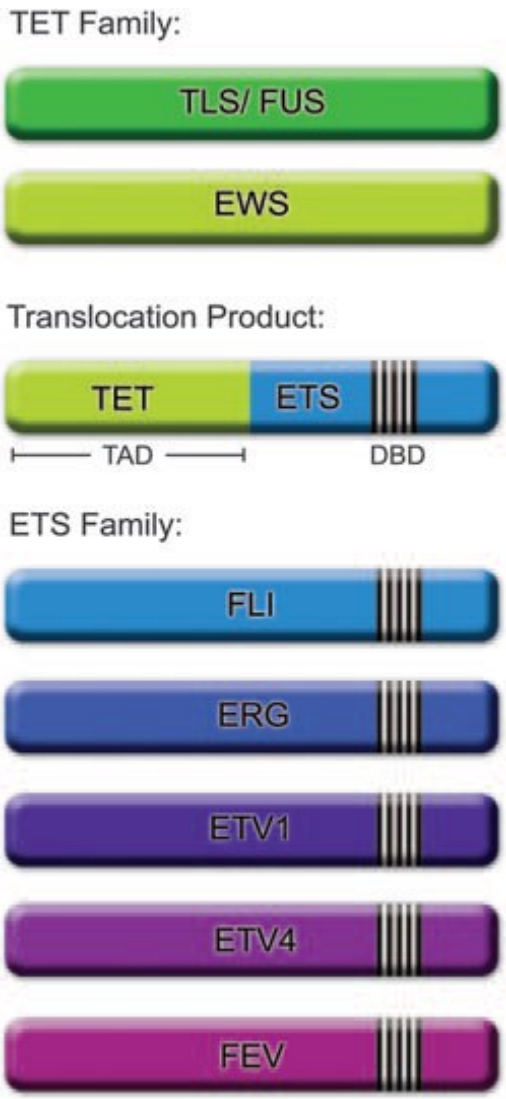

Fig 3: Ewing's sarcoma fusion protein organization. The Ewing's sarcoma translocation product is the result of a chromosomal rearrangement involving the N-terminal transcriptional activation domain (TAD) of a TET family member (either TLS/FUS or more commonly EWS) and the C-terminal portion of an ETS family member (FLI, ERG, ETV1, ETV4, or FEV), including the ETS DNA-binding domain (DBD). ***Picture from "Toomey E.C. et al, Oncogene (2010), 29, 4504-16".***

EWS/FLI1 fusion protein localizes to the cell nucleus. The main difference between EWS/FLI1 and FLI1 is the substitution of the amino-terminal domain of EWS for the putative transcriptional activation domain of FLI1. This substitution converts a non-transforming gene (FLI1) into a transforming gene (EWS/FLI1), with the alteration of the transcriptional activation properties of the amino terminal domains of these two proteins.

The EWS amino-terminal domain present in the EWS/FLI1 fusion protein, is a much more potent transcription activator than the amino terminus of FLI1. EWS/FLI1 can activate a broader repertoire of genes than FLI1 (Madoz-Gurpide, 2009).

2.1.1 Ewing's sarcoma cell of origin

When first described in 1921 James Ewing proposed an endothelial origin (Ewing, 1921). Numerous hypotheses have been put forth regarding the histogenesis of this tumor including hematopoietic (Kadin & Bensch, 1971), fibroblastic (Dickman *et al*, 1982), neural crest (Cavazzana *et al*, 1988) and mesenchymal progenitor stem cells (Riggi *et al*, 2005; Tirode *et al*, 2007).

The cell of origin for Ewing sarcoma is unknown and also the permissive cellular environment for the expression of EWS/FLI1 has also been problematic.

Neural hypothesis

Several evidences suggest that the cell of origin could be effectively represented by the neural crest cell. Both Ewing's sarcoma and primitive neuroectodermal tumors (PNET) harbour the same t(11;22)(q24;q12) rearrangement. This suggest that these are the same tumor demonstrating differences in extent of neural differentiation (Kovar, 1998). A gene expression profiling study evidences that gene expressed in neural tissues or during neuronal differentiation are highly expressed in Ewing's sarcomas, and that Ewing's sarcomas clustered with fetal and adult brain tissues (Staege *et al*, 2004). There is a parallel hypothesis: Ewing's sarcoma neural phenotype could be a result of EWS/FLI1 expression, rather than a reflection of the cell of origin.

This latter hypothesis is further supported by work demonstrating that genes critical for neural crest development were upregulated when EWS/FLI1 was ectopically expressed in rhabdomyosarcoma, neuroblastoma, or human foreskin fibroblast cell lines (Hu-Lieskovan *et al*, 2005) (Lessnick *et al*, 2002).

Mesenchymal hypothesis

There are growing evidences that the cell of origin of Ewin'g sarcoma could be a mesenchymal stem or progenitor cell. To support this hypothesis there is a study that demonstrated that EWS/FLI1 and EWS/ERG blocked the differentiation of pluripotent murine bone marrow-derived mesenchymal progenitor cells (mMPCs); (Torchia *et al*, 2003). Furthermore different studies suggest that the introduction of EWS/FLI1 into unselected primary murine bone-marrow cells or into mMPCs allowed the transduced cells to form tumors in immunocompromised mice with a small round cell morphology (Castillero-Trejo *et al*, 2005; Riggi *et al*, 2005).

In contrast to other normal human cell types with forced EWS/FLI1 expression, human mesenchymal stem cells (MSCs) retain the ability to propagate in the presence of fusion protein (Riggi *et al*, 2008). The gene expression profile derived from these cells are similar to which of Ewing's sarcoma but not to other bone and soft tissue tumors (Miyagawa *et al*, 2008). Because Ewing's cells were unable to form tumors when injected into immunocompromised mice (Riggi *et al*, 2008), it seems that EWS/FLI1 is necessary, but not sufficient, for oncogenic transformation of human MSCs.

EWS/FLI1 is able to transform (as oncogene) immortalized murine NIH3T3 cells but not any normal human cell type suggesting that critical differences might exist between human and mouse cells in their abilities to respond to EWS/FLI1. In NIH3T3 cells some gene targets of the chimeric protein, that have been shown to be critical for oncogenic transformation in patient-derived Ewing sarcoma cell lines (such as NKX2.2 and NR0B1) are not induced. These data suggest that the molecular pathways used in NIH3T3 mouse fibroblasts may be different from those used in *bona fide* Ewing sarcoma.

The fact that the presence of EWS/FLI1 is not sufficient to transform any human cell type *in vitro*, is an indication that there are parallel pathways and/or mutations that work in conjunction with the chimeric protein in the transforming process.

The exact "molecular combination" that provides the "Ewing sarcoma oncogenic cocktail" is currently unknown and requires more studies.

2.1.2 EWSR1 gene and EWS protein

The EWSR1 gene spans about 40Kb on chromosome 22 and is encoded by 17 exons (Plougastel *et al*, 1993).

The EWS protein is an RNA – binding protein containing the transcriptional activation domain (s) in the N-terminus and the RNA recognition motif and three arginine – glycine – glycine repeats (RGG boxes 1-3) in its C-terminal domain. EWS may function as transcriptional factor. EWS belongs to a subgroup of RNA-binding proteins (TET family) which also includes liposarcoma / fusion protein (TLS /FUS), and human TATA binding protein-associated factor (hTAFII68).

These proteins contain an RNA recognition motif (87aa) commonly found in most RNA-binding proteins and possess a number of RGG repeats that seem to facilitate the binding to RNA. A zinc finger domain with four cysteines is present in their C-terminus.

TET proteins bind RNA as well as DNA and are implicated in the regulation of gene expression and in cell signalling. All the members of this family contribute to human pathologies, as they are involved in sarcoma translocations (Delattre *et al*, 1992; Lessnick & Ladanyi, 2012) and neurological diseases (Mackenzie *et al*, 2010; Vance *et al*, 2009).

They contain several conserved domains: a serine-tyrosine-glycine-glutamine (**SYGQ**) domain, an RNA-recognition motif (**RRM**), a zinc finger motif, and three RNA binding Arginine-Glycine-Glycine (**RGG-**) rich domains (Morohoshi *et al*, 1998) (Figure 4).

The first 7 exons encode the N-terminal domain of EWS, which consist of a repeated degenerated polypeptide of 7 to 12 residues rich in tyrosine, serine, threonine, glycine and glutamine (SYGQ).

Exons 8 to 17 encode regions associates with RNA binding while the RGG motifs are mainly encoded by exons 8,9,14 and 16; RRM regions are encoded by exons 11,12 and 13.

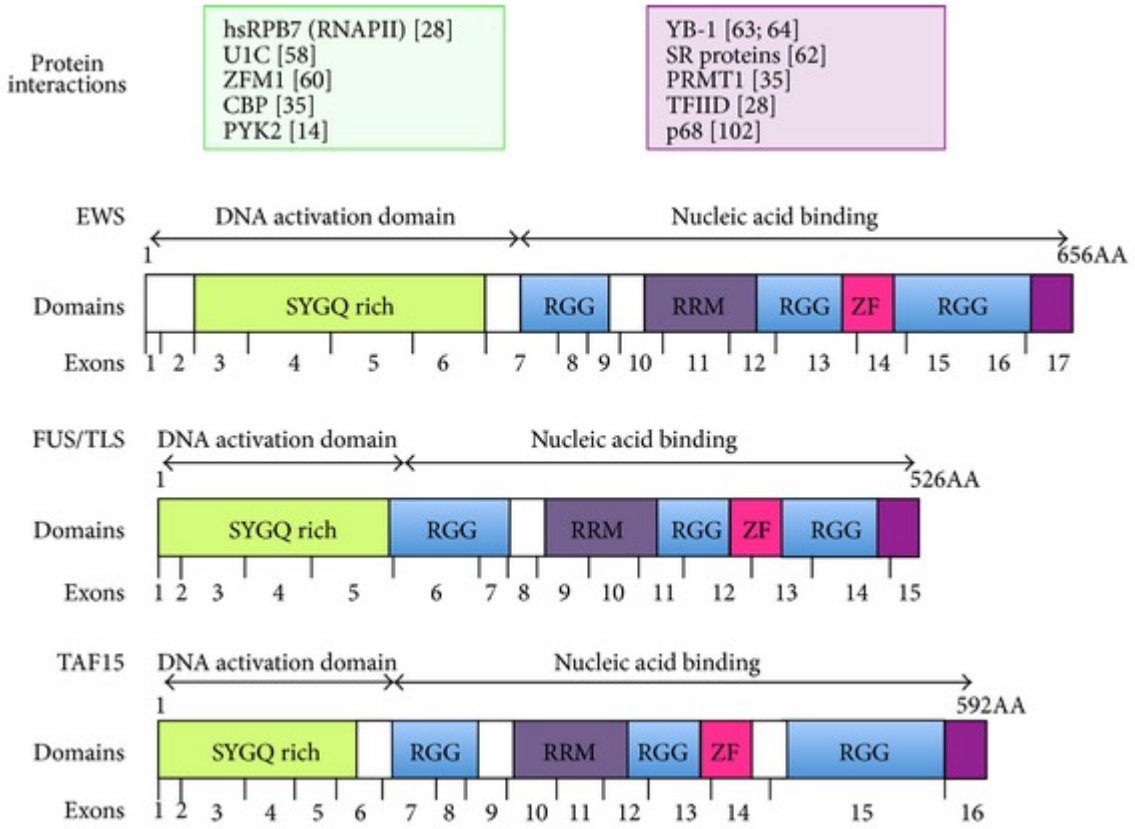

Figure 4: Domain structure of TET proteins.

Picture from: (Paronetto, 2013)

The DNA sequence in the 5' region of EWSR1 gene lacks canonical promoter elements such as TATA and CCAAT consensus sequences but contain G/C rich stretches, suggesting a housekeeping role for TET proteins.

The EWS protein, belonging to the TET family, is probably encoded by an housekeeping gene for the reasons described above and because:

1) Is expressed ubiquitously
2) Its expression is stable throughout the cell cycle
3) Its mRNA has a long half-life

EWS is a nuclear protein that appears to be recruited to promoter regions where it associates with other factors to act as a promoter specific transactivator. This protein is also a transcriptional coactivator in a cell type- and promoter-specific manner.

The role of native EWS protein and the regulatory mechanism controlling its coactivator function are largely unknown.

The oncogenic conversion of EWS follows a common scheme of activation, by exchanging its RNA binding domain with different DNA binding domains, thus generating tumor-specific fusions proteins (Paronetto, 2013).

As reported the involvement of EWS in transcriptional regulation of gene expression. EWS is able to associate with different subunits of the transcription factor TFIID. This feature is not maintained by the oncogenic fusion protein EWS-FLI1 suggesting that EWS and the chimeric protein behave differently in this respect. EWS binds various transcription factors and may regulate transcription both positively and negatively.

The amino terminus of EWS protein was shown to act as a transcriptional activator when fused to a DNA-binding domain (Bailly *et al*, 1994); it may regulate transcription both positively or negatively.

EWS is critically important for the homologous recombination during meiosis and could be involved in the DDR (DNA-damage response) pathway (Li *et al*, 2007). EWSR1 is a gene required for resistance to ionizing radiations (IR) (Hurov *et al*, 2010), which release intermediary ions and free radical that cause DNA lesions, and to CPT, a topoisomerase I-DNA adducts and prevents DNA relegation, leading to formation of single – strand breaks (SSBs) (O'Connell *et al*, 2010). EWS depletion results in alternative splicing (AS) changes of genes involved in DNA repair and genotoxic stress signalling, including ABL1, CHEK2 and MAP4K2. The association of EWS with its target is reduced upon irradiation of cells with ultraviolet light, concomitant with EWS accumulation in nucleoli and with alternative splicing changes that parallel those induced by EWS depletion and lead to reduced c-ABL protein expression.

2.1.3 ETS transcription factors

ETS factors act by binding to promoter and/or enhancer elements of target genes and result in transcriptional activation or repression. The identification of physiologic direct target genes of ETS factors is quite bit difficult. The in vitro DNA binding specificities of different ETS factors can be nonstringent and a single DNA site could potentially be occupied by multiple ETS factors.

Starting from the evidence that different ETS factors can be simultaneously expressed in cells, the ability of a particular ETS protein to bind to a specific gene's regulatory sequence *in vitro* does not necessarily mean that the ETS factor is actually regulating the gene *in vivo (Arvand & Denny, 2001).*

ETS factors typically form heteromeric complexes with non-ETS transcription factors that coordinately bind to target gene sites. To facilitate the DNA binding at regulatory elements, protein-protein interactions can be important for recruiting additional factors necessary for transcriptional modulation of specific target genes. These data indicate that the intrinsic physiologic specificity on any particular ETS protein depends on both its protein-DNA and protein-protein interactions.

They activate specific target genes by binding to cognate DNA sequences through their DNA-binding regions (in the carboxy terminal region). The ETS family of transcription factors is defined by a conserved ETS domain that recognizes a core DNA motif of GGAA/T. This family of approximately 30 genes including FLI1, ERG, ETV1, ETV4, FEV and ZSG controls, various cellular function in cooperation with other transcription factors and cofactors. The target genes of these transcription factors are oncogenes, tumor suppressor genes, genes related to apoptosis, differentiation, angiogenesis and invasion.

2.1.4 Fli1 gene and protein

The Friend leukemia virus integration 1 gene (Fli1), is a member of the ETS family of transcription factors. The gene is located on human chromosome 11q24.1, a region of several abnormalities in human disease (Ben-David *et al*, 1990) (Truong & Ben-David, 2000).

The fli1 gene encodes two isoforms of 51 and 48 kDa, synthesized by alternative translation initiation sites, as mentioned above. Loss of function studies have provided evidence to suggest that both the p51 and p48 isoforms retain the same functional domains and activity (Melet *et al*, 1996).

FLI1 is highly expressed in all hematopoietic tissues and endothelial cells, and at a lower level in the lungs, heart and ovaries (Ben-David *et al*, 1991) (Hewett *et al*, 2001; Melet *et al*, 1996; Pusztaszeri *et al*, 2006). The ubiquitous expression of FLI1 in all endothelial cells suggests a role for FLI1 in endothelial cell fate and angiogenesis (Hewett *et al*, 2001). It has been suggested that FLI1 is the first dependable nuclear marker of endothelial differentiation (Rossi *et al*, 2004), is essential for embryonic vascular development (Spyropoulos *et al*, 2000), and acts as a master regulator establishing the blood and endothelial programmes in the early embryo (Liu *et al*, 2008). Moreover immunohistochemical analysis has revealed that FLI1 expression is a valuable tool in the diagnosis of benign and malignant vascular tumors.

FLI1 is the predominant EWS fusion partner in Ewing's sarcoma tumors and contains a typical Dna Binding Domain (DBD) located towards the C-terminus (Truong & Ben-David, 2000).

At the amino acid level FLI1 is very similar to ERG, the second most common ETS gene involved in Ewing's sarcoma translocations.

FLI1 is primarily a nuclear protein. Several FLI1 proteins have been defined but their physiologic significance is still being investigated.

Consistent with in vivo expression and oncogenic data, genetic animal model systems also confirm a significant role for FLI1 in normal hematopoietic development.

FLI1 plays an important role in erythropoiesis. The constitutive activation of FLI1 in erythroblasts leads to a dramatic shift in the Epo/Epo-R signal transduction pathway, blocking erythroid differentiation, activating the Ras pathway, and resulting in massive Epo-independent proliferation of erythroblasts (Tamir *et al*, 1999; Zochodne *et al*, 2000). These results suggest that FLI1 overexpression in erythroblasts alters their responsiveness to Epo and triggers abnormal proliferation by switching the signaling event(s) associated with terminal differentiation to proliferation (Zochodne *et al*, 2000). The constitutive suppression of FLI1, mediated through RNA interference or dominant negative protein expression has revealed an essential role for continuous FLI1 overexpression in the maintenance and survival of the malignant phenotype in both murine and human erythroleukemia (Cui *et al*, 2009).

2.1.5 EWS-ETS chimeric proteins

The high prevalence of EWS/ETS fusions in Ewing's sarcoma tumors suggested that these chimeric proteins are important for the genesis and maintenance of these tumors. Different chimeric proteins could be observed, due to the different ETS members could be involved in the fusion protein (table1, below).

Karyotype	*Fusion*	*Malignancy*	*Reference*
t(11;22)(q24;q12)	EWS/FLI1	EFT	(Delattre *et al*., 1992)
t(21;22)(q22;q12)	EWS/ERG	EFT	(Sorensen *et al*., 1994; Zucman *et al*., 1993b)
t(7;22)(p22;q12)	EWS/ETV1	EFT	(Jeon *et al*., 1995)
t(2;21;22)(q33;q22;q12)	EWS/FEV	EFT	(Peter *et al*., 1997)
t(17;22)(q12;q12)	EWS/E1AF	EFT	(Kaneko *et al*., 1996; Urano *et al*., 1996)
		undifferentiated sarcoma	
t(12;16)(q13;p11)	TLS(FUS)/CHOP	myxoid liposarcoma	(Crozat *et al*., 1993; Rabbitts *et al*., 1993)
t(12;22)(q13;q12)	EWS/CHOP	myxoid lipsarcoma	(Panagopoulos *et al*., 1996)
t(9;22)(q22;q12)	EWS/CHN(TEC)	myxoid chondrosarcoma	(Clark *et al*., 1996; Labelle *et al*., 1995)
t(9:17)(q22:q11)	TAFII68/CHN(TEC)	myxoid chondrosarcoma	(Attwooll *et al*., 1999; Sjögren *et al*., 1999)
t(12;22)(q13;q12)	EWS/ATF1	MMSP	(Zucman *et al*., 1993a)
t(11;22)(p13;q12)	EWS/WT1	DSRCT	(Ladanyi and Gerald, 1994; Rauscher *et al*., 1994)
t(1;22)(p36;q12)	EWS/ZSG	round cell sarcoma	(Mastrangelo *et al*., 2000)
t(16;21)(p11;q12)	TLS/ERG	myeloid leukemia	(Ichikawa *et al*., 1994)

Karyotypic abnormalities and resultant fusion genes are shown. Abbreviations for malignancies are as follows: EFT, Ewing's family tumor; MMSP, malignant melanoma of soft parts; DSRCT, desmoplastic small round cell tumor

Table1: List of cancer associated gene fusions involving TET family members. ***Table from "Arvand A. and Denny C.T., Oncogene (2001), 20, 5747-54"***

The experiments conducted in animal model systems support the view that EWS/ETS fusions act as dominant oncogenes (May *et al*, 1993a).

This is in agreement with the observation that the treatment of Ewing's sarcoma tumor cell lines with antisense EWS/FLI1 oligonucleotides induces a decreased in vivo tumor growth in immunodeficient mice (Ouchida *et al*, 1995).

The chimeric protein could act as strong transcriptional activator (Bailly *et al*, 1994; Lessnick *et al*, 1995; May *et al*, 1993b) or as transcriptional repressor at some gene targets (Hahm *et al*, 1999; Nakatani *et al*, 2003). The most representative chimera found in the Ewing's sarcoma tumors is represented by EWS-FLI.

The structure of EWS-FLI1 chimeric protein is represented in figure 5.

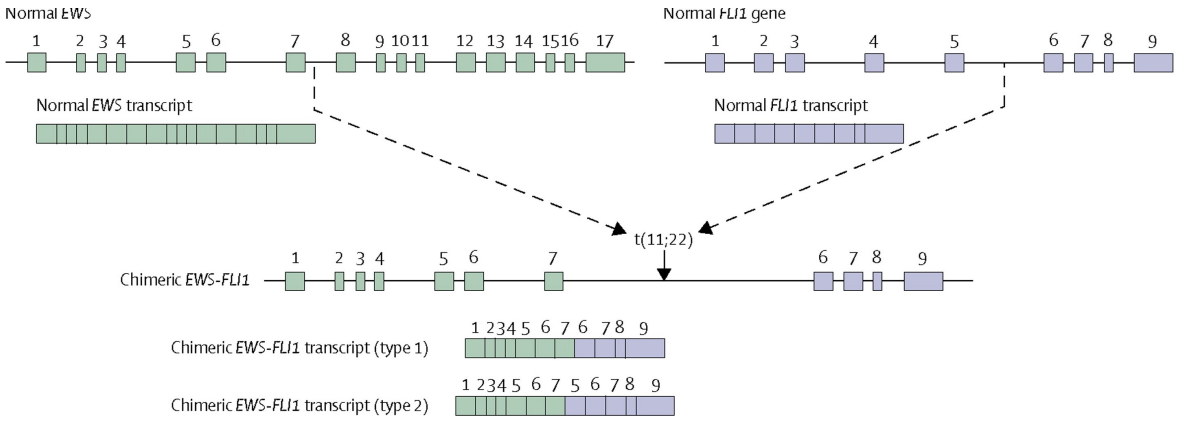

Figure 5: the chimeric protein EWS-FLI1 derived from the fusion of N-terminal part of EWS with COOH terminal part of FLI1. The type I and Type II chimeras differ for the number of exons of FLI1 gene involved in the fusion. The type I chimera derived from the fusion of the first 7exons of EWS with exons 6-7-8-9 of FLI1. The type II chimera is composed of the first 7 exons of EWS gene and exons 5-6-7-8-9 of FLI1 gene.

Picture adapted from Boo Messahel et al., The Lancet Oncology, Volume 6, N°6, p421-430, June 2005.

ETS family members (EWS/FLI1 included) bind to sequences containing a GGAA “core” motif surrounded by bases that provide affinity and specificity to the interaction (Seth and Watson 2005).

In the chimeric protein the N-terminal EWS domain can act as a potent transcriptional activation domain. The N-terminus of EWS encodes a stronger transcriptional activation domain than the native FLI1 domain that is displaced by the t(11;22). This data suggests that EWS/FLI1 could function as a dominant active FLI1 protein. All EWS/ETS fusions contain an intact ETS DNA-binding domain.

2.1.6 Ewing’s Sarcoma: Clinical point of view

The symptomatology of ES is not very extensive and includes mostly pain severe enough to wake up patients (96%) with or without a mass in the involved area (61%).

The prognosis in Ewing’s Sarcoma has improved considerably with current therapy, and approximately two thirds of patients are cured of their disease. However, outcome for patients with disseminated disease or early relapse remains dismal, and the presence of metastatic disease appears to be the major prognostic factor.

Local therapy supplemented with chemotherapy /radiotherapy is the current standard of care for a vast number of solid tumors, including Ewing’s Sarcoma. This type of treatment does not specifically target the pathogenetic mechanisms of Ewing’s Sarcoma, and therefore drug-related resistance frequently emerges. First-line therapy consists of neoadjuvant therapy usually combining 4 to 6 chemotherapeutic agents among vincristine (V), doxorubicin (D), etoposide (E), cyclophosphamide (C), ifosfamide (I) and /or actinomycin-D (A), followed by surgery and/or radiotherapy (Ladenstein R *et al*, 2010). These multimodality treatments were able to increase overall survival up to 60% to 70% in localized disease.

Regarding relapsed and metastatic disease, in which patients present much worse prognosis, there are several nonrandomized ongoing clinical trials at the moment.

These studies include treatment with trabectedin (NCT01222767); Src family tyrosine kinase (TK) inhibitor Dasatinib (NCT01643278); PARP inhibitor Olaparib (NCT01583543) or proteasome inhibitor bortezomib (NCT00027716) among others, in monotherapy, as well as in combination regimens.

The results obtained in a phase II clinical trial (NCT00070109) in refractory relapsed pediatric tumors including 16 Ewing's sarcoma patients, showed insufficient activity of trabectedin used in monotherapy, even if safely tolerated in children (Baruchel *et al*, 2012; Lau *et al*, 2005). The Ewing's Sarcoma is a relatively uncommon disease with different problems in terms of research on new therapies.

3. ANTICANCER DRUGS AND THERAPIES FROM NATURAL COMPOUNDS

For over 50 years, the research of anticancer drugs has been governed by the fact that tumor cells replicate more rapidly than normal cells and that DNA is the most important molecule in cell division. As a result, DNA is often the therapeutic target of anticancer drugs; the vast majority of the currently used drugs cause DNA damage, interrupting cell division and subsequently causing cell death.

Empirically identified compounds with anti-cancer activity were later shown to target DNA either directly or through inhibition of enzymes that control DNA integrity or provide building blocks for DNA. There are different therapeutic agents for which the main target is DNA such as: alkylating agents, antimetabolites, inhibitors of topoisomerases (TOPO) I and II, and agents causing covalent modification of DNA (mitomycin C and platinum compounds), as well as γ-irradiation.

A) ANTICANCER DRUGS THAT DIRECTLY TARGET TUMORAL CELLS

Alkylating agents

Alkylating agents represent a class of anticancer drugs actively used in the clinical approach to cancer therapy.

hese compounds are known for their ability to become strong electrophilic intermediates able to covalently interact with nucleophilic centres (phosphate, aminic, sulphydrilic, hydroxylic, carboxylic and hymidazolic groups) located on proteins and nucleic acids. It has been demonstrated that the most important target of such drugs is the genomic DNA. The alkylating agents are compounds that react with electron-rich atoms in biologic molecules to form covalent bonds. Traditionally, these agents are divided into two types: those that react directly with biologic molecules and those that form a reactive intermediate, which then reacts with the biologic molecules. These intermediates, represented in figure 7, are termed SN1 and SN2, respectively.

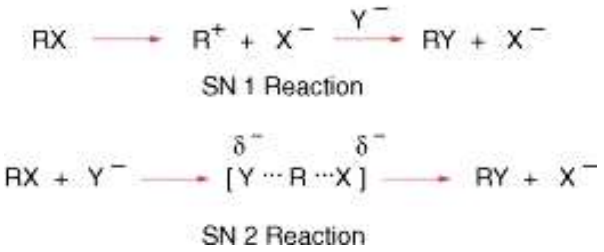

Figure 6: SN1 and SN2 intermediates

Picture from Colvin M. et al, Holland-Frei Cancer Medicine. 6th edition

The terms SN1 and SN2 refer to the kinetics of the reactions. The rate of reaction of an SN1 agent is dependent only on the concentration of the reactive intermediate, whereas the rate of reaction of an SN2 agent is dependent on the concentration of the alkylating agent and of the molecule with which it reacts. This distinction has important implications in understanding the cellular and molecular pharmacology of specific alkylating agents. The *nitrogen mustards* and *nitrosoureas* are examples of SN1 agents, whereas *busulfan* is an SN2 agent. These compounds are known for their ability to become strong electrophilic intermediates able to covalently interact with nucleophilic centres (phosphate, aminic, sulphydrilic, hydroxylic, carboxylic and hymidazolic groups) located on proteins and nucleic acids.

Within DNA, the most frequently alkylated sites are: N^7 and O^6 of guanine, N^7 and N^3 of adenine and N^3 of cytosine.

Several studies provided the evidence that these drugs exert their cytotoxic activity by altering the physiological DNA metabolism, in terms of replication, transcription and repair processes, thus producing molecular signals that can trigger apoptosis.

Major groove alkylators, such as nitrogen mustards (for example, melphalan) and alkylsulfonates (for example, busulfan), covalently bind N^7 only of guanines located in a run of guanines (5'-GGG-3') thus producing interstrand cross-links. Minor groove alkylating agents, such as benzoyl mustard tallimustine and CC-1065, covalently bind to N^3 of adenines with the highest sequence specificity ever seen for alkylators: in fact, these agents are able to alkylate only the N^3 of adenines located in the 5'-TTTTGA-3' and 5'-PuNTTA-3' or 5'-AAAA-3' respectively (Broggini *et al*, 1995; Broggini *et al*, 1991; Colella *et al*, 1996).

Class of alkylating agents	Drugs	Clinical use
Nitrogen mustards	Melphalan	Hematologic tumors, Myeloma, Ovarian cancers, Solid tumors
	Chlorambucil	
	Bendamustine	
	Estramustine	Prostate cancers
Oxazaphosphorines	Cyclophosphamide	Hematologic tumors, Solid tumors, Sarcoma
	Ifosfamide	Sarcoma, Solid tumors
	Trofosfamide	Palliative care
Ethylene imines	Thiotepa	Ovarian, Breast, Bladder cancers
	Altretamine	Ovarian, Lung cancers
	Mitomycin C	Gastrointestinal tumors, Breast and Bladder cancers
Nitrosoureas	Carmustine (BCNU)	Lymphoma, Brain tumors, Melanoma
	Lomustine (CCNU)	
	Nimustine	Brain tumors, Solid tumors
	Fotemustine	Melanoma
	Streptozotocine	Pancreatic and Neurorendocrine tumors
Alkyl alcane sulfonates	Busulfan	Chronic Myeloid leukemia (CML)
Triazenes and hydrazines	Dacarbazine	Melanoma, Lymphoma, Sarcoma
	Temozolomide	Glioma
	Procarbazine	Lymphoma, Glioma
Platinum derivatives	Cisplatin	Solid tumors
	Carboplatin	Solid tumors
	Oxaliplatine	Colorectal cancers
Tetrahydroisoquinolines	Trabectedine	Sarcoma, Ovarian cancers

Table 2: the most important alkylating agents. ***Table from S. Puyo et al, Critical Reviews in Oncology/Hematology, volume 89, pp 43–61, 2014.***

There are several possible consequences of N^7 guanine alkylation:

1. Cross-linkage. Bifunctional alkylating agents, such as the nitrogen mustards, may form covalent bonds with each of two adjacent guanine residues. Such interstrand cross-linkages will inhibit DNA replication and transcription. Intrastrand cross-links also may be produced between DNA and a nearby protein.

2. Mispairing of bases. Alkylating at N^7 changes the O^6 of guanine to its enol-tautomer, which can then form base pairs with thymine. This may lead to gene miscoding, with adenine thymine pairs replacing guanine–cytosine. The result is the production of defective proteins.
3. Depurination. N^7 alkylation may cause cleavage of the imidazole ring and excision of the guanine residue, leading to DNA strand breakage.

Alkylating drugs differs in their electrophilic reactivity, the structure of their reactive intermediates, and their pharmacokinetic properties. These differences will be reflected in the spectrum of their antitumor activities and in the toxicity they produce in normal tissues. An example of alkylating agent is represented by *cyclophosphamide*.

This alkylating chemotherapeutic agent (the structure is represented in figure 9) possess a strong immunosuppressive activity, for many years usually used in the chemotherapeutic regimens in lymphoproliferative diseases as well as in a wide range of solid tumors.

Figure 7: structure of cyclophosphamide

Picture adapted from "Chemsynthesis.com"

Depending on the dose of administration, cyclophosphamide affects tumors either through direct cytotoxic activity or through immune-enhancing mechanisms. Administering cyclophosphamide at high doses is cytotoxic, due to its activity as an alkylating agent, which leads to inhibition of DNA replication and apoptosis of both tumor and lymphoid cells. This cytotoxic effect on lymphoid cells is observed in actively replicating as well as resting, nonreplicating lymphocytes (de Jonge *et al*, 2005).

Cyclophosphamide administration results in the formation of crosslinks within DNA due to a reaction of the two chloroethyl moieties of cyclophosphamide with adjacent nucleotide bases. Cyclophosphamide must be activated metabolically by microsomal enzymes of the cytochrome P450 system before ionization of the chloride atoms and formation of the cyclic ethylenimmonium ion can occur. The metabolites phosphoramide mustard and acrolein are thought to be the ultimate active cytotoxic moiety derived from cyclophosphamide. The high doses of cyclophosphamide lead to the nonspecific depletion of immune cells and are therefore used for inducing lympho-depletion before adoptive cell transfer, conditioning patients before allogeneic stem cell transplantation, as well as chemotherapeutic approaches in aggressive types of lympho-proliferative disorders.

Low doses of cyclophosphamide can have antitumor effects by enhancing the immune response. These doses are effective in treating tumors in immune competent, but not nude, mice, indicating that the effect of low-dose cyclophosphamide is immune mediated, whereas high-dose cyclophosphamide led to antitumor responses in both types of mice. High doses of cyclophosphamide have also been found to decrease lymphocyte infiltration into tumors, whereas low doses lead to higher lymphocyte infiltration. Additionally, low-dose cyclophosphamide enhances vaccine-induced immune responses, whereas higher doses impeded vaccination

Cyclophosphamide is a component of CMF (cyclophosphamide, methotrexate, 5-fluorouracil) and other drug combinations used in the treatment of breast cancer.

Cyclophosphamide is used in combination for the treatment of different solid tumors including: Hodgkin’s and non-Hodgkin's lymphoma, Burkitt’s lymphoma, chronic lymphocytic leukemia (CLL), chronic myelocytic leukemia (CML), acute myelocytic leukemia (AML), acute lymphocytic leukemia (ALL), t-cell lymphoma, multiple myeloma, neuroblastoma, retinoblastoma, rhabdomyosarcoma, Ewing's sarcoma, breast, testicular, endometrial, ovarian, and lung cancers.

In the family of alkylating agents, another important component is *Ifosfamide.*

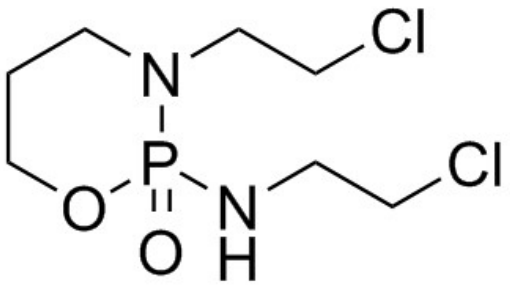

Figure 8: structure of ifosfamide

Picture adapted from "Chemsynthesis.com"

This drug is an analog of cyclophosphamide. It is in the oxazaphosphorine class of alkylating agents, and it is effective against solid tumors such as sarcomas and hematologic malignancies (Chugh *et al*, 2007).

Following activation in the liver, ifosfamide interferes with DNA through formation of phosphotriesters and DNA-DNA crosslinks, thereby inhibiting protein synthesis and DNA synthesis. Ifosfamide is cell cycle-specific, but cell cycle phase non-specific.

Ifosfamide is used in combination chemotherapy, therefore drug-drug interactions are a possible source of increased toxicity as well as genetic variation or a combination of both (Zaki *et al*, 2003).

Ifosfamide has lower myelotoxicity relative to its structural analog cyclophosphamide but higher rates (45% compared to 10%) of the nephrotoxic metabolite chloroacetaldehyde (CAA) (Cheung *et al*, 2011). Glomerular and tubular dysfunctions represent serious side effects, especially in children who are co-treated with other nephrotoxic drugs. Major clinical toxicities include urotoxicity, nephrotoxicity, encephalopathy and cardiotoxicity, as well as neurotoxicity (which occurs in approximately 20% of patients) (Shin *et al*, 2011).

Minor groove alkylating agents, such as benzoyl mustard tallimustine and CC-1065, covalently bind to N^3 of adenines with the highest sequence specificity ever seen for alkylators: in fact, these agents are able to alkylate only the N^3 of adenines located in the 5'-TTTTGA-3' and 5'-PuNTTA-3' or 5'-AAAA-3' respectively (Colella *et al*, 1996; LH *et al*, 1984).

Trabectedin is a minor groove alkylator that binds the exocyclic N2 amino groups of guanines with a sort of sequence specificity with a guanine located in the central position of triplets 5'-purine-GC-and 5'-pyrimidine-GG (TGG,CGG,AGC and GGC sequences), as described in the following paragraph.

Platinum-based antineoplastic agents are sometimes described as "alkylating-like" due to similar effects as alkylating antineoplastic agents, although they do not have an alkyl group.

These anticancer agents are able to covalently bind N^7 of guanine with a certain degree of sequence selectivity thus producing various types of DNA adducts.

Antimetabolite drugs

They are structural analogues of enzymatic cofactors or nucleosides, include inhibitors of folate synthesis, uracil analogues, cytidine analogues and purine analogues. These molecules are able to inhibit the synthesis of DNA precursors and/or can be themselves incorporated into nucleic acids, thus altering DNA replication and repair processes.

An example of these drugs is represented by 5FU (5-fluorouracil).

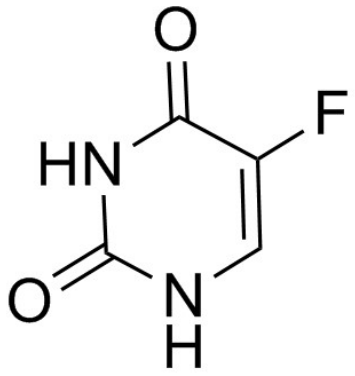

Figure 9: structure of 5-fluorouracil

Picture adapted from "Chemsynthesis.com"

It was synthesized by Duschinsky and Heidelberger, in 1957.

5-FU is a pyrimidine base containing a fluoride atom at the 5 carbon position on the ring. Uracil is a naturally occurring pyramidine base used in nucleic acid synthesis. It is converted to thymidine by enzyme action. 5-FU is similar in structure to uracil and is converted to two active metabolites (FdUMP and FUTP) that inhibit the activity of the enzyme thymidylate synthetase. The enzyme normally converts uracil to thymidine by adding a methyl group at the fifth carbon of the pyrimidine ring. 5-FU mimics the natural base and functions to inhibit DNA synthesis. The carbon group cannot be added because of the fluoride atom at the five position. Normal DNA synthesis fails. dUTP and FdUTP are incorporated into DNA so that it cannot function normally. In addition, FUTP is incorporated into RNA leading to faulty translation of the RNA. Thus, the synthesis of multiple forms of RNA (messenger, ribosomal, transfer and small nuclear RNAs) is blocked. These combined actions on DNA and RNA are cytotoxic to the rapidly dividing cancer cells.

5-FU is used for the treatment of many malignancies: breast, head and neck, adrenal, pancreatic, gastric, colon, rectal, esophageal and G-U (bladder, penil and vulva).

DNA topoisomerase I and II enzymes

Another important class of anticancer drugs is represented by the poisons of the DNA topoisomerase I and II enzymes. By covalently binding the binary complex DNA-topoisomerase I, camptothecins are able to produce a 'cleavable' ternary complex of DNA-topoisomerase I-drug in which topoisomerase I activity is blocked. The presence of such cleavable complexes on genomic DNA seems to interfere with the DNA replication machinery thus altering normal DNA synthesis. Other drugs, such as DNA-topoisomerase II poisons doxorubicin, daunorubicin, mitoxantrone and etoposide are able to stabilize the binary complex DNA-topoisomerase II forming a ternary drug-DNA topoisomerase II complex, thus leaving on the cellular DNA highly toxic double-strand breaks.

Topoisomerases are highly conserved enzymes that are present in virtually all life forms, from bacteria to humans, and they regulate DNA topology to facilitate DNA replication, transcription, and other nuclear processes. The mechanism of action of doxorubicin involves topoisomerase II poisoning, resulting in double-strand DNA breaks and cell death at clinically relevant drug concentrations (Gewirtz, 1999; Thorn *et al*, 2011).

Topoisomerase II is essential for decatenation of DNA during mitosis, and deficiency in topoisomerase II prevents normal cytokinesis resulting in cell death (Carpenter & Porter, 2004). Doxorubicin, like etoposide, traps topoisomerase II at breakage sites, stabilizes the cleavage complex and impedes DNA resealing (Nitiss, 2009; Wu *et al*, 2011).

However, there are many examples in which doxorubicin-mediated cell killing is independent of topoisomerase II. However there are different findings that suggest that anthracycline-induced topoisomerase II poisoning by trapping topoisomerase II at cleavage sites is unlikely to be the only mechanism of cancer cell killing by anthracycline drugs.

An example of a drug that acts blocking the topoisomerase I enzyme is represented by irinotecan (figure 10).

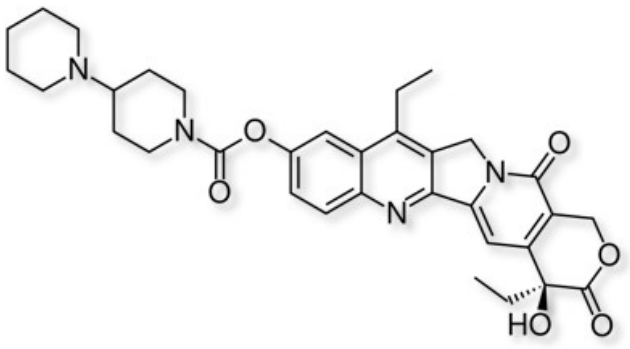

Figure 10: chemical structure of irinotecan.

Picture adapted from "Chemsynthesis.com"

Irinotecan (CPT-11; Campto®) is a semisynthetic, water-soluble derivative of the plant alkaloid camptothecin. Following conversion, by ubiquitous carboxylesterases, to its active metabolite SN-38, irinotecan acts by inhibiting DNA topoisomerase I, thereby interfering with DNA replication and cell division (Creemers *et al*, 1994). Irinotecan interacts with cellular Topo I-DNA complexes and has S-phase –specific cytotoxicity (Liu *et al*, 2000). The nuclear enzyme topoisomerase I relaxed supercoiled DNA and appears to be important for semiconservative replication of double-helical DNA, transcription and chromosomal decondensation (Wang, 1985). This enzyme cleaves and reseal the phosphodiester backbone of DNA, which allows the passage of another single- or double-stranded DNA through the nicked DNA. Topo I binds to single-stranded DNA breaks, and the reversible Topo I-irinotecan-DNA cleavable complex is not lethal to the cells by itself. However, upon their collision with the advancing replication forks, the formation of a double-strand DNA break occurs, leading to irreversible arrest of the replication fork and cell death (Liu *et al*, 2000).

The collision of irinotecan-Topo I complex with the replication fork also results in G2 arrest/delay by signaling the presence of DNA damage to an S-phase checkpoint mechanism (Shao *et al*, 1999).

Irinotecan has shown activity against colorectal, esophageal, gastric, non-small-cell lung cancers, leukemia and lymphomas, as well as central nervous system malignant gliomas (Rothenberg, 2001). On October 2015, the US Food and Drug Administration (FDA) approved the cytotoxic agent, irinotecan liposome injection (Onivyde; Merrimack Pharmaceuticals), for use in combination with leucovorin and 5-FU, for the treatment of patients with advanced or metastatic pancreatic cancer that progressed after gemcitabine-based chemotherapy, making it the first and only FDA-approved treatment option for patients in this setting.

The approval of irinotecan liposome injection was based on the demonstration of improved overall survival in the NAPOLI-1 study, a phase 3, multicenter clinical trial of 417 patients with metastatic pancreatic cancer, whose disease relapsed after gemcitabine-based chemotherapy (Wang-Gillam *et al*, 2016).

The major toxicities of irinotecan in clinical use are myelosuppression and diarrhea.

The elimination of irinotecan and SN-38 is through biliary excretion.

An example of a drug that acts blocking the topoisomerase II enzyme is represented by doxorubicin (figure 11).

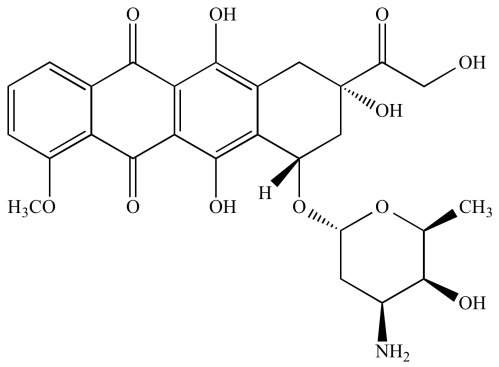

Figure 11: chemical structure of doxorubicin.

Picture adapted from "Chemsynthesis.com"

Doxorubicin (also called adriamycin) was isolated from *Streptomyces peucetius*, a soil bacterium (Arcamone *et al*, 1969; Di Marco *et al*, 1969).

Doxorubicin has shown great efficacy in cancer cell killing for both solid and hematological malignanices, but the emergence of drug resistance and potential side effects such as heart muscle damage after doxorubicin treatment are major limitations for successful cancer treatment (Thorn *et al*, 2011). Despite the extensive usage in the clinics, the molecular mechanism(s) by which doxorubicin causes cell death or cardiotoxicity remains unclear.

Antimitotic drugs

Molecules which exert their cytotoxic activity acting on the mitotic spindle assembly or disassembly. Compounds such as vinblastine, vincristine and vinorelbine are able to prevent mitotic spindle formation by inhibiting microtubule polymerisation, whereas taxanes act by inhibiting microtubule depolymerisation thus stabilising the mitotic spindle.

All these drugs act exerting their activity in proliferating cells since they normally used DNA, DNA synthesis and cell cycle progression as targets. In this wide family of anticancer agents also the chemical inhibitors of kinases that regulate the cell cycle progression, must be included. A new generation of cancer drugs ('targeted therapy') are in development, in order to interfere with a specific molecular target (typically a protein) that could have a critical role in tumor growth or progression. This approach presents some advantages, such as the reduction of side effects thanks to the improvement of tumor specificity and the choice of the therapy after the identification of the molecular target alteration in the specific neoplasm. Among these new drugs, inhibitors of kinases represent one of the most important because kinases are a promising class of targets for cancer therapy. Kinases play key roles in cancer as they are directly or indirectly involved in most signaling pathways.

Protein phosphorylation is the most common form of reversible post-translational modification (Khoury *et al*, 2011). The phosphorylation state of any given protein is controlled by the coordinated action of specific kinases and phosphatases that add and remove phosphate, respectively. There are at least 518 kinases (Manning *et al*, 2002)) and 156 phosphatases (Shi, 2009). Notwithstanding, signaling networks that employ phosphorylation to modulate target activities have been shown to be critically involved in all aspects of cellular function, and in cancer, the abnormal activation of protein phosphorylation is frequently either a driver or direct consequence of the disease (Cohen, 2002).

For instance, kinase signaling pathways have been shown to drive many of the hallmark phenotypes of tumor biology (Hanahan & Weinberg, 2011), including proliferation, survival, motility, metabolism, angiogenesis, and evasion of antitumor immune responses. Currently, there are multiple examples of small molecule kinase inhibitors with both selectivity and suitable pharmaceutical properties that have produced meaningful clinical benefit. For instance, *imatinib* is used to inhibit BCR-ABL1 in chronic myelogenous leukemia (CML) and acute lymphoblastic leukemia with the Philadelphia chromosome (Kantarjian *et al*, 2002); *crizotinib* and other ALK kinase inhibitors for cancers driven by *ALK* fusions (Shaw *et al*, 2014); *lapatinib* for *ERBB2/HER2*-amplified tumors (Arteaga & Engelman, 2014); *gefitinib* and *erlotinib* for *EGF* mutated tumors (Arteaga & Engelman, 2014); and *vemurafenib* for *BRAF* mutant tumors (Chapman *et al*, 2011).

Our evolving ability to genomically characterize tumors heralds a new era in which selective kinase inhibitors can be utilized to inactivate molecular drivers of the malignant state.

B) ANTICANCER DRUGS THAT DO NOT DIRECTLY TARGET THE TUMORAL CELLS

Anticancer therapies linked to tumor-associated macrophages

It is now well established that chronic inflammation contributes to cancer development. Clinical and experimental data indicate that the presence and activation of chronic innate immune cell types, e.g., neutrophils, macrophages and mast cells (MCs) promote cancer development. Therefore, whereas the past point of view was that host immunity was protective against cancer, it is now clear that some subsets of chronically activated innate cells promote the growth and/or facilitate the survival of neoplastic cells (Hanahan & Coussens, 2012). Preclinical evidence supports the use of anti-inflammatory drugs in cancer prevention and therapy.

Several tumor-promoting inflammation inhibitors are designed to: (*a*) inhibit signal transducers and transcription factors that mediate survival and growth, such as nuclear factor κ-light-chain-enhancer of activated B cells (NF-κB) or signal transducer and activator of transcription 3 (STAT3); (*b*) inhibit tumor-promoting chemokines and cytokines that promote tumor infiltration by inflammatory cells such as interleukin 1 (IL-1), IL-6, tumor necrosis factor-α, or receptor antagonists targeting C-C chemokine receptor types 2 and 4 and C-X-C chemokine receptor type 4; (*c*) deplete the tumor-promoting immune and inflammatory cells that promote tumor development and progression such as MDSCs and macrophages.

Several anti-inflammatory drugs have been found to reduce tumor incidence when used as prophylactics, and to slow down tumor progression and reduce mortality when used as therapeutics, such as cyclooxygenase 2 inhibitors in colorectal cancer and in breast and colorectal cancer resistant to chemotherapy (Kang *et al*, 2011); nonsteroidal anti-inflammatory drugs in breast, colorectal, and prostate cancer; and the anti-inflammatory steroid dexamethasone in brain tumors. Several inhibitors of NF-κB or STAT3 have been reported to enhance the effect of therapeutic agents in the treatment of bone metastasis in prostate cancer. However, sustained NF-κB inhibition can result in severe side effects caused by immune deficiency, leading to neutrophilia, enhanced acute inflammation due increased IL-1β secretion, and liver damage (Greten *et al*, 2007). Recent preclinical studies, anti-RANKL (anti–receptor activator of NF-κB ligand) antibodies inhibited bone metastasis in prostate and breast cancer (Smith *et al*, 2012), and IL-1 inhibition blocked myeloma progression (Lust *et al*, 2009). Although targeting single cytokines, chemokines, or transcription factors has led to interesting results in preclinical assays, their potential as single agents in the treatment of human cancers is limited. Combinations with other targets are needed in clinical trials to ensure their efficacy and to limit their side effects.

Targeting Angiogenesis

Tumor growth and expansion are dependent on oxygen and nutrients provided by the newly formed blood vessels. This capability to shift to a vascularized state, called the angiogenic switch, is dependent on cancer cell interaction with the local microenvironment (Hanahan & Weinberg, 2011). More than 1000 clinical trials have been conducted worldwide with antiangiogenic drugs. In the case of vascular endothelial growth factor (VEGF), the anti-VEGF antibody *bevacizumab* increases overall survival or progression-free survival of patients with metastatic colorectal cancer, non–small cell lung cancer, and breast cancer when given in combination with conventional chemotherapeutic regimens (Ebos & Kerbel, 2011). *Sunitinib*, a multireceptor tyrosine kinase inhibitor, also offers a clinical benefit for patients with renal cell carcinoma and advanced gastrointestinal stromal tumors, a benefit that could be in part due to its c-KIT–inhibitory activity. **Sorafenib**, an antiangiogenic tyrosine kinase inhibitor that also targets Raf kinase activity, has been approved for the treatment of renal cell carcinoma and liver cancer. Overall, the survival benefits of antiangiogenic drugs have been rather modest so far, and surprisingly most cancer patients stop responding or do not respond at all to the antiangiogenic therapy (Ebos & Kerbel, 2011).

Emerging challenges in the development of antiangiogenic drugs for cancer treatment have led to increased interest in the development and/or optimization of antiangiogenic drugs as adjuvant or neoadjuvant therapies combined with traditional cytotoxic chemotherapies. It is worth noting that most of the clinical trials with antiangiogenic drugs were conducted during advanced stages of tumor development, whereas the most promising preclinical tests were conducted in animal models at early stages of tumor development.

Moreover, antiangiogenic drugs used in the clinic are centered on the blockade of the VEGF-signaling pathway, whereas VEGF-independent angiogenic factors such as fibroblast growth factor, angiopoietins, placental growth factor (PlGF) and matrix metalloproteases (MMPs).

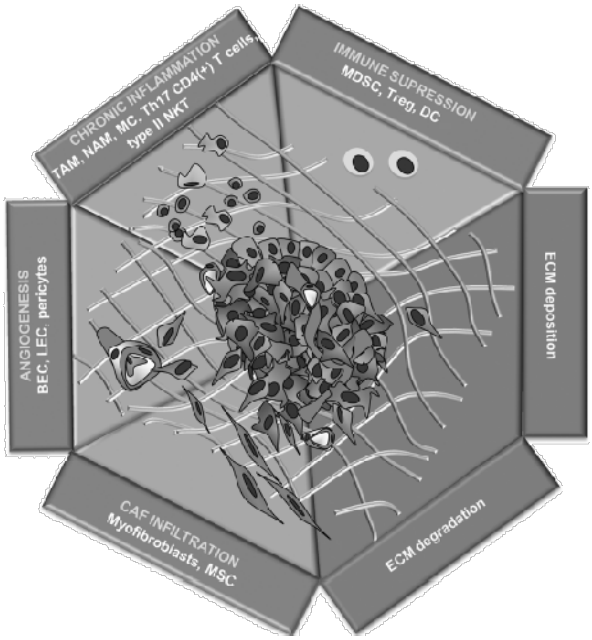

Figure 12: Cellular and noncellular elements of the tumor microenvironment.
Picture from "Sounni NE and Noel A., Clin.Chem, 2013, 59(1):85-93. doi: 10.1373/clinchem.2012.185363"

Targeting Extracellular Matrix

The ability of the stroma to suppress carcinogenesis apparently correlates with organismal survival and contribute to longevity. However, once transformed to a tumor-associated neighbor by various stimuli, the stroma-derived effect turns to be adverse and can significantly promote cancer progression. Under such conditions, the stromal cells co-evolve with the cancer cells by being frequently educated, coopted, or modified by the latter to synthesize a wide variety of cytokines, chemokines, growth factors, and proteinases, together dramatically accelerating disease progression (Junttila & de Sauvage, 2013). ECM molecules and their metabolites are known to regulate cell proliferation, migration, angiogenesis, and cancer metastasis.

Any perturbation of ECM synthesis, degradation, density, and rigidity can considerably influence the capacity of the tumor microenvironment to promote cancer cell proliferation, migration, and invasion, as well as modulate inflammatory responses and lymphangiogenesis (Barker *et al*, 2012; Detry *et al*, 2012). The Matrix Metalloproteinases (MMP) mediates the collagen-remodeling and can regulate tissue architecture through different mechanisms. These phenomena can generate extracellular space for cell migration and unmask cryptic sites within ECM molecules, thereby modifying cell-to-matrix adhesion. By promoting the release of matrix-associated growth factors or cytokines, they modulate the activity or bioavailability of signaling molecules during vascular response to physiological or pathological stimuli. In addition to this MMP-driven ECM degradation process, MMP activities also result in the generation of matrix fragments displaying novel biological activity. It is now well recognized that collagen proteolysis may release a number of endogenous angiogenesis inhibitors, including type IV (arresten, canstatin, tumstatin), type V (restin), and type XVIII (endostatin, neostatins) collagen fragments among other fragments of ECM proteins that may display antiangiogenic activity (Kessenbrock *et al*, 2010). These bioactive fragments become released upon proteolysis of both the interstitial matrix and the vascular basement membrane. These molecules can be found both in the circulation and sequestered in the ECM surrounding cells. These angioinhibitory fragments regulate primarily endothelial cell proliferation and apoptosis by interfering with integrins. Although the role of matrix-derived angiogenesis inhibitors has been well studied in animal models of cancer, their role in human cancers is less established.

The ECM-derived inhibitors have a potential use as cancer therapeutics agents and biomarkers.

In the table 3 is shown a panel of therapeutic agents that target specific compartments of tumor microenvironment.

Molecule	Target	Molecular type	Company	Status
ECM/fibroblasts				
Sonidegib	SMO	Small molecule	Novartis	Phase II (NCT01708174, NCT01757327, NCT02195973)
Vasculature				
Bevacizumab	VEGFA	Antibody	Genentech/Roche	FDA-approved ((BLA) 125085)
Vandetanib	VEGFRs, PDGFRs, EGFR	Small molecule	AstraZeneca	FDA-approved ((NDA) 022405)
Sunitinib	VEGFRs, PDGFRs, FLT3, CSF1R	Small molecule	Pfizer	FDA-approved ((NDA) 021938)
Axitinib	VEGFRs, PDGFRs, KIT	Small molecule	Pfizer	FDA-approved ((NDA) 022324)
Sorafenib	VEGFRs, RAF PDGFRs, KIT	Small molecule	Bayer	FDA-approved ((NDA) 021923)
Pazopanib	VEGFRs, PDGFRs, KIT	Small molecule	GlaxoSmithKline	FDA-approved ((NDA) 022465)
Cabozantinib	VEGFR2, RETMET	Small molecule	Exelixis	FDA-approved ((NDA) 023756)
Ziv-aflibercept	VEGFA, VEGFB, PIGF	Receptor-Fc fusion	Regeneron	FDA-approved ((BLA) 125418)
AMG-386	ANG2	RP-Fc fusion protein	Amgen	Phase III (NCT01204749, NCT01493505, NCT01281254)
Parsatuzumab	EGFL-7	Antibody	Genentech/Roche	Phase II (NCT01399684, NCT01366131)
Enoticumab	DLL4	Antibody	Regeneron	Phase I (NCT00871559)
Demcizumab	DLL4	Antibody	OncoMed	Phase I (NCT00744562, NCT01189968, NCT01189942, NCT01189929)
Nesvacumab	ANG2	Antibody	Regeneron	Phase I (NCT01688960, NCT01271972)
Immune				
Ipilimumab	CTLA-4	Antibody	Bristol-Myers Squibb	FDA-approved ((BLA) 125377)
Sipuleucel-T	PAP	DC vaccine	Dendreon	FDA-approved ((BLA) 125197)
Aldesleukin	IL-2	RP	Prometheus	FDA-approved ((BLA) 103293)
IFN-α-2b	IFN-α receptor	RP	Merck	FDA-approved ((BLA) 103132)
MK-3475	PD1	Antibody	Merck	Phase III (NCT01866319)
Nivolumab	PD1	Antibody	Bristol-Myers Squibb	Phase III (NCT01642004, NCT01668784, NCT01673867, NCT01721746, NCT01721772, NCT01844505)
Nivolumab	OX40	Antibody	Bristol-Myers Squibb and PPMC	Phase III (NCT01642004, NCT01668784, NCT01673867, NCT01721746, NCT01721772, NCT01844505)
MPDL-3280A	PDL1	Antibody	Genentech/Roche	Phase II (NCT01846416)
PLX-3397	KIT, CSF1R, FLT3	Small molecule	Plexxikon	Phase II (NCT01349036)
BMS-663513	CD137 (4-1BB)	Antibody	Bristol-Myers Squibb	Phase II (NCT00612664)
Blinatumomab	CD3 and CD19	Bi-specific scFv	Amgen	Phase II (NCT01741792, NCT01466179, NCT01207388, NCT01471782, NCT00560794, NCT01209286)
AMG-820	CSF1R	Antibody	Amgen	Phase I (NCT01444404)
AMP-224	PD1	Antibody	GlaxoSmithKline	Phase I (NCT01352884)
TRX-518	GITR	Antibody	GITR, Inc.	Phase I (NCT01239134)
IMC-CS4	CSR1R	Antibody	ImClone/Eli Lilly	Phase I (NCT01346358)
CP-870,893	CD40	Antibody	Pfizer	Phase I (NCT00711191, NCT01008527, NCT00607048, NCT01456585, NCT01103635)

Table 3: A list of some therapeutic agents that target specific compartments of tumor microenvironment, with the relative clinical phase trials.

Table from "Chen F. et al, BMC Medicine, 2015, 13:45 DOI: 10.1186/s12916-015-0278-7".

4. DNA REPAIR: NER AND HR PATHWAYS

4.1 Nucleotide excision repair (NER)

The NER system is one of the most important DNA repair mechanisms, because of its wide substrate range (Sancar, 1996; Wood, 1996). In humans, the NER pathway has been studied by means of three inherited disorders (Xeroderma pigmentosum (XP), Cockayne syndrome (CS) and TTD (a photosensitive form of trichotiodystrophy) in which a defective NER mechanism is involved. Genes encoding for proteins involved in NER have been named as the subclasses of XP in which they are lacking, whereas others have been designated ERCC genes (excision repair cross-complementing genes). Some independently identified XP proteins and ERCC gene products are identical (for example, ERCC2 is identical to XPD and ERCC3 is identical to XPB) (O'Donovan & Wood, 1993). The **NER reaction mechanism** is represented in Figure 13.

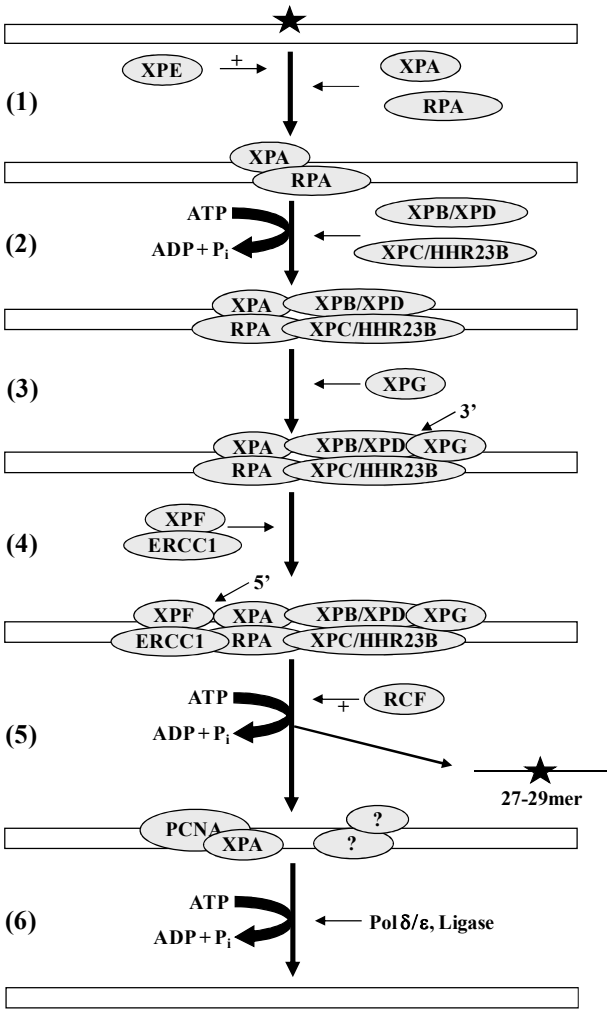

Figure 13: Model for nucleotide excision repair (NER) in humans. Damage (*) is recognised by the XPA-RPA complex, stimulated by XPE (Step 1). Subsequently, two subfactors of TFIIH, XPB and XPD, unwind the DNA after which the XPC-HR23B complex is recruited (Step 2). Next, XPG makes the 3' incision (Step 3) and XPF-ERCC1 makes the 5' incision (Step 4). The damaged part is released and the postincision complex is dissociated by RCF, leaving behind the gapped DNA protected by RPA, PCNA and other proteins (Step 5). Finally, the gap is filled and ligated (Step 6).

Picture adapted from "PhD thesis – Molecular analysis of DNA damage induced by a ovel trinuclear platinum complex (BBR3464) of Doctor Gennaro Giovanni Domenico Colella, 2001"

In the first step the damage is recognised by **XPA-RPA** (replication protein A, also referred to as 'human single-stranded binding protein' (HSSB) complex). XPA contains a zinc finger and has a high affinity for damaged DNA. The addition of **XPE** in this step seems to have an important role as a stimulatory or accessory factor for the binding of XPA-RPA to DNA.

In the subsequent step (step 2), the DNA is unwound by two sub-factors of the general transcription factor TFIIH: **XPB** and **XPD**. These two factors exhibit helicase activities, each in opposite direction (XPB 3→5 and XPD 5→3). The **XPC-HHR23B** complex also binds to the damaged strand in this phase of the process and acts as a stabiliser for the unwound state of the DNA. In the steps 3 and 4 the dual incisions are made. First, **XPG** incises 3' of the lesion and remains bound to the damaged site. It plays a structural role in maintaining a stable complex and in recruiting **XPF-ERCC1**, which incises 5' of the lesion (Hoeijmakers & Bootsma, 1994). XPA also acts as an anchor to recruit XPF-ERCC1. The damaged part is now released as a 27-29 nucleotide long fragment (step 5) then the post incision complex is dissociated by a protein called **RCF** (replication factor C). Both the gapped DNA and the excised oligomer are complexed with proteins. Two of these proteins are proliferating cell nuclear antigen (**PCNA**) and **RPA**; the others have not yet been identified. Complexation is a necessary step in order to protect the excision gap from non-specific nucleases until repair synthesis take place. Repair is performed by DNA polymerases δ or ε. Finally, a ligase seals the remaining nicks (step 6).

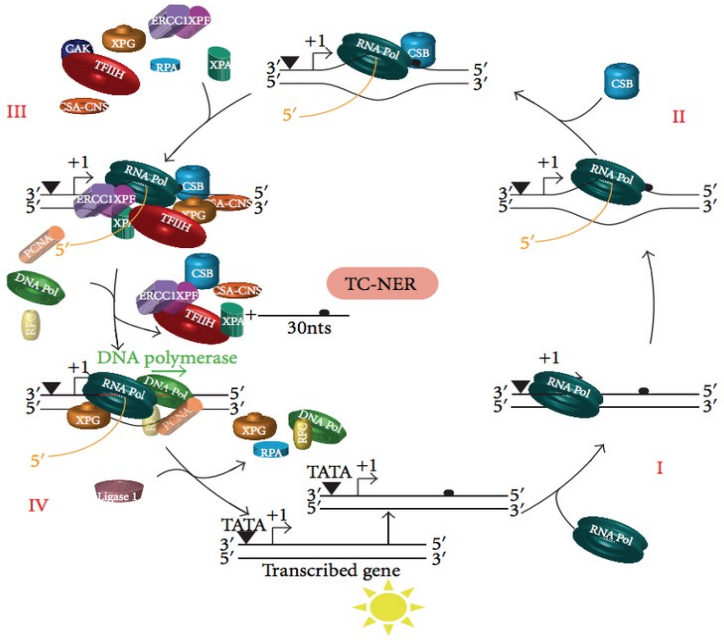

Figure 14: The different phases of NER mechanism.

Picture from: Le May N. et al, Journal of Nucleic Acids, 2010, doi: 10.4061/2010/616342.

4.2 Homologous Recombination (HR)

HR is considered a more accurate mechanism for DSB repair because broken ends use homologous sequences elsewhere in the genome (sister chromatids, homologous chromosomes, or repeated regions on the same or different chromosomes) to prime repair synthesis. If the repair template is perfectly homologous, repair can be 100% accurate, although even in this case there is evidence from yeast that the repair polymerase is more error-prone than replicative polymerases, and point mutations arise at increased frequencies adjacent to DSB repair sites (Strathern *et al*, 1995). This DNA repair mechanism is a highly complex process that involves multiple proteins and occurs during the S and G2 phases of the cell cycle (Shrivastav *et al*, 2008), when the sister chromatids are present and can also be a model for DNA repair (Takata *et al*, 1998).

The isolation and characterization of relevant mutants in *Escherichia coli*1, and later in the budding yeast *Saccharomyces cerevisiae*, uncovered the role of HR in DNA repair and led to the recognition that HR prevents the death of damaged DNA replication forks, orchestrates the segregation of homologous chromosomes in meiosis I and functions in telomere maintenance (Michel *et al*, 2004; Symington, 2002).

Many tumor suppressors proteins participate in this pathway as reported in the table 4.

BRCA1 and BRCA2	BRCA1 and BRCA2 mutation carriers have increased risk of breast, ovarian, prostate, pancreatic, melanoma and other gastrointestinal, gynaecological and haematological malignancies. Methylation of the *BRCA1* promoter is common in spontaneous breast, ovarian and lung cancers
XRCC2 and RAD51	XRCC2 is a RAD51 paralogue, frameshift mutation owing to microsatellite slippage that in MSI tumors confers sensitivity to crosslinking agents
RAD 50	Frameshift mutations in the *RAD50*-associated microsatellite, which results in a truncated protein, occur in 31% of gastrointestinal cancers
FANC proteins	Fanconi's anaemia is associated with haematological malignancies and oesophageal and gynaecological cancer. Most mutations occur in FANCA (65%), FANCC (15%) or FANCG (10%). *FANCD1* (*BRCA2*), *FANCN*

	(*PALB2*) and *FANCJ* (*BACH1*; also known as *BRIP1*) are breast cancer susceptibility genes. Methylation of FANC genes is common in sporadic cancers; for example, *FANCF* is methylated in lung, ovarian and cervical cancer

Table 4: tumor suppressor proteins with an important role in HR pathway.

Table adapted from Curtis N.J., Nature Reviews, 2012, Vol12, 801-817.

In eukaryotic cells, DNA repair is supported by several protein complexes. Protein ATM (Ataxia Telangiectasia Mutated) has a role in DSB signaling via its activation induced by the MRN protein complex (MRE11-Rad50-NBS1 complex). MRE11 is a 5'-3' exonuclease that leads to a 3' end of DNA which is required for the process (Uziel *et al*, 2003). This resection of single-stranded DNA is followed by the recruitment of many proteins such as RPA, BRCA1, BRCA2, Rad51, Rad52, and Rad54. Rad52 is one of the first to settle on the DSB. BRCA1 then recruits BRCA2, Rad54 and Rad51 to form the nucleoprotein filament with ssDNA, whose role is to move the blade to the homologous sequence required for HR. Rad51 protein is the main element involved in the HR process. This recombinase catalyzes the homology search and the strand exchange with a homologous sequence and thus ensures the accurate repair of the DSB. In eukaryotes, Rad51 recombinase (RecA homolog in *Escherichia coli*) catalyzes the essential steps of homologous recombination and interacts directly with protein suppressors of breast cancer (BRCA1, BRCA2) (Aihara *et al*, 1999) and p53 (Bearss *et al*, 2002) which also indicates the importance of Rad51 in apoptosis.

HR involves a large number of protein complexes and can be divided into three main stages (figure 15).

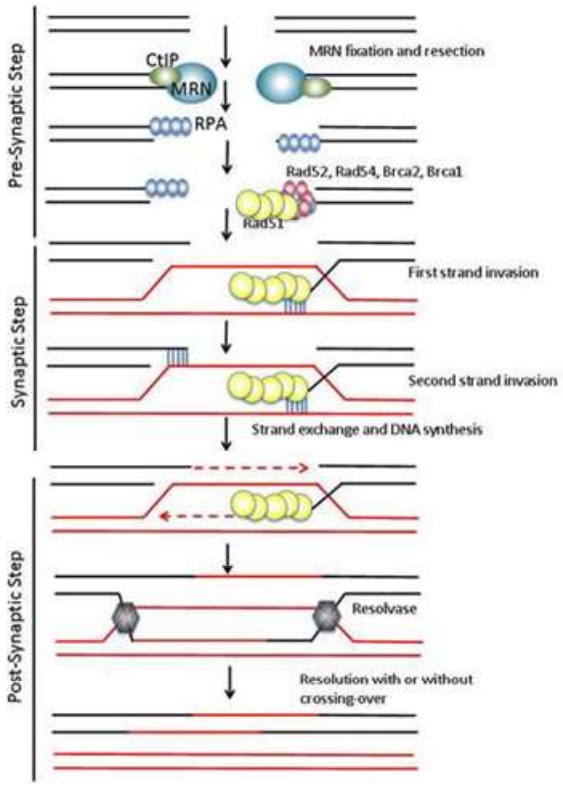

Figure 15: schematization of HR pathway

Picture from "Renodon-Corniere A. et al, Biochemistry, Genetics and Molecular Biology, Book edited by Clark Chen, ISBN 978-953-51-1114-6".

Pre-synaptic step: DNA DSBs are resected by nuclease to generate 3'-protruding ends. The complex MRN (MRE11-RAD50-NSB1) contributes to DNA resection which is followed by formation of the replication protein A (RPA) complex. This ssDNA-binding factor removes secondary structures of ssDNA and is subsequently replaced by Rad51. Rad51 is recruited onto ssDNA to form the nucleofilament. Protein mediators such as Rad52 and Rad51 paralogs, Rad51B-C-D, BRCA1/2, facilitate the loading of Rad51 onto the ssDNA. The DNA binding sites of Rad51 are located in the N-terminal domain of each Rad51 monomer (Aihara *et al*, 1999).

Synaptic step: the nucleofilament of Rad51 is involved in the search for homologous DNA. Once a homologous sequence is located, the Rad51 filament invades the duplex DNA and generates a displacement of the homologous DNA strand to form a D-loop.

Exchange and resolution of the DNA intermediate structure or post-synaptic phase. The second 3' ssDNA overhang anneals to the displaced DNA strand and serves as a model strand for DNA synthesis. Two Holliday Junctions (HJ) are then formed.

Post-Synaptic Step: resolution of the Holliday Junctions with consequent generation of two dsDNA. HJ can be either resolved or dissolved resulting in crossover or non-crossover products.

It is clear that Rad51 plays an essential role at different levels of HR and several interactions are involved such as Rad51/ssDNA, Rad51/Rad51, Rad51/dsDNA, and Rad51/nucleotide. In addition, Rad51 interacts with its partners involved in HR (e.g. Rad52, Rad54).

The function of the entire pathway can be compromised by mutation in one or more genes.

HR impairment is probably the underlying cause of breast, ovarian and other cancers in individuals who harbour mutations in the BRCA1 and BRCA2 (Jasin, 2002; Moynahan, 2002).

Tumors with HR defects are highly sensitive to crosslinking agents (such as cisplatin, carboplatin and nitrosoureas) and DSBs that are induced by IR and topoisomerase I poisons.

5. CELL CYCLE AND CELL CYCLE REGULATION

The cell cycle in eukaryotic cells consists of four phases: gap (G1), synthesis (S), G2 and M and an additional phase outside the cycle, G_0.

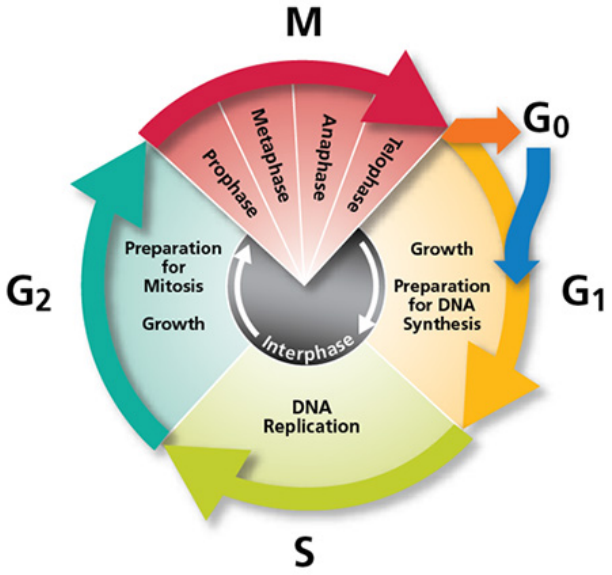

Figure 16: the different phases of the cell cycle.

Picture from BD Bioscience website

In the G1 phase, directly after mitosis, the cell increases in size and starts synthesizing RNA (transcription) and proteins (translation). In the subsequent S phase, DNA is replicated to produce an exact copy of the genome for the subsequent daughter cells.

During G2, the cells will grow and make extra proteins to ensure that two viable daughter cells can be formed. RNA and protein syntheses that started in the G1 phase are continued during S and G2 phases. As final step the cells will go into the M phase where the chromosomes are organized in such a way that two genetically identical daughter cells can be produced. After these events the whole cell cycle can start again or cells can stop dividing and remaining in G_0 phase.

In a normal cell cycle, the passage from one stage to another is thoroughly controlled. In all cells the cell cycle checkpoint pathways are active and up-regulated when DNA damage occurs. The term checkpoint is defined more upon the transition between phases, which is being inhibited by DNA damage at G1/S, intra-s, and G2/M checkpoints.

The DNA damage response during any phase of the cell cycle has the same pattern. After the detection of DNA damage by sensor proteins, signal transducer proteins transduce the signal to effector proteins. These effector proteins launch a cascade of events that causes cell cycle arrest, apoptosis, DNA repair, and /or activation of damage-induced transcription programs (Figure 17).

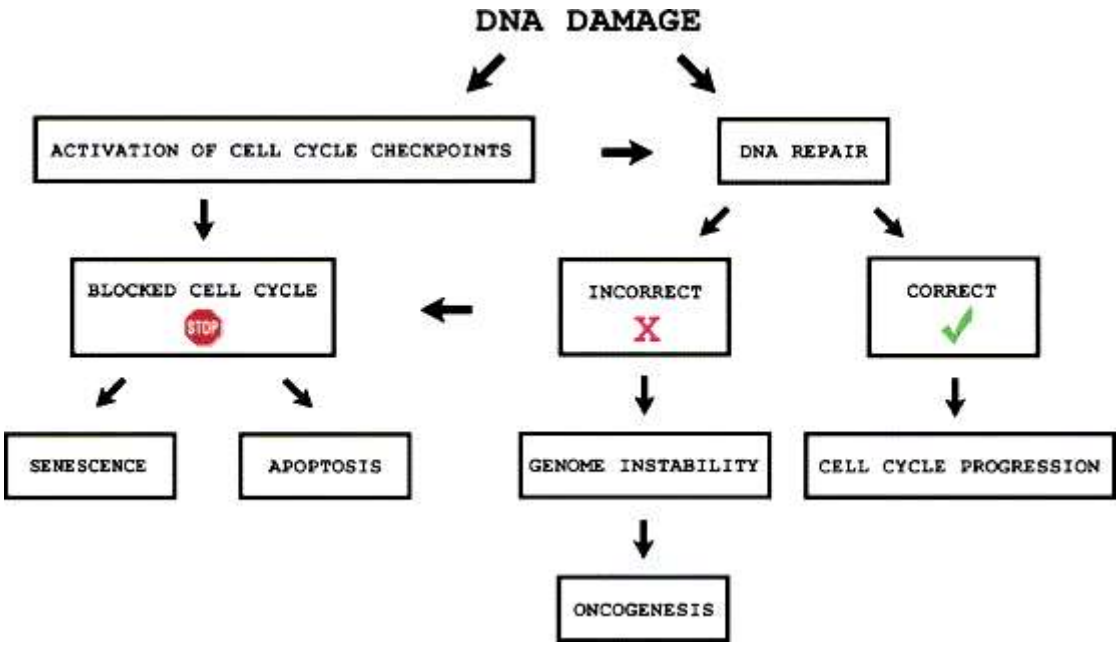

Figure 17: flowchart of the cellular response to any kind of DNA damage.

Picture adapted from "Khalil H.S. et al., Biodiscovery, 2012, 1:3"

There are different signal transducers and effectors associated to specific checkpoint of the cell cycle, that function as damage sensors. ATM and ATR, important players in the early response to DNA damage, phosphorylate most of these mediators. ATM (that respond to ionizing radiations) and ATR (that respond to UV, MMS and replication inhibitors) phosphorylate Chk1 and Chk2 that are serine/threonine protein kinases that in turn phosphorylate protein targets to finally result in the cell cycle arrest.

The double strand breaks (DSB) signal sensed by ATM is transduced by Chk2 while the UV damage signal sensed by ATR is transduced by Chk1, with some overlap between the functions of these two proteins.

Summarizing the cell cycle is controlled by multiple overlapping checkpoints that regulate progression through the cell cycle. Entry into the cell cycle is controlled by the “restriction point” and the progression through the different phases is regulated by multiple distinct checkpoints: the cyclin-dependent kinases.

These are serine/threonine kinases whose activity depends on a regulatory subunit: the cyclin.

One of the most important regulators of the cell cycle is WEE1 that prevents the mitotic entry via inhibitory phosphorylation of CDK1(Tyr15) (Lindqvist *et al*, 2009). A more detailed description of this kinase is reported in the following paragraph.

5.1 ChK1 Kinase

Checkpoint kinase 1, commonly named ChK1, is a serine-threonine kinase encoded by the CHK1 gene, that is located on chromosome 11 (11q22-23), in humans. Chk1 is highly conserved from budding yeast (Rad27) to humans (Rhind & Russell, 2000). Chk1 has a C-terminal regulatory domain which may be involved in its translocation between the cytoplasm and the nuclear compartment. Chk1 is one of the key proteins in cell cycle control which activates cell cycle checkpoint initiation. This kinase is involved in several steps of the cell cycle from S to G2/M phase; in addition it is a cell regulator and a DNA damage sensor. In response to DNA damage, Chk1 phosphorylates, inhibiting, the Cdc25 phosphatases, particularly Cdc25A, which is the main target. This phosphorylation induces the degradation of Cdc25 with consequent inhibition of cyclin-Cdk and prevention of mitotic phase entry (Xu *et al*, 2012).

The activation of Chk1 results in the initiation of cell cycle checkpoints, cell cycle arrest, DNA repair and cell death, in order to prevent damaged cells from progressing through the cell cycle. Therefore, Chk1 is crucial in genomic stability but can also be a source of resistance to anticancer therapies.

Chk1 activation occurs through ATR-mediated phosphorylation of two conserved sites, Ser317 and Ser345 (Goto *et al*, 2015).

These phosphorylation events promote the autophosphorylation of Chk1 on Ser296, which triggers its cell cycle arrest and DNA repair functions (Goto *et al*, 2012; Merry *et al*, 2010). Chk1 pSer345 site has been described as an important phosphorylation site for its catalytic activation and is considered as a marker of DNA damage (Walker *et al*, 2009). These post-translational modifications trigger the release of Chk1 from the chromatin fraction into the soluble compartments (Smits *et al*, 2006) which allows cell cycle arrest and repair processes. Released and activated Chk1 then phosphorylates a number of downstream targets to control cell cycle transition and DNA damage repair (Bryant *et al*, 2014). DNA Double Strand Breaks (DSB) repair proteins involved in homologous recombination, such as the key protein RAD51, have been identified among the targeted proteins (Sorensen *et al*, 2005) , so Chk1 is involved in the activation of DNA repair by homologous recombination (Morgan *et al*, 2010). In response to DNA lesions, Chk1 physically interacts with and phosphorylates RAD51 on Thr309, promoting the recruitment of RAD51 at DNA damage sites (Sorensen *et al*, 2005).Treatment with Chk1 inhibitors impairs HU-induced RAD51 foci formation, confirming the essential role of Chk1 as activator of HR (Sorensen *et al*, 2005). Starting from these information about the role of Chk1, it is clear that a target therapy directed against this kinase could represent a novel strategy in cancer therapy.

Chk1 plays a key role in regulating replication checkpoints and the DNA Damage Response (DDR) since this kinase is mainly responsible for G2/M checkpoint. The main checkpoint regulator in G1/S phase is p53 and in numerous cancers (about 50% of cases) p53 is either mutated or null. Given that most tumor cells suffer defects in the p53 pathway, cancer cells have to maintain functional S and G2/M phases mediated by Chk1 to avoid premature mitotic entry which could lead to mitotic catastrophe. This latter status is characterized by phosphorylation of Histone H3 (on Ser10) and aberrant mitotic spindle formation (Wei *et al*, 1999). These p53-related defects have been taken advantage of to kill cancer cells and it has been shown that using Chk1 siRNA enables to enhance apoptosis in p53-deficient tumor cell lines (Chen *et al*, 2003; Chen *et al*, 2006).

P53 inhibitors were already described (Benada & Macurek, 2015). In addition, a high level of Chk1 is often described in various types of cancers, including breast cancer, pancreatic cancer, non-small cell lung carcinoma and leukemia. In one report, lung cancer cells expressing high levels of Chk1 were hypersensitive to Chk1 inhibitors. Recently, Sarmento et al. have shown that Chk1 overexpression in T-cell acute lymphoblastic leukemia (T-ALL) enables cellular proliferation and survival by preventing replication stress (Sarmento *et al*, 2015). Chk1 overexpression contributes to cancer resistance by delaying mitotic entry and thereby it has been associated with tumor grade and poor prognosis (Grabauskiene *et al*, 2014; Zhang & Hunter, 2014). Chk1 contributes to cell survival by inducing G2 arrest and signaling to the HR pathway for DNA repair (Sorensen *et al*, 2005). These data highlighted the importance to use inhibitors of Chk1 as possible therapy.

PF-477736 is a selective and competitive inhibitor for the Chk1 ATP site. Its specificity is one hundred times stronger for Chk1 than for Chk2. Ovarian cancer often responds well to treatment with PF-477736 but it rapidly generates metastasic and chemoresistant forms (Kim *et al*, 2015). The treatment of HGS (high grade serous) cells by PF-477736 combined with topotecan (topoisomerase I inhibitor) improved and synergized the cellular toxicity by inducing apoptosis (Kim *et al*, 2015). PF-477736-induced Chk1 inhibition led to impaired replication combined with the abrogation of G2/M checkpoint in T-ALL cells. Interestingly, this inhibitor did not significantly affect normal thymocyte cells in vitro which shows the ability of PF-477736 to discriminate normal and cancer cells (Sarmento *et al*, 2015).

5.2 WEE1 Kinase

WEE1 is an evolutionarily conserved nuclear tyrosine kinase that is markedly active during the S/G2 phase of the cell cycle (Featherstone & Russell, 1991; McGowan & Russell, 1995). It was first discovered many years ago (1980_s), as a cell division cycle (cdc) mutant-*wee1*- in the fission yeast, *Schizosaccharomyces pombe* (Russell & Nurse, 1987). Fission yeast lacking WEE1 are characterized by a smaller cell size, and this phenotype has been attributed to the ability of WEE1 to regulate negatively the activity of the cyclin-dependent kinase CdK1 (Cdc2), in the CdK1/Cyclin B complex (Gould & Nurse, 1989). In 2012 Mahajan K. et al (Mahajan *et al*, 2012) demonstrated that the inhibition of WEE1 kinase activity by a specific inhibitor (MK-1775) or RNA interference technology, abrogated the H2B Y37-phosphorylation with a concurrent increase in histone transcription. WEE1 kinase in normal condition phosphorylates H2B at site 2, with a consequent suppression of Hist1 mRNA transcription.

All these data suggest that WEE1 could have a role as a “chromatin synthesis sensor” by two sequential phosphorylation events: 1) Y15-phosphorylation of CDK1, to prevent the exit from S phase until DNA replication is completed and 2) Y37-phosphorylation of H2B at the end of S phase to terminate histone synthesis, thus maintaining the correct histone-DNA stoichiometry prior to mitotic entry (Mahajan *et al*, 2012). All eukaryotic cells maintain a precise ratio of core histones to the newly synthesized DNA; both higher or lower ratios of histones to the DNA have deleterious effects. The alterations of histone stoichiometry or mutations in histone genes are linked to chromosome loss, altered chromatin architecture, and cancer (Meeks-Wagner & Hartwell, 1986; Singh *et al*, 2009).

WEE1 deposits pY37-H2B marks the nucleosomes located upstream of HIST1 cluster to disengage NPAT (nuclear protein, ataxia-telangiectasia locus), a transcriptional activator of mammalian histone genes and RNA polymerase II (Zhao *et al*, 2000). Cell cycle analysis indicated that cells rapidly exit S phase once the histone transcription is completed and the pY37-H2B marks are quickly erased (Mahajan *et al*, 2012).

The mechanisms of action of WEE1 make the protein a “master regulator of chromatin integrity”. Agents that compromise WEE1 function cause mitotic infidelity, chromosome loss, and apoptosis causing the so called “mitotic catastrophe” (Mir *et al*, 2010). Wee1 knockout is lethal for embryonic mice because the embryos do not proceed the blastocyst stage due to defects in cell proliferation. The abnormalities exhibited by Wee1-deficient cells are more severe than that noted for other checkpoint proteins such as ATM (which regulates G2/M entry); this observation suggests that the loss of proliferation may not be solely attributed to early entry into mitosis (Tominaga *et al*, 2006). Consistent with these data Wee1-deficient cells exhibit increase DNA damage in S phase as evidenced by increased H2AX S139-phosphorylation (hallmark of DNA damage and chromosome aneuploidy) (Beck *et al*, 2010; Tominaga *et al*, 2006).

5.2.1 WEE1: mechanism of action

When DNA replication is disrupted by endogenous or exogenous factors (alkylating agents, oxidative free radicals, UV radiation, nucleotide depletion) cells rapidly mobilize checkpoint and DNA repair proteins to sites of damage. Subsequently the DNA replication checkpoint ATR is activated. ATR regulates activation of the checkpoint kinase CHK1, a serine/ threonine kinase that negatively regulates CDC25 phosphatase, dephosphorylates CDK1 and stabilizes WEE1 (Fasulo *et al*, 2012; Sorensen *et al*, 2003). As consequence WEE1 phosphorylates Tyr15 of CDK1 in the CDK1/Cyclin B complex, to prevent mitotic entry until the damaged DNA is repaired.

WEE1 is a negative regulator of entry into mitosis (G2 to M transition) because protects the nucleus from cytoplasmically - activated cyclin B1-complexed CDK1 before the onset of mitosis by mediating phosphorylation of CDK1 on Tyr-15. Specifically phosphorylates and inactivates cyclin B1-complexed CDK1 reaching a maximum during G2 phase and a minimum as cells enter M phase. Phosphorylation of cyclin B1-CDK1 occurs exclusively on Tyr-15 and phosphorylation of monomeric CDK1 does not occur. Its activity increases during S and G2 phases and decreases at M phase when it is hyperphosphorylated.

WEE1 is also crucial for the delay in chromosome condensation when DNA replication is perturbed by treatment with specific inhibitors that interfere with S-phase progression and for the metaphase delay in cells treated with topoisomerase inhibitors (Fasulo *et al*, 2012). Wee1 definitely coordinates completion of multiple chromosomal processes before cells divide by dynamically surveying events to ensure proper chromatin duplication and segregation. All the knowledge about WEE1 suggests that this kinase is an important regulation in DNA replication, histone transcription and chromatin condensation; perturbations of any of these processes affect the chromatin integrity and faithful transmission of genetic and epigenetic information to the progeny.

5.2.2 Inhibition of WEE1 as therapeutic option

WEE1 is overexpressed in glioblastoma multiform (GBM) (Mir *et al*, 2010) , luminal and triple-negative breast cancers (TNBC) (Iorns *et al*, 2009; Murrow *et al*, 2010), as well as in malignant melanomas (Magnussen *et al*, 2012). WEE1 overexpression and the resulting decrease in histone levels could lead to inefficient chromatin packaging, making the DNA more accessible to the DNA damage repair machinery and promoting radioresistance (Liang *et al*, 2012). The overexpression of WEE1 in different cancer types could be exploited by using WEE1-specific-small-molecule inhibitors such as AZD-1775 that is used in different clinical trials (Hirai *et al*, 2009). This inhibitory drug (AZD-1775) is able to radiosensitize human lung, breast, skin, brain and prostate cancer cells to DNA-damaging agents, and WEE1 inhibitors were shown synergize with CHK1 inhibitors to induce cytotoxicity (Aarts *et al*, 2012; Sarcar *et al*, 2011).

6. SYNTHETIC LETHALITY

Many of the defects that transform normal cells into malignant consist of mutations in key classes of genes that are responsible for the reproduction, or growth, of cells with a final disruption of the functions that control cell division.

The defects targeted by molecular therapy are found in three classes of genes.

The first class, known as *oncogenes*, stimulates cell progression through the cell cycle. Members of the second class are *tumor suppressor genes*. Genes in the third group govern the *replication and repair of DNA*.

Most tumors possess mutations in one or more of these gene categories.

In particular the third class of genes are those that help to check and maintain the integrity of DNA, which is often damaged during replication. Without these mechanisms, the chances that a damaged gene will be repaired fall drastically, and the likelihood rises that the damage will ultimately be transmitted to the cell's progeny as a permanent mutation. Indeed, tumor cells frequently have defects in their DNA repair processes. Starting from these observations, oncologists are designing drug-screening assays to identify agents that inhibit checkpoint proteins. These agents could be useful, for example, to attack tumor cells possessing a known defect in a checkpoint gene. Nonetheless the standard chemotherapies that exploit the ability to kill rapidly dividing cells, unfortunately are frequently toxic for the rapidly dividing normal cells.

With many such defects, the cancerous cells should readily die or at least succumb easily to other treatments.

One anticancer drug discovery strategy that shows great promise in specifically targeting cancer cells that possess genetic mutations that are not present in normal cells is the exploitation of synthetic lethality (Hartwell *et al*, 1997; Kaelin, 2005; Kaelin, 2009; Kroll *et al*, 1996).This concept is based on the interaction of two genes that both contribute, often nonlinearly, to an essential process or processes (Guarente, 1993). When either gene is mutated alone, the cell is viable (FIG. 18a); however, the combination of mutations in both of these genes results in lethality (FIG. 18b).

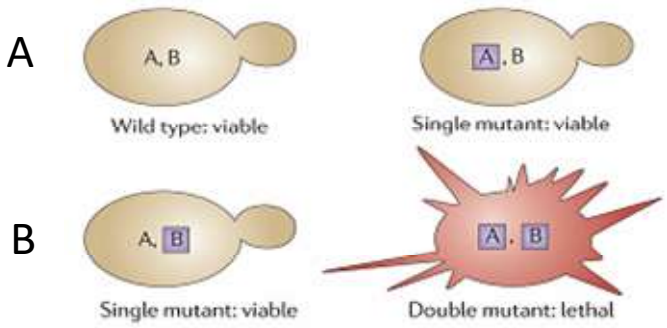

Figure 18 A and B: the graphic representation of the synthetic lethality's concept. Cells with a mutation in one of the vital gene (B gene) will survive; the induction of mutation (or inhibition) of gene A in a cell with gene B mutated induced the formation of a double mutant that results in the die of the cell.

Picture from: Chan & Giaccia, 2011.

This process is referred to as synthetic lethality because cells with both gene mutations are not viable, and so it is not possible to directly isolate such cells. Nevertheless, various approaches can be used to evaluate and target potential synthetic lethal interactions. The interactions revealed by synthetic lethality studies can indicate a range of both predicted and unexpected connections. In the most conceptually straightforward scenario, two parallel pathways both contribute to an essential process. Consequently, disruption of a gene in one pathway is non-lethal, as the alternative pathway can sufficiently maintain the essential process, whereas disruption of both pathways is lethal to the cell.

Other associations may include two divergent pathways that are both needed for a response to a cellular insult, or a pathway that is only connected to another pathway as a result of a gain-of-function oncogenic mutation. High-throughput screening may prove to be particularly useful in identifying these more complex, unpredictable interactions.

The technological advances have made it possible to screen for genes involved in synthetic lethal interactions in a mammalian setting (figure 19).

Notably, the advent of libraries of either siRNAs or short hairpin RNAs (shRNAs), as well as combinatorial and diversity-oriented libraries of small molecules, enables genome-wide investigation of specific mutations in a rapid manner in mammalian cells.

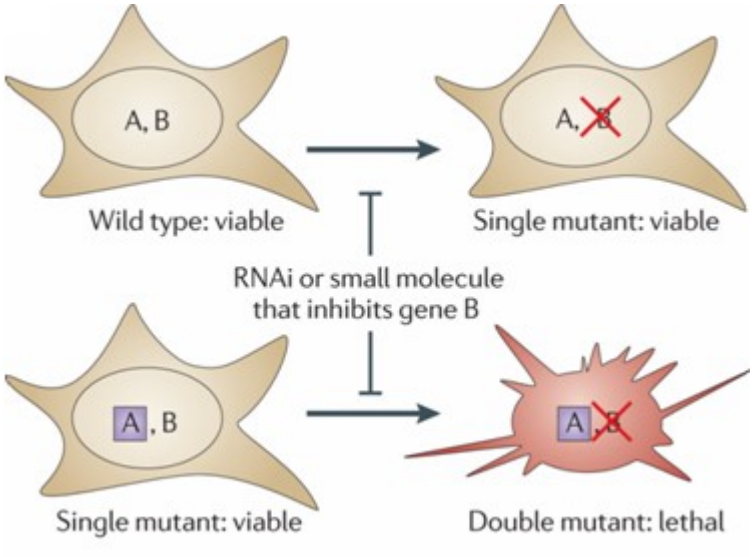

Figure 19: Mammalian synthetic lethality screens for anticancer efficacy.

Picture from: Chan & Giaccia, 2011.

One approach for RNAi-based genome-wide screening requires a reverse transfection step, in which cells are plated onto pre-seeded plates containing the RNAi library along with a transfection reagent. Following incubation to allow for expression, the cells are then assayed for changes in viability.

6.1 siRNA and esiRNA theory for the development of libraries

The small interfering RNA (siRNA), sometimes known as short interfering RNA or silencing RNA, is a class of double-stranded RNA molecules, 20-25 base pairs in length with 2-nt at 3' overhangs. siRNAs play many roles but the most important is the ability to function in the RNA interference (RNAi) pathway, where they interfere with the expression of specific genes with complementary nucleotide sequence. They are naturally produced as part of the RNA interference (RNAi) pathway by the enzyme Dicer. They can also be exogenously (artificially) introduced by investigators to bring about the knockdown of a particular gene.

RNA interference (RNAi) is a biological process in which RNA molecules inhibit gene expression, typically by causing the destruction of specific mRNA molecules.

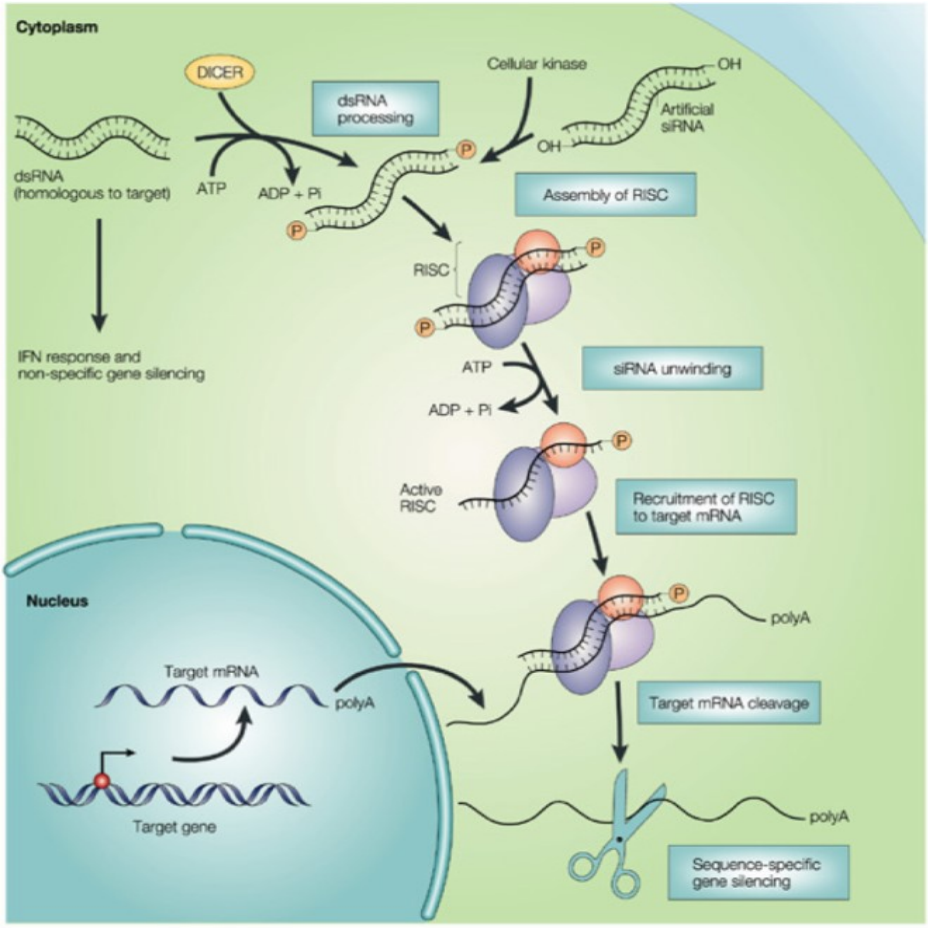

Figure 20: Long double-stranded (dsRNA) is cleaved by DICER — a conserved RNase III protein into RNA duplexes of 21–23 nucleotides that contain two unpaired nucleotides at the 3' end of each strand. This reaction has been documented mainly in lower eukaryotic systems. In higher eukaryotes, dsRNA promotes non-specific inhibition of gene expression through the activation of the interferon (IFN) response. Artificial small interfering RNAs (siRNAs) are converted into functional siRNAs that have 5' phosphate groups by a cellular kinase. These artificial siRNAs obviate the need for processing of siRNAs from long dsRNA, thereby, allowing activation of RNAi without concomitant activation of the IFN response. siRNAs assemble with cellular proteins to form an RNA-induced silencing complex (RISC), which contains a helicase that unwinds the duplex siRNA and a ribonuclease that cleaves target sequences. The RISC is directed by the antisense strand of the unwound siRNA, through sequence complementarity, to the target messenger RNA, which is subsequently cleaved. Micro-RNAs (miRNAs) and small temporal RNAs (stRNAs) are genomically encoded as ~70 nucleotide stem-loop RNA precursors, which are then processed by DICER to single-stranded 21 nucleotide forms. The mature stRNA or miRNA binds to mismatched target sequences, and in this case, translational repression, rather than degradation of the target mRNA occurs. ***Picture from: Stevenson, 2003.***

The RNAi pathway is found in many eukaryotes and it is initiated by the enzyme Dicer, which cleaves long double-stranded RNA(dsRNA) molecules into short double stranded fragments of ~20 nucleotides that are called siRNAs. Each siRNA is unwound into two single-stranded (ss) ssRNAs, namely the passenger strand and the guide strand (Figure 21).

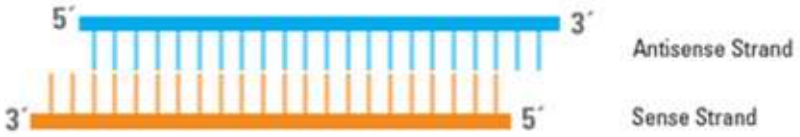

Figure 21: Schematic diagram of a duplex siRNA with two RNA strands that form a duplex 21 bp long with 3' dinucleotide overhangs on each strand. The antisense strand (or guide strand, blue) is a perfect reverse complement of the intended target mRNA. The sense strand is also called "passenger strand" (orange).

Picture from website: *http://dharmacon.gelifesciences.com/applications/rna-interference/sirna/*

The passenger strand is degraded while the guide strand is incorporated into the RNA-induced silencing complex (RISC).

The most well-studied outcome of this pathway is post-transcriptional gene silencing, which occurs when the guide strand base pairs with a complementary sequence in a messenger RNA molecule and induces cleavage by Argonaute, the catalytic component of the RISC complex.

esiRNA or Endoribonuclease-prepared siRNAs are pools of siRNAs resulting from the cleavage of long double-stranded RNA (dsRNA) by the *Escherichia coli* RNase III. The template for *in vitro* transcription is generated by PCR amplification of the cDNA from the clone using primers specific for the vector backbone or target-specific primers appended with RNA-Polymerase promoter sequences. The PCR product is sequence verified and the amplified region is selected based on the highest possible number of highly effective siRNA based on the "DEQOR" siRNA design program. esiRNAs are designed to cover all known transcript variants of the target gene.

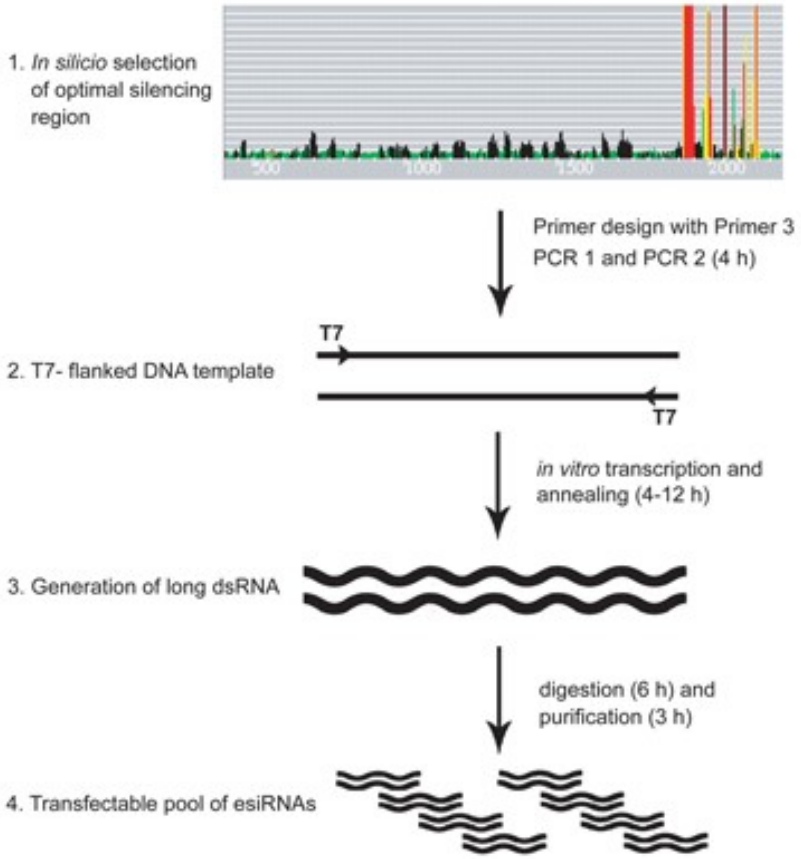

Figure 22: the experimental design used for the esiRNAs synthesis.

Picture adapted from "Sigma Aldrich" explanation.

6.2 siRNA and esiRNA libraries

RNA interference is the mechanism whereby introduction of dsRNA (double strand RNA) into a cell results in the degradation of a mRNA product that is highly complementary with the dsRNA. Since its discovery, advances in the generation of tools that mediate RNAi have resulted in an extensive set of genome-wide RNAi libraries (Iorns *et al*, 2007). These libraries can be divided into two major classes: synthetic siRNA and vector-based shRNA libraries. The siRNA libraries can be subdivided into those derived from algorithm-driven design and chemical synthesis, and those which are enzymatically generated by RNaseIII digestion of dsRNA fragments of approximately 500 bp (endoribonuclease-prepared siRNAs). The wide availability and ease of use of synthetic siRNAs have led to their extensive application in many studies (Mullenders & Bernards, 2009).

Although knockdown efficiency of siRNAs is high, it is transient, restricting the use of siRNAs to short-term experiments. In addition, testing siRNAs across multiple cell lines can be challenging, as it may require optimization of transfection conditions for every individual cell line.

In the phenomenon of drug resistance, in most cases, the factors that contribute to this phenomenon are not known and RNAi screens can be useful to identify genes that modulate drug responses.

The siRNA libraries could be used to screen important component in tumor progression (as the kinase and phosphatase component) of the human genome, in order to detect the target that have a key role for the cell survival. The development of inhibitors directed against these genes may lead to a new anti-cancer strategy (MacKeigan *et al*, 2005).

Another way to find modulators of drug responses is to search for genes whose suppression enhances the response to a given cancer drug. This is in fact a variation on the theme of synthetic lethality and is also referred to as '*chemical synthetic lethality'*. To find factors that can potentiate the effects of a drug, the screen should be performed in presence of a low concentration of the drug, which causes only a small decrease of cell viability.

In this way genes that significantly enhance loss of cell viability can be identified.

Similar screens have been performed aiming at the identification of sensitizers of the well-known anticancer drugs gemcitabine, cisplatin and paclitaxel (Bartz *et al*, 2006; Giroux *et al*, 2006; Ji *et al*, 2007; Swanton *et al*, 2007; Whitehurst *et al*, 2007).

7. TRABECTEDIN (Ecteinascidin-743 or Yondelis®)

Figure 23: A picture of Ecteinascidia Turbinata. ***Picture adapted from "PharmaMar website".***

In the continuous search of new effective compounds useful for the anticancer therapy, the nature represents a vast source. Over 60% of the currently approved drugs for the treatment of cancer derived from natural sources like plants (taxanes as paclitaxel and docetaxel) and microbe-derived agents (bleomycin and doxorubicin). In the last years the interest for the compounds deriving from the sea has increased (Cragg *et al*, 1997; D'Incalci, 1998; da Rocha *et al*, 2001; Schwartsmann *et al*, 2001). Due to the advance in diving techniques and deep-sea sample collection, the marine ecosystem became an accessible source for new chemical classes. The advanced techniques developed provide a means for the production of these potential anticancer agents on a larger scale, with a consequent facilitation of its development.

Trabectedin is an *ecteinascidia turbinata* that grows preferentially on mangrove roots in the Carribean sea. The potent cytotoxicicty of its extracts was first discovered in the late 1960s and the purification of active compounds was not established until 1986.

Trabectedin (or Yondelis) was one of the selected compounds (isolated from the sea) for further development as an anticancer agent, based on its promising cytotoxic activity: the positive therapeutic index and activity in resistant solid tumors as well as sarcomas and pretreated ovarian cancer (Demetri *et al*, 2009; Monk *et al*, 2012b).

Trabectedin is an antineoplastic agent originally isolated from a *Caribbean tunicate*, currently produced synthetically. This compound is clinically used for the treatments of advanced soft tissue sarcoma and platinum-sensitive ovarian cancer patients. The compound was approved by the **E**uropean **M**edicines **A**gency (EMA) in 2007 in monotherapy (1.5mg/m^2 as a 24h-infusion every 3 weeks) for the treatment of adult patients with advanced soft tissue sarcoma, after failure of anthracyclines and ifosfamide-based regimens, or who are unsuited to receive these agents.

In 2009 EMA approved the use of trabectedin for the treatment of ovarian cancer patients, who have relapsed after 6 months from Platinum-based therapy in combination with pegylated liposomal doxorubicin. The U.S. **F**ood and **D**rug **A**dministration (FDA) approved the administration of trabectedin for the treatment of specific soft tissue sarcomas (STS) – liposarcoma and leiomyosarcoma – that cannot be removed by surgery (unresectable) or in advanced metastatic stage (October 2015).

Trabectedin is an alkylating agent that, differently from the other agents belonging to this category, covalently binds the minor groove of DNA inducing a cascade of several interactions like: inhibition of gene activation by a promoter-specific mechanism, inhibition of transcription-dependent nucleotide-excision repair (NER) by trapping proteins responsible for NER, thereby driving cells to undergo apoptosis.

Trabectedin is not just a simple DNA binder but a drug with a more complex mechanism that affects key processes in tumor cells as well as tumor microenvironment (Galmarini *et al*, 2014).

The antitumor efficacy of trabectedin derived from its different mechanisms of action that nowadays are not completely understood.

7.1 Trabectedin: chemical structure

Trabectedin is characterized by a pentacyclic skeleton of two fused tetrahydroisoquinoline rings (A and B), linked to a 10-member lactone bridge through a benzylic sulfide linkage and attached through a spiroring to an additional ring system made up of a tetrahydroisoquinoline (subunit C). Differently from the traditional alkylating agents that bind guanine in N7 or O6 position, in the major groove of DNA, trabectedin binds the N2 amino group of guanines in the minor groove of DNA. The binding of trabectedin to N2 guanine induces the formation of an iminium intermediate, generated in situ by dehydration of the carbinolamine moiety present in the ring A. The fact that the carbinolamine moiety is essential for the pharmacological activity of trabectedin is that the absence of this group in the derivative ET-745 induces a reduction of 100 times in the activity of the drug.

The resulting adduct is stabilized through Van der Waals interactions and one or more hydrogen bonds between ring A and B, with neighboring nucleotides in the same or opposite strand of DNA double helix, creating the equivalent to a functional interstrand crosslink.

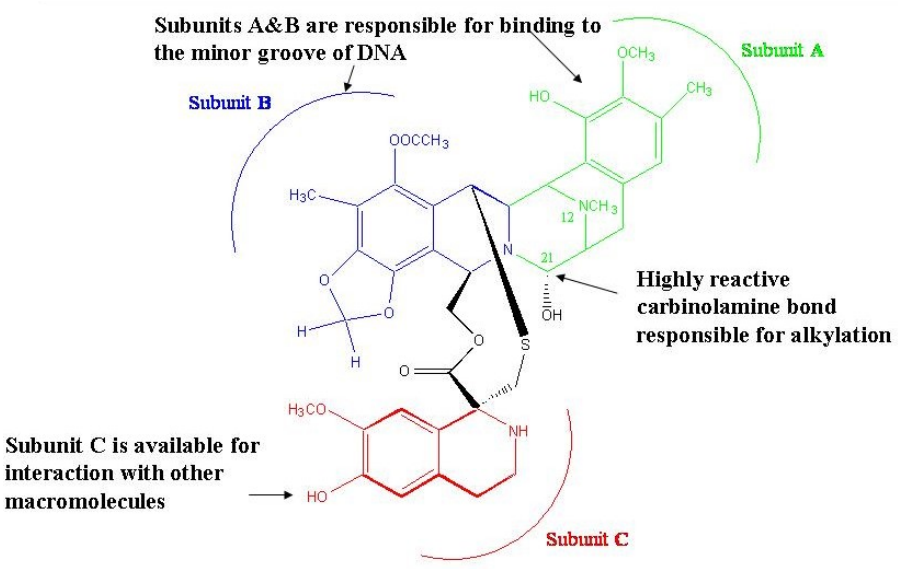

Figure 24: chemical structure of trabectedin; the three subunits are represented.

Picture adapted from: www-chemdrug.com

The chemical structure of trabectedin is characterized by three chemical moiety subunits named A, B and C important for the functional activity of the drug. Subunits A and B are important for the binding to DNA; the carbinolamine group in the subunit A alkylate DNA causing crosslinks that finally induced cell death. Subunit C apparently does not participate in DNA binding but protrudes out of DNA and interacts with DNA binding proteins, such as transcription factors or DNA repair proteins (Bonfanti *et al*, 1999). Trabectedin binds covalently to the exocyclic 2-amino group of a central guanine in certain triplet sequences of double-stranded DNA (dsDNA). The resulting adducts are additionally stabilized through the establishment of van der Waals interactions, and one or more hydrogen bonds with the sugar- phosphate backbone and other nucleobases in both the strand containing the adduct and the opposite strand of the same duplex (Feuerhahn *et al*, 2011; Zewail-Foote & Hurley, 1999). The triplets TGG, CGG, AGC and GGC provide an optimal arrangement of hydrogen-bonding donor / acceptor atoms on both DNA strands that is believed to properly orentiate the drug in the minor groove and catalyze dehydration of the carbinolamine and generation of the reactive iminium intermediate (Marco *et al*, 2006).

By linking the two complementary strands of the double helix, DNA strand separation is hampered regardless of which strand bears the lesion, and RNA Pol II is arrested during transcription elongation. The drug induced lesions, for the mechanism described above, has been suggested to functionally mimic an interstrand crosslink (ICL) (a type of DNA damage that blocks transcription).

Some important characteristics differentiate trabectedin from other minor groove monoalkylating agents: a unique ability to bend DNA towards the major groove by alkylating the minor groove, duplex stabilization and extrahelical protrusion of the C-subunit (Zewail-Foote & Hurley, 1999).

The alkylation reaction is not random but DNA sequence specific (5'-PuGC, 5'-PyGG) (Pommier *et al*, 1995).

The minor groove alkylation (caused by trabectedin) causes an interference in the DNA-topoisomerase I cleavage sites. At high concentration (micromolar levels) trabectedin causes a topoisomerase I-induced formation of cleavage complexes (enzyme-linked and –mediated DNA strand breaks) which are the catalytic intermediates of topoisomerization reactions.

The mechanism of alkylation induced by trabectedin is represented in figure 25.

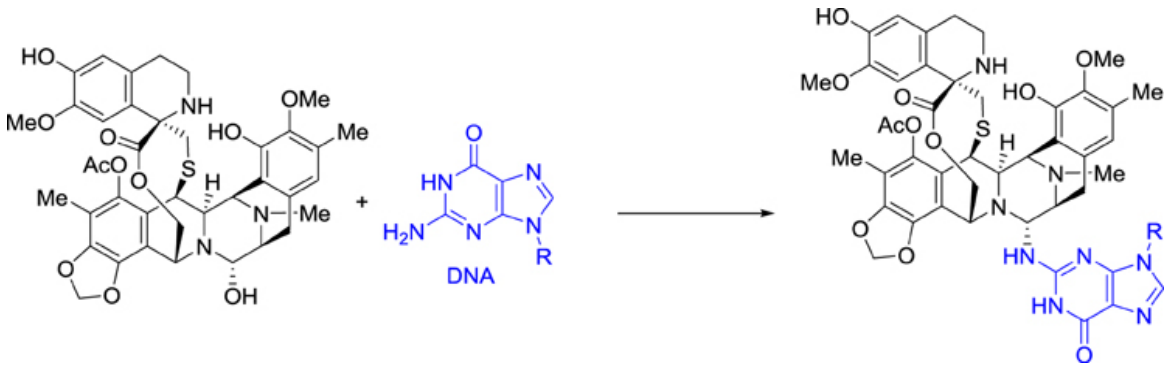

Figure 25: DNA Alkylation by trabectedin.

Picture from Christine Basmadjian et al, Front. Chem., 01 May 2014; https://doi.org/10.3389/fchem.2014.00020.

7.2 Trabectedin metabolism

Trabectedin biotransformation at the microsomal level is mainly due to CYP3A4, 2C9, 2C19, 2D6 and, to a minor extent, 2E1 (Brandon *et al*, 2006). These data have been confirmed *in vitro* by the increased cytotoxicity of trabectedin (measured as IC50 decrease) observed in a HepG2 cell line after incubation with CYP inhibitors (Beumer *et al*, 2005). Since CYP3A4 has an important role in trabectedin metabolism, the risk of *in vivo* drug–drug interactions must be considered when the agent is combined with other CYP3A4 substrates.

Given the complexities of trabectedin metabolism, it is unlikely that a single polymorphism or the inhibition of a single metabolic pathway can change its metabolic profile.

7.3 Trabectedin toxicities

The liver is a key organ not only for trabectedin metabolism but also for its collateral effects.

- Preclinical studies in animals demonstrated liver toxicity as an important side effect of trabectedin. Repeated treatment cycles were able to increase the extent of clinical chemistry changes, suggesting cumulative toxicity. Interestingly advanced sarcoma patients receiving dexamethasone before starting trabectedin administration shown a lower liver and bone marrow toxicities than patients not receiving dexamethasone, even though any relationship between the two toxicities remains to be elucidated (Grosso *et al*, 2006).
- Several case reports described another rare toxicity of trabectedin treatment: rhabdomyolysis. Rhabdomyolysis is a syndrome caused by injury to skeletal muscle and involves leakage of large quantities of potentially toxic intracellular contents into plasma. Its final common pathway may be a disturbance in myocyte calcium homeostasis.
- Another important and dose-limiting trabectedin toxicity is represented by myelosuppression. Reversible dose-dependent neutropenia was the most frequently reported toxicity in Phase II studies, observed at approximately 14 days (Villalona-Calero *et al*, 2002). There are different suggestions that trabectedin could have a direct immunomodulatory effect through inhibition of monocytes and macrophages and reduction of production of CCL2 and IL-6 (Allavena *et al*, 2005; Germano *et al*, 2013).

7.4 TRABECTEDIN: DIFFERENT MECHSNISMS OF ACTION

7.4.1 Trabectedin inhibits active transcription and displaces oncogenic transcription factors from their target promoters

Trabectedin interferes directly with activated transcription (Friedman *et al*, 2002; Minuzzo *et al*, 2000), induces a poison of transcription-coupled nucleotide excision repair (TC-NER) system (Damia *et al*, 2001; Herrero *et al*, 2006; Takebayashi *et al*, 2001) and generates double-strand DNA breaks (DSBs) (Soares *et al*, 2007).

Inhibition of active transcription is one of the major effects of trabectedin; only the transcription of activated genes is affected by the drug, not the constitutive transcription (Scotto, 2002).

One of the mechanisms by which trabectedin interferes with the transcriptional regulation is based on the displacement of oncogenic transcription factors that are over-expressed in different tumor types. The most important example of this mechanism, with clinical relevance, is represented by the important antitumor activity of trabectedin in patients with advanced myxoid liposarcoma tumors (MLS). This tumor is characterized by the presence of a chimeric protein (FUS-CHOP) deriving from the chromosomal translocation t(12;16) (q13;p11). Less frequently the translocation could be t(12;22) (q13;q12) with the formation of EWS-CHOP chimera (Sandberg, 2004).

Trabectedin in myxoid liposarcoma patients induces an objective response in approximately 50% of cases and progression free survival exceeding 2 years in 80% (Grosso *et al*, 2007; Le Cesne *et al*, 2012).

The activity of this drug in myxoid liposarcomas is explained also by a regression of the capillary network and reappearance of mature lipoblasts (Gronchi *et al*, 2012).

The particular sensitivity of myxoid liposarcomas to trabectedin treatment could be related to the ability of the drug to block the activity of the chimeric protein FUS-CHOP with a consequent differentiation of the tumor into benign lipoblasts (Di Giandomenico *et al*, 2014; Forni *et al*, 2009; Frapolli *et al*, 2010).

The ability of trabectedin to induce a displacement of the chimeric protein FUS-CHOP from the promoter of its target genes, blocking its transactivating function, with a consequent derepression of the adipocytic differentiation process, was confirmed also in tumor biopsies of patients with MLS and treated with the drug. Di Giandomenico et al. (Di Giandomenico *et al*, 2014) demonstrated also the specificity of trabectedin for the different type of FUS-CHOP chimeric protein.

Myxoid liposarcoma tumors with type I and II are more sensitive to trabectedin treatment than tumors belonging the type III chimera. This major sensitivity seems to be correlated to the ability of trabectedin to detach the chimeric protein from its target promoters and to induce adipogenic differentiation in type I and II while not in type III.

The findings observed in myxoid liposarcomas can be extended in other sarcomas in which specific translocations result in an altered regulation of the expression of transcription factors. A representative example is some responses observed in patients with Ewing sarcoma tumors in which the trabectedin activity can be explained by the detachment of EWS-FLI1 chimera generated by the t(11;22)(q24;q12) chromosomal translocation, from its target promoters. The high sensitivity of Ewing sarcoma cell lines to trabectedin treatment is associated with a direct and specific inhibitory effect of the drug on the aberrant transcriptional activity of this oncogenic chimera, thereby reversing the gene signature of induced downstream targets of EWS-FLI1 and inducing apoptosis (Grohar *et al*, 2011).

Among the proteins that trabectedin is able to displace from its promoter targets there are also the high mobility group proteins. A study performed by D'Angelo et al. (D'Angelo *et al*, 2013) showed that trabectedin treatment displaces HMGA proteins from the HMGA-responsive promoters, including ATM promoter, impairing their transcriptional activity. These observations might have important clinical implications since it suggests that trabectedin could be potentially used for the treatment of neoplasias expressing abundant HMGA levels, that are frequently associated to chemoresistance and poor prognosis.

7.4.2 The high mobility group proteins: an overview

The high mobility group (HMG) proteins are ubiquitous nuclear proteins that regulate and facilitate various DNA-related activities such as transcription, replication, recombination and repair.

Three different families of HMG proteins were identified and named on the basis of their DNA binding domains and their substrate binding specificity: HMG-AThook families (HMGA), HMG-box families (HMGB) and HMG-nucleosome binding families (HMGN) (Bustin, 2001).

The family of **HMGA proteins**, HMGA1a, HMGA1b and HMGA2, can bind the minor groove of DNA in the AT-rich regions using three domains called "AT hooks" (Reeves & Nissen, 1990).

HMGA1a and HMGA1b, also known as HMG-I and HMG-Y, respectively, are the products of the same gene (*HMGA1*), and they are identical in sequence except for an 11-amino acid internal deletion in HMGA1b due to alternative splicing (Johnson *et al*, 1988; Johnson *et al*, 1989). The HMGA2 protein, encoded by HMGA2 gene, distinguishes from HMGA1a in the first 25 amino-acid residues; HMGA2 contains a short peptide located between the third AT-hook and the acidic tail, which is absent in HMGA1a (Manfioletti *et al*, 1991).

HMGA1 proteins, considered as "hubs" of nuclear function, have been suggested to play roles in regulating gene transcription (more than 40 target genes have been reported), DNA replication, chromatin changes during cell cycle and chromatin remodeling (Reeves, 2003; Reeves & Beckerbauer, 2001). HMGA proteins are expressed abundantly in embryonic, rapidly proliferating, and tumor cells, but they are absent or expressed at very low levels in normal, differentiated cells (Bandiera *et al*, 1998; Sgarra *et al*, 2004). Many reports indicate that HMGA proteins are oncogenic and contribute to many common diseases, including benign and malignant tumors (Sgarra *et al*, 2004), obesity (Anand & Chada, 2000), diabetes (Foti *et al*, 2005) and atherosclerosis (Schlueter *et al*, 2005).

The **HMGB proteins** (HMGB1, HMGB2 and HMGB3) are encoded by *HMGB1*, *HMGB2* and *HMGB3* genes (Stros *et al*, 2007).

They were found to be abundant non histone DNA-binding proteins and their name originate from their (anomalous) high electrophoretic mobility in triton-urea gels (High Mobility Group, HMG), due to a high content of positively and negatively charged amino acid residues explaining their extractability in diluted solutions of acids (Goodwin & Johns, 1973). HMGB1 protein exhibits not only high mobility in polyacrylamide gels, but also in the nucleus being the most mobile and dynamic nuclear protein (Scaffidi *et al*, 2002). These proteins are characterized by the presence of HMG boxes which can bind to the minor groove of DNA with limited or no sequence specificity both in vitro and in vivo (Read *et al*, 1993; Weir *et al*, 1993) producing a strong bend in DNA backbone. In general, HMGB binds preferentially to distorted DNA structure, such as four-way junctions (Bianchi *et al*, 1989), cisplatin- and UV-damaged DNA (Hughes *et al*, 1992; Pil & Lippard, 1992). HMGB1 is present in the serum of patients affected by mesothelioma and represents an important biomarker for this tumor. Other tumor cells, such as erythroleukemia, neuroblastoma, and colon cancer cells, have also been shown to secrete HMGB1 (Passalacqua *et al*, 1997; Wahamaa *et al*, 2007).

Once extracellular, HMGB1 triggers inflammation (Schiraldi *et al*, 2012) and when secreted by tumor cells promotes their proliferation, migration, invasion, and neoangiogenesis (Sparatore *et al*, 2005; van Beijnum *et al*, 2006). Inhibitors of HMGB1 are important in the impairment of the anchorage-independent growth of mesothelioma cells, a hallmark of malignant transformation (Hanahan & Weinberg, 2011). Several studies are in progress in order to identify inhibitors exploitable in the clinic.

The **HMGN family**, which binds specifically to the 147-base pair nucleosome core particle, consists of four closely related proteins with a molecular weight of ~10 kDa: HMGN1 (previously known as HMG-14), HMGN2 (previously known as HMG-17), HMGN3 (previously known as Trip-7) as well as the recently identified member of HMGN4 (Birger *et al*, 2001).

7.5 Trabectedin: DNA repair mechanisms and cell cycle

Several studies conducted on cell lines with DNA repair mechanism defects suggest a role of TC-NER and homologous recombination (HR) DNA repair mechanisms in the antitumor activity of trabectedin. The evaluation of the antiproliferative activity of trabectedin in CHO (Chinese Hamster Ovary) cell lines proficient or deficient in nucleotide excision repair (NER), showed that this drug is approximately 7-8 times less active in XPG and ERCC1 deficient cells than in the control one (Erba *et al*, 2001). The sensitivity to trabectedin of cells TC-NER deficient is an unusual observation that has not been reported before for other anticancer agents.

The levels of trabectedin-induced DNA double strand breaks are less for XPG deficient cells than for XPG proficient human cells. Moreover, in contrast to proficient cells, CHO-NER-deficient cells do not suffer the post-replication G2 arrest induced by trabectedin, indicating that the G2 checkpoint is not activated (Tavecchio *et al*, 2007). It has also been demonstrated that homologous recombination (HR) is particularly relevant for trabectedin; the lack of HR was associated with the persistence of unrepaired DSBs during the S phase of the cell cycle accompanied by apoptosis (Soares *et al*, 2007; Tavecchio *et al*, 2008). This particular sensitivity has been confirmed in the clinic; in fact the drug is highly active in patients with recurrent ovarian cancer carrying the BRCA1 mutation (Monk *et al*, 2015).

NER proteins are involved in repairing the DNA damage caused by many DNA binding drugs commonly used in cancer treatment, such as nitrogen mustard, cisplatin, or mitomycin C (Beljanski *et al*, 2004). As a consequence, defects in the NER repair system usually increase drug sensitivity. This is not what happens after trabectedin treatment; the sensitivity to the drug is decreased in NER deficient cells (Colmegna *et al*, 2015; Erba *et al*, 2001; Takebayashi *et al*, 2001). It is thought that DNA-bound trabectedin prevents the correction of DNA lesions by TC-NER mechanism, creating cytotoxic ternary complexes with DNA-binding proteins of the NER system, such as XPG (Damia *et al*, 2001; Erba *et al*, 2001).

Several reports highlighted that the cell-killing ability of trabectedin is linked to the transcription-coupled NER (TC-NER) (David-Cordonnier *et al*, 2005; Herrero *et al*, 2006; Takebayashi *et al*, 2001). The DNA bending induced by the binding of trabectedin to the minor groove is detected by the TC-NER machinery which in the repair process makes single strand breaks (SSBs) on each side of the lesion (David-Cordonnier *et al*, 2005). These breaks are then made irreversible by the DNA-protein crosslinking abilities of trabectedin (Takebayashi *et al*, 2001)

Herrero et al. (Herrero *et al*, 2006) suggested a slightly different model based on their observations made in the yeast model *Schizosaccharomyces pombe*. In this model, cells deficient for Rad13 (the yeast equivalent to the human XPG, which is an endonuclease of the NER system), were resistant to trabectedin, while those with an inactive Rad51 (a protein of the homologous recombination repair (HR) pathway, involved in the repair of double stand breaks) were more sensitive to trabectedin than the wild-type cells.

A further evidence of the involvement of NER pathway in trabectedin response is shown in the study performed by Colmegna et al.(Colmegna *et al*, 2015). They demonstrated that the development of an ovarian cancer cell line resistant to trabectedin, is associated with the loss of XPG protein.

Soares et al. showed that human cell lines deficient for the HR proteins XRCC3, BRCA2, RAD51C and XRCC2 were 8 to 23 times more sensitive to treatment with trabectedin (Soares *et al*, 2007). Furthermore, their data showed that trabectedin-DNA adducts induce the formation of highly cytotoxic double strand breaks during the S-phase of the cell cycle (Soares *et al*, 2007), thereby confirming, the scenario suggested by Herrero (Herrero *et al*, 2006).

The adducts created by trabectedin functionally mimic a typical interstrand crosslink (ICL); despite the fact that this drug binds covalently to only one DNA strand, its interaction with the opposite strand is mediated through Van der Waals contacts and hydrogen bonds (Feuerhahn *et al*, 2011).

Different footprinting assays demonstrated that the drug protect the high-affinity CGG sequence, as well as the complementary triplet in the opposite strand, from DNase I digestion. The binding of trabectedin to a particular sequence triplets, located within certain responsive elements of the promoter of a given gene, might prevent the formation of the transcription complex. During the elongation phase of transcription, the transcribing RNA polymerase II (Pol II) can collide directly with trabectedin, preventing further movements of Pol II along the DNA template and causing the premature ending of the RNA transcript. The transcription arrest caused by the treatment is solved by ubiquitination of Pol II and degradation by proteasome machinery (Svejstrup, 2007). All the data produced in the studies of characterization of trabectedin's mechanism of action, clearly highlighted the important role played by the mechanism of DNA repair NER in the activity of the drug.

Like many other different DNA-interacting drugs, trabectedin causes strong perturbations of the cell cycle with a delay of cells progressing from G1 to G2, an inhibition of DNA synthesis and a marked blockade in G2M phase, which does not appear to be p53-dependent, as it could be observed in both cells expressing or not a functional p53. A peculiarity of trabectedin is its strong activity in cells in the G_1 phase of cell cycle (Erba *et al*, 2001). Independently from the NER status of the cells, the G_1 phase seems to represent an important checkpoint for trabectedin's activity: cells treated in G_1 phase were affected in crossing this cell cycle phase, and cells treated in S-late or G_2/M phases were perturbed when they reached G1 phase. Behaviour of S-early cells, which had just started to synthesize DNA, appears very similar to that of G_1 cells (Tavecchio *et al*, 2007).

The resistance to trabectedin of cells deficient in NER pathway is associated with differences in the cell response to DNA damage, inducing different cell cycle perturbations.

Normally, when the DNA is damaged, different cell cycle checkpoints are activated to cause a transient arrest (mainly in G1 or G2/M phase) of cell cycle that allows the cells to repair the damage and restore its integrity before moving on S phase or mitosis.

This is a very important mechanism used to protect cells from synthesizing DNA or undergoing cell divisions when there is still a damage in the genome.

The studies performed on the perturbations induced by trabectedin, highlighted that when cells are exposed to this drug the mechanism of cell cycle blocking is more complex. The cells that were exposed to trabectedin appear to be able to overcome blocks in progression through the cell cycle, even when damage is not completely repaired.

7.6 Effects of trabectedin on tumor microenvironment

The tumor microenvironment (TME) is populated by different non-neoplastic cells like inflammatory leukocytes, activated fibroblasts and endothelial cells.

Physiologically, the stroma in healthy individuals is a physical barrier against tumorigenesis; however, neoplastic cells elicit various changes to convert the adjacent TME into a pathological entity.

The structurally and functionally essential elements in the stroma of a typical TME includes fibroblasts, myofibroblasts, neuroendocrine cells, adipose cells, immune and inflammatory cells, the blood and lymphatic vascular networks, and the extracellular matrix (ECM). The naive stroma is a critical compartment in maintaining physiological homeostasis of normal tissue, and recent studies strengthened the concept that some stromal components have anticancer activities by regulating immunosuppression and restraining carcinogenesis, which is particularly the case of pancreatic ductal adenocarcinoma (Ozdemir *et al*, 2014). The ability of the stroma to suppress carcinogenesis apparently correlates with organismal survival and contribute to longevity. However, once transformed to a tumor-associated neighbor by various stimuli, the stroma-derived effect turns to be adverse and can significantly promote cancer progression.

It has been estimated that up to 20% of all tumors arise from conditions of persistent inflammation due to chronic infections or other causes (Balkwill & Mantovani, 2001). The prominent role of inflammatory mediators has been shown in several studies.

For example in mouse models of skin carcinogenesis, deletion of selected proinflammatory cytokines reduced tumor susceptibility (Moore *et al*, 1999). In addition the activation of the transcription factor nuclear factor kB (NFκB) has been implicated in the formation and progression of inflammation-associated tumors (Balkwill & Coussens, 2004).

Macrophages infiltrating the tumor tissue, or tumor-associated macrophages (TAM), constitute a peculiar macrophage population. The role of TAMs in the tumor microenvironment and tumor development is complex and multifaceted. Macrophages activated by bacterial products and Th1 cytokines (e.g., lipopolysaccharide and IFN-γ) are regarded as M1 or classically activated macrophages, with high bactericidal activity and cytotoxic function against tumor cells. Macrophages activated by Th2 cytokines [e.g., interleukin (IL)-4 and IL-13] or immunosuppressors (e.g., corticosteroids, vitamin D_3, and IL-10) are defined as M2 macrophages, with low cytotoxic functions but high tissue-remodeling activity. M1 cells have immunostimulatory properties and defend the host against pathogenic infections, M2 cells attenuate the acute inflammatory reaction, potently scavenge cellular debris, and secrete a variety of growth and angiogenic factors essential to repair the injured tissues. When their activation (especially that of M1 macrophages) persists over time, pathologic conditions and tissue injury may occur.

Trabectedin treatment induced a reduction of inflammatory mediators (in *in vitro* and *in vivo* models). In a myxoid liposarcoma model the inhibition of CXCL8 and CCL2 with a partial reduction of PTX3 was observed (Germano *et al*, 2010). The macrophage-derived product CCL2 is a chemoattractant for monocytes and lymphocytes and is produced both by mononuclear phagocytes and by tumor cells. In ovarian and pancreatic carcinomas, serum levels of CCL2 significantly correlate with the macrophage content of tumors (Monti *et al*, 2003; Negus *et al*, 1995); thus, CCL2 is a major determinant of the monocyte recruitment within the tumor tissue. Trabectedin significantly inhibits the production of selected pro-inflammatory cytokines such as CCL2, IL-6 CXCL8, VEGF and PTX3.

Downregulation of key inflammatory molecules in the tumor microenvironment might be important to sustain the increasingly clear relationship between persistent inflammation and cancer progression (Allavena *et al*, 2005).

7.7 Preclinical and Clinical evidences

The first preclinical evidence of trabectedin antitumor activity was demonstrated in human tumors explanted from patients (Izbicka *et al*, 1998), ovarian carcinoma (Hendriks *et al*, 1999; Valoti *et al*, 1998), melanoma and non-small-cell lung cancer xenografts (Valoti *et al*, 1998). A gene expression profile analysis in human STS cell lines, explanted from chemonaive patients revealed that trabectedin treatment induced the upregulation of 86 genes and downregulation of 244 genes, suggesting an important impact of the drug in tumor cell biology (Martinez *et al*, 2005). Trabectedin promotes differentiation in myxoid liposarcoma tumors by detachment of the pathogenic FUS-CHOP chimeric protein from its target promoters (Di Giandomenico *et al*, 2014; Forni *et al*, 2009).

Another important and peculiar aspect of trabectedin is the showed “sequence-dependent synergistic cytotoxicity” with paclitaxel (administered before trabectedin) in human breast cancer cell lines *in vitro* and *in vivo* (Takahashi *et al*, 2002). This synergistic activity was also shown in STS cells; in this model the synergism was evidenced not only with paclitaxel (administered before trabectedin) but also with doxorubicin (administered after trabectedin) (Takahashi *et al*, 2001).

Conversely the combination of cisplatin with trabectedin was observed to be additive or additive-to-synergistic when given simultaneously or trabectedin after cisplatin (D'Incalci *et al*, 2003). The combination of trabectedin and irinotecan is synergic in vivo but additive in vitro, in a rhabdomyosarcoma model (Riccardi *et al*, 2005). Also the combination of trabectedin with doxorubicin seems to be additive in a rhabdomyosarcoma model (Meco *et al*, 2003).

A more recent study showed a potent synergistic combination in vitro and in a xenograft model of Ewing’s sarcoma, administering trabectedin and irinotecan (Grohar *et al*, 2014).

Another important combinatorial effect induced by trabectedin is its radiosensitizing properties. More recent findings showed a significant in vitro radiosensitizing effect and the induction of cell-cycle changes and apoptosis in several human cancer cell lines in the presence of pharmacologically appropriate (nanomolar range) concentrations of the drug (Romero *et al*, 2008).

Following the preclinical studies a large number of clinical trials have been carried out in order to evaluate the in vivo effect of trabectedin. These results suggested that the maximum tolerated dose slightly changes with the stabilized schedule (administration by 24 hours continuous infusion 1 time per week for 3 weeks) and the dose-limiting toxicities are mainly hematological toxicities and asthenia rather than transient transaminase elevation. Trabectedin does not interact with other common chemotherapeutic agents (e.g. doxorubicin, gemcitabine and cisplatin) from a pharmacodynamic / pharmacokinetic point of view. Therefore, combination therapies could be suitable and useful in the management of advanced diseases.

Several Phase II trials have been carried out and are currently ongoing; they revealed that trabectedin seems to be a very promising drug for the treatment of a wide spectrum of tumors; nevertheless the drug failed against gastrointestinal stromal tumors (Taamma *et al*, 2001; van Kesteren *et al*, 2000) and pre-treated advanced colorectal cancer (Puchalski *et al*, 2002). Overall the most promising results have been achieved against soft tissue sarcomas (especially leiomyosarcomas and myxoid liposarcoma) and ovarian cancers. As for trabectedin hepatic effects, plasma liver enzymes level (transaminase, bilirubin, alkalin phosphatases and 5'-nucleotidase) should be checked before each course.

7.8 Combination of trabectedin with other anticancer agents

The ability of trabectedin to modulate the tumor microenvironment and to interfere with the transcriptional activity are two important features that make this drug a good candidate for pharmacological combinations.

The improved understanding of the mechanism of action of anticancer agents could be used to establish the so called “intelligent” drug combinations and, based on its mechanism of action, trabectedin could represent an excellent candidate for this strategy.

An important example in this direction is represented by the recent work published by Grohar et al. that showed the strong synergism obtained combining trabectedin and irinotecan, in Ewing’s sarcoma cells and xenograft models (Grohar *et al*, 2014).

Briefly the rationale of the active combination is that trabectedin blocks the activity of EWS-FLI1 chimeric protein (hallmark of Ewing’s sarcoma), down-regulating the expression of Werner RecQ helicase (WRN), and consequently sensitizing tumor cells to the DNA-damaging effects of irinotecan, which would in turn feedback and increases the suppression of EWS-FLI1 downstream targets.

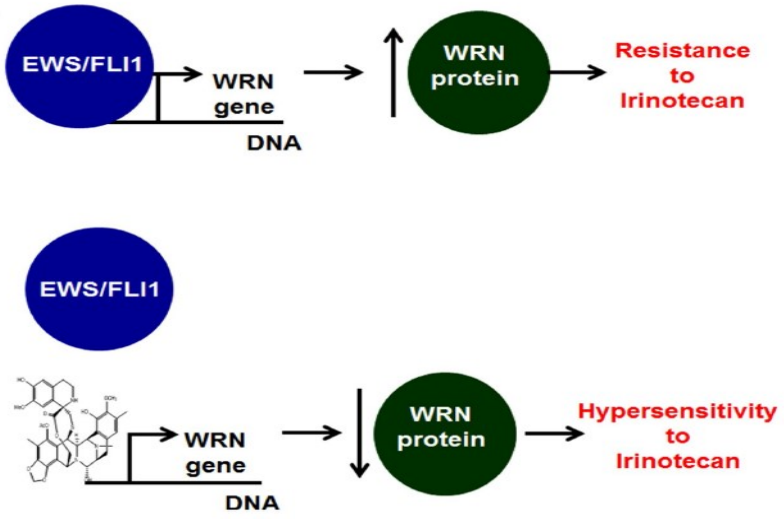

Figure 26: the mechanism of action of trabectedin in Ewing’s sarcoma. The drug interferes with the transcription of the WRN gene; the downregulation of WRN protein enhances the sensitivity to irinotecan treatment.

Picture from: Larsen A.K. et al, “Unique features of trabectedin mechanism of action”, Cancer Chemother Pharmacol, 2016, 77:663–671.

Several in vitro and in vivo experiments showed additive or synergistic effects derived from the combination of trabectedin with doxorubicin. In vitro, concomitant exposure of human sarcoma cells (TE671, HT-1080, HS-18) to trabectedin and doxorubicin produces additive or synergistic effects.

Today the improved understanding of the mechanism of action of anticancer agents could be used to establish what it can be called “intelligent” combinations. According to this idea, it would be possible to develop “molecularly targeted” strategies to increase the therapeutic index of a drug combination in order to achieve the best synergistic effects at the lowest doses, concentrating the pharmacodynamics effect on tumor cells and thus avoiding unnecessary toxicities.

Based on its mechanism of action, trabectedin is excellently suited for this strategy. One example is the strong synergism derived from the combination trabectedin and irinotecan (Grohar *et al*, 2014). Another example is the synergistic activity of combinations of platinum compounds and trabectedin that showed activity in preclinical models as well as in the clinical setting (D'Incalci *et al*, 2003; Sessa *et al*, 2009; Soares *et al*, 2011). The fact that trabectedin is a good drug useful for combination treatments, is probably related to its mechanism of action, particularly to its ability to interfere with the NER machinery, inducing a sensitization of tumor cells to platinum compounds (Soares *et al*, 2011).

Also the peculiar ability of trabectedin to induce cell cycle perturbations in G2/M phase of the cell cycle could be exploitable for combinations with drugs that are able to abrogate the cell cycle checkpoints.

In addition to all these evidences, trabectedin binds the minor groove of DNA, so the possibility that could physically interact with drugs that bind the major groove of DNA is low. This effect could be useful in order to exploit the peculiarity of trabectedin for the combination with a second alkylating agent, avoiding interferences in the “physical” binding to DNA of the second drug.

AIMS of the PROJECT

The general scope of the project was to identify potential new effective combinations of trabectedin with other compounds in a Ewing sarcoma(ES) cellular model.

A first aim was to test the hypothesis that inhibitors of the cell cycle checkpoints could potentiate the activity of trabectedin.
The rationale behind this hypothesis is based on the findings that in ES cells trabectedin-induced DNA damage activates cell cycle checkpoints, and the arrest of the cells in pre-mitotic phase protect them from death.

A second aim was to test the hypothesis that the inhibition of some specific molecular targets is synthetically lethal with low dose trabectedin pretreatment, in ES cells.
The rationale behind this hypothesis is based on the findings that in ES cells trabectedin transiently affects the aberrant transcription program driven by the oncogenic EWS-FLI1 chimera, thus possibly increasing its sensitivity to a second hit. The finding that trabectedin downregulates the Werner (WRN) gene in ES cells lead to the discovery that the sequential treatment of trabectedin and topoisomerase I inhibitors, known to be more effective in cells that do not express WRN gene, is highly synergistic.
The identification of new molecular targets exploitable for this sequential combination approach required the development of a new methodology based on a screening of RNA silencing libraries.

Therefore an important part of the thesis was directed at developing and setting up the methodologies to pursue this approach.

MATERIALS and METHODS

1. DRUGS and CELL CYCLE CHECKPOINTS INHIBITORS

Trabectedin was provided as lyophilized formulation by PharmaMar (S.A. Colmenar Viejo, Spain), dissolved in DMSO at the final concentration of 1mM and stored at -20°C. Just before use the drug was diluted in Iscove's Modified Dulbecco's Medium (IMDM, Biowest) medium supplemented with 10% Fetal Bovine Serume (FBS, Biowest), 1% L-glutamine (2mmol/L, Biowest) and 1% (1000U/ml) penicillin-streptomycin (PS), 10.000 U/ml (Biowest).

Dasatinib (Sigma), PF-477736 (Pfizer) and AZD-1775 (Astra Zeneca) were provided as lyophilized formulation, dissolved in DMSO and stored at -20°C; just before use the drugs were diluted in IMDM (Biowest) supplemented with 10% of FBS (Biowest), 1% L-glutamine (2mmol/L, Biowest) and 1% (1000 U/ml) PS (Biowest).

2. TUMOR CELL LINE

TC71 (Ewing's sarcoma) cell line (p53 null), kindly provided by Dr. Scotlandi (Istituto Ortopedico Rizzoli, Bologna, Italy) was maintained in IMDM supplemented with 10% FBS and 1% L-glutamine (2mmol/L). This cell line derived from the biopsy of a tumor localized in the humerus in a 22 years old male (Whang-Peng *et al*, 1984).

Cultures were grown in a humidified incubator at 37°C with 5% CO2.

All tumour cells were cultured as follow: at set time points, specific growth medium was removed from the flasks and the cellular monolayer was washed twice with 37°C-heated PBS and 1 ml of a trypsin-EDTA solution (Trypsin 0.05% EDTA (1X), GIBCO, Thermo Fisher) was added to each flask. After incubation at 37°C with gentle shaking, cell detachment was checked under the microscope (Olympus CKX41) and trypsin activity was blocked by addition of 10 ml of complete growth medium.

Ten ml-suspension containing detached cells was transferred in a sterile 15 ml conical tube (Eppendorf) and centrifuged at 1200 rpm for 10 minutes at room temperature in a centrifuge (Eppendorf, centrifuge 5810). The pellet was then resuspended in 10 ml of growth medium and a small aliquot (500µl) was transferred in a plastic becker containing 9.5 ml of the PBS solution. The solution was checked and counted using a Cell Counter (Coulter Counter "Multisizer 3", Beckman Coulter).

Frozen stocks of each cell line were prepared as follows. Cells in logarithmic growth phase were detached from the flasks and counted as previously described. After counting, the cell suspension was centrifuged at 1200 rpm for 10 minutes at room temperature. The supernatant was removed and the cell pellet was carefully resuspended in 4°C-cold "freezing medium" composed as follow: medium used for cells growth supplemented with equal volume of FBS and a double volume of "Cryoprotective medium" (Lonza). Cells at a density of 5 x 10^6 viable cells/ml were resuspended in one ml of the "freezing medium", transferred in a 2 ml sterile Nalgene tube (Nalgene Company), placed on ice for 30 minutes and stored at -80°C for the initial freezing step. After 16-24 hrs, frozen cells were removed from the freezing container and stored under liquid nitrogen vapours in the "CRYO"containers (CRYO 200 or CRYO PLUS2, Thermo Electron Corporation, Analytical Service).

For cell thawing, frozen cells were incubated in a 37°C water bath (shaking water bath SBS40, Stuart, Barloworld Scientific), transferred into a sterile 15 ml conical tube containing 10 ml of complete growth medium and centrifuged at 800 rpm for 10 minutes at room temperature. The cell pellet was then resuspended in 5 ml of growth medium and cells were seeded in a T25cm^2 flask.

3. CELL CYCLE and GROWTH INHIBITION

Cell cycle perturbations induced by trabectedin and AZD-1775 were evaluated by standard flow cytometric methods (Erba *et al*, 2001).

Briefly cells in the logarithmic growth phase were seed in 6 wells/plate, in 2 ml of fresh media containing 10% FBS, 1% L-glutamine and 1% PS. The cellular density is function of the cell line considered. 48hrs after the seed, exponentially growing cells were treated for 1h with different doses of the analyzed drug and the medium was replaced with new free-drug medium (medium addition of FBS, glutamine and PS). 24 - 48 and 72 hours after treatment, cells were detached from the plate, counted by coulter counter (Beckman Coulter), centrifuged at 1200rpm for 10 minutes and fixed for the cell cycle analysis.

At any time point the cells were counted in order to evaluate the cytotoxic effect of the drugs (defining the growth inhibition) and define the quantitative of fixing solution to use (1ml for $2*10^6$cells).

During this step it was very important the use of polypropylene 15ml falcons for the recovering of the cells; this material is important to avoid the adhesion (with consequent loss) of the cells to the walls.

FIXING SOLUTION

1part of saline GM solution and 3 parts of ethanol 100%.

SALINE GM SOLUTION

GLUCOSE	1.1g/l
NaCl	8 g/l
KCl	0.4g/l
$Na_2HPO_4.2H_2O$	0.2g/l
KH_2PO_4	0.15g/l
EDTA	0.2g/l (0.5mM)

During this step it was important to add the ethanol drop by drop in order to avoid the cellular aggregation. The samples fixed with this procedure were maintained 20 minutes in ice and kept at 4°C before DNA staining.

Each experimental sample was run in triplicate and the results were expressed as the number of cells in treated samples compared with control one.

At the end of the last experimental time point, fixed cells were washed in cold PBS+FBS 5% and stained with the appropriate volume (~ 2millions of cells/ml) of a solution of 25µg/ml of Propidium Iodide (PI) in PBS and 12.5µl/ml of RNAse 1mg/ml in water, overnight at 4°C in the dark. The following day the DNA was analyzed by FACS calibur (Becton Dickinson).

4. CHROMATIN IMMUNOPRECIPITATION

Chromatin Immunoprecipitation experiments were performed as previously described by Di Giandomenico et al. (Di Giandomenico *et al*, 2014).

From cellular samples

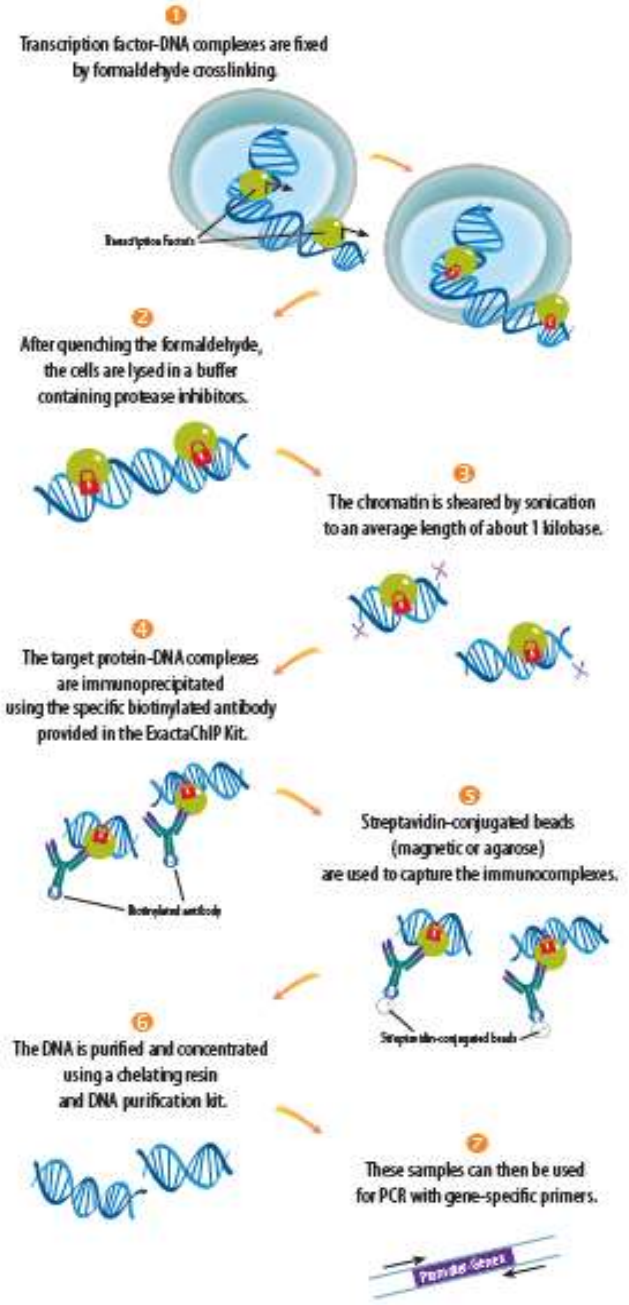

Figure 27: a schematic representation of the different steps of the Chromatin Immunoprecipitation assay. ***Picture adapted from: R&D System protocol***

Briefly cells were detached (approximately $1*10^6$ cells/sample) and washed with PBS, to perform the chromatin immunoprecipitation assay. The pellet was incubated for 10 minutes with 1% formaldehyde (VWR International PBI), in order to obtain the crosslinking between the transcription factors and the DNA.

After quenching the reaction with glycine 0.125M, the cross-linked pellet was resuspended in sonication buffer and sonicated in 1.5ml eppendorf. The sonication was performed on ice, with the following scheme: 1min sonication followed by 1 min stop. This step is necessary to obtain chromatin fragments of an average length of 500/800bp, that were evaluated by agarose gel 1%. The chromatin was subsequent kept at -80°C until the immunoprecipitation step. Immunoprecipitations were performed using Prot-G-Sepharose (KPL, Milan, Italy) and 5 µg of specific antibodies were used: Fli-1 (C-19) (sc-356 Santa Cruz Biotechnology), and anti-Flag antibody (F7425, Sigma Aldrich). The “Prot-G solution” was prepared by adding Prot-G-Sepharose blocked with 1 µg/l salmon sperm (Sigma Aldrich) and 10 µg/l bovine serum albumin (BSA) and immunoprecipitation buffer (containing inhibitors of proteases and phosphatases). The “chromatin solution” was prepared adding the immunoprecipitation buffer (added with inhibitors) to the solution of sonicated chromatin. “Prot-G” and “chromatin solution” were pre-cleaned for 2hours at 4°C on a rotating wheel; after the pre-cleaning the “chromatin solution” was transferred in a new eppendorf 1,5ml coated with Sigmacote® (Sigma Aldrich). The Sigmacote® reacts with the surface of the eppendorf to produce a neutral, hydrophobic microscopically film that allows the precipitation of Prot-G-Sepharose and prevents its loss along the walls. The antibodies selected for the immunoprecipitation were added to the “chromatin solution” and incubated overnight at 4°C on a rotating wheel.

The day after, the “Prot-G-solution” was added to the “chromatin“ samples and incubated 3hours at 4°C on a rotating wheel. After this incubation the supernatants of FLAG samples were taken and named “INPUT”; since FLAG is the negative control, the INPUT material is the whole chromatin’s sample. The immunoprecipitated material, deriving from the incubation with the specific antibody, was washed 5 times with RIPA wash buffer, 1 with LiCl buffer and 1 with TE buffer. To reverse the crosslinks the pellets were resuspended in 100µl of TE buffer and incubated overnight at 65°C with 4µl of RNase 10µg/µl.

To the “INPUT” pellets were added 10µl of RNase 10µg/µl and were incubated overnight at 65°C. Recovered material was treated with proteinase K, extracted with phenol/chloroform / isoamyl alcohol (25:24:1), and precipitated. The immunoprecipitated DNAs were resuspended in 50µl of H_2O and analyzed by quantitative Real Time PCR. Values are reported as fold enrichment over the control antibody–Flag (Sigma Aldrich). Satellite sequences repeated at multiple 94 positions in the genome were used as a control for unspecific precipitation and as a loading control (sequence: forward CAATTATCCCTTCGGGGAATCGG and reverse GGCGACCAATAGCCAAAAAAGTGAG primers). The receipts for each buffer used and the primers used for the final analysis by RT-PCR were described in the following section.

From tumoral samples

When the sample of origin is a tumor and not cells, it is necessary to pre-treated it in order to finally obtain the cellular suspension. From the final cellular suspension the steps of the chromatin immunoprecipitation assay are exactly the same used for the cells and described above.

The tumors were taken and immediately fragmented and crosslinked with 1% of formaldehyde solution for 10 minutes; the quenching was performed with an incubation of 5 minutes with glycine 0.125M. The samples were washed three times with PBS and incubated at 37°C for 30 minutes with a volume of collagenase 1X proportionally to the size of the pellet (the tumor sample must be covered by the solution). After that time the tumor sample was further homogenized using a turrax or a dounce tissue grinder (depending on the consistency of the tumor), in a solution of lysis buffer.

When the final cellular concentration was obtained, the sample was washed and resuspended in sonication buffer. From this step the procedure followed the same used for the cellular samples, described above.

4.1 CHROMATIN IMMUNOPRECIPITATION: BUFFERS AND PRIMERS

LYSIS BUFFER

Final volume of 50ml:

2.5 ml of **0.1M PIPES pH 8.0**

4.25 ml of **1M KCl**

2.5ml of **10% NP40**

40.5 ml of **dH_2O**

Store the solution at 4°C – the proteases inhibitors were added at the time of use

SONICATION BUFFER

Final volume of 50ml:

2.5 ml of **1M Tris HCl pH 8.0**

1ml of **0.5M EDTA**

0.5ml of **10% SDS**

5ml of **5% deoxycholic acid**

41ml of **dH_2O**

Store the solution at 4°C - the proteases inhibitors were added at the time of use

IMMUNOPRECIPITATION BUFFER

Final volume of 50ml:

2.5 ml of **1M Tris HCl pH 8.0**

1ml of **0.5M EDTA**

0.5ml of **10% SDS**

5ml of **5% deoxycholic acid**

1.5ml of **LiCl 5M**

39.5ml of **dH_2O**

Store the solution at 4°C - the proteases inhibitors were added at the time of use

RIPA BUFFER

Final volume of 50ml:

0.5 ml of **1M Tris HCl pH 8.0**

0.05ml of **0.5M EDTA**

0.1ml of **EGTA 250mM**

0.5ml of **10% SDS**

1ml of **5% deoxycholic acid**

1.4ml of **NaCl 5M**

0.5ml of **Triton X-100**

45.95ml of **dH_2O**

Store the solution at 4°C- the proteases inhibitors were added at the time of use

LiCl BUFFER

Final volume of 50ml:

0.5 ml of **1M Tris HCl pH 8.0**

0.1 ml of **0.5M EDTA**

2.5 ml of **LiCl 5M**

2.5 ml of **10% NP40**

5ml of **5% deoxycholic acid**

39.4 ml of **dH_2O**

Store the solution at 4°C

TE BUFFER

Final volume of 1lt:

10 ml of **0.1M Tris HCl pH 8.0**

2 ml of **0.5M EDTA**

988 ml of **dH_2O**

Store the solution at room temperature

PRIMERS USED FOR REAL TIME PCR

Target	Forward Primer (5'- 3')	Reverse Primer (5'- 3')
CD99 prom	TTGTTAAGTGTGGGAAGGGC	CTGCTCACCTCAGGGAGTTC
TGFβR2 prom	GTGTGGGAGGGCGGTGAGGGGC	GAGGGAAGCTGCACAGGAGTCCGGC
NR0B1 prom	GATTCTGTATCAGCTGGTATATACC	GCATCAGGAAGCCTGGATCC

Table 5: Primer pairs list for Real Time PCR of ChIP samples

4.2 CHROMATIN IMMUNOPRECIPITATION - DATA ANALYSIS

The immunoprecipitated DNAs were resuspended in 50µl of H_2O and analyzed by quantitative Real Time PCR. Values were reported as fold enrichment over the control antibody Flag (Sigma Aldrich). Satellite sequences repeated at multiple 94 positions in the genome were used as a control for unspecific precipitation and as a loading control.

5. NUCLEIC ACIDS QUANTIFICATION

Concentration and quality of solutions containing DNA was determined by spectrophotometric analysis using the "Nanodrop".

The nucleic acid concentration was expressed as the mean of the values (µg/ml) obtained in the two independently- prepared and – measured dilutions.

The quality of nucleic acid solutions was evaluated by calculating the A_{260nm}/A_{280nm} ratio. It is well known that for DNA, a ratio of 1.8-2 was indicative of a good-quality preparation.

6. PROTEIN EXTRACTION

Total proteins were extracted from cultured cells by a "lysis method". Basically cell cultures were washed twice with ice-cold PBS and then detached with a disposable scraper. The suspension was then centrifuged at 1500 rpm for 5 minutes and the pellet was resuspended in an amount of lysis buffer dependent on the size of cell pellet.

Lysis buffer composition: 50 mM Tris-HCl pH 7.5, 250 mM NaCl, 0,1% Nonidet (NP40), 5mM EDTA, 0.21g NAF per 100ml solution, in the presence of 1X protease cocktail inhibitor (Sigma).

Lysates were incubated on ice for 30 minutes. Insoluble cellular debris were pelleted at 13000 x g for 10 min at 4°C and the total protein present in the supernatant was recovered and placed in a fresh Eppendorf tube (1.5 ml). An aliquot (2 µl) was used to determine protein concentration.

To evaluate proteins in *ex vivo* samples (tumor from xenografts), explanted tumours were immediately snap-frozen. Frozen specimens were diluted into an appropriate volume of ice-cold lysis buffer and homogenized with a “ultra-turrax” homogenizer. Lysates were incubated on ice for 45-60 minutes and then centrifuged at 13000 rpm (17000 x g) for 20 min at 4°C at least two times to pellet insoluble cellular debris. 2 µl of clear lysates were used to measure protein concentration.

6.1 PROTEIN CONCENTRATION

Protein concentration was determined according to Bradford (Bradford, 1976).

The concentration of proteins in the samples was determined by mixing 2 µl of protein cellular extract to the BioRad diluted solution as done for the calibration curve points (see paragraph “Calibration Curve Preparation”, below).

Samples were rapidly transferred into disposable cuvettes and the absorbance read by spectrophotometer, at 595 nm wave length. Protein sample concentration was found by interpolating the registered absorbance with the standard curve.

6.2 CALIBRATION CURVE – PREPARATION

For the calibration curve, a solution of bovine serum albumin (BSA) (1 mg/ml) was prepared dissolving powdered BSA (Sigma) in water. For each calibration point, 800 µl of distilled water were mixed with 200 µl of BioRad Protein Assay (BioRad) and transferred into disposable cuvettes (PBI International).

Calibration points of the standard curve were generated by adding 2,4,6, 8 and 10 µl of BSA solution to 1 ml of BioRad diluted solution. The absorbance at 595 nm was measured with the spectrophotometer. The absorbance value corresponding to the blank sample was subtracted from the values obtained from the BSA-containing samples. The calibration curve obtained in such a way allows extrapolation of the exact absorbance value corresponding to 1 µg of proteins present in the solution.

7. WESTERN BLOTTING

The TruPAGE™gels (Sigma Aldrich) 4-12% polyacrylamide were used as resolving gels.

The equivalent of 30 to 50 µg of proteins were mixed with 4X Laemmli buffer with the addition of 1/10 of volume of β-mercaptoethanol.

The loading Laemmli buffer contains SDS that negatively charged the proteins and permits the migration of the proteins on the basis of its molecular weight.

Samples were heated at 100°C for 5 minutes, chilled on ice for an additional 5 minutes, centrifuged at 4°C at 12000 rpm for 5 seconds and loaded onto the SDS-PAGE system.

Proteins were resolved on a minigel apparatus (BioRad) and run for approximately 1.5 hrs at 130-150V in 1X TruPAGE™ TEA-Tricine SDS Running Buffer (Sigma Aldrich); electrophoresis progress was followed using pre-stained molecular weight marker “Precision Plus Protein WesternC standards” (10-250KDa - BioRad).

At the end of the run, the glass plates holding the gel were removed from the electrophoresis tank, opened and, by means of a scalpel, the stacking gel was removed. The resolving gel was placed on the precast Trans-Blot® Turbo Transfer Pack Mini sandwich in nitrocellulose (Biorad), for the blotting step. Possible air bubbles trapped were displaced by repeated rolling with a pipette tip. The sandwich was then placed in the Trans-Blot® Turbo™ Transfer System with the “Universal Power Supply”, and the right program was selected on the basis of molecular weight of the proteins.

This dispositive allows to change the conditions of the blotting, in function of the molecular weight of the proteins analyzed.

The programs for 1mini gel were the following:

STANDARD PROTEIN: up to 1.0A; 25V constant for 30 minutes

HIGH MW PROTEIN (>150KDa): 1.3A constant; up to 25V for 10 minutes

LOW MW PROTEIN (<30KDa): 1.3A constant; up to 25V for 5 minutes

MIXED MW PROTEIN (5-150KDa): 1.3A constant; up to 25V for 7 minutes

The protein's transfer, from the gel to nitrocellulose membrane, was carried out at room temperature.

7.1 Immunological detection of nitrocellulose-immobilised proteins

At the end of the transfer step, the nitrocellulose filter was recovered from the sandwich and, in order to verify the correct protein blotting, it was stained for 5 minutes in a clean tray containing a "Ponceau S red dye" solution (Sigma Aldrich) with gentle agitation at room temperature. When the bands of proteins were visible, the filter was destained with several washes of distilled water at room temperature.

On the basis of the molecular weight marker position, membrane slices containing the proteins of interest were excised with a scalpel and placed in separate clean trays. The nitrocellulose slices were incubated with blocking solution, 5% (w/v) dried non-fat milk solubilised in TBST buffer (composed by 20mM Tris-HCl, 500mM NaCl and 0.5% tween20, with final pH equal to 7.4), at room temperature on a shaking platform for at least one hour, in order to mask potential nonspecific antibodies binding sites and, thus, to reduce general background. After 1 hour, blocking solution was removed and filter slices were washed 1 time with TBST washing solution and incubated over night at 4°C, on a shaking platform, with the specific antibody-containing solution. Detection of proteins of interest was achieved by using polyclonal antibodies anti β-Actin (GOAT) and Chk1(G4) (MOUSE) were purchased by Santa Cruz Biotechnology, diluted in 5% milk-TBST solution (Actin and ChK1) or 5% BSA-TBST solution (Chk1 (G4)).

At the end of the overnight incubation, primary antibodies were removed and filter slices were washed 3 times for 20 minutes with TBST solution at room temperature, on a shaking platform. Nitrocellulose filters were then incubated at room temperature on a shaking platform with the appropriate secondary peroxidase-linked whole antibodies (Amersham Pharmacia Biotech) diluted 1:3000, in blocking solution. After a 1-hour hybridisation, secondary antibodies were removed and filter slices were washed three times for 20 minutes at room temperature on a shaking platform with TBST solution. Antibodies bound to proteins of interest on nitrocellulose slices were detected by enhanced chemoluminescence system (ECL), SuperSignal Chemiluminescent HRP Substrates (Thermo Fisher Scientific) and, according to the manufacturer's instructions, revealed by using Hyperfilm MP films (Amersham-Pharmacia Biotech).

8. ANIMALS

Female athymic nude mice, 6- to 9-week old obtained from “Envigo Laboratories” were used. They were maintained under specific pathogen-free conditions, housed in individually ventilated cages and handled using aseptic procedures. Procedures involving animals and their care were conducted in conformity with the institutional guidelines that are in compliance with national (Legislative Decree 26, March, 2014) and international (EEC Council Directive 2010/63, August, 2013) laws and policies in line with guidelines for the welfare and use of animals in cancer research (Workman P. Et al. (2010), Guidelines, BRJ, 102,1555-1577).

Animals studies were approved by the Mario Negri Institute Animal Care and Use Committee and by the Italian Ministerial decree no. 84-2013.

9. SiRNA and esiRNA LIBRARIES TRANSFECTION

A “Mission siRNA Human Kinase Panel” (719 targets) and a “esiRNA Nucleic Acid Binding Panel” (310 targets) libraries were purchased from Sigma Aldrich.

As concerns the “Mission siRNA Human Kinase Panel” three individual siRNAs were provided per gene and the siRNA duplexes were spotted in 96 well microplates, with 80 duplexes per plate to reach the final quantity of 0.25 nmol per duplex; the library was diluted in order to obtain a final concentration of 2μM.

The siRNAs were designed using the “Rosetta algorithm” that provides an efficient gene knockdown and a good target specificity.

The Rosetta siRNA Design Algorithm utilizes “Position-Specific Scoring Matrices (PSSM)” and knowledge of the all-important siRNA seed region to predict the most effective and specific siRNA sequences for the target gene of interest. Additionally, the Rosetta siRNA Design Algorithm has been trained with feedback from over 3 years of gene-silencing experiments, ensuring that the algorithm’s in-silico rules are guided and bolstered by real-world empirical evidence.

The library “Nucleic Acid Binding Panel” were performed using esiRNAs because the library with siRNAs was discontinued from Sigma Aldrich. The Endoribonuclease-prepared siRNAs (esiRNAs) “esiFLEX- esiRNA” library (291genes) was provided at the concentration of 5μM in each well; the library was diluted to obtain a final concentration of 2 μM.

Each library contains siRNA or esiRNA negative controls, carefully designed to have no homology to known gene sequences; they did not contain known immune-response motifs.

9.1 Optimization of TC71 cell culture conditions

A) Different pilot experiments were designed to find the best cellular concentration to use for the seed in 384 wells/plate. This was a very important step in order to perform the experiments when the cells were in their exponential-growth phase.

The experimental schedule was the following:

Each column (from well B to O) was seed with a defined cellular concentration (300-600-1250-2500 and 5000cells/well), in order to obtain 14 (vertically represented) replicates with the same cellular concentration. The frame of PBS (grey wells in figure 28) was used to avoid the phenomenon of evaporation during the incubation in a humidified incubator at 37°C with 5% CO2.

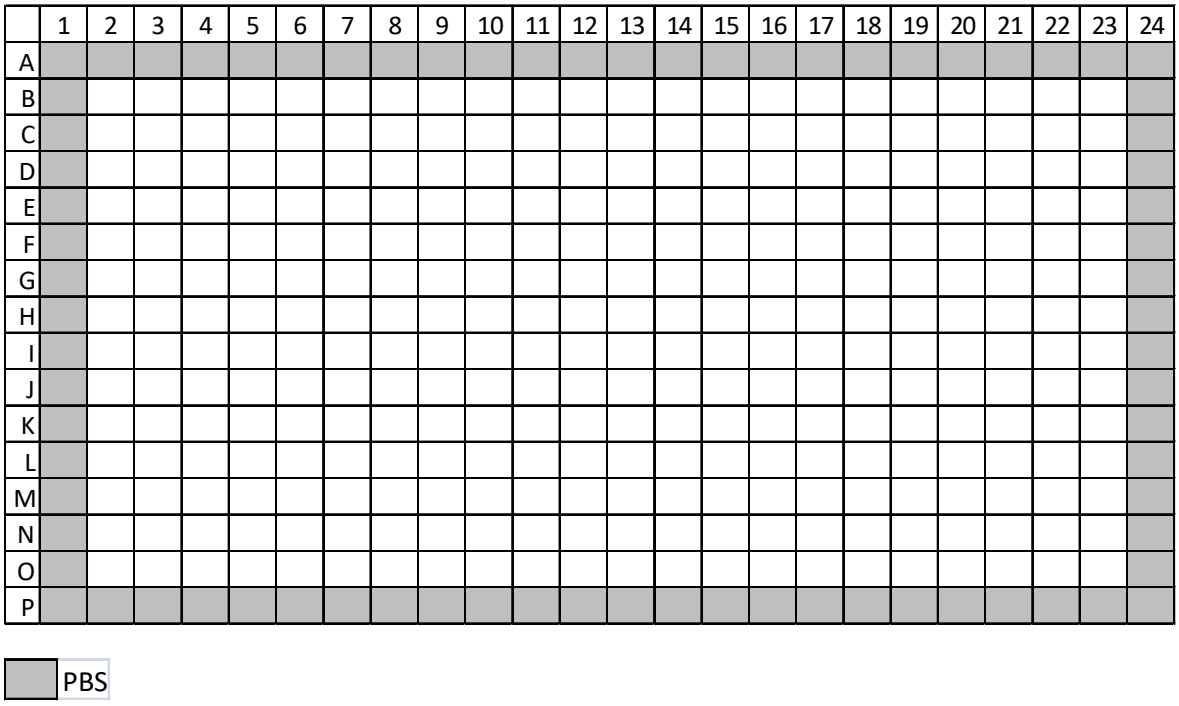

Figure 28: the 384 wells/plate used for the assessment of best cellular concentration. The grey wells were filled with PBS. For each concentration 14 replicates (from B to O) were performed. 48 hours after the seed (time delay), the cell's growth was evaluated by microscope and MTS assay, at 24-48 and 72 hours.

The results obtained showed that the cellular concentration of 300 cells/well is the ideal in order to use cells in the exponential phase of growth, without reaching the confluence state.

B) Pilot experiments were performed to determine the best volume of lipofectamine to use for the transfection. The final goal was to transfect the cells without any evidence of cytotoxicity.

1) Cells were seed in a 384 wells/plate at day 0 and treated with different µl of lipofectamine at day 2. After 24 – 48 and 72 hours the MTS assay was performed and the toxicity of lipofectamine was assessed evaluating the % of cell survival after treatment with lipofectamine compared to not treated, control cells.

   For each time point a plate (like the representative in figure 29) was seeded. For each condition 14 (vertically represented) replicates were seeded.

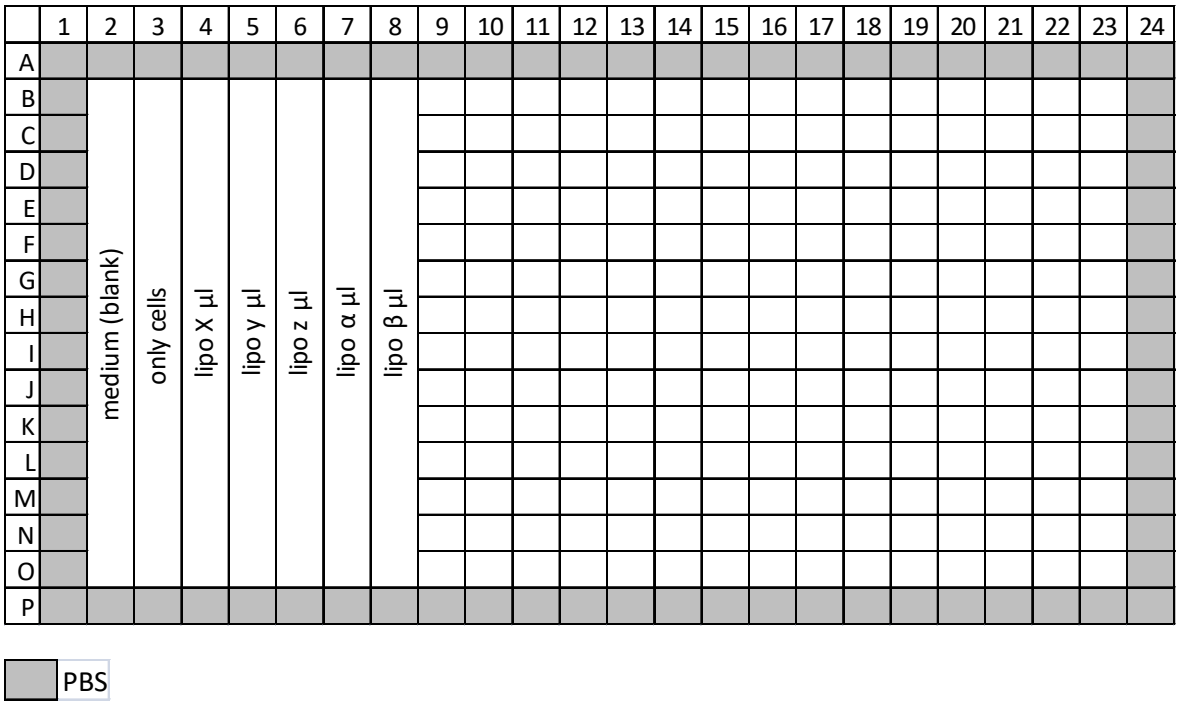

Figure 29: the 384 wells/plate used for the assessment of the best volume of lipofectamine to use. The grey wells were filled with PBS. Cells were seed at time 0 and treated with different µl of lipofectamine (from 0.01 to 0.1Vl per well). For each condition 14 replicates (from B to O) were performed. 48 hours after the seed (time delay), the cytotoxicity of lipofectamine was evaluated by MTS assay, at 24-48 and 72 hours.

From this experiment were selected two volumes of lipofectamine not toxic for the cells (0.05 and 0.09 µl/well).

2) Cells were seed in a 384 wells/plate at day 0 and transfected with two different concentrations of sichK1 (used as probe in the pilot experiments); the two volumes of lipofectamine selected in the point 1 were used (figure 30). The range of concentration of sichK1 to use for the transfection was assessed in preliminary experiments performed in the laboratory.

   24 – 48 and 72 hours after transfection the cells were pelleted and the efficacy of transfection was evaluated by western blotting analysis.

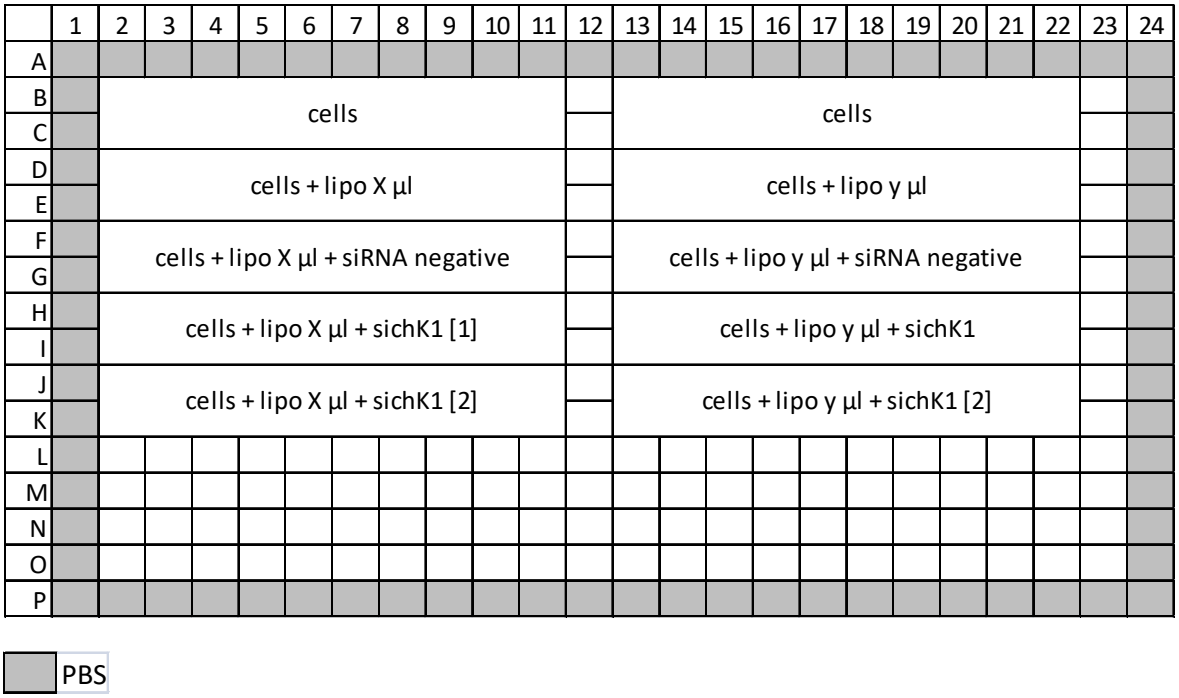

Figure 30: the 384 wells/plate used for the evaluation of the efficacy of transfection with sichK1. The grey wells were filled with PBS. Cells were seed at time 0 (concentration 300cells/well) and treated as reported in the figure. For each condition 20 replicates (from column 2 to 11 for two rows) were assessed. 48 hours after the seed (time delay), the cells were treated. 24-48 and 72 hours after treatment the cells were pelleted and prepared for the western blotting analysis.

The volume of lipofectamine that allow the transfection without cytotoxicity, assessed by this experiment, was 0.05 µl/well.

The best time point to observe the results, determined from these experiments, was 48hours after continuous treatment. At this time point the transfection with sichK1 induced downregulation of the protein without causing cytotoxicity.

3) The evaluation of the cytotoxicity derived from the treatment with trabectedin and transfection with lipofectamine was assessed, as shown in figure 31.

   Preliminary pilot experiments were performed to determine the concentration of trabectedin to use in order to obtain an IC30.

   The cytotoxicity was evaluated by MTS, 48hrs after transfection.

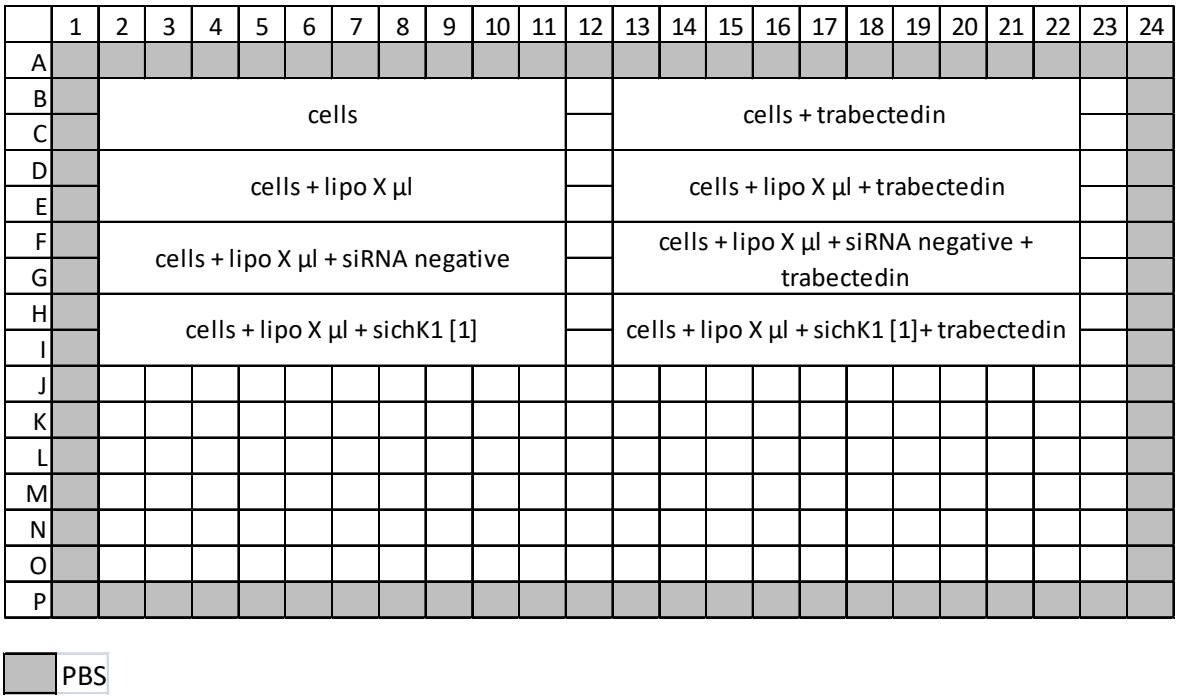

Figure 31: the 384 wells/plate used for the evaluation of the toxicity derived from the combined transfection with trabectedin and sichK1. The grey wells were filled with PBS. Cells were seed at time 0 and treated as reported in the scheme For each condition 20 replicates (from column 2 to 11 for two rows) were assessed. 48 hours after the seed (time delay), the cells were treated. The cytotoxicity parameter was evaluated by MTS, 48 hours after treatment.

For the experiments performed in 384 wells/plate, cells were seeded using an automated robot “Janus” (Perkin Elmer), in a sterile flowhood, in order to maintain sterile condition.

This is an automated Workstation that offers multiple pipetting technologies in the same instrument platform. The instrument provides an automated liquid handling solution with flexibility in throughput, plate capacity, and dynamic volume range.

This is a very important tool to avoid the variability and to increase the feasibility of the methodology. Dispense heads can be automatically switched, within a single protocol, to go from nanoliters to microliters.

Three pictures of the robot are shown below in figure 32.

Figure 32: Janus robot

9.2 Transfection with libraries

The experimental schedule used for the transfection with the libraries was the following:

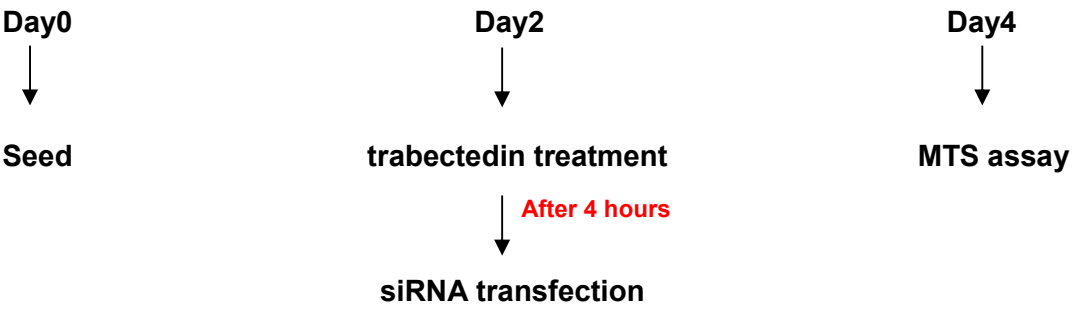

Figure 33: the diagram of the experimental design.

The cells were seeded at day 0 and treated 48 hours later.

As concerns the siRNA library, composed by different 96 wells/plates, in which each well contained a mix of siRNAs directed versus a specific kinase. The big library was composed by thirteen 96 wells/plate. The experimental design was planned in order to perform the experiments in 384 wells/plate. Each 384 wells/plate was examined in triplicate; each triplets was transfected with a pool of two 96 well/plates, containing the siRNAs against a specific target.

The esiRNA library is composed by five 96 wells/plate.

The schematic representation of the procedure used for the transfection is represented in the following figure 34.

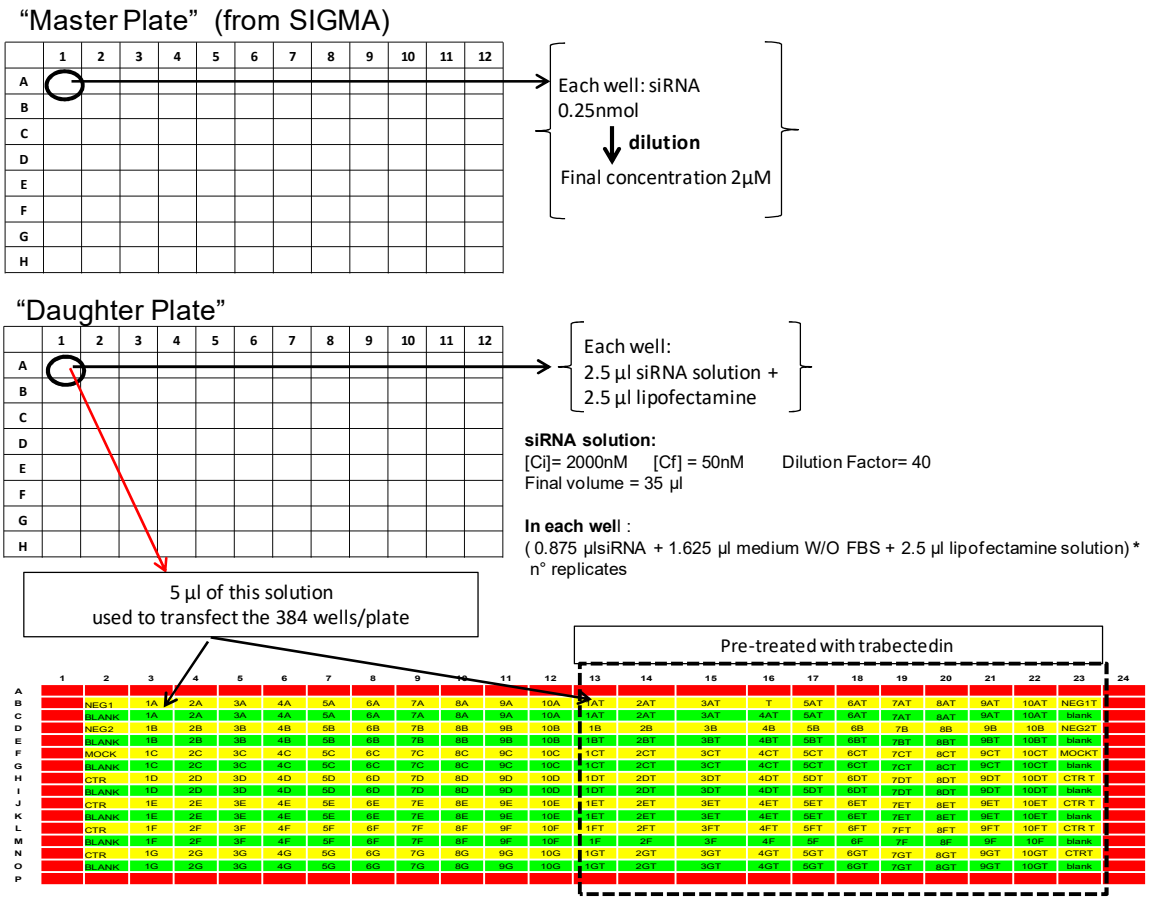

Figure 34: schedule of dilution of siRNAs and preparation of "daughter plates" for the transfection.

The same schedule was used to prepare the “Daughter Plates” for the “esiRNA Nucleic Acid Binding Panel”; the final concentration of esiRNA used was 30nM.

Figure 35 shows two 96 wells/plate as example of the 13 plates of the library and the 384 wells/plate seeding at day 0 and treated and transfected at day 2.

Plate 1

NEG1	ABL1	ADRBK1	AMHR2	BMPR1B	DDR1	CAMK2D	CDK2	CHEK1	CKMT1B	CLK2	
NEG2	ABL2	ADRBK2	ARAF	BMPR2	CALM1	CAMK2G	CDK3	CHEK1	CKMT2	CLK3	
	ACVR1	AK1	ATM	BMX	CALM2	CDC2	CDK4	CHKA	CKMT2	CLK3	
	ACVR1B	AK2	ATR	BRAF	CALM3	CDC2L1	CDK5	CHKB	CKS1B	PLK3	
	ACVR2A	AK3L1	AXL	BRDT	CAMK4	CDC2L2	CDK6	CHKB	CKS2	MAP3K8	
	ACVR2B	AKT1	BCR	BTK	CAMK2A	CDC2L2	CDK7	CHUK	CLK1	CPT1B	
	ACVRL1	AKT2	BLK	BUB1	CAMK2B	CDC2L2	CDK8	CKB	CLK1	CRKL	

Plate 2

NEG1	CSF1R	CSNK2A2	DAPK3	DLG4	MARK2	EPHB2	ERN1	FGFR2	FRK	GK2	
NEG2	CSK	CSNK2B	DCK	DMPK	EPHA1	EPHB3	ERN1	FGFR2	FRAP1	GRK4	
	CSNK1A1	DGKA	DGUOK	DMPK	EPHA3	EPHB4	PTK2B	FGFR2	FYN	GRK5	
	CSNK1D	DGKB	DLG1	DTYMK	EPHA4	EPHB6	FER	FGFR4	GAK	GRK6	
	CSNK1E	DGKG	DLG1	DYRK1A	EPHA5	ERBB2	FES	FGR	GALK1	MKNK2	
	CSNK1G2	DGKG	DLG2	DYRK1A	EPHA7	ERBB3	FGFR1	FLT1	GALK2	GSK3A	
	CSNK1G3	DGKQ	DLG3	EGFR	EPHA8	ERBB4	FGFR1	FLT3	GCK	GSK3B	

Figure 35: an example of the 96wells/plate contained in the siRNA library.

These two plates were used and pooled for the transfection of the same 384 wells/plate. For some gene it could be present more than one pool of siRNAs, in order to cover the different known isoforms.

Figure 36 represents an example of the 384 wells/plate; columns 13 to 23 represent cells pre-treated with trabectedin. 4 hours after trabectedin treatment the whole plate was transfected with the different siRNAs derived from 96 wells/plate represented in figure 35.

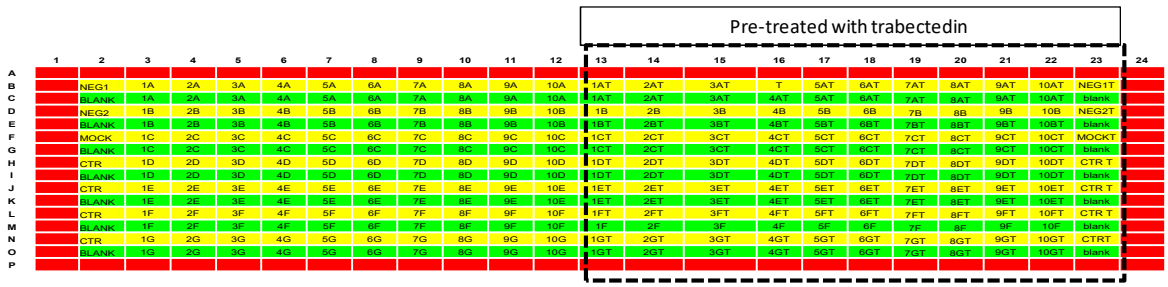

Figure 36: the 384 wells/plate treated and transfected.

RED wells represent the frame of PBS.

From column 2 to 12 each well was transfected with the respective siRNA (deriving from the 96 wells/plate, figure 35) alone, while from column 13 to 23 each well was treated with trabectedin and, 4 hours later, transfected with the same siRNA of the first half of the plate.

In each plate were used different controls to assess:

1) The specificity of siRNAs: the siRNA negative controls were included in the libraries.
2) The cytotoxicity derived from the transfection. Wells transfected with lipofectamine alone using the same volume used for the transfection of the library.
3) The cytotoxicity derived from the treatment with trabectedin. Wells treated with the dose of trabectedin selected for the experiment; the importance of this control was to verify that the activity of trabectedin during the experiments were maintained around the desired IC value (in this case IC30).
4) The background. Wells with only medium. The values of absorbance obtained from these wells were used as “blank”, that is the medium background.

Each plate was performed in triplicate and incubated in a humidified incubator at 37°C with 5% CO2. 48hours after the treatment and transfection, the wells were stained with MTS and the absorbance read at 490nm by spectrophotometer (Tecan). Trabectedin treatment was performed in IMDM medium supplemented with 10% FBS, 1% L-glutamine (2mmol/L, Biowest) and 1% penicillin-streptomycin 10.000 µg/ml. The transfection with siRNA and esiRNA libraries was performed using 0.05µl/ well of Lipofectamine 2000 (cod.11668019, Life Technologies), in IMDM medium without FBS, glutamine or PS.

The final “Working Protocol” that I obtained from the assessment of the methodology is reported here.

- **WORKING PROTOCOL**

1. At day 0 seed the cells in a 384 well/plates (300 cells/well), in a final volume of 25µl. It is important to create a frame of PBS, in order to avoid the phenomenon of evaporation. Incubate the plates for 48 hours in a humidified incubator at 37°C with 5% CO2.

2. At day 2 (48 hours after seed), treat half plate with the dose of 0.15nM (IC30) of trabectedin. A final volume of 5µl for the treatment is used. Prepare the solution of trabectedin in medium containing FBS, glutamine (1%) and PS (1%). Treat the other half plate with 5µl of the same medium used to dilute trabectedin, in order to obtain the same final volume in each volume.

3. Prepare the lipofectamine solution in medium without FBS.

Use 0.05µl/well of lipofectamine.

2.5µl of this solution will be added to 2.5µl of "siRNA solution" to finally tranfect the cells with a final volume of 5µl.

For the lipofectamine solution the calculation is:

2.5µl * **X** samples = **Y** total volume

0.05µl* **X** samples = **Z** volume of lipofectamine

The final solution is composed as followed:

Z volume of lipofectamine + (Y – Z) volume of medium without FBS .

4. Prepare the "siRNA solution", in medium without FBS.

2.5µl of siRNA solution is prepared to add to the 2.5µl of lipofectamine solution to finally tranfect the cells with a final volume of 5µl.

For the siRNA solution the calculation is:

- The dilution factor is calculated by [initial concentration]/[final concentration]
- The final volume is 35 µl for each well.
- Final volume / dilution factor = **A** volume of each siRNA to be used
- 2.5µl final volume of this solution – **A** volume = **B** volume of medium without FBS to be used for each siRNA.

- **B** volume * total number of siRNAs = **C** value of total volume of medium without FBS to be used for the transfection of all the siRNAs considered.

5. Add the **C** volume of medium without FBS to the lipofectamine solution

6. Use the robot to dispense in a 96wells/plate the final volume of lipofectamine (2.5µl for each replicate of siRNA that is need) and siRNA solution (2.5µl for each replicate of siRNA that is need). Incubate this solution for 5 minutes.

7. 4 hours after trabectedin treatment dispense, using the robot, 5µl of the final solution of siRNA obtained in the point 6 to each 384 well.

8. Incubate the 384 wells/plate treated and transfected in a humidified incubator at 37°C with 5% CO2.

9. At Day 4: (48 hours after the transfection) perform the MTS analysis. Read the absorbance of each well using the spectrophotometer, at 490nm.

The siRNAs and esiRNAs used for the transfection with the two libraries are reported in Table 6 and 7, respectively.

siRNA Kinase Panel

plate1

NEG1	ABL1	ADRBK1	AMHR2	BMPR1B	DDR1	CAMK2D	CDK2	CHEK1	CKMT1B	CLK2
NEG2	ABL2	ADRBK2	ARAF	BMPR2	CALM1	CAMK2G	CDK3	CHEK1	CKMT2	CLK3
	ACVR1	AK1	ATM	BMX	CALM2	CDC2	CDK4	CHKA	CKMT2	CLK3
	ACVR1B	AK2	ATR	BRAF	CALM3	CDC2L1	CDK5	CHKB	CKS1B	PLK3
	ACVR2A	AK3L1	AXL	BRDT	CAMK4	CDC2L2	CDK6	CHKB	CKS2	MAP3K8
	ACVR2B	AKT1	BCR	BTK	CAMK2A	CDC2L2	CDK7	CHUK	CLK1	CPT1B
	ACVRL1	AKT2	BLK	BUB1	CAMK2B	CDC2L2	CDK8	CKB	CLK1	CRKL

plate2

NEG1	CSF1R	CSNK2A2	DAPK3	DLG4	MARK2	EPHB2	ERN1	FGFR2	FRK	GK2
NEG2	CSK	CSNK2B	DCK	DMPK	EPHA1	EPHB3	ERN1	FGFR2	FRAP1	GRK4
	CSNK1A1	DGKA	DGUOK	DMPK	EPHA3	EPHB4	PTK2B	FGFR2	FYN	GRK5
	CSNK1D	DGKB	DLG1	DTYMK	EPHA4	EPHB6	FER	FGFR4	GAK	GRK6
	CSNK1E	DGKG	DLG1	DYRK1A	EPHA5	ERBB2	FES	FGR	GALK1	MKNK2
	CSNK1G2	DGKG	DLG2	DYRK1A	EPHA7	ERBB3	FGFR1	FLT1	GALK2	GSK3A
	CSNK1G3	DGKQ	DLG3	EGFR	EPHA8	ERBB4	FGFR1	FLT3	GCK	GSK3B

plate3

NEG1	GUCY2F	IKBKB	ITPKA	LCK	MATK	MAP3K9	MST1R	NEK1	NTRK1	PAK2
NEG2	GUK1	ILK	ITPKB	LIMK1	MAP3K1	MAP3K10	MUSK	NEK2	NTRK2	PAK3
	GUCY2D	INSR	JAK1	LIMK2	MAP3K1	MAP3K11	MVK	NEK3	NTRK3	PCK1
	HCK	INSRR	JAK2	LTK	MAP3K3	MOS	MYLK	NME1	ROR1	PCK2
	HK1	IRAK1	JAK3	LYN	MAP3K4	MPP1	MYLK	NME3	ROR1	PCTK1
	HK2	IRAK2	KDR	MAK	MAP3K5	MPP2	MYLK	NME4	ROR2	PCTK2
	HK3	ITK	KHK	MARK1	MET	MPP3	MYLK	NPR1	DDR2	PCTK3

plate4

NEG1	PDGFRB	PFKFB3	PHKA1	PIK3C2G	PI4KA	POLR2K	PRKAG1	PRKCE	PRKCZ	MAPK7
NEG2	PDK1	PFKFB4	PHKA1	PIK3C3	PI4KA	PRKAA1	PRKAR1A	PRKCG	PRKDC	MAPK8
	PDK2	PFKL	PHKA2	PIK3CA	PI4KB	PRKAA2	PRKAR1B	PRKCH	PRKG1	MAPK11
	PDK3	PFKM	PHKB	PIK3CB	PIN1	PRKAB1	PRKAR2A	PRKCI	PRKG2	MAPK9
	PDK4	PFKP	PHKG1	PIM1	PIP4K2A	PRKAB2	PRKAR2B	PKN1	MAPK1	MAPK10
	PDPK1	PFTK1	PHKG2	PIK3CD	PKLR	PRKACA	PRKCA	PKN2	MAPK3	MAPK10
	PFKFB1	PGK1	PIK3C2A	PIK3CG	PKM2	PRKACB	PRKCB	PRKD1	MAPK4	MAPK13

plate 5

NEG1	MAP2K2	PRPS1	ALDH18A1	RNASEL	RPS6KB2	SRC	AURKA	TAF9	TJP1	TYRO3
NEG2	MAP2K3	PRPS2	ALDH18A1	BRD2	RPS6KB2	SRMS	CDKL5	MAP3K7	TK1	UCK2
	MAP2K5	PSKH1	MAP4K2	ROCK1	RYK	SRPK1	STK10	TEC	TK2	VRK1
	MAP2K6	PTK2	RAGE	ROS1	MAPK12	SRPK2	STK11	TEK	TRIO	VRK2
	MAP2K7	PTK6	RAF1	RPS6KA1	MAP2K4	STC1	AURKC	TESK1	TTK	WEE1
	EIF2AK2	PTK7	RALB	RPS6KA2	SGK1	NEK4	SYK	TGFBR1	TTN	YES1
	PRKX	PTK7	RET	RPS6KA3	SKP1	STK3	TAF1	TGFBR2	TXK	ZAP70

plate6

NEG1	MAPKAPK3	ULK1	IKBKG	CDC14B	STK16	DYRK4	PRPF4B	BRSK2	DGKI	MAPKAPK2
NEG2	BRD3	STK24	DGKZ	CDK10	STK16	TRIM24	HERC2	PKD2L1	MAP3K13	STK17B
	TRRAP	DYRK3	DGKZ	CDK10	CDC2L5	TRIM24	CDK5R2	PAPSS2	DCLK1	STK17A
	CDC7	DYRK2	DGKE	CDK10	TNK1	CDKL1	RPS6KA4	PAPSS1	AURKB	TAOK2
	NME5	CDC42BPA	DGKD	PDXK	RIPK1	KSR1	KALRN	MAP3K6	MAGI1	TJP2
	PIP5K1B	MAP4K3	CAMK1	MKNK1	RIPK2	CDK5R1	KALRN	PKMYT1	DLG5	MAP4K4
	PIP5K1B	PIK3R3	MAPKAPK5	CASK	RIOK3	STK19	CDKL2	LATS1	RPS6KA5	EIF2AK3

plate7

NEG1	CDC42BPB	MELK	TANK	TNK2	TESK2	PLK4	RIPK3	CHEK2	MAST1	PASK
NEG2	AATK	MAGI2	TANK	NME6	BAIAP2	MAP3K2	PIM2	IRAK3	STK38L	SNF1LK2
	AATK	TLK1	GNE	TRIB1	MERTK	PLK2	RAPGEF4	AKAP13	MAST3	KIAA0999
	AATK	NUAK1	COL4A3BP	SPEG	STK25	NEK6	RAPGEF4	STK38	PDZD2	PIP5K1C
	IKBKE	XYLB	SGK2	BCKDK	CCT2	FASTK	CIT	TWF2	TNIK	BRD4
	ULK2	OXSR1	HIPK3	BCKDK	ERN2	RAB32	MAP4K5	AAK1	SMG1	CCRK
	SLK	AKT3	HIPK3	PAK4	CAMKK2	TLK2	MAP4K1	LMTK2	CDC2L6	DAPK2

plate8

NEG1	SGK3	DAK	PKD2L2	HIPK2	MINK1	CDKL3	TRIM33	RP6-213H19.1	TRPM7	ULK4
NEG2	RAB38	AK5	EIF2AK1	TBK1	AK3	TXNDC3	MPP6	ZAK	SNRK	ULK4
	PRKD3	HSPB8	TJP3	EEF2K	TNNI3K	TAOK3	NLK	PANK1	PXK	OXSM
	SHPK	LATS2	STK36	NME7	TNNI3K	PRKAG2	CMPK1	PANK1	UCKL1	ETNK2
	RIPK5	SRPK3	RPS6KA6	PKN3	IRAK4	POLK	POLR3K	PRKAG3	ULK4	FGGY
	PRKD2	RPS6KC1	STK39	NRBP1	IRAK4	IHPK2	CRKRS	MYO3A	ULK4	FGGY
	PRKD2	TPK1	TRIB2	HUNK	VRK3	IHPK2	CRKRS	CSNK1G1	ULK4	PI4K2B

plate 9

NEG1	STK32B	BMP2K	SPHK2	CAMK1G	MPP4	WNK1	PANK3	YSK4	NUAK2	OBSCN
NEG2	STYK1	SCYL2	RAD18	CLK4	RBKS	NADK	LRRK1	HKDC1	UCK1	OBSCN
	PI4K2A	AGK	PAK6	SCYL1	FN3K	WNK4	SGK269	ALPK1	RPS6KL1	SGK196
	STRADB	RIOK2	CABC1	SCYL1	MPP5	WNK3	SGK269	ALPK1	RIOK1	CAMKK1
	ETNK1	PBK	CAMK1D	ALPK3	CERK	WNK2	SGK269	ITPKC	GSG2	C1orf57
	ETNK1	TEX14	ADCK1	TAOK1	CERK	STK33	PIP4K2C	COASY	STK40	BRSK1
	CDC42BPG	STK31	PAK7	TRIB3	PINK1	CAMKV	NEK11	COASY	TSSK1B	KIAA1804

plate 10

NEG1	MASTL	MYLK3	ALPK2	PLK5P	MYO3B	SNF1LK	FUK	HIPK1	KSR2	FLJ40852
NEG2	MYLK2	MARVELD3	EVI5L	UHMK1	MYO3B	NEK10	MLKL	C6orf199	TSSK4	MYLK4
	DCLK3	MARVELD3	IHPK3	ACVR1C	NEK7	DGKH	PIP5K3	PRPS1L1	NEK8	NRBP2
	DCLK3	STRADA	LRRK2	ACVR1C	TRPM6	TCEB3C	PIP5K3	MAPK15	EPHA10	NEK5
	PSKH2	STRADA	CSNK1A1L	GRK7	STK35	DCLK2	STK32A	IPMK	EPHA10	CDKL4
	ADCK2	MGC16169	AK7	LRGUK	TTBK2	GPR125	STK32A	ANKK1	EPHA10	TXNDC6
	SGK493	TP53RK	FLJ25006	TAF1L	HIPK4	MGC42105	ADCK5	PAN3	EPHA6	CERKL

plate 11

NEG1	ADK	ALK	BMPR1A	BUB1B	CAMK2B	CDC2L2	CDK9	CKM	CLK2	MAPK14
NEG2	CSNK2A1	DAPK1	DLG3	EPHA2	EPHB1	ERBB4	FGFR3	FLT4	GK	GUCY2C
	IGF1R	ITPK1	KIT	MARK3	MIP	ABCC1	NDUFA10	NPR2	PAK1	PDGFRA
	PFKFB2	PGK2	PIK3C2B	PIK3R2	PLK1	PRKACG	PRKCD	PRKCQ	MAPK6	MAP2K1
	PRKY	TWF1	GRK1	RPS6KB1	SKP1	STK4	TAF9	TIE1	TYK2	MAP3K12
	PIP4K2B	PIK3R3	CDC14B	CASK	RIOK3	SPHK1	MAP3K14	DYRK1B	MAPKAPK2	ROCK2
	IHPK1	NAALADL1	TRIM28	RAPGEF3	PMVK	TLK2	MAP4K1	ICK	MAST2	TSSK2

plate 12

NEG1	ULK3	TPK1	HIPK2	PIK3R4	CDKL3	IHPK2	RP6-213H19.1	RIPK4	ULK4	RFK
NEG2	NAGK	STK31	SCYL3	MARK4	PFTK2	CARD14	ADCK4	TSSK3	TSSK6	TTBK1
	NEK9	LMTK3	PLK5P	PNCK	PDIK1L	C9orf96	NRK	STK32C	EPHA6	CERKL
	MAST4	FGR	CDC2L1	PAK3	CDC2L2	PLK5P	ABL2	MYLK	ULK4	IKBKG
	MAP3K15	NME1-NME2	MAST4	PAK4	PIP5K1A	RAPGEF3	SNRK	MKNK1	ULK4	CSK
	PIM3	SBK1	LOC442075	ACVR1C	ABL2	PRKG1	COASY	MAST3	IHPK1	BRD2
	EIF2AK4	WEE2	LOC390975	LYN	LCK	PRKDC	CDC2L2	LMTK3	CAMK2B	DYRK1B

plate 13

	CSNK1G1	DGKZ								
	TTN	PLK5P								
	ATM	NEG1								
	CAMK2B	NEG2								
	CAMK2G									
	CSNK2A1									
	PAK7									

Table 6: siRNA Kinase Panel – list of genes

esiRNA Kinase Panel

plate 1

	AOF2	BOLL	CBX1	CHD2	DAZL	DDX52	DNTT	ENPP4	ERCC5	FEN1	
	APEX1	BRCA2	CDC45L	CNBP	DCLRE1A	DHFRL1	EEF1D	ENPP5	ERCC6	FMR1	
	APEX2	BRD4	CDC6	CPSF3L	DCLRE1B	DKC1	EIF2C2	EPRS	EWSR1	GADD45A	
	APTX	BRD7	CENPA	CRNKL1	DCLRE1C	DMC1	EIF3S8	ERCC1	EXO1	GADD45G	
	ASF1A	BRD9	CENPC1	CRY1	DDB1	DMRT1	EIF4G2	ERCC2	EZH1	GSPT1	
	ATRX	BRD9	CHAF1B	CUGBP1	DDX11	DNMT1	ELAVL4	ERCC3	EZH2	GSPT2	
	BLM	BRIP1	CHD1	CXorf34	DDX46	DNMT3B	ENDOGL1	ERCC4	FARSLB	RLUC (NEG)	

plate 2

	HCFC1	HDAC8	INTS6	LIG3	MCM6	MLH3	MSH6	NEIL3	NTHL1	PARP14	
	HDAC1	HDAC9	KHDRBS1	LIG4	MCM7	MPG	MUTYH	NGDN	NUCB2	PARP15	
	HDAC11	HIRA	KHSRP	LRPPRC	MCM8	MPHOSPH10	NBN	NIN	NUP153	PARP16	
	HDAC2	HIST1H4J	KIAA0664	LSM1	MECP2	MRE11A	NCBP2	NIPBL	OGG1	PARP6	
	HDAC3	HTF9C	KLHDC3	MCM2	MGMT	MSH2	NDN	NOL6	ORC1L	PARP8	
	HDAC4	IGHMBP2	LEF1	MCM3	MKI67IP	MSH3	NEIL1	NOVA1	PARP11	PARP9	
	HDAC5	INCENP	LIG1	MCM5	MLH1	MSH4	NEIL2	NSUN6	PARP12	FLUC (NEG)	

plate 3

	PCBP4	PMS2L2	POLG	POLR1C	RAD51C	RARS	RCL1	RFC5	RPL7L1	RRM2	
	PCNA	PNPT1	POLH	POLR2C	RAD51L1	RBBP4	RECQL	RIF1	RPS16	RRM2B	
	PELO	POLB	POLI	PRPF31	RAD51L3	RBM10	RECQL4	RNASE2	RPS27A	SETD1A	
	PES1	POLD1	POLL	PRPF8	RAD52	RBM14	RECQL5	RPA1	RPS27L	SETDB1	
	PMS1	POLD4	POLM	RAD1	RAD54B	RBM5	REV3L	RPA4	RPS3	SETDB2	
	PMS2	POLE	POLN	RAD50	RAD54L	RBM7	REXO4	RPL24	RPS3A	SETMAR	
	PMS2L11	POLE2	POLQ	RAD51	RAG2	RCC1	RFC4	RPL7	RPS4X	EGFP (NEG)	

plate 4

	SETX	SIRT6	SMARCB1	SMC6	SUV39H1	TERF1	TOP1MT	WDR33	XRCC5	HSA9761	
	SF3B3	SIRT7	SMARCD3	SMN1	SUV39H2	TERF2	TOP2A	WRN	XRCC6	NOL1	
	SHFM1	SLBP	SMC1A	SMUG1	SYCP1	TIGD2	TOP2B	WRNIP1	ZC3HAV1	INOC1	
	SIRT2	SMARCA2	SMC1B	SS18	TCF7	TIPARP	TOP3A	XPA	ZCCHC11	HDAC7A	
	SIRT3	SMARCA4	SMC2	STAG1	TCF7L2	TMEM62	TOPBP1	XPC	ZRANB3	KIAA1008	
	SIRT4	SMARCAD1	SMC3	STAG2	TDG	TOE1	TRMT1	XRCC2	EIF3S5	EIF3S6	
	SIRT5	SMARCAL1	SMC4	STAG3	TEP1	TOP1	UNG	XRCC3	BRCTD1	ANG	

plate 5

	C13orf21	ITGB4BP									
	C21orf55	POLA									
	C20orf179	TREX2									
	DDX12	PMS2L8									
	DHFR										
	DKFZp686O24166										
	DNMT2										

Table 7: esiRNA Panel – list of genes of the "Nucleic Acid Binding" Panel

9.3 Analysis

The cytotoxicity induced by the treatment with siRNA or esiRNA alone or in combination with trabectedin was evaluated 48 hours after trabectedin treatment and transfection with siRNA or esiRNA libraries, by MTS assay.

9.3.1 MTS assay

Tetrazolium reagents can be reduced by viable cells to generate formazan products that are directly soluble in cell culture medium. The negative charge of the formazan products, that contribute to solubility in cell culture medium, are thought to limit cell permeability of the tetrazolium.

This set of tetrazolium reagents is used in combination with intermediate electron acceptor reagents such as phenazine methyl sulfate (PMS) which can penetrate viable cells, become reduced in the cytoplasm or at the cell surface and exit the cells where they can convert the tetrazolium to the soluble formazan product. The general reaction scheme for this class of tetrazolium reagents is shown in figure 37.

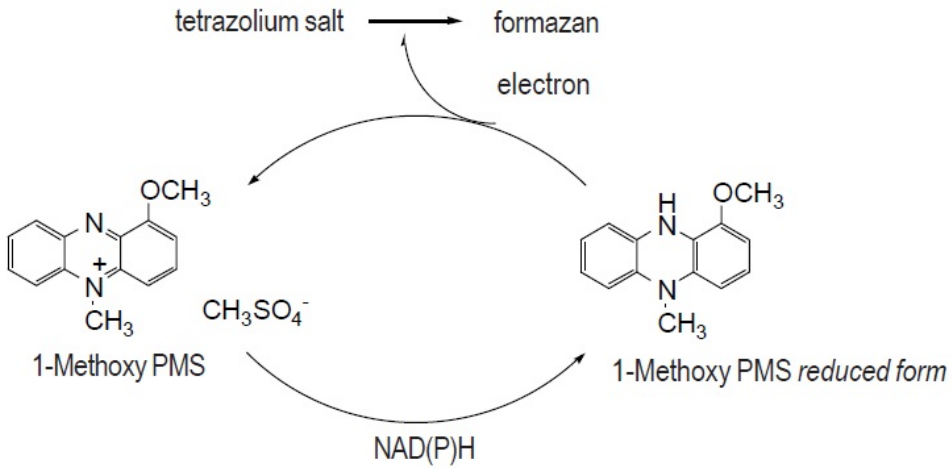

Figure 37: mechanism of action of MTS assay.

Picture from: http://www.dojindo.com/store/p/309-1-Methoxy-PMS.html

Cells were incubated with MTS (5µl/well) until the medium changed color (approximately 3-4 hours); this phenomenon indicates that cells metabolized the tetrazolium. The absorbance for each well was assessed by spectrophotometer (Tecan) at 490nm.

9.3.2 Analysis of the results obtained from the combination of trabectedin with the siRNA Kinase Panel library or esiRNA Panel of "Nucleic Acid Binding" molecules

Two types of analysis were performed using the absorbance values.

A) The absorbance of cells treated with trabectedin and transfected with siRNA (siRNA + trabectedin) / absorbance of cells transfected with siRNA alone. The final values obtained were multiply *100 to obtain the percentage, represented in the graphs (in the "results" section).

B) The absorbance of cells treated with trabectedin and transfected with siRNA (siRNA + trabectedin) / absorbance of cells treated with trabectedin. The final values obtained were multiply *100 to obtain the percentage, represented in the graphs (in the “results” section).

For each analysis:

- Were evaluated the outliers values. These are values that were outside the prefixed interval of confidence equal to 0.2.
- The blank values (only medium) were subtracted to each value of absorbance read. This represent the “noise”.
- Each sample was normalized for the correspondent value of siRNA negative present in each plate.
- For each plate were evaluated the cytotoxic effects derived from the lipofectamine (MOCK samples) and trabectedin treatment. This evaluation was important to be sure that the lipofectamine was not toxic for the cells and that the cytotoxic effect of trabectedin was closely the IC30, in each plate.

RESULTS

FIRST AIM

1. COMBINATION of TRABECTEDIN and CELL CYCLE CHECKPOINTS INHIBITORS

Trabectedin is an anticancer agent that exerts its activity by different mechanisms of action, related to the different type of tumors and cellular microenvironments.

The ability to induce DNA damage and G2 cell cycle blockade seems to represent the most common features that could generally describe the activity of this drug in different tumors, like Ewing's sarcomas.

Since the focus of my project was to find "intelligent combinations" with trabectedin I hypothesized that the combination of this drug with specific checkpoints inhibitors could induce a drastic alteration of the cell cycle regulation.

Using this approach I expected to potentiate the activity of trabectedin in Ewing's sarcoma cells.

To test my hypothesis, I combined trabectedin with chemical inhibitors of ChK1 and WEE1, two of the most important checkpoints regulators.

1.1 COMBINATION of TRABECTEDIN and ChK1 INHIBITOR PF-477736

ChK1 is a serine/threonine kinase that plays a crucial role in the regulation of G2/M transition.

To perform the experiments, I selected an inhibitor of ChK1, the chemical compound PF-477736 (figure 38), that acts with an ATP- competitive mechanism. I decided to use this compound because was already used in the laboratory and represents one of the most specific inhibitors for this kinase.

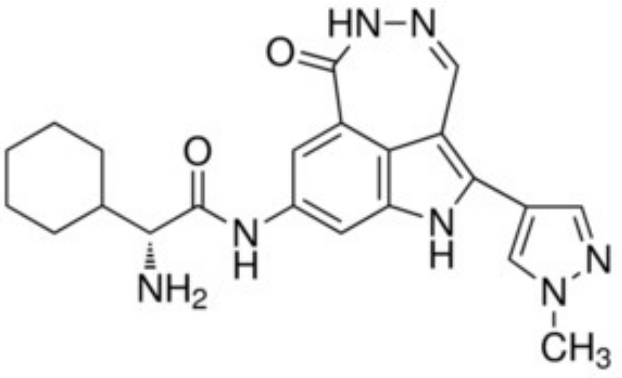

Figure 38: the chemical structure of PF-477736 ((2R)-2-Amino-2-cyclohexyl-N-[2-(1-methyl-1H-pyrazol-4-yl)-6-oxo-5,6-dihydro-1H-[1,2]diazepino[4,5,6-cd]indol-8-yl]-acetamide). ***Picture from Sigma Aldrich website (http://www.sigmaaldrich.com/catalog/product/sigma/pz0186?lang=it&region=IT).***

Since no data were available in literature as concern the sensitivity of TC1 Ewing's sarcoma cells to PF-477736, I performed preliminary "pilot experiments" using in parallel trabectedin and the ChK1 inhibitor.

Starting from these results I selected a range of concentrations for both drugs (from the ineffective to very toxic doses) to be used for the experiments of combination.

Figures 39 and 40 show the effects of trabectedin and PF-477736 given alone.

Figure 41 shows the results obtained treating TC-71 cells with different concentrations of trabectedin and three different concentrations of PF-477736, that were not cytotoxic when given alone.

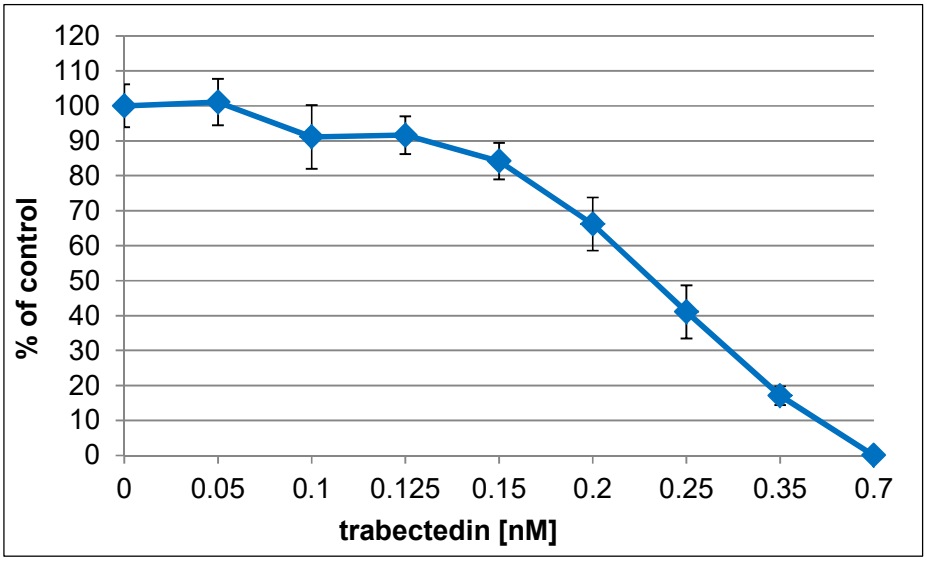

Figure 39: The dose-response curve of trabectedin (MTS analysis). Cells were seed in a 96 wells plate and after 48 hours (when the exponential growth was reached), treated with different drug concentrations. The cytotoxicity was evaluated by MTS assay, 48 hours after drug treatment. The time 48 hours was selected by previous experiments performed to determine the point in which the cytotoxicity was visible and the phenomenon of confluence in the control cells (not treated) was not reached. The values are the mean of six replicates. Bars ±sd.

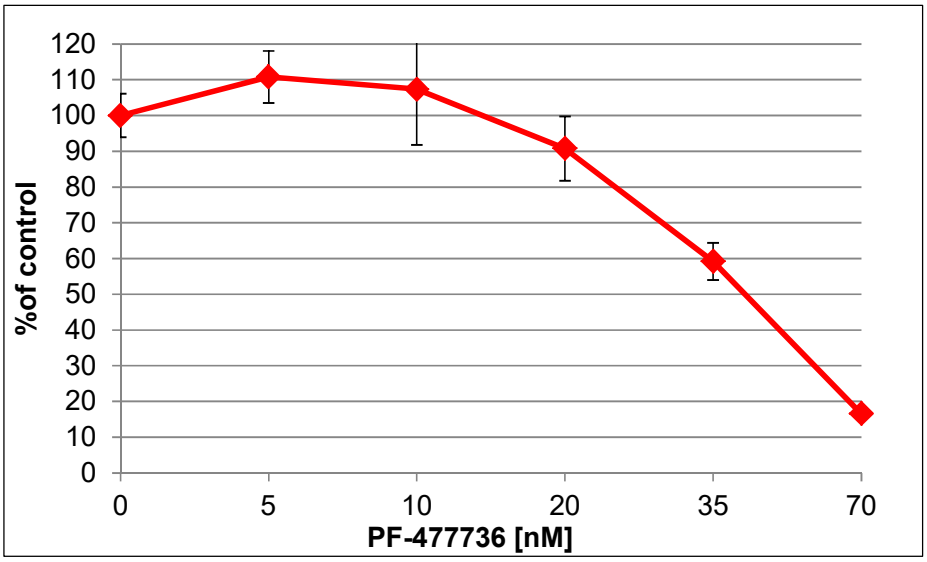

Figure 40: The dose-response curve of PF-477736 (MTS analysis). Cells were seed in a 96 wells plate and after 48 hours (when the exponential growth was reached), treated with different drug concentrations. The cytotoxicity was evaluated by MTS assay, 48 hours after drug treatment. The time 48 hours was selected by previous experiments performed to determine the point in which the

cytotoxicity was visible and the phenomenon of confluence in the control cells (not treated) was not reached. The values are the mean of six replicates. Bars ±sd.

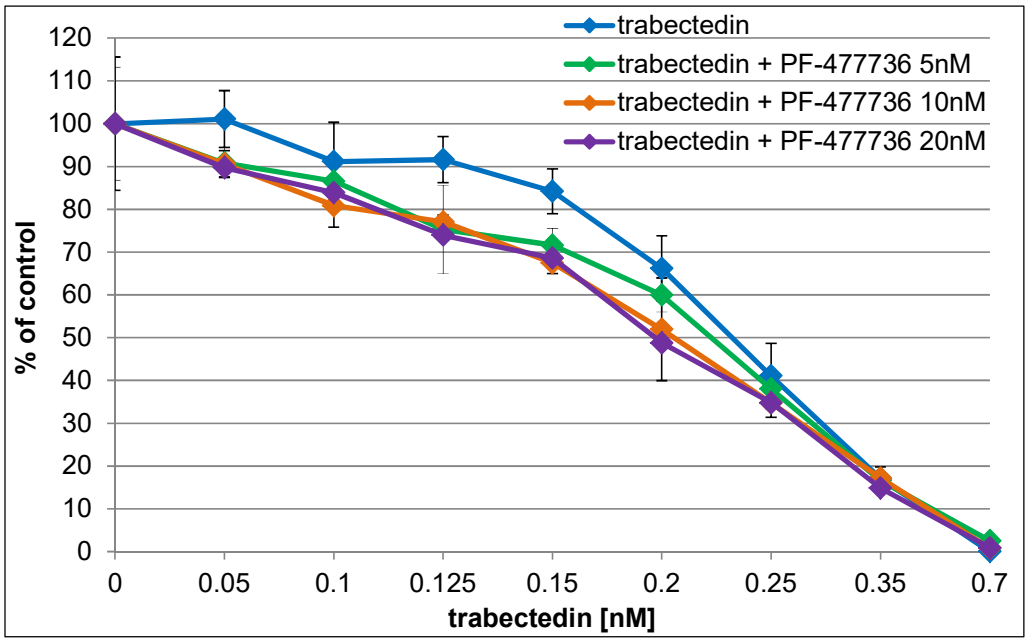

Figure 41: The MTS analysis of the combination trabectedin and PF-477736.

Cells were seed in a 96 wells plate and treated, simultaneously, with different drugs concentrations, 48 hours after (when the exponential growth phase was reached). The cytotoxicity was evaluated by MTS assay, 48 hours after drug treatment. The time 48 hours was selected by previous experiments performed to determine the point in which the cytotoxicity was visible and the phenomenon of confluence in the control cells (not treated) was not reached.

The values reported are expressed as the % of control. Bars ±sd. The statistical analysis (one-way ANOVA) showed that at all the concentrations there was not any significant difference between trabectedin alone or given in combination with different concentrations of PF-477736.

The dose-response curves represented in figure 41 clearly show that the addition of PF-477736 (ChK1 inhibitor) did not potentiate the cytotoxicity induced by trabectedin treatment.

This finding was unexpected since previous data reported in the literature indicated that PF-477736, or other ChK1 inhibitors, potentiate the cytotoxicity of DNA damage agents, causing a G2/M block, particularly when p53 is mutated or absent (like in the TC71 cell line analysed) (Koniaras *et al*, 2001; Luo *et al*, 2001; Mitchell *et al*, 2010).

One of the hypothesis that could be considered to explain my results is that trabectedin could interferes with the expression of the kinase ChK1.

In fact, if trabectedin as single agent is able to interfere with the expression of ChK1 (the target of PF-477736), it could act antagonizing the effect of the inhibitor.

This hypothesis is based on the fact that trabectedin was previously reported to modulate the transcription and expression of several genes including those involved in the cell cycle regulation (Minuzzo *et al*, 2005; Uboldi *et al*, 2012).

As illustrated in figure 42 the treatment with doses of trabectedin around the IC50 induced a marked reduction of ChK1 expression.

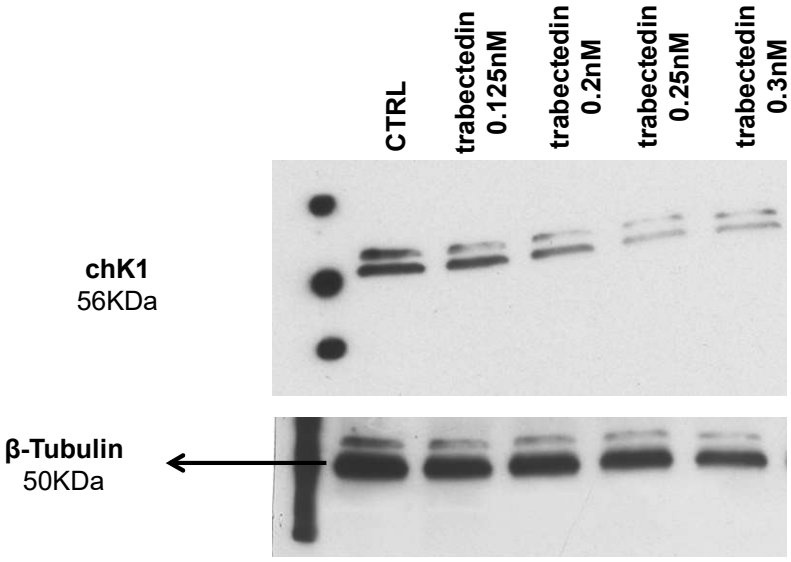

Figure 42: Western blotting analysis. The cells were pelleted 72hours after continuous treatment with trabectedin. Lysates were performed as described in "material and methods" and 30µg of proteins were load for each sample. Antibodies against ChK1 and the housekeeping β-tubulin were used.

The western blotting analysis was performed after 72 hours of continuous treatment. This time point was selected to be sure that the impact of trabectedin on ChK1 protein expression could be clearly evidenced; although it could not be denied that also at early time points trabectedin's treatment could induce a downregulation of ChK1.

This data confirmed the hypothesis that trabectedin interferes with ChK1 expression and could probably represents the reason why the concomitant treatment with the chemical ChK1 inhibitor (PF-477736) was not effective to potentiate the trabectedin activity.

The indication obtained by these results is that trabectedin itself is an inhibitor of ChK1, not acting on the catalytic activity of the enzyme, but on its expression.

1.2 COMBINATION of TRABECTEDIN and WEE1 INHIBITOR AZD-1775

Previous data in literature showed that the combination of ChK1 and Wee1 inhibitors is synergistic against different human tumors cell lines (Carrassa *et al*, 2012; Davies *et al*, 2011; Guertin *et al*, 2012; Russell *et al*, 2013). These data combined with the previously results obtained (the ability of trabectedin to interfere with the ChK1 expression) prompt me to hypothesize that the mechanism of action of trabectedin could be exploited in order to potentiate the cytotoxic effects of the WEE1 inhibitor, AZD-1775 (figure 43).

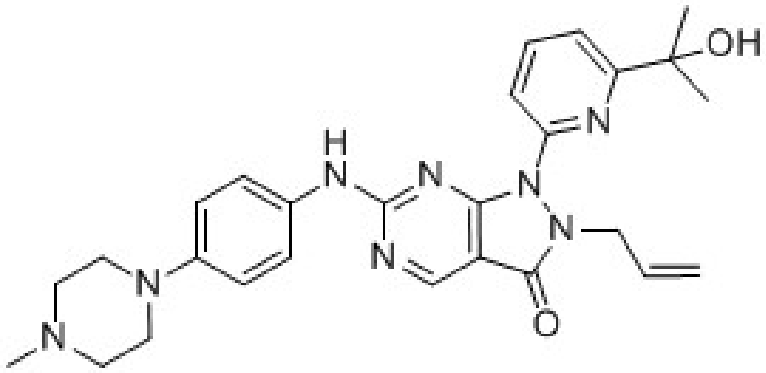

Figure 43: Chemical structure of AZD-1775 (2-allyl-1-(6-(2-hydroxypropan-2-yl)pyridin-2-yl)-6-((4-(4-methylpiperazin-1-yl)phenyl)amino)-1H-pyrazolo[3,4-d]pyrimidin-3(2H)-one).

Picture adapted from : http://www.medkoo.com/products/4700

Figures 44 and 45 show the dose response curves of trabectedin and AZD-1775 used as single agents, respectively.

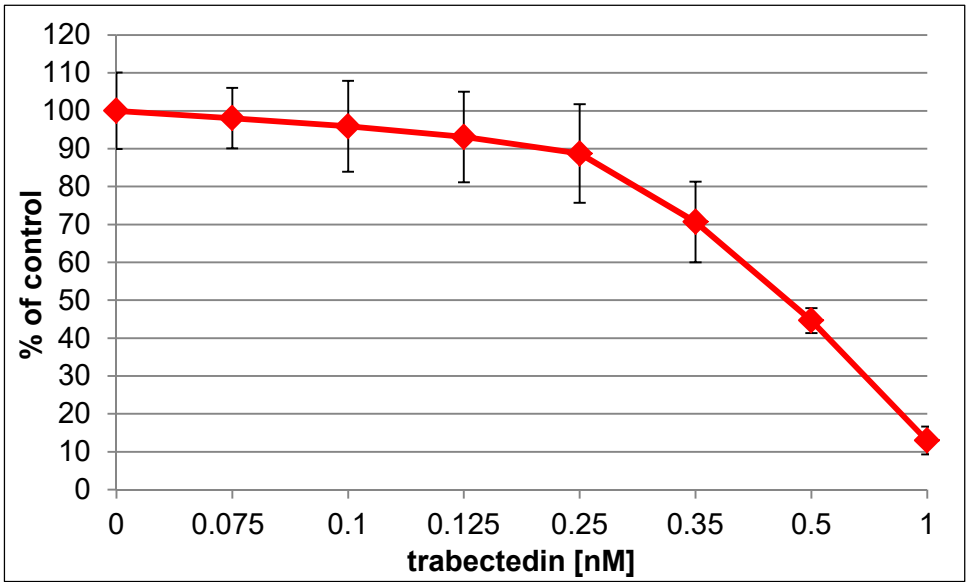

Figure 44: The dose-response curve of trabectedin (MTS analysis).

Cells were seed in a 96 wells plate and after 48 hours (when the exponential growth was reached), treated with different drug concentrations. The cytotoxicity was evaluated by MTS assay, 48 hours after drug treatment. The time 48 hours was selected by previous experiments performed to determine the point in which the cytotoxicity was visible and the phenomenon of confluence in the control cells (not treated) was not reached. The values are the mean of six replicates. Bars ±sd.

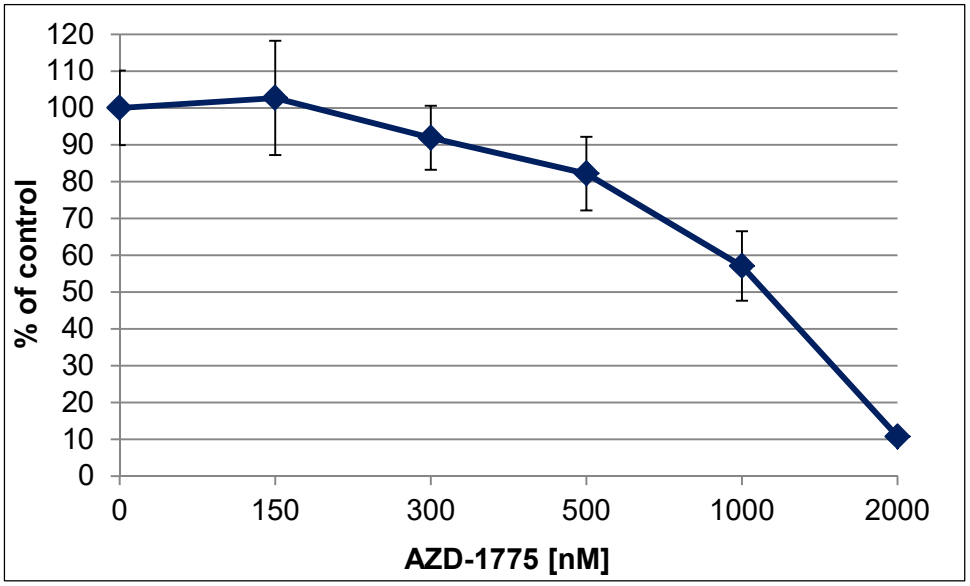

Figure 45: The dose-response curve of AZD-1775 (MTS analysis). Cells were seed in a 96 wells plate and after 48 hours (when the exponential growth was reached), treated with different drug concentrations. The cytotoxicity was evaluated by MTS assay, 48 hours after drug treatment.
The time 48 hours was selected by previous experiments performed to determine the point in which the cytotoxicity was visible and the phenomenon of confluence in the control cells (not treated) was not reached. The values are the mean of six replicates. Bars ±sd.

Figure 46 shows the combination of different concentrations of trabectedin combined with three different concentrations of AZD-1775, that were not or slightly toxic when used as single agent. To perform the experiment of combinations I arbitrarily decided to use different concentrations of trabectedin combined with three concentrations of AZD-1775 that represent approximately an inactive dose, the IC50 and a very active (around IC70) dose of AZD-1775.

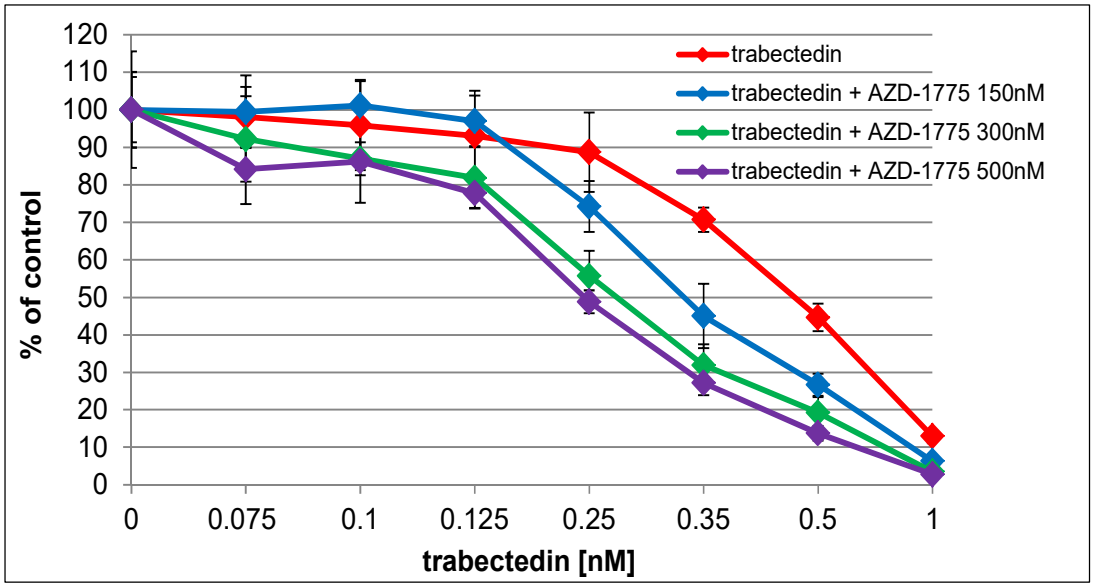

Figure 46: **The MTS analysis of the combination trabectedin and AZD-1775. The values, mean of six replicates, are expressed as the % of control. Bars ±sd.**

Cells were seed in a 96 wells plate and treated, simultaneously, with different drugs concentrations, 48 hours after (when the exponential growth phase was reached). The evaluation of the cytotoxicity was evaluated by MTS assay, 48 hours after drug treatment. The time 48 hours was selected by previous experiments performed to determine the point in which the cytotoxicity was visible and the phenomenon of confluence in the control cells (not treated) was not reached.

The results obtained show that the combination of AZD-1775 with trabectedin is effective to enhance the cytotoxicity induced by trabectedin given as single agent; these data suggest that the combination of the two drugs could be defined as synergic.

The possibility to define synergic or not the combination of trabectedin and AZD-1775 derived from the use of the isobologram's analysis. In this approach the isobolograms were generated fixing three doses of trabectedin and AZD-1775 that, for each drug, represented the IC30, 50 and 70. The blue dots in each graph (figure 48) represent each combination that reaches the IC30, 50 or 70.

The isobolograms represented in figure 47 demonstrate that the combination of trabectedin with AZD-1775 is synergic, especially at doses around the IC50 and 70.

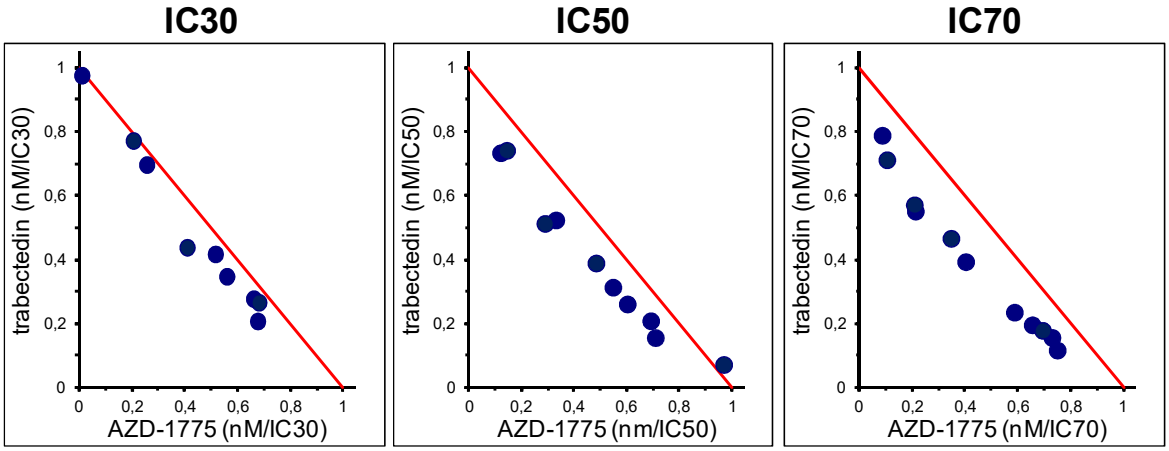

Figure 47: The isobolograms referred to the combination of trabectedin and AZD-1775. Each dot represents the value of combination trabectedin and AZD-1775. To define synergistic the combination the dot must be <1. Values >1 define an antagonistic effect, =1 an additive effect.

Both drugs (trabectedin and AZD-1775) act by interfering with the cell cycle progression. To better characterize the cell cycle effects and perturbations induced by the combination of trabectedin and AZD-1775, a flow cytometric (FACS) analysis was performed.

The goal of this approach was to determine if the combination of AZD-1775 (WEE1 inhibitor) with not or only marginally cytotoxic doses of trabectedin, could potentiate the cell cycle perturbations usually caused by trabectedin treatment. To reach this result I decided to perform the cell cycle experiments using doses of trabectedin around the IC30 and 40.

The effects induced by trabectedin treatment on cell cycle are well known; this anticancer agent induces a block in the G2/M phase of the cell cycle (Tavecchio *et al*, 2007), starting from the 24 hours after administration. The entity of the block is proportionally related to the concentration of drug used; a higher concentration of trabectedin (= or > IC50) induces a G2/M block that was not normally solved in the 72 hours, whether a less toxic concentration (<IC50) induces a G2/M block that is normally solved until 72 hours.

Figure 48 shows the cytotoxic effects induced by trabectedin and AZD-1775 given alone, or in combination, at 24 - 48 and 72 hours after continuous treatment, in TC71 cells.

The Ewing's sarcoma cells were seeded in a 6wells/plate and treated with trabectedin or AZD-1775 as single agents or in combination, when they reached the exponential growth phase. Twenty-four, 48 and 72 hours after treatment the cells were detached, counted by coulter counter, and fixed for the FACS analysis. Further details are described in the section "Materials and Methods".

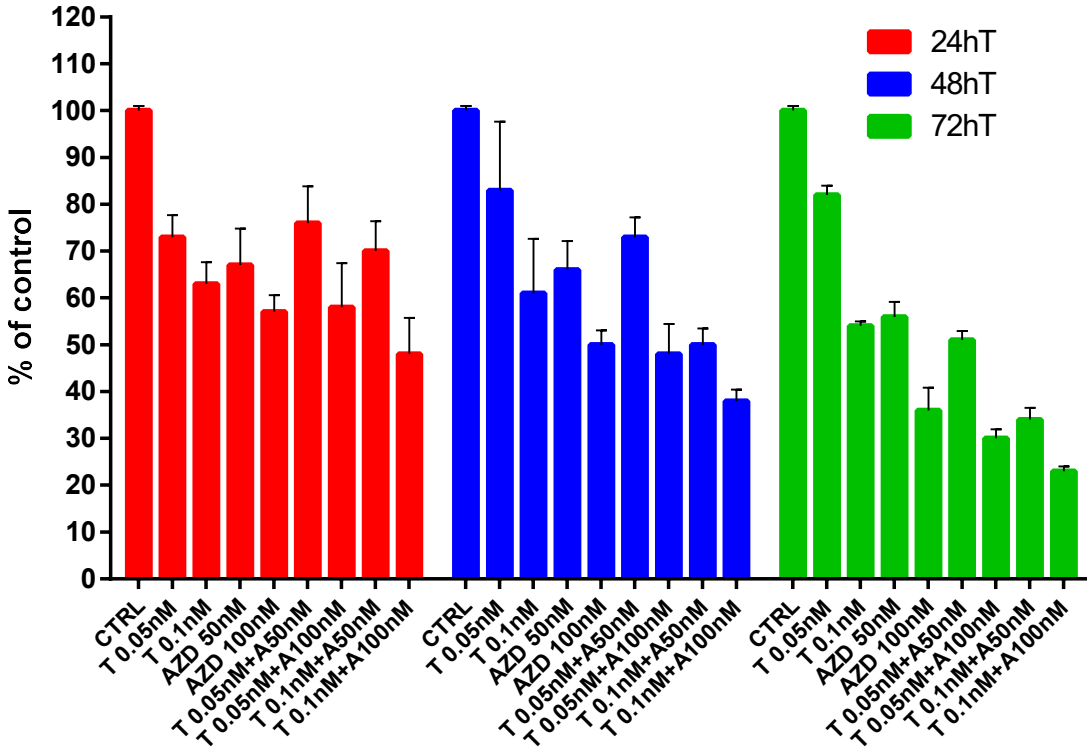

Figure 48: analysis of the cytotoxicity induced by trabectedin alone (T), AZD-1775 alone (AZD) or by the combination trabectedin with AZD-1775 (T concentration + AZD concentration). The values, mean of six replicates, are expressed as the % of control. Bars ±sd.

The concentrations of trabectedin (0.05 and 0.1nM) and AZD-1775 (50 and 100nM) used represented approximately the IC30 and IC40, respectively, at 24 hours of continuous treatment, as shown in figure 48.

Figure 49 shows the cell cycle perturbations induced by trabectedin and AZD-1775 given as single agents or in combination at 24, 48 and 72 hours after continuous treatment.

The results obtained showed that trabectedin, as expected, induced a G2/M block at 24 hours after treatment that was solved until the 48 hours (trabectedin 0.05nM) or 72 hours (trabectedin 0.1nM) of continuous treatment (blue histograms) (figure 49).

The inhibitor of WEE1, AZD-1775, used as single agent did not cause any detectable block in the cell cycle at any concentration or time considered (green histograms).

The combination of trabectedin and AZD-1775 induced an alteration of the cell distribution in the cell cycle phases (figure 49), in comparison to the distribution of the cells treated with trabectedin alone.

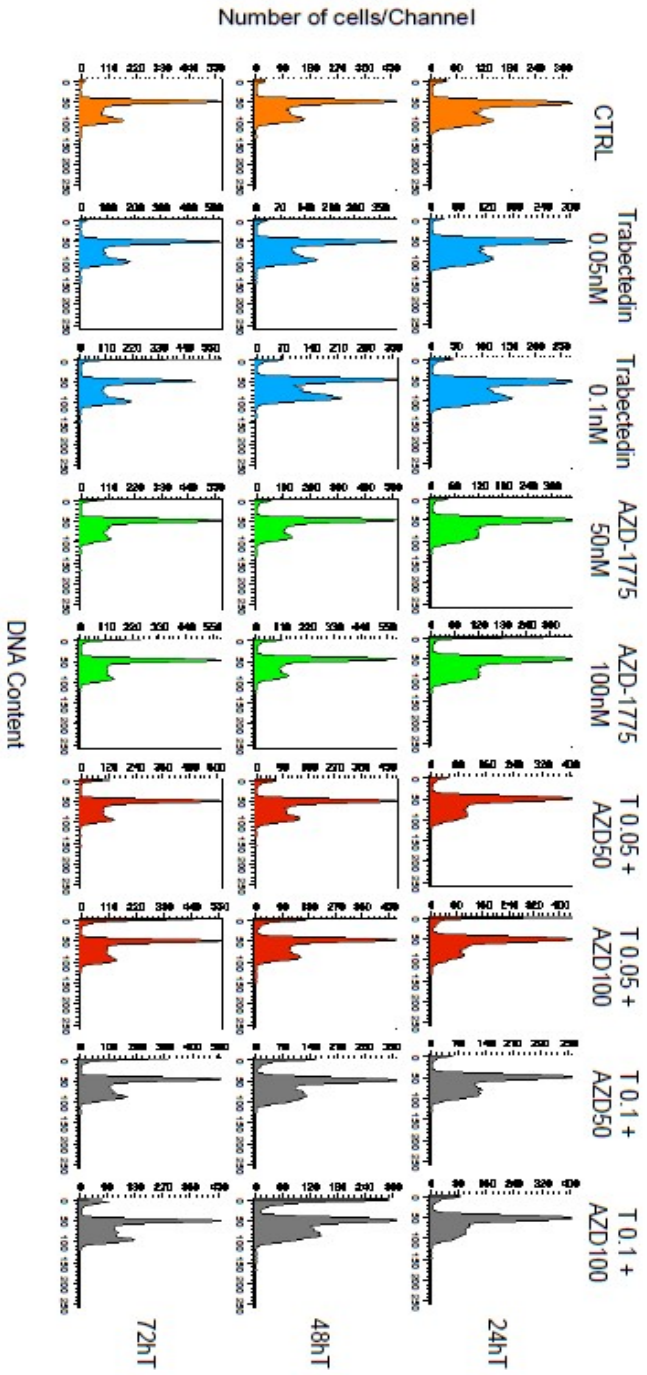

Figure 49: Flow cytometric analysis of cell cycle perturbations induced by trabectedin (T) and AZD-1775 (AZD) used as single agents or in combination (T concentration + AZD concentration), performed at 24, 48 and 72 hours after continuous treatment. The blue histograms are referred to trabectedin used as single agent, the green one to AZD-1775 used as single agent, the red one to the combination of trabectedin 0.05nM with both the AZD-1775 concentrations and the grey one to the combination of trabectedin 0.1nM with both the AZD-1775 concentrations.

These data are consistent with the synergism effects derived from the combination of trabectedin and AZD-1775, previously showed and discussed in figures 46 and 47.

SECOND AIM

1. THE TRANSCRIPTIONAL MECHANISM of ACTION of TRABECTEDIN IN EWING'S SARCOMA*: THE EFFECTS of THE DRUG on the BINDING of CHIMERIC PROTEIN EWS-FLI1 to SELECTED TARGET PROMOTERS.*

Previous studies performed by Grohar et al. showed that in Ewing's sarcoma (ES) trabectedin acts inducing the modulation of the transcription of several genes that are under the control of the fusion gene EWS-FLI1 (Grohar *et al*, 2011).

A similar mechanism of action was previously observed in myxoid liposarcomas in which was demonstrated the ability of trabectedin to displace the chimeric protein FUS-CHOP (hallmark of this pathology) from different target genes. Di Giandomenico *et al*, 2014, showed, by Chromatin Immunoprecipitation (ChIP) analysis, in *in vitro* and *ex vivo* experiments, that trabectedin treatment induced a detachment of the chimeric protein FUS-CHOP from its target promoters with the consequent modulation of the transcription of the target genes.

Starting from these observations I evaluated if the modulation of gene transcription observed by Grohar et al. (Grohar *et al*, 2011) was related to the ability of trabectedin to detach the EWS-FLI1 from its target promoters, in Ewing's sarcoma. To reach this result I performed the ChIP analysis on TC71 cells treated with a concentration of trabectedin that represent the IC50. I chose a higher concentration of trabectedin in order to better appreciate the effect induced by the drug at the molecular level.

I evaluated the binding of the chimeric protein EWS-FLI1 to three of its target promoters, CD99, TGFβR2 and NR0B1, using specific antibodies. I chose these target genes because represents three of the most important recognized target for the chimeric protein.

The schematic representation of the usual procedure used for the chromatin immunoprecipitation assay is shown in figure 50.

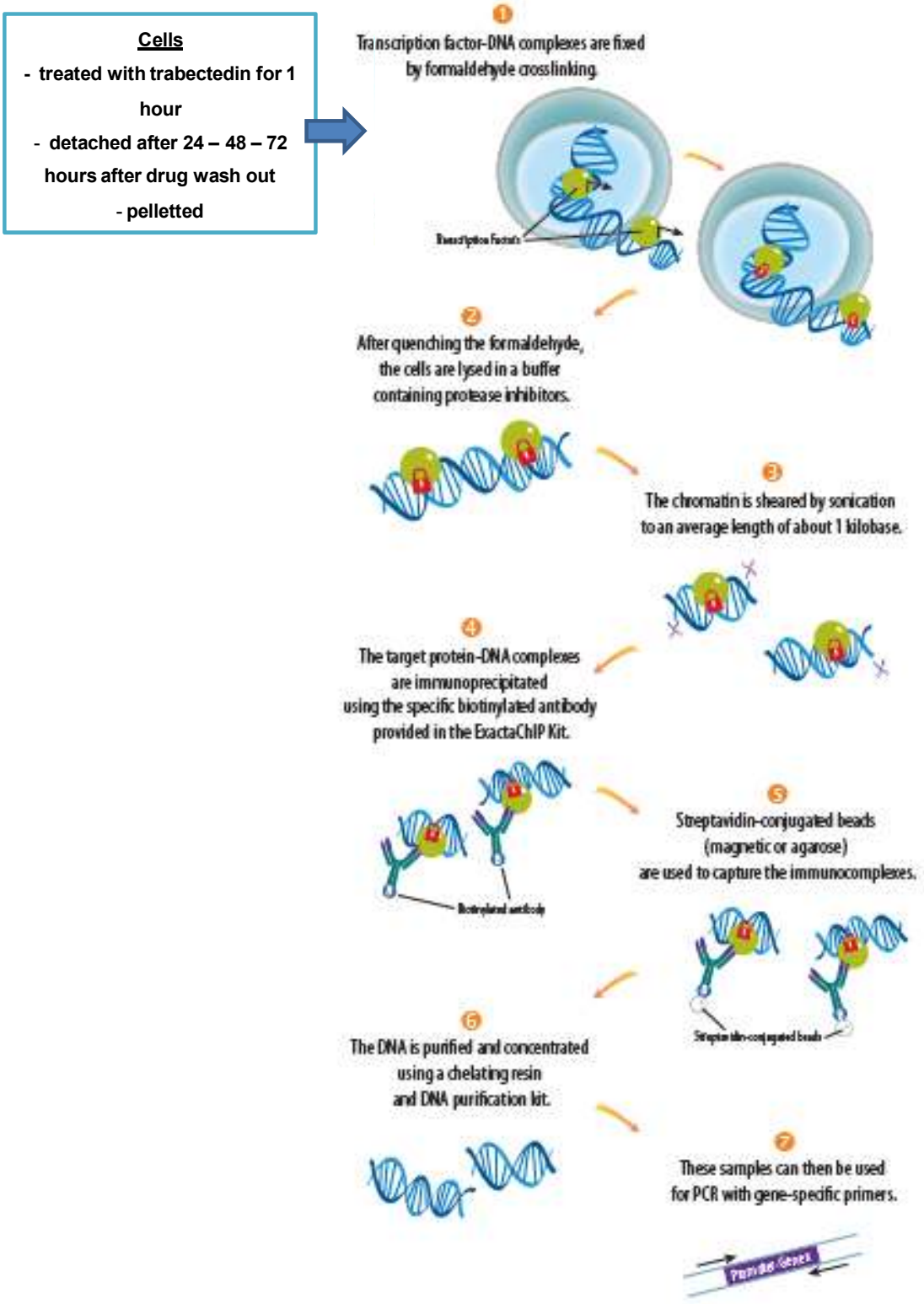

Figure 50: the different steps of the chromatin immunoprecipitation assay performed starting from a cellular sample.

Details of the ChIP method are reported in “Material and Methods” at the section “Chromatin Immunoprecipitation assay”.

Figure 51 shows the binding of the EWS-FLI1 chimeric protein to the promoters of CD99, TGFβR2 and NR0B1, after 1 hour of treatment with trabectedin (used at a concentration around the IC50: 2.5nM) and 24 - 48 and 72 hours after drug washout.

For the chromatin immunoprecipitation assay I decided to perform the drug washout, to avoid that the high dose of drug selected (IC50) could become extremely cytotoxic, especially at 48 and 72 hours.

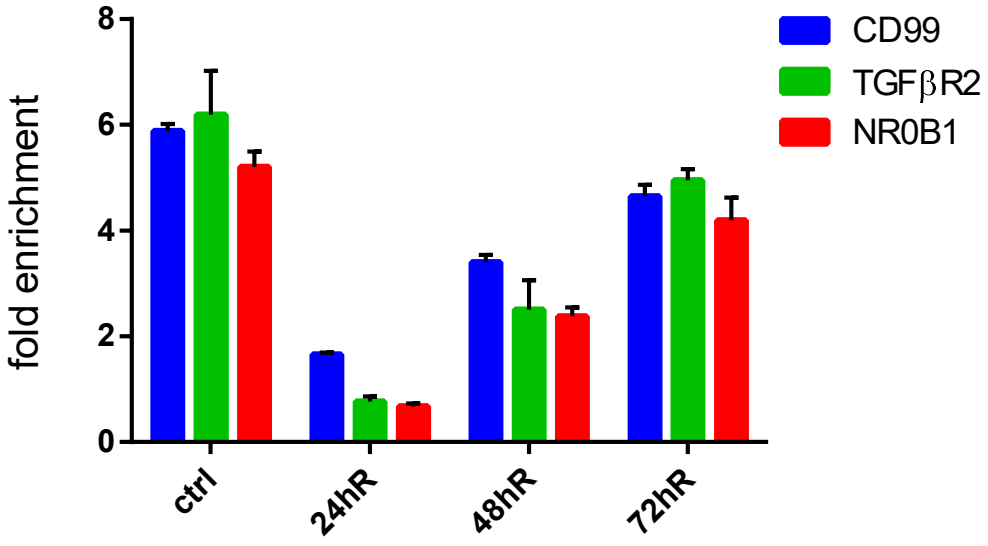

Figure 51: The promoter region of CD99, TGFβR2 and NR0B1 were amplified using specific designed primers. Values were measured as fold enrichment over a Flag control antibody in quantitative RT-PCR analysis. Cells were seed in flasks T75 (in order to recover a higher number of cells) and treated for 1 hour with trabectedin when they reached the exponential growth phase (48 hours after the seed). Cells were finally collected 24, 48 and 72 hours after recovery. Each sample was analyzed in triplicate and three independent RT-PCR were performed. Bars ±sd.

The results show that trabectedin induced a detachment of the chimeric protein (EWS-FLI1) from all the three target promoters analyzed, appreciable already at 24 hours after drug washout. These data are in agreement with the data previously obtained by Di Giandomenico et al. (Di Giandomenico *et al*, 2014) in a myxoid liposarcoma model.

Differently from what observed in the myxoid liposarcoma model, the re-attachment of the chimeric protein to the target promoters in Ewing's sarcomas is more rapid, starting from 48 hours after drug washout (figure 51).

In order to evaluate if this mechanism was active and effective also in *in vivo* models, the ChIP assay was performed in *ex vivo* samples, from xenografts tumors treated or not with trabectedin. The antitumor activity of trabectedin, evaluated in TC71 xenografts after intravenous (i.v.) administration of 0.15 mg/kg of trabectedin with the classical schedule q7dX3 (every seven days for three times), is shown in figure 52.

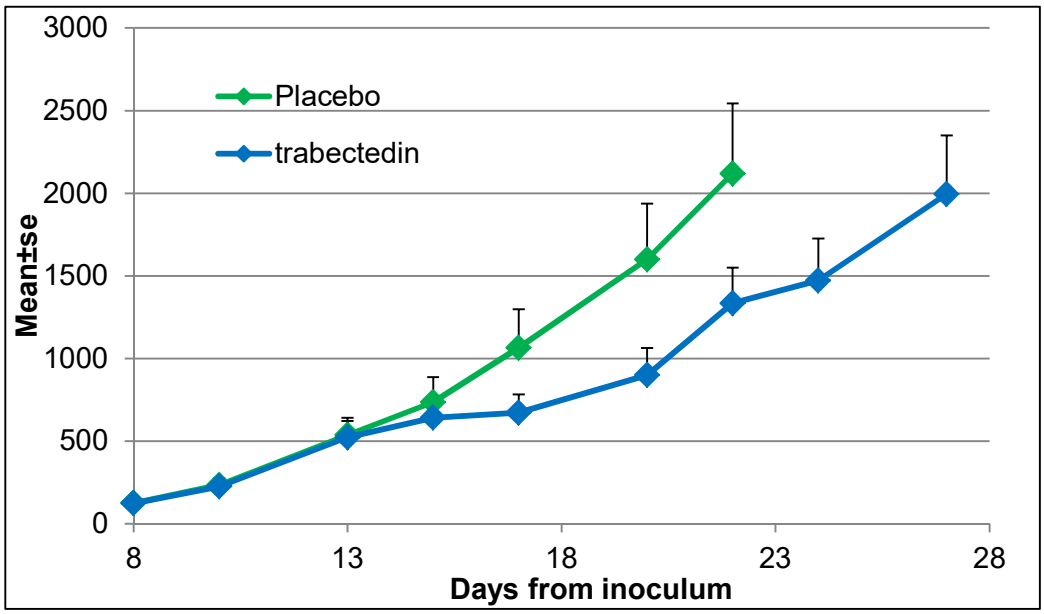

Figure 52: Antitumor activity of trabectedin (blue line) in TC71 xenograft model, compared to a placebo (green line).

The antitumor activity was expressed as T/C%, where T and C were the mean tumor weight of treated and control groups, respectively. The results show that trabectedin was able to slightly reduce the tumor growth with a best T/C of 56.2% (day 20).

To perform the Chromatin Immunoprecipitation assay the tumor samples were collected 24 hours after the first dose in order to evaluate the acute effect induced by trabectedin treatment on the target promoters; the collection of tumor samples at 24 hours and seven days after the third dose is important in order to evaluate the effects derived from the accumulation of perturbations induced by three administrations of trabectedin. The tumor samples collected were sectioned, crosslinked and, after quenching and washes with PBS, fragmented and homogenized, to obtain a cellular suspension. Further details are described in the “Materials and Methods” section.

The results, shown in figure 53, highlighted the ability of trabectedin to detach the EWS-FLI1 chimeric protein from the target promoters CD99, TGFβR2 and NR0B1, already 24 hours after the first dose.

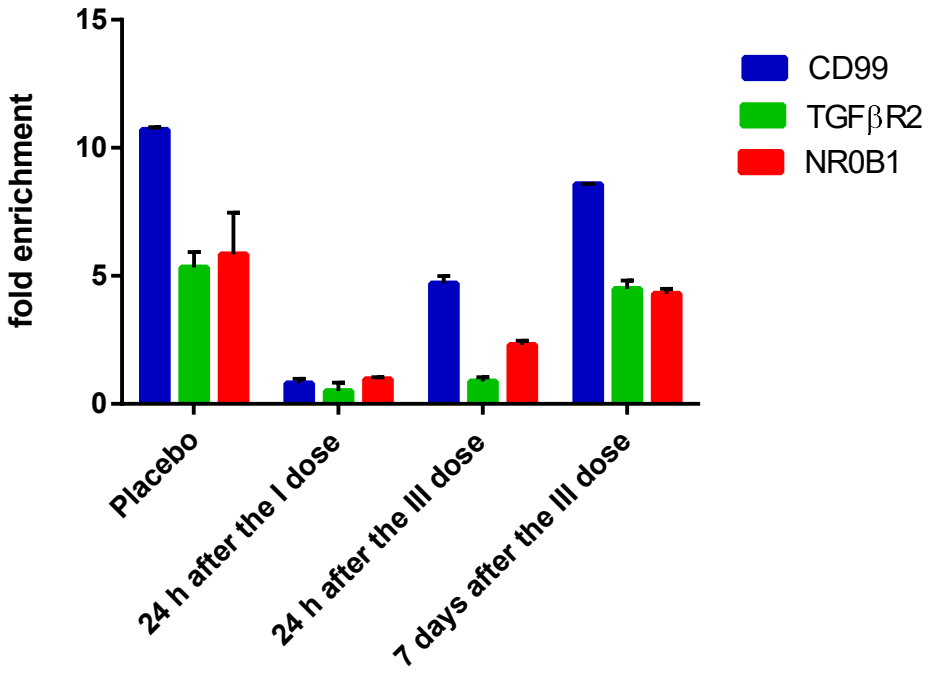

Figure 53: The promoter region of CD99, TGFβR2 and NR0B1 were amplified using specific designed primers. Values were measured as fold enrichment over a Flag control antibody in quantitative RT-PCR analysis. The tumor samples were collected 24 hours after the first and third doses and 7 days after the third dose. Each sample was analyzed in triplicate and three independent RT-PCR were performed. Bars ±sd.

The re-attachment of the EWS-FLI1 chimeric protein, in absence of trabectedin treatment, is appreciable from 24 hours (CD99 promoter) to 7 days after the third dose (TGFβR2 and NR0B1).

The rapid reversibility of this effect suggests that the slight antitumor activity of trabectedin, administered as single agent, could be due to a too short change in gene transcription that did not result in a significant pharmacologically effect.

These preclinical findings are in keeping with the relative limited antitumor activity of trabectedin (administered as single agent) observed in patients affected by ES (Baruchel *et al*, 2012) and highlighted the need to find new ways to increase the efficacy of this drug by the identification of effective combinations.

The identification of new effective combinations with trabectedin is subordinate to the development of a methodology useful to find new targets.

2. THE USE of siRNA LIBRARIES to IDENTIFY NEW TARGETS SUITABLE for the COMBINATORIAL APPROACH with TRABECTEDIN

In this work I approached the possibility to find new targets for “intelligent combination” with trabectedin by a siRNA libraries approach.

The idea was to use a sequential treatment, anticancer drug followed by a siRNA library that targets, inhibiting, a selected class of molecules.

To my knowledge no previous reports are available on this type of sequential treatment.

In order to develop a methodology suitable for this new approach I decided to start with two siRNA libraries: one made of siRNAs that downregulate genes encoding for kinases and the other one with siRNAs that downregulate genes encoded for proteins that bind DNA. I decided to start with these libraries because my preliminary experiments indicated a possible synergism between trabectedin and the inhibition of a kinase (WEE1) and because the involvement of trabectedin in mechanisms of DNA repair are well known.

Details about the two libraries are reported in the “Materials and Methods“ section.

The experimental plan was designed to obtain detailed information about:

A) The optimal number of cells to be seeded in order to treat them in the exponential growth phase, not reaching confluence at the end of the experiment.

   This step was very important as the TC71 cells appear to be prone to detach as soon as they reach the confluence status.

B) The definition the best concentration of trabectedin to detect the potential synergism.

C) The definition the best time point to evaluate the cytotoxic effects induced by the combination of trabectedin with the siRNA libraries.

- Experiments performed in relation to the item **A**

  In these preliminary experiments I seeded the cells using different cellular concentration (from 300 to 5000 cells/well) that, in exponential phase, were treated or not with lipofectamine (0.05 µl/well).

  The evaluation of the toxicity was performed using MTS assay and evaluating the fraction of surviving cells after transfection, compared with not transfected controls.

  Figure 54 shows that the lipofectamine was not toxic neither at 48 hours (Panel A) nor at 72 hours (Panel B) after treatment.

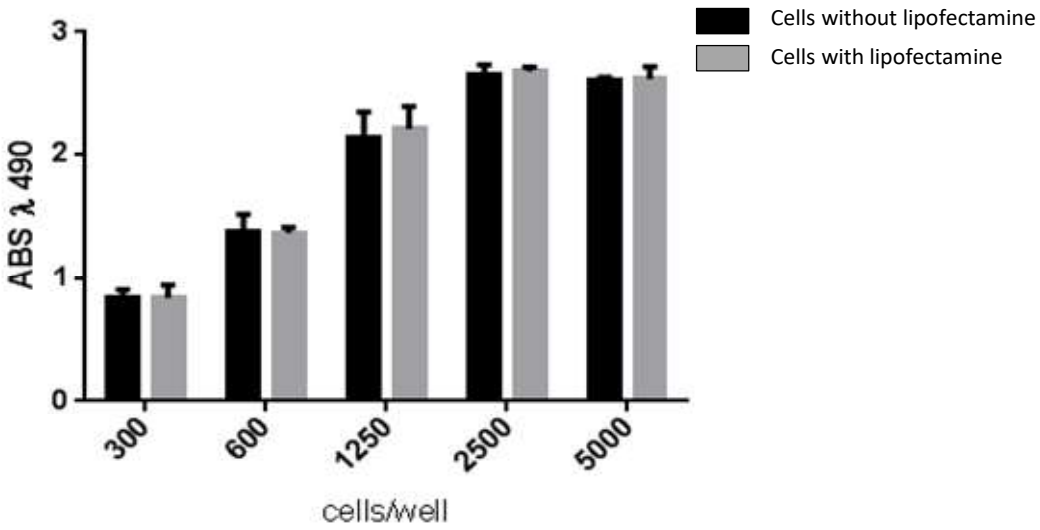

Figure 54 - Panel A: Evaluation of the toxicity of lipofectamine (0.05 µl/well) in TC71 cells. The cells were seed at different concentrations in 384 wells/plate and treated with lipofectamine or with medium (as control), 48 hours later. The time 48 hours was selected by previous experiments performed to determine the point in which the cytotoxicity was visible and the phenomenon of confluence in the control cells (not treated) was not reached. The evaluation was performed by MTS assay, 48 hours after transfection. The values represent the mean of six replicates. Bars ±sd.

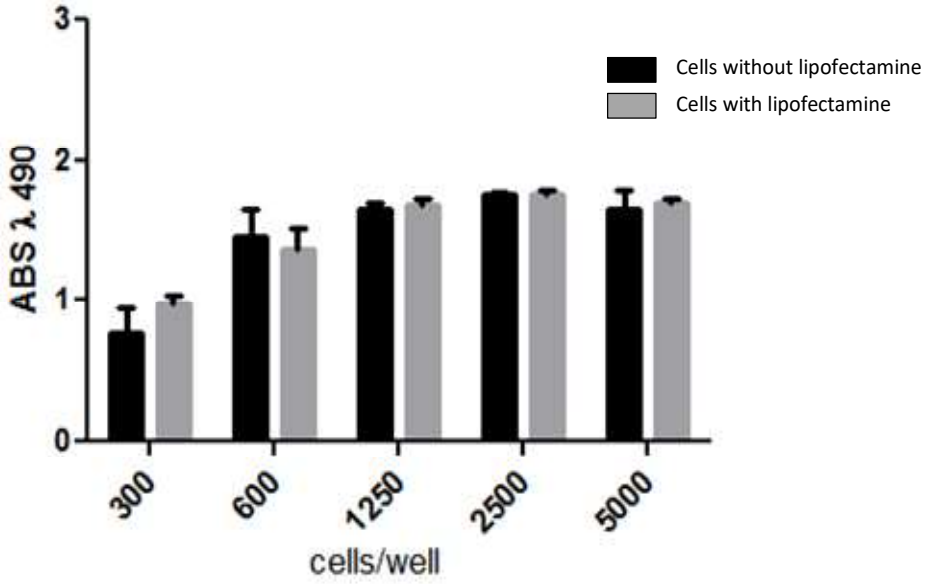

Figure 54 - Panel B: Evaluation of the toxicity of lipofectamine (0.05 µl/well) in TC71 cells. The cells were seed at different concentrations in 384 wells/plate and treated with lipofectamine or with medium (as control), 48 hours later. The time 48 hours was selected by previous experiments performed to determine the point in which the cytotoxicity was visible and the phenomenon of confluence in the control cells (not treated) was not reached. The evaluation was performed by MTS assay, 72 hours after transfection. The values represent the mean of six replicates. Bars ±sd.

The observation of the cells by microscope showed that using concentrations equal or higher than 600 cells/well the confluence was already reach at 24 hours. Therefore I decided to perform the subsequent experiments using the cellular concentration of 300 cells/well to be sure to avoid the phenomenon of confluence.

During the "pilot" experiments the transfection efficiency was evaluated using a commercial siRNA against ChK1 (a gene already evaluated in the studies performed combining the inhibitor of ChK1 and trabectedin in the paragraph 1 of this section) and evaluating the expression by western blotting.

The figure 55 shows that the quantity of lipofectamine used for the transfection (0.05 µl/well) was not toxic and sufficient to downregulate, but not abrogate, the ChK1 expression.

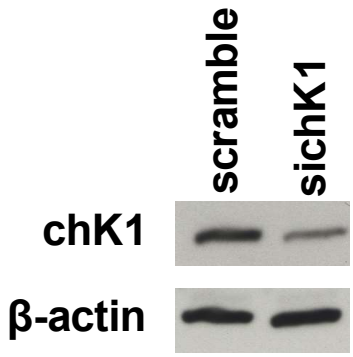

Figure 55: Western Blotting analysis of TC71 cells transfected with a siRNA negative (scramble) or a siRNA against ChK1 (siChK1).

Cells were seeded in 384 well plates at the concentration of 300 cells/well and transfected with siChK1 after 48hours. 24-48 and 72 hours after transfection the cells were pelleted and processed for the western blotting analysis. The results reported here are referred to the time of 48hours, the best time point to observe the results avoiding the phenomenon of confluence, as assessed by the preliminary experiments.

- Experiments performed in relation to the item **B**

Figure 56 shows the cytotoxicity induced by 48 hours of exposure to trabectedin.

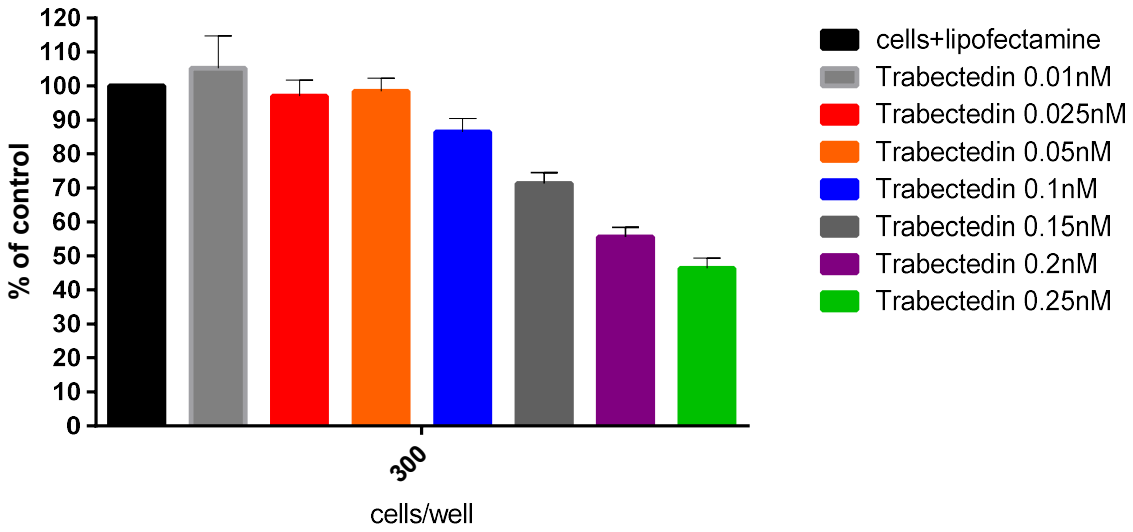

Figure 56: Evaluation of the toxicity induced by 48 hours of exposure to different concentrations of trabectedin. TC71 cells, seeded in 384 well/plates at the concentration of 300 cells/well, were treated 48 hours later, when reached the exponential phase. The evaluation was performed by MTS assay, 48 hours after treatment. The values represent the mean of six replicates. Bars ±sd.

I have then decided to use a concentration of trabectedin (0.15nM) that induced a 30% of mortality (IC30), for the experiments of combination. I selected this concentration because during the experiments of combination is important to use a drug concentration not extremely toxic, in order to avoid that the final results will derived from the toxicity of the single drug used.

- Experiments performed in relation to the item **C**

The time point selected was 48hours after treatment and transfection. At this time point the downregulation of ChK1 – a marker of the transfection efficiency - induced by the siChK1 transfection was evident. The lipofectamine was not toxic and cells have not reached the confluence.

2.1 siRNA kinase Panel transfection

Considering the very high number of siRNAs, I decided to fraction the library into two parts to increase the feasibility and reduce the possibility to introduce errors and variability.
In the first experiment I used the first 420 siRNAs pre-seeded in the library.
Each siRNA was assessed in triplicate, in three different plates.

The pilot experiments performed to define a “working protocol” for the experiments of combination of trabectedin and siRNA library, in TC71 cells, were described in the paragraph ”7.2 Transfection with libraries” in the “Materials and Methods” section.
The final protocol that I obtained and optimized will be used as a draft for this kind of experiments, in different cell lines, using different anticancer agents, prior assessment of the right conditions.

- **WORKING PROTOCOL**

1. At day 0 seed the cells in a 384 well/plates, in a final volume of 25 µl, making a frame of PBS, in order to avoid the phenomenon of evaporation. Incubate the plates for 48 hours in a humidified incubator at 37°C with 5% CO2.
2. At day 2 (48 hours after seed), treat half plate with 5µl of the selected concentrations of trabectedin. Treat the other half plate with 5µl of the same medium used to dilute trabectedin.
3. Prepare the lipofectamine solution in medium without FBS.
4. Prepare the "siRNA solution", in medium without FBS.
5. Use the robot to dispense in a 96wells/plate the right volumes of lipofectamine and siRNA solutions. Incubate this solution for 20 minutes.
6. 4 hours after trabectedin treatment dispense, using the robot, 5µl of the final solution of siRNA obtained in the point 5, to the correct 384 well.
7. Incubate the 384 wells/plate treated and transfected in a humidified incubator at 37°C with 5% CO2.
8. At Day 4: (48 hours after the transfection) perform the MTS analysis. Read the absorbance of each well using the spectrophotometer, at 490nm.

Two types of analysis were performed:

A) The ratio of each siRNA treated with trabectedin / siRNA alone *100.

B) The ratio of each siRNA treated with trabectedin / trabectedin alone*100.

A and B represent two different analyses to identify the genes whose downregulation induced an enhancement of the cytotoxicity of trabectedin.

In order to analysed the wide number of results obtained I arbitrarily decided to fixed a cut off (60%) that evidenced only the few genes whose downregulation could significantly potentiate the activity of trabectedin (40% of enhancement of trabectedin activity). I decided to fix this point in order to skim rationally the data.

The MTS analysis was performed 48 hours after trabectedin treatment and siRNA transfection since the preliminary experiments, discussed above, evidenced that this time point was the best compromised between the risk to reach the cellular confluence (more than 48hours) and the risk to did not see any effects (time points under 48hours).

Analysis of the first part of the siRNA library

A) The results obtained from the analysis of the first part of the library, shown in figure 57, evidenced that the downregulation of 7 kinases (BLK, CSK, FGFR1, PDK2, PDK1, PDK2, PDK3 and PDK4) enhanced the cytotoxicity of trabectedin, in this cellular model.

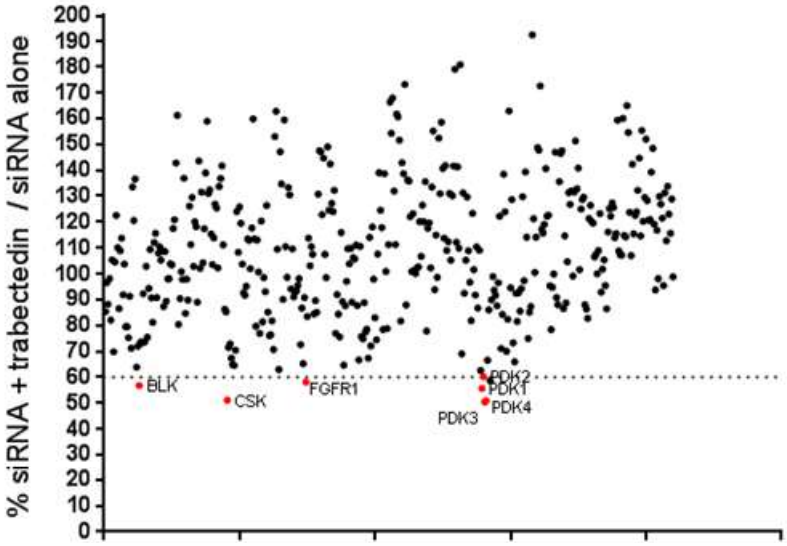

Figure 57: The schematic representation of the results obtained by the transfection with the first part of the siRNA library using the analysis siRNA+ trabectedin / siRNA alone *100.

Each dot represents a different gene.

The horizontal axis represents the genes that are grouped using an alphabetic order (from A to Z).

The vertical axis represents the values of % of siRNA+ trabectedin / siRNA alone for each gene.

B) Figure 58 shows the results obtained using this analysis (siRNA +trabectedin / trabectedin alone*100) of the first part of the library. The downregulation of 9 kinases (ACVRL1, BLK, CSK, FGFR1, MAP2K3, MAP2K6, MAP3K6, PDK3 and PDK4) enhanced the cytotoxicity of trabectedin, in this cellular model.

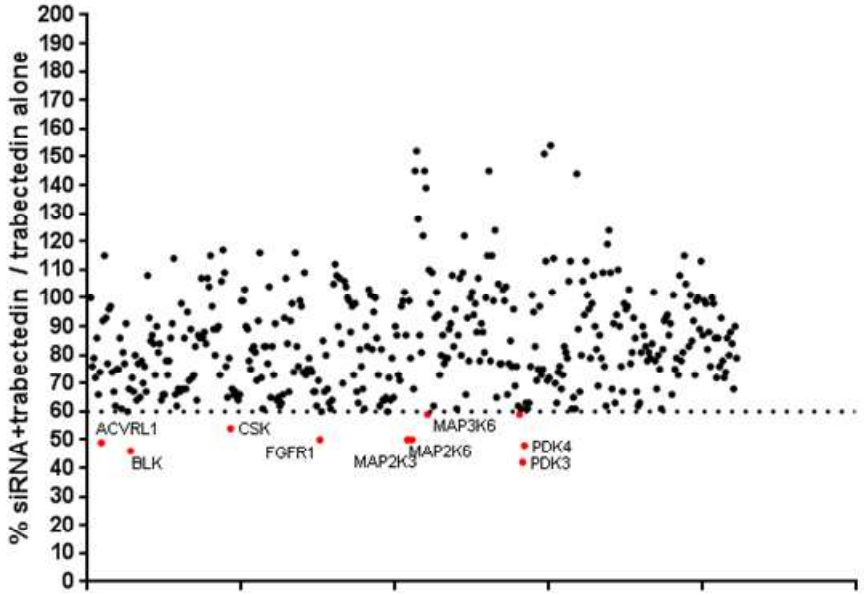

Figure 58: The schematic representation of the results obtained by the transfection with the first part of the siRNA library using the analysis siRNA+ trabectedin / trabectedin alone *100.

Each dot represents a different gene.

The horizontal axis represents the genes that are grouped using an alphabetic order (from A to Z).

The vertical axis represents the values of % of siRNA+ trabectedin / trabectedin alone for each gene.

The cytotoxicity induced by lipofectamine transfection and the efficacy of trabectedin treatment are shown in figures 59 and 60, respectively

The results obtained showed that the transfection with lipofectamine (MOCK) is not toxic, as shown in figure 59.

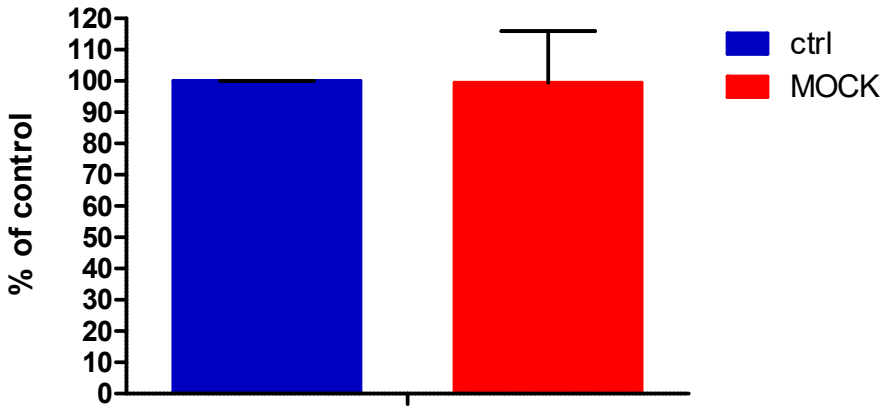

Figure 59: MTS assay performed in a 384 wells/plate. Cells (300cells/well) were seed in a 384 wells plate and after 48 hours (when the exponential growth was reached), treated with medium (CTRL) or lipofectamine (MOCK). The cytotoxicity was evaluated by MTS assay, 48 hours after drug treatment. The time 48 hours was selected by previous experiments performed to determine the point in which the cytotoxicity was visible and the phenomenon of confluence, in the control cells (not treated), was not reached. The values are reported as the % of the cells treated with lipofectamine (MOCK) versus the control cells not transfected (CTRL). The values are the mean of three replicates and two independently experiments. Bars ±sd. The t-student test analysis showed that the difference between control and MOCK is not statistically significant.

Figure 60 shows the cytotoxicity induced by trabectedin treatment and evaluated by MTS assay. The results evidenced that the trabectedin treatment (0.15nM) induced a 30% of cytotoxicity (IC30), compared with the cells not treated.

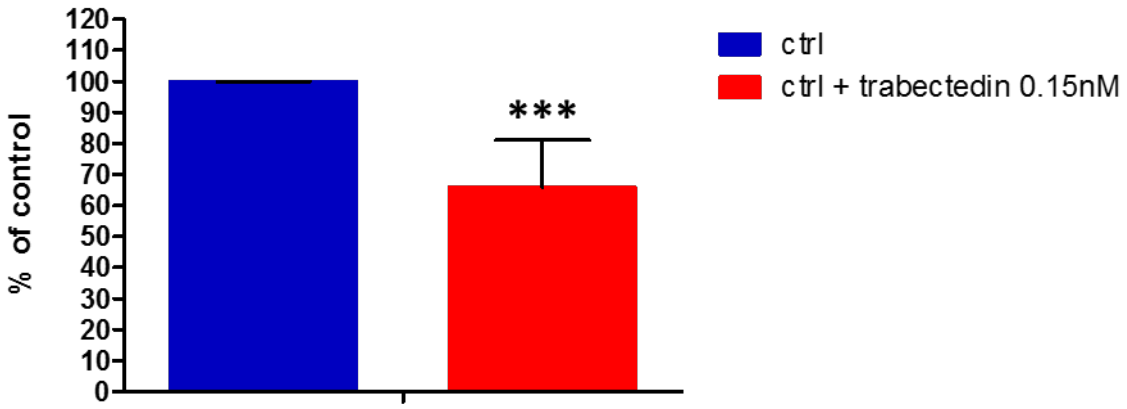

Figure 60: MTS assay performed in a 384 wells/plate. Cells (300cells/well) were seed in a 384 wells plate and after 48 hours (when the exponential growth was reached), treated with medium (CTRL) or trabectedin 0.15nM. The cytotoxicity was evaluated by MTS assay, 48 hours after drug treatment. The time 48 hours was selected by previous experiments performed to determine the point in which the cytotoxicity was visible and the phenomenon of confluence, in the control cells (not treated), was not reached. The values are reported as the % of the cells treated with trabectedin 0.15nM versus the control cells not treated. The values are the mean of three replicates and two independently experiments. Bars ±sd. The t-student test analysis showed that the difference between control and trabectedin 0.15nM is statistically significant (* P<0.0001)**

Analysis of the second part of the siRNA library

The second part of the library (299 genes) was analysed as described above.

A) The results obtained from the analysis of the second part of the library showed that the downregulation of 4 kinases (ADCK2, MAST4, PAK7 and RIPK4) enhanced the cytotoxicity of trabectedin, in this cellular model (figure 61).

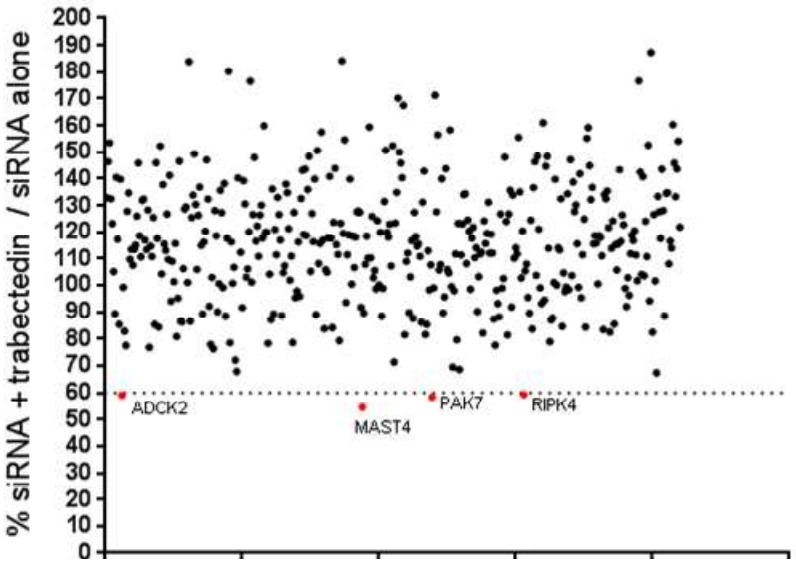

Figure 61: The schematic representation of the results obtained by the transfection with the first part of the siRNA library using the analysis siRNA+ trabectedin / siRNA alone *100.

Each dot represents a different gene.

The horizontal axis represents the genes that are grouped using an alphabetic order (from A to Z).

The vertical axis represents the values of % of siRNA+ trabectedin / siRNA alone for each gene.

B) The results obtained using the second analysis (siRNA +trabectedin / trabectedin alone*100) showed that the downregulation of 8 kinases (ADCK2, ADCK5, MLKL, OBSCN, MAST4, PLK5P, PAK7 and RIPK4) enhanced the cytotoxicity of trabectedin, in this cellular model (figure 62).

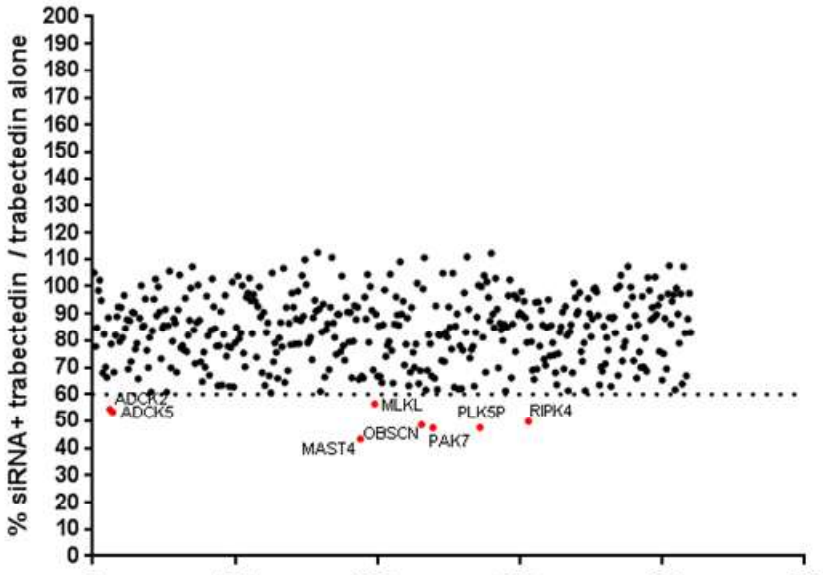

Figure 62: schematic representation of the results obtained by the transfection with the first part of the siRNA library using the analysis siRNA+ trabectedin / trabectedin alone *100.

Each dot represents a different gene.

The horizontal axis represents the genes that are grouped using an alphabetic order (from A to Z).

The vertical axis represents the values of % of siRNA+ trabectedin / trabectedin alone for each gene.

The cytotoxicity induced by lipofectamine transfection and the efficacy of trabectedin treatment are shown in figures 63 and 64, respectively

The results obtained showed that the transfection with lipofectamine (MOCK) is not toxic, as shown in figure 63.

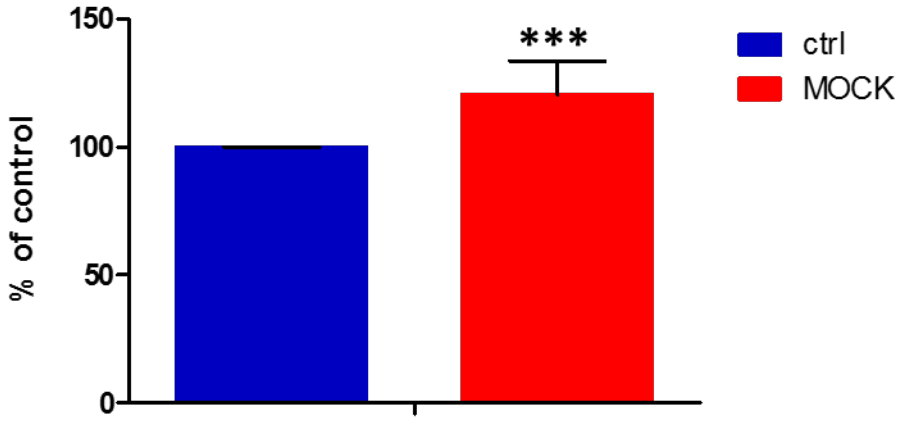

Figure 63: MTS assay performed in a 384 wells/plate. Cells (300cells/well) were seed in a 384 wells plate and after 48 hours (when the exponential growth was reached), treated with medium (CTRL) or lipofectamine (MOCK). The cytotoxicity was evaluated by MTS assay, 48 hours after drug treatment. The time 48 hours was selected by previous experiments performed to determine the point in which the cytotoxicity was visible and the phenomenon of confluence, in the control cells (not treated), was not reached. The values are reported as the % of the cells treated with lipofectamine (MOCK) versus the control cells not transfected (CTRL). The values are the mean of three replicates and two independently experiments. Bars ±sd. The t-student test analysis showed that the difference between control and trabectedin 0.15nM is statistically significant (* P<0.0001).**

Figure 64 shows the cytotoxicity induced by trabectedin treatment and evaluated by MTS assay. The results evidenced that the trabectedin treatment (0.15nM) induced a 30% of cytotoxicity (IC30), compared with the cells not treated.

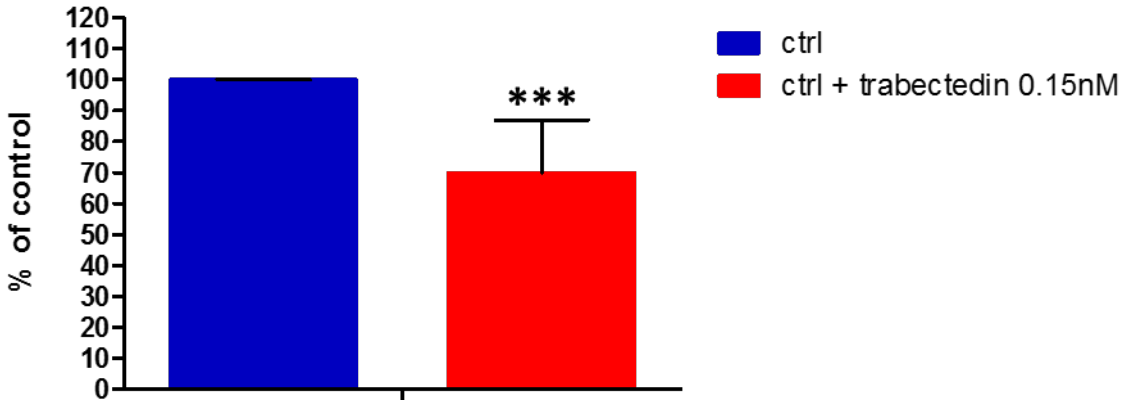

Figure 64: MTS assay performed in a 384 wells/plate. Cells (300cells/well) were seed in a 384 wells plate and after 48 hours (when the exponential growth was reached), treated with medium (CTRL) or trabectedin 0.15nM. The cytotoxicity was evaluated by MTS assay, 48 hours after drug treatment. The time 48 hours was selected by previous experiments performed to determine the point in which the cytotoxicity was visible and the phenomenon of confluence, in the control cells (not treated), was not reached. The values are reported as the % of the cells treated with trabectedin 0.15nM versus the control cells not treated. The values are the mean of three replicates and two independently experiments. Bars ±sd. The t-student test analysis showed that the difference between control and trabectedin 0.15nM is statistically significant (* P<0.0001).**

2.2 esiRNA "Nucleic Acid Binding "Panel transfection

The transfection with the "esiRNA Nucleic Acid Binding Panel" was performed with the same schedule used for the transfection with the siRNA kinase Panel. The dose of trabectedin 0.15nM (IC30) was used for the treatment.

The two types of analysis, A and B already described in the 2.1 paragraph, were performed.

A) The results obtained using this analysis (esiRNA + trabectedin/ esiRNA alone *100) showed that the downregulation of 3 genes (NOVA1, POLQ and XRCC3) enhanced the cytotoxicity of trabectedin, in this TC71 cellular model (figure 65).

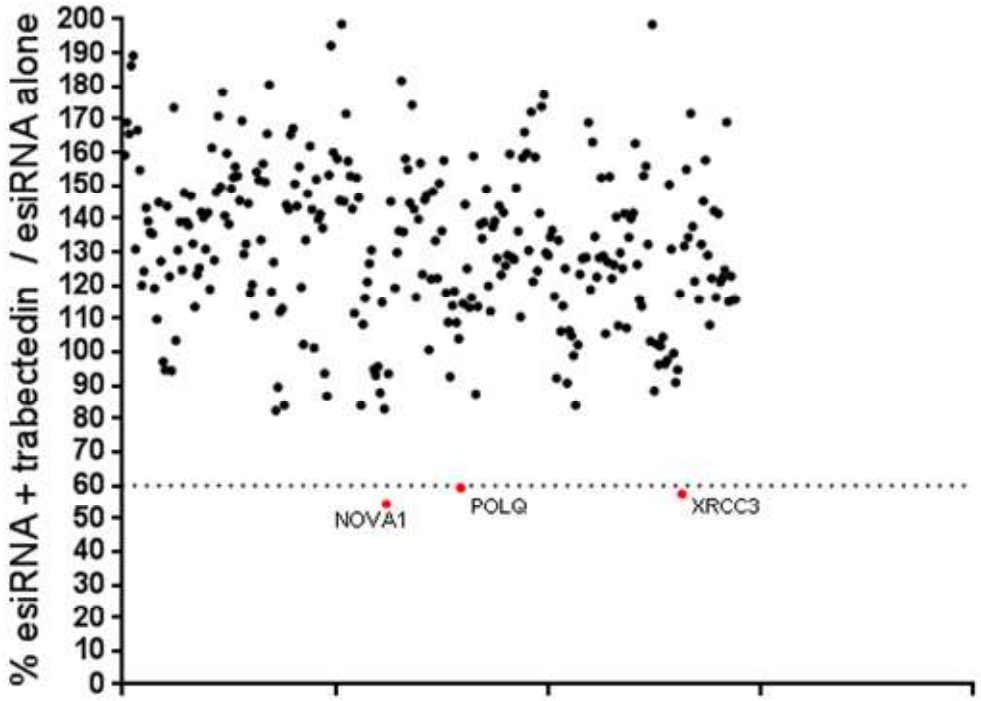

Figure 65: schematic representation of the results obtained by the transfection with esiRNA library using the analysis esiRNA+ trabectedin / esiRNA alone *100.

Each dot represents a different gene.

The horizontal axis represents the genes that are grouped using an alphabetic order (from A to Z).

The vertical axis represents the values of % of siRNA+ trabectedin / siRNA alone for each gene.

B) The results obtained using the second analysis (esiRNA +trabectedin / trabectedin alone*100) showed that the downregulation of 6 genes (NOVA1, PARP9, POLL, POLQ, SIRT4 and XRCC3) enhanced the cytotoxicity of trabectedin, in this cellular model (figure 66).

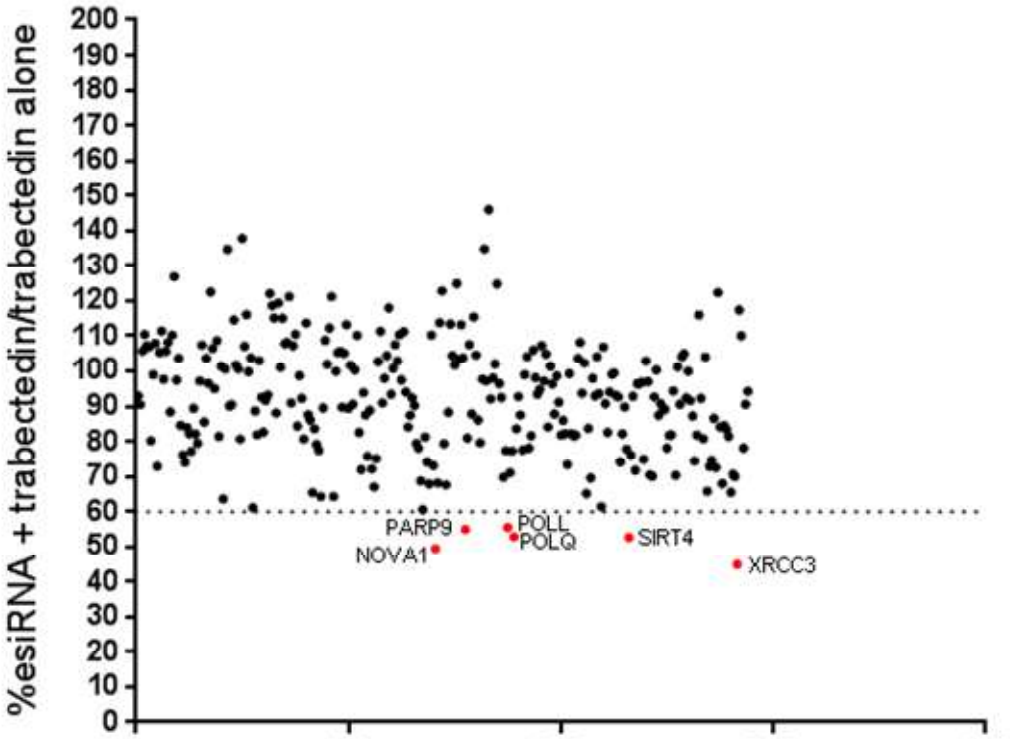

Figure 66: schematic representation of the results obtained by the transfection with esiRNA library using the analysis esiRNA+ trabectedin / trabectedin alone *100.

Each dot represents a different gene.

The horizontal axis represents the genes that are grouped using an alphabetic order (from A to Z).

The vertical axis represents the values of % of siRNA+ trabectedin / trabectedin alone for each gene.

The cytotoxicity induced by lipofectamine transfection and the efficacy of trabectedin treatment are shown in figures 67 and 68, respectively

The transfection with lipofectamine (MOCK) is not toxic, as shown in figure 67.

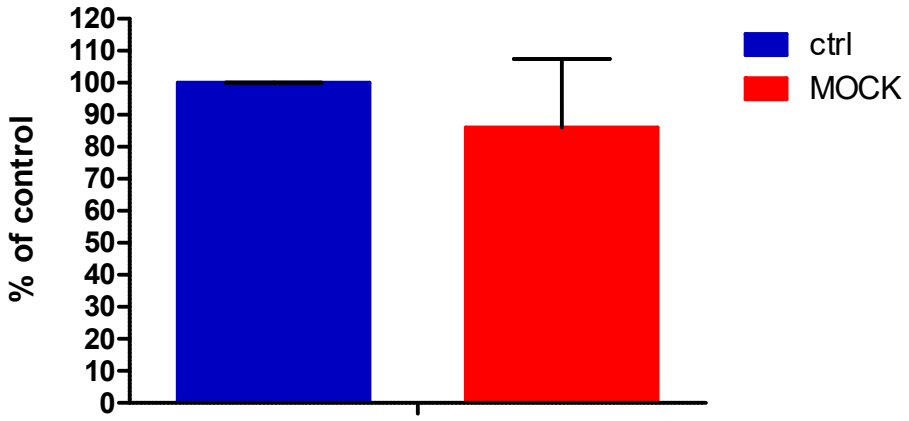

Figure 67: MTS assay performed in a 384 wells/plate. Cells (300cells/well) were seed in a 384 wells plate and after 48 hours (when the exponential growth was reached), treated with medium (CTRL) or lipofectamine (MOCK). The cytotoxicity was evaluated by MTS assay, 48 hours after drug treatment. The time 48 hours was selected by previous experiments performed to determine the point in which the cytotoxicity was visible and the phenomenon of confluence, in the control cells (not treated), was not reached. The values are reported as the % of the cells treated with lipofectamine (MOCK) versus the control cells not transfected (CTRL). The values are the mean of three replicates and two independently experiments. Bars ±sd. The t-student test analysis showed that the difference between control and MOCK is not statistically significant.

Figure 68 shows the cytotoxicity induced by trabectedin treatment and evaluated by MTS assay. The results evidenced that the trabectedin treatment (0.15nM) induced a 30% of cytotoxicity (IC30), compared with the cells not treated.

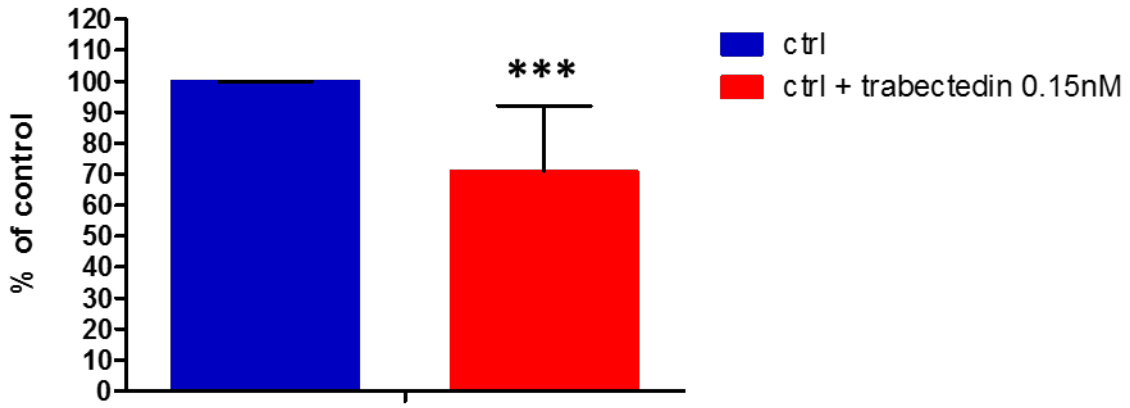

Figure 68: MTS assay performed in a 384 wells/plate. Cells (300cells/well) were seed in a 384 wells plate and after 48 hours (when the exponential growth was reached), treated with medium (CTRL) or trabectedin 0.15nM. The cytotoxicity was evaluated by MTS assay, 48 hours after drug treatment.

The time 48 hours was selected by previous experiments performed to determine the point in which the cytotoxicity was visible and the phenomenon of confluence, in the control cells (not treated), was not reached. The values are reported as the % of the cells treated with trabectedin 0.15nM versus the control cells not treated. The values are the mean of three replicates and two independently experiments. Bars ±sd. The t-student test analysis showed that the difference between control and trabectedin 0.15nM is statistically significant (* P<0.0001).**

3. RESULTS OBTAINED BY THE ANALYSIS OF THE LIBRARIES

3.1 genes obtained from the siRNA library kinase panel

The results obtained by the two types of analysis of the whole siRNA kinase panel showed that the downregulation of the kinases listed below increased the trabectedin activity.

An increase of the trabectedin activity equal or higher than 40% was considered.

Kinases whose downregulation enhanced trabectedin activity:

BLK, CSK, FGFR1, PDK1, PDK2, PDK3, PDK4, ACVRL1, MAP2K3, MAP2K6 and MAP3K6, ADCK2, MAST4, PAK7, RIPK4, ADCK5, MLKL, OBSCN and PLK5P.

A brief description of each kinase is reported below.

- **BLK**: This gene encodes a non-receptor tyrosine-kinase of the src family of proto-oncogenes that are typically involved in cell proliferation and differentiation. The protein has a role in B-cell receptor signalling and B-cell development. The protein also stimulates insulin synthesis and secretion in response to glucose and enhances the expression of several pancreatic beta-cell transcription factors.
- **CSK**: C-Src Tyrosine Kinase. Non-receptor tyrosine-protein kinase that plays an important role in the regulation of cell growth, differentiation, migration and immune response. Phosphorylates tyrosine residues located in the C-terminal tails of Src-family kinases (SFKs) including LCK, SRC, HCK, FYN, LYN or YES1.

  Upon tail phosphorylation, Src-family members engage in intramolecular interactions between the phosphotyrosine tail and the SH2 domain that result in an inactive conformation. To inhibit SFKs, CSK is recruited to the plasma membrane via binding to transmembrane proteins or adapter proteins located near the plasma membrane. Suppresses signalling by various surface receptors, including T-cell receptor (TCR) and B-cell receptor (BCR) by phosphorylating and maintaining inactive several positive effectors such as FYN or LCK. CSK is associated to colorectal cancer and breast cancer.

- **FGFR1**: Tyrosine-protein kinase that acts as cell-surface receptor for fibroblast growth factors and plays an essential role in the regulation of embryonic development, cell proliferation, differentiation and migration. Required for normal mesoderm patterning and correct axial organization during embryonic development, normal skeletogenesis and normal development of the gonadotropin-releasing hormone (GnRH) neuronal system. Phosphorylates PLCG1, FRS2, GAB1 and SHB. Ligand binding leads to the activation of several signalling cascades. Activation of PLCG1 leads to the production of the cellular signalling molecules diacylglycerol and inositol 1,4,5-trisphosphate.

Phosphorylation of FRS2 triggers recruitment of GRB2, GAB1, PIK3R1 and SOS1, and mediates activation of RAS, MAPK1/ERK2, MAPK3/ERK1 and the MAP kinase signalling pathway, as well as of the AKT1 signalling pathway. Promotes phosphorylation of SHC1, STAT1 and PTPN11/SHP2. In the nucleus, enhances RPS6KA1 and CREB1 activity and contributes to the regulation of transcription. FGFR1 signalling is down-regulated by IL17RD/SEF, and by FGFR1 ubiquitination, internalization and degradation. Diseases associated with FGFR1 include osteoglophonic dysplasia and hypogonadotropic hypogonadism 2 with or without anosmia. Among its related pathways are Adherens junction and Central carbon metabolism in cancer.

- **PDK**: pyruvate dehydrogenase kinase (PDK) that phosphorylates, inactivating, the Pyruvate dehydrogenase (PDH). PDH is a mitochondrial multienzyme complex that catalyzes the oxidative decarboxylation of pyruvate and is one of the major enzymes responsible for the regulation of homeostasis of carbohydrate fuels in mammals. Multiple alternatively spliced transcript variants have been found for this gene.
- **PDK1**: Kinase that plays a key role in regulation of glucose and fatty acid metabolism and homeostasis via phosphorylation of the pyruvate dehydrogenase subunits PDHA1 and PDHA2. This inhibits pyruvate dehydrogenase activity, and thereby regulates metabolite flux through the tricarboxylic acid cycle, down-regulates aerobic respiration and inhibits the formation of acetyl-coenzyme A from pyruvate. Plays an important role in cellular responses to hypoxia and is important for cell proliferation under hypoxia. Protects cells against apoptosis in response to hypoxia and oxidative stress.
- **PDK2**: same activity of PDK1; Mediates cellular responses to insulin. Plays an important role in maintaining normal blood glucose levels and in metabolic adaptation to nutrient availability.

Via its regulation of pyruvate dehydrogenase activity, plays an important role in maintaining normal blood pH and in preventing the accumulation of ketone bodies under starvation. Plays a role in the regulation of cell proliferation and in resistance to apoptosis under oxidative stress. Plays a role in p53/TP53-mediated apoptosis. Overexpression of this gene may play a role in both cancer and diabetes.

- **PDK3**: same activity of PDK1; plays a role in the generation of reactive oxygen species.
- **PDK4**: same activity of PDK1.
- **ACVRL1**: This gene encodes a type I cell-surface receptor for the TGF-beta superfamily of ligands. The encoded protein sometimes is termed ALK1. Type I receptor for TGF-beta family ligands BMP9/GDF2 and BMP10 and important regulator of normal blood vessel development. On ligand binding, forms a receptor complex consisting of two type II and two type I transmembrane serine/threonine kinases. Type II receptors phosphorylate and activate type I receptors which autophosphorylate, then bind and activate SMAD transcriptional regulators.
- **MAP2K3:** The protein encoded by this gene is a dual specificity protein kinase that belongs to the MAP kinase family. The MAPKs are involved in directing cellular responses to a diverse array of stimuli, such as mitogens, osmotic stress, heat shock and proinflammatory cytokines. They regulate cell functions including proliferation, gene expression, differentiation, mitosis, cell survival, and apoptosis. This kinase is activated by mitogenic and environmental stress, and participates in the MAP kinase-mediated signalling cascade. It phosphorylates and thus activates MAPK14/p38-MAPK. This kinase can be activated by insulin, and is necessary for the expression of glucose transporter. Expression of RAS oncogene is found to result in the accumulation of the active form of this kinase, which thus leads to the constitutive activation of MAPK14, and confers oncogenic transformation of primary cells.

The inhibition of this kinase is involved in the pathogenesis of Yersina pseudotuberculosis. Multiple alternatively spliced transcript variants that encode distinct isoforms have been reported for this gene.

- **MAP2K6:** Dual specificity protein kinase which acts as an essential component of the MAP kinase signal transduction pathway. With MAP3K3/MKK3, catalyzes the concomitant phosphorylation of a threonine and a tyrosine residue in the MAP kinases p38 MAPK11, MAPK12, MAPK13 and MAPK14 and plays an important role in the regulation of cellular responses to cytokines and all kinds of stresses. Especially, MAP2K3/MKK3 and MAP2K6/MKK6 are both essential for the activation of MAPK11 and MAPK13 induced by environmental stress, whereas MAP2K6/MKK6 is the major MAPK11 activator in response to TNF. Within the p38 MAPK signal transduction pathway, MAP3K6/MKK6 mediates phosphorylation of STAT4 through MAPK14 activation, and is therefore required for STAT4 activation and STAT4-regulated gene expression in response to IL-12 stimulation. Has a role in osteoclast differentiation through NF-kappa-B transactivation by TNFSF11, and in endochondral ossification and since SOX9 is another likely downstream target of the p38 MAPK pathway. MAP2K6/MKK6 mediates apoptotic cell death in thymocytes. Acts also as a regulator for melanocytes dendricity, through the modulation of Rho family GTPases.
- **MAP3K6:** This gene encodes a serine/threonine protein kinase that forms a component of protein kinase-mediated signal transduction cascades. The encoded kinase participates in the regulation of vascular endothelial growth factor (VEGF) expression. Alternative splicing results in multiple transcript variants. Activates the JNK, but not ERK or p38 kinase pathways.
- **ADCK2:** The function of this protein is not yet clear. It is not known if it has protein kinase activity and what type of substrate it would phosphorylate (Ser, Thr or Tyr).
- **ADCK5:** the same of ADCK2.

- **MAST4:** This gene encodes a member of the microtubule-associated serine/threonine protein kinases. The proteins in this family contain a domain that gives the kinase the ability to determine its own scaffold to control the effects of their kinase activities. Alternative splicing results in multiple transcript variants encoding different isoforms.
- **PAK7:** The protein encoded by this gene is a member of the PAK family of Ser/Thr protein kinases This kinase is predominantly expressed in brain. It is capable of promoting neurite outgrowth, and thus may play a role in neurite development. PAK7 is associated with microtubule networks and induces microtubule stabilization. The subcellular localization of this kinase is tightly regulated during cell cycle progression. Alternatively spliced transcript variants encoding the same protein have been described.
- **RIPK4:** The encoded protein can also activate NF-kappaB and is required for keratinocyte differentiation. Among its related pathways are NF-kappaB Signaling and Wnt / Hedgehog / Notch.
- **MLKL:** The encoded protein contains a protein kinase-like domain; however, is thought to be inactive because it lacks several residues required for activity. This protein plays a critical role in tumor necrosis factor (TNF)-induced necroptosis, a programmed cell death process, via interaction with receptor-interacting protein 3 (RIP3), which is a key signaling molecule in necroptosis pathway. Inhibitor studies and knockdown of this gene inhibited TNF-induced necrosis. High levels of this protein and RIP3 are associated with inflammatory bowel disease in children. Alternatively spliced transcript variants have been described for this gene.
- **OBSCN:** The encoded protein is protein belongs to the family of giant sarcomeric signaling proteins that includes titin and nebulin, and may have a role in the organization of myofibrils during assembly and may mediate interactions between the sarcoplasmic reticulum and myofibrils. Alternatively spliced transcript variants encoding different isoforms have been identified.

- **PLK5P:** Inactive serine/threonine-protein kinase that plays a role in cell cycle progression and neuronal differentiation.

3.2 genes obtained from the esiRNA library “molecules that bind DNA”

The results obtained from the analysis of the esiRNA library of molecules that bind DNA showed that the downregulation of the genes listed below enhanced the trabectedin activity.

An increase of the trabectedin activity equal or higher than 40% was considered.

List of genes: NOVA1, POLQ, POLL, XRCC3, SIRT4 and PARP9.

- **NOVA1:** This gene encodes a neuron-specific RNA-binding protein, a member of the Nova family of paraneoplastic disease antigens, that is recognized and inhibited by paraneoplastic antibodies. These antibodies are found in the sera of patients with paraneoplastic opsoclonus-ataxia, breast cancer, and small cell lung cancer. Nova1 may regulate RNA splicing or metabolism in a specific subset of developing neurons.
- **POLQ:** this gene encodes a DNA polymerase that promotes microhomology-mediated end-joining (MMEJ), an alternative non-homologous end-joining (NHEJ) machinery triggered in response to double-strand breaks in DNA. MMEJ is an error-prone repair pathway that produces deletions of sequences from the strand being repaired and promotes genomic rearrangements, such as telomere fusions, some of them leading to cellular transformation. POLQ acts as an inhibitor of homology-recombination repair (HR) pathway by limiting RAD51 accumulation at resected ends. POLQ-mediated MMEJ may be required to promote the survival of cells with a compromised HR repair pathway by resolving unrepaired lesions. The polymerase acts by binding directly the 2 ends of resected double-strand breaks, allowing microhomologous sequences in the overhangs to form base pairs.

It then extends each strand from the base-paired region using the opposing overhang as a template. POLQ also exhibits low-fidelity DNA synthesis, translesion synthesis and lyase activity, and it is implicated in interstrand-cross-link repair, base excision repair and DNA end-joining. It is frequently a target of mutational inactivation in sporadic tumors.

- **POLL:** polymerase lambda. Pol λ is a member of the X family of DNA polymerases. It is thought to re-synthesize missing nucleotides during non-homologous end joining, a pathway of DNA double-strand break repair. The crystal structure of pol λ shows that, unlike the DNA polymerases that catalyze DNA replication, pol λ makes extensive contacts with the 5' phosphate of the downstream DNA strand. This allows the polymerase to stabilize the two ends of a double-strand break and explains how pol λ is uniquely suited for a role in non-homologous end joining. In addition to NHEJ, pol λ can also participate in base excision repair, where it provides backup activity in the absence of Pol β. Pol λ participates in V(D)J recombination, the process by which B-and T-cell receptor diversity is generated in the vertebrate immune system. Pol λ has been shown to interact with PCNA. Alternatively spliced transcript variants have been described.
- **XRCC3:** This gene encodes a member of the RecA/Rad51-related protein family that participates in homologous recombination to maintain chromosome stability, genomic integrity and repair DNA damage. The XRCC3 protein is one of five paralogs of RAD51, including RAD51B (RAD51L1), RAD51C (RAD51L2), RAD51D (RAD51L3), XRCC2 and XRCC3. They each share about 25% amino acid sequence identity with RAD51 and each other. The RAD51 paralogs are all required for efficient DNA double-strand break repair by homologous recombination and depletion of any paralog results in significant decreases in homologous recombination frequency. Two paralogs form a complex designated CX3 (RAD51C-XRCC3). Four paralogs form a second complex designated BCDX2 (RAD51B-RAD51C-RAD51D-XRCC2). These two complexes act at two different stages of homologous recombinational DNA repair.

A rare microsatellite polymorphism in this gene is associated with cancer in patients of varying radiosensitivity.

- **SIRT4:** This gene encodes a member of the sirtuin family of proteins. Members of the sirtuin family are characterized by a sirtuin core domain and grouped into four classes. The functions of human sirtuins have not yet been determined; however, yeast sirtuin proteins are known to regulate epigenetic gene silencing and suppress recombination of rDNA. Studies suggest that the human sirtuins may function as intracellular regulatory proteins with mono-ADP-ribosyltransferase activity. Acts as NAD-dependent protein lipoamidase, ADP-ribosyl transferase and deacetylase. Catalyzes the transfer of ADP-ribosyl groups onto target proteins. SIRT4 is a mitochondrial ADP-ribosyltransferase that inhibits mitochondrial glutamate dehydrogenase 1 activity, thereby downregulating insulin secretion in response to amino acids. It has been shown that SIRT4 regulates fatty acid oxidation and mitochondrial gene expression in liver and muscle cells.
- **PARP9**: Poly (ADP-ribose) polymerase (PARP) catalyzes the post-translational modification of proteins by the addition of multiple ADP-ribose moieties. PARP transfers ADP-ribose from nicotinamide dinucleotide (NAD) to Glu/Asp residues on the substrate protein. In concert with DTX3L PARP 9 plays a role in PARP1-dependent DNA damage repair. PARP1-dependent PARP9/BAL1-DTX3L-mediated ubiquitination promotes the rapid and specific recruitment of 53BP1/TP53BP1, UIMC1/RAP80, and BRCA1 to DNA damage sites. Involved in inducing the expression of IFN-gamma-responsive genes. PARP 9 also plays a role in the regulation of cell migration.

4. ANALYSIS of ONE TARGET OBTAINED BY THE COMBINATION of TRABECTEDIN and the siRNA KINASE PANEL LIBRARY.

The results obtained by the analysis of the libraries showed that the downregulation of different genes could potentiate the cytotoxic effects induced by trabectedin treatment. One example is the downregulation of BLK, a gene encoding for a kinase that belongs to the “Src“ family of proteins.

Since one of the inhibitors of this gene, dasatinib, is currently used in the clinic, I used this compound to inhibit BLK gene and verify if the combination with trabectedin was synergic.

Figures 69 and 70 show the dose response curves of the treatment with trabectedin or dasatinib alone, respectively.

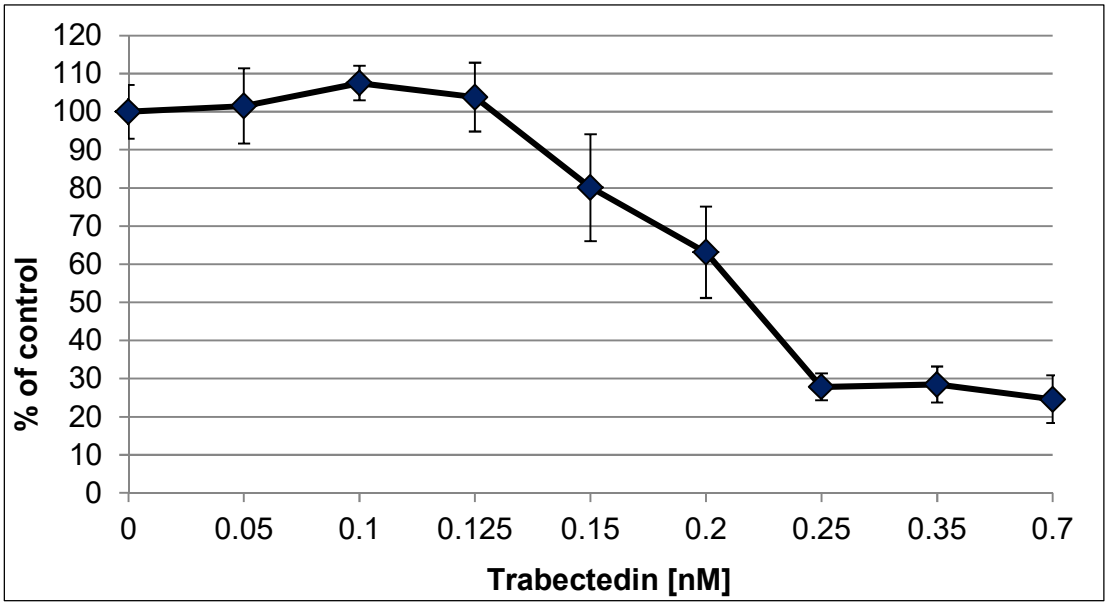

Figure 69: The dose-response curve of trabectedin, derived from the MTS analysis at 48 hours. The values are the mean of six replicates. Bars ±sd.

Cells were seed in a 96 wells plate and after 48 hours (when the exponential growth was reached), treated with different drug concentrations. The cytotoxicity was evaluated by MTS assay, 48 hours after drug treatment. The time 48 hours was selected by previous experiments performed to determine the point in which the cytotoxicity was visible and the phenomenon of confluence, in the control cells (not treated), was not reached.

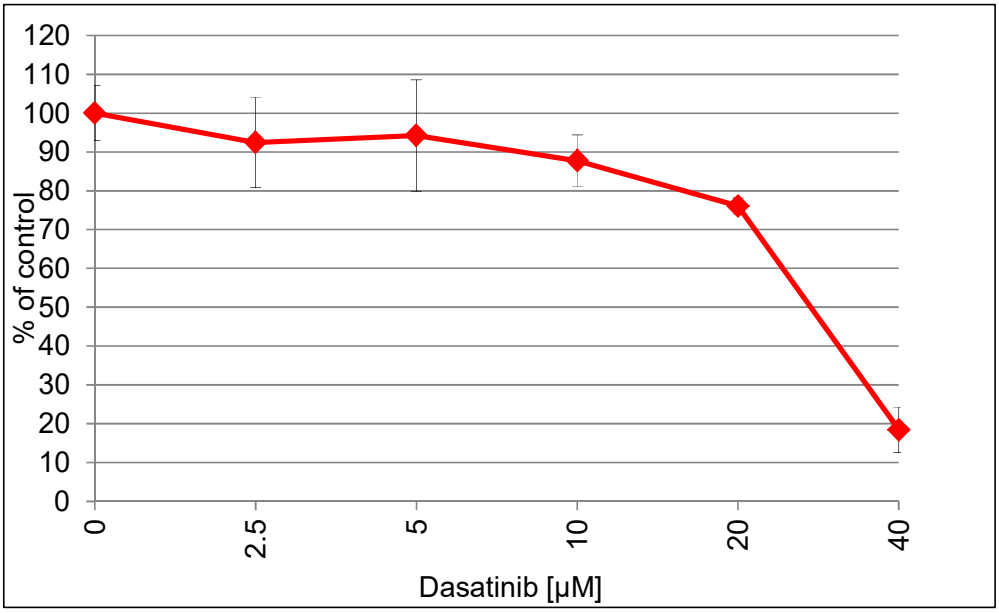

Figure 70: The dose-response curve of dasatinib, derived from the MTS analysis at 48hours The values are the mean of six replicates. Bars ±sd.

Cells were seed in a 96 wells plate and after 48 hours (when the exponential growth was reached), treated with different drug concentrations. The cytotoxicity was evaluated by MTS assay, 48 hours after drug treatment. The time 48 hours was selected by previous experiments performed to determine the point in which the cytotoxicity was visible and the phenomenon of confluence, in the control cells (not treated), was not reached.

The dose-response curves of the combination were generated using three concentrations of dasatinib that were marginally effective when used as single agent (figure 71).

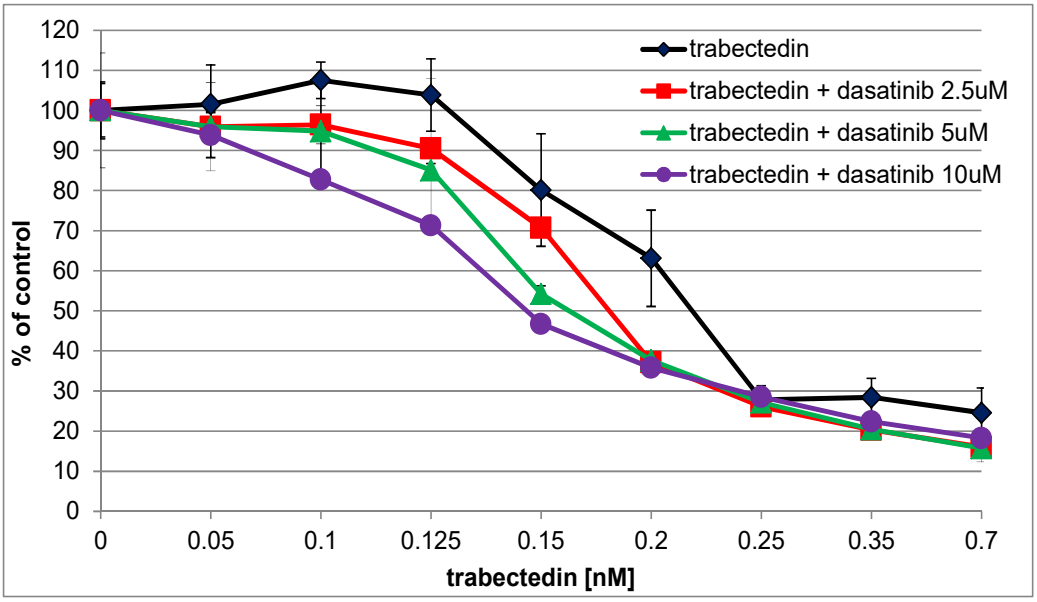

Figure 71: **The MTS analysis of the combination trabectedin and dasatinib. The values are the mean of six replicates. Bars ±sd.**

Cells were seed in a 96 wells plate and treated, simultaneously, with different drugs concentrations, 48 hours after (when the exponential growth phase was reached). The cytotoxicity was evaluated by MTS assay, 48 hours after drug treatment. The time 48 hours was selected by previous experiments performed to determine the point in which the cytotoxicity was visible and the phenomenon of confluence, in the control cells (not treated), was not reached.

The results in figure 71 show that the combination trabectedin and dasatinib was slightly synergic.

The isobolograms were generated fixing three doses of trabectedin and dasatinib that, for each drug, represented the IC30, 50 and 70.

The isobolograms represented in figure 72 show that at doses around the IC30 and 50 the combination is additive or slightly synergic. Instead at doses around the IC70 the two drugs became antagonist.

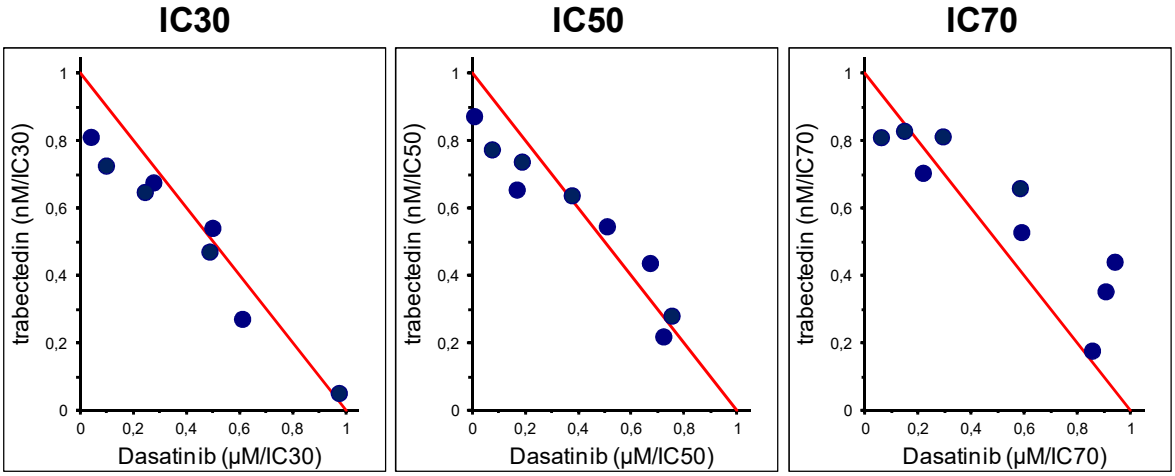

Figure 72: The isobolograms referred to the combination of trabectedin and Dasatinib. Each dot represented the value of combination. To define synergic the combination the dot must be <1. Values>1 define an antagonistic effect, =1 an additive effect.

The results showed that the combination of trabectedin and dasatinib at the selected doses that were in the range of activity defined in ES cells was not synergic (Bai *et al*, 2012). I choose dasatinib to perform this experiment because this drug is already used in the clinic, but is not a selective inhibitor for BLK protein. It is important to consider that the chemical inhibitors (like dasatinib) act on the protein level while siRNAs act on the mRNA level; for this reason a drug like dasatinib is not specific as inhibitor like a siRNA, expressly designed to downregulate a specific mRNA target.

These considerations could be the explanation of the unexpected results obtained combining dasatinib and trabectedin.

DISCUSSION

Ewing's sarcoma (ES) is a rare, aggressive childhood disease characterized by the expression of a chimeric protein derived from the fusion of the EWS and FLI1 genes (in approximately 90% of cases). The ES normally have the tendency to recur and to metastasize. For the15-25% of patients who are in an advanced stage of the pathology at the time of the diagnosis, the average survival at five years is around the 30%.

Therefore there is an urgent need to develop new treatment regimens for the therapy of ES. Among the recently registered drugs for the therapy of sarcomas, trabectedin could be of potential great interest as it seems very active in some "translocated sarcomas" (Delaloge *et al*, 2001; Garcia-Carbonero *et al*, 2004; Gronchi *et al*, 2012; Monk *et al*, 2012a). However in spite of some initial promising reports, the overall clinical results indicated only a marginally activity of trabectedin given as single agent in ES (Baruchel *et al*, 2012; Lau *et al*, 2005).

The drug shows some activity but seems to have a modest impact on the disease progression.

Thus it would be important to identify new combinations of trabectedin with other drugs that are potentially effective in ES and act synergistically.

The mechanism of action of trabectedin is complex and not fully elucidated, yet.

One of the mechanisms by which trabectedin exerts its antitumor activity is related to its interference with the nucleotide excision repair (NER) and homologous recombination (HR) mechanisms of DNA repair. Trabectedin-induced DNA damage activates cell cycle checkpoints with consequent cell cycle perturbations. A G2/M block caused by trabectedin treatment was reported in NER-positive cells (sensitive to the treatment) but not in NER-negative cells (partially resistant to trabectedin treatment) (Colmegna *et al*, 2015; Erba *et al*, 2001).

The first aim of my thesis was to test if inhibitors of two important cell cycle checkpoints (chK1 and WEE1) were able to potentiate the activity of trabectedin.

The results obtained showed that the chK1 inhibitor PF-477736 and trabectedin were not synergic, probably because trabectedin in this cellular model was able to downregulate the expression of chK1, that is the target of PF-477736.

In a recent paper Natarajan S. et al demonstrated a correlation between the levels of the high mobility group proteins HMGAs (particularly the HMGA2) and the axis ATR-CHK1 that is activated in response to a DNA damage (Natarajan *et al*, 2013). In this paper the authors proposed a model in which in the presence of a genotoxic stress, HMGA2 interacting with ATR-CHK1 facilitated and sustains the repair of damaged DNA and promotes the cell survival. The ability of trabectedin to interfere with the activity of the high mobility group proteins, displacing the binding of these proteins to their target promoters, were reported (D'Angelo *et al*, 2013), thus possibly suggesting that this mechanism is responsible for the observed downregulation of chk1. In other words trabectedin could interfere with the binding of the HMGA proteins with chK1, with a consequent downregulation of this kinase.

Further investigations are necessary to better understand the mechanism underlying this data.

Since several studies in the literature showed that the concomitant inhibition of chK1 and WEE1 is synergic in different solid tumors (Carrassa *et al*, 2012; Davies *et al*, 2011; Guertin *et al*, 2012; Russell *et al*, 2013), I evaluated the possibility to exploit the ability of trabectedin to downregulate the chK1 expression, to potentiate its activity in combination with a WEE1 inhibitor, AZD-1775.

The results obtained clearly showed that this combination is synergic especially using higher doses of the two drugs.

This data was further confirmed by the cell cycle analysis performed treating the cells with two different concentrations of trabectedin and AZD-1775, as single agents or in combination.

As expected trabectedin caused a G2/M block while AZD-1775 did not cause a significant perturbation in the cell cycle. The combination of the two drugs modify the cell distribution in the cell cycle phases.

The synergism and the enhancement of perturbations observed after the combined treatment of trabectedin with AZD-1775 could be probably attributed to the simultaneously lack of two important checkpoints: the chK1 downregulated by trabectedin and WEE1 inhibited by AZD-1775. In the cells exposed to the combination of trabectedin and AZD-1775 the G2/M block is partially abolished and a fraction of cells died for “mitotic catastrophe”. My experiments, deliberately performed using a very low dose of trabectedin, close the IC30 value, showed a synergism but not a complete disruption of cancer cells. On the other hand the IC30 of trabectedin (0.15nM) can be achieved in plasma of cancer patients receiving standard dose of trabectedin. Therefore my finding might be translated in the clinic.

Previous data showed the ability of trabectedin to sensitize cells to another anticancer agent, such as irinotecan. The mechanism behind this interaction appeared to be related to the ability of trabectedin to strongly reduce the expression of WRN gene (in ES), that encodes for an helicase whose downregulation is associated to hypersensitivity to camptothecins (Grohar *et al*, 2014).

In the present thesis the molecular mechanism by which trabectedin modifies the transcriptional regulation by displacing EWS-FLI1 from target promoters, in ES cells, is shown. The results were in keeping with several other observations that were previously published. Previous studies showed that in many cellular systems trabectedin interferes with transcriptional regulation (Friedman *et al*, 2002; Minuzzo *et al*, 2000).This effect was explained by its binding to GC-enriched DNA sequences and changes of DNA structure that modify the affinity of some transcription factors for DNA (Bonfanti *et al*, 1999).

This mechanism was studied in detail in myxoid liposarcomas. In this sarcoma trabectedin was reported to displace the oncogenic FUS-CHOP chimeric protein (hallmark of this disease) from the promoter of its targets(Di Giandomenico *et al*, 2014). This observation provides the biochemical explanation for the very high sensitivity of myxoid liposarcomas to trabectedin treatment (Grosso *et al*, 2007).

The present thesis shows that a similar mechanism occurs also in ES, in which trabectedin displaces the EWS-FLI1 chimeric protein from its target promoters, likewise in the myxoid liposarcomas.

Differently from what observed in myxoid liposarcomas, in ES the reattachement of the chimeric protein to its consensus sequences was fast. This data might explain why the results obtained in the clinic using trabectedin as single agent in ES were not as good as in myxoid liposarcomas (Baruchel *et al*, 2012).

The peculiar effect of trabectedin on the oncogenic EWS-FLI1 chimera - responsible for the pathogenesis of ES – stimulated me to find new ways to exploit this mechanism.

I asked the question:

How can we identify new potentially effective combinations of trabectedin with other drugs for the therapy of ES, exploiting this specific effect of the drug on transcription?

Most of my efforts were directed to find out new experimental approaches suitable to answer this question. In particular I developed a novel strategy based on siRNA libraries, that I started to validate and apply.

The set up the right conditions to perform these sequential treatments required a systematic study of different variables. The “working protocol”, that has been shown in the “Results” section, is feasible and sufficiently robust to be used by other laboratories as well.

This protocol has been applied to perform experiments that have allowed me to identify targets that when inhibited increased the sensitivity of ES cells to trabectedin.

Many of the genes that I have identified as possible targets for the combination with trabectedin are involved in the cell cycle proliferation; this is in line with the ability of trabectedin to interfere with the DNA repair pathways and to cause perturbations in the cell cycle.

Among the genes whose downregulation was found to enhance the cytotoxicity of trabectedin I identified *PAK7*. This is a member of the serine threonine PAK kinases. It is expressed in brain and have a role in the neurite development. One of the hypothesis about the origin's cell of Ewing's sarcomas (discussed in the "Introduction" section) is the neuronal hypothesis; it could be speculated that the combination of trabectedin with an inhibitor of PAK7 could possess some degree of specificity.

Another target evidenced from the analysis is *XRCC3*, that is a gene encoding for a protein that belongs to the RecA/Rad51 family of proteins and participates to the homologous recombination DNA repair mechanism (HR).

Since it is known that cells deficient in HR pathway are exquisitively sensitive to trabectedin treatment (Grohar *et al*, 2014; Soares *et al*, 2007; Tavecchio *et al*, 2008), the observation that the downregulation of XRCC3, with consequent impairment on HR activity, potentiate the activity of the drug, is in line with the previous studies.

Interesting to note that irinotecan, that is highly synergistic given in combination with trabectedin, is one of the most active inhibitors of XRCC3. This data suggests that in addition to the downregulation of WRN gene also the inhibition of XRCC3 could be important to explain the synergism between trabectedin and irinotecan (Grohar *et al*, 2014).

These data suggest that an additional mechanism behind the synergism of the combination of trabectedin with irinotecan is the downregulation of XRCC3.

A further finding is that the downregulation of PARP9 induces the enhancement of trabectedin activity. PARP9, that belongs to the poly (ADP-ribose) polymerase family, in concert with DTX3L (ubiquitin ligase) plays a role in PARP1-dependent DNA damage repair.

PARP1-dependent *PARP9/BAL1-DTX3L*-mediated ubiquitination promotes the rapid and specific recruitment of 53BP1/TP53BP1, UIMC1/RAP80, and BRCA1 to DNA damage sites.

PARP1 is one of the most important protein in the BER (Base excision repair) mechanism of DNA repair; in the presence of single-strand breaks the BER pathway is responsible for the repair of DNA. In the absence of a functional BER, the single-strand breaks evolve in double – strand breaks, that represent the most lethal lesion for the cells.

Ewing's sarcoma cells are sensitive to PARP inhibitors treatment (Garnett *et al*, 2012; Stewart *et al*, 2014) and in addition PARP1 (that is the main target of PARP inhibitors) acts as transcriptional regulator of EWS-FLI1, by a physical interaction with the chimeric protein (Brenner *et al*, 2011). A recent study by Ordonez et al. demonstrates the efficacy of the combined treatment trabectedin – olaparib (one of the most used PARP1 inhibitor) in *in vitro* and *in vivo* models of ES (Ordonez *et al*, 2015).

The result that I obtained is in line with this work: the downregulation of PARP9 enhances the activity of trabectedin, possibly by the indirect downregulation of PARP1.

Another target whose downregulation enhanced the activity of trabectedin is BLK, that encodes for a tyrosine kinase involved in cell proliferation and differentiation.

The availability of inhibitors of BLK enzyme allowed me to perform pilot experiments to verify the effectiveness of the combination with trabectedin. I selected dasatinib, among the inhibitors of BLK, because it is already used in the clinic (e.g. for the treatment of imatinib-resistant or intolerant chronic myeloid leukemia) and therefore, if positive results were achieved, they could be applied for patients treatment more easily.

It should be noted, however, that dasatinib inhibits not only BLK but other kinases (e.g. c-KIT) and thus the results could be affected by lack of specificity.

I found that the combination of trabectedin with dasatinib was slightly synergic, at the lower doses. Therefore the results were only partially satisfactory.

It should be considered that the results obtained with siRNAs do not necessarily fully predict those obtained with a chemical inhibitor.

For genes encoding for proteins with a high turnover it is expected a rapid decrease in the protein whereas, in some cases, would be necessary to maintain the transcription inhibition for a very long time.

The initial results obtained by using this RNA silencing-based approach indicate its feasibility to discover potential new drug combinations.

Once further validated this “platform” could represent an important tool for the identification of specific targets whose inhibition can enhance the activity of an anticancer agent supposedly acting by modulating gene transcription.

There are however a number of caveats to this approach.

It should be considered that the RNA silencing methodology does not directly act on the protein and thus its effect depends on the time and efficiency of the downregulation, also in respect of the protein turnover.

I have arbitrarily used a concentration of trabectedin that was not very effective (i.e. IC30). Therefore it cannot be excluded that using higher concentrations I could have identified other targets suitable for combinations.

This seems to be the case as for example of WRN gene, whose downregulation required a concentration of trabectedin higher than the IC50.

In my choice I have preferred to select highly stringent conditions, with the risk of missing some potential useful target, selecting the conditions that might increase the potential application in the clinic, where the toxicity issues might require the use of relatively low doses of each drug that will used in combination.

In summary the experimental work performed in this thesis has shown that:

1) In a ES cellular model (TC71), the WEE1 inhibitor, AZD-1775, enhances trabectedin cytotoxicity.
2) A new approach based on RNA silencing library was developed to identify potential synergism in cells pre-treated with trabectedin.

   A number of targets, whose inhibition could potentiate the activity of trabectedin, have been identified.

   After further validations they may be exploited to set up new combination regimens for the treatment of ES.

APPENDIX

1. LIST OF PUBLICATIONS

1. **Mechanism of action of trabectedin in desmoplastic small round cell tumor cells.**
   Uboldi S, Craparotta I, Colella G, Ronchetti E, Beltrame L, Vicario S, Marchini S, Panini N, Dagrada G, Bozzi F, Pilotti S, Galmarini CM, D'Incalci M, Gatta R.
   BMC Cancer. 2017 Feb 6;17(1):107. doi: 10.1186/s12885-017-3091-1.
   PMID:28166781

2. **Increased sensitivity to platinum drugs of cancer cells with acquired resistance to trabectedin.**
   Colmegna B, **Uboldi S**, Frapolli R, Licandro SA, Panini N, Galmarini CM, Badri N, Spanswick VJ, Bingham JP, Kiakos K, Erba E, Hartley JA, D'Incalci M.
   Br J Cancer. 2015 Dec 22;113(12):1687-93. doi: 10.1038/bjc.2015.407. Epub 2015 Dec 3.
   PMID:26633559

3. **Trabectedin efficacy in Ewing sarcoma is greatly increased by combination with anti-IGF signaling agents.**
   Amaral AT, Garofalo C, Frapolli R, Manara MC, Mancarella C, **Uboldi S**, Di Giandomenico S, Ordóñez JL, Sevillano V, Malaguarnera R, Picci P, Hassan AB, De Alava E, D'Incalci M, Scotlandi K.
   Clin Cancer Res. 2015 Mar 15;21(6):1373-82. doi: 10.1158/1078-0432.CCR-14-1688. Epub 2015 Jan 21.
   PMID:25609059

4. **Mode of action of trabectedin in myxoid liposarcomas**.
   Di Giandomenico S, Frapolli R, Bello E, **Uboldi S**, Licandro SA, Marchini S, Beltrame L, Brich S, Mauro V, Tamborini E, Pilotti S, Casali PG, Grosso F, Sanfilippo R, Gronchi A, Mantovani R, Gatta R, Galmarini CM, Sousa-Faro JM, D'Incalci M.
   Oncogene. 2014 Oct 30;33(44):5201-10. doi: 10.1038/onc.2013.462. Epub 2013 Nov 11.
   PMID:24213580

5. **Role of macrophage targeting in the antitumor activity of trabectedin.**
   Germano G, Frapolli R, Belgiovine C, Anselmo A, Pesce S, Liguori M, Erba E, **Uboldi S**, Zucchetti M, Pasqualini F, Nebuloni M, van Rooijen N, Mortarini R, Beltrame L, Marchini S, Fuso Nerini I, Sanfilippo R, Casali PG, Pilotti S, Galmarini CM, Anichini A, Mantovani A, D'Incalci M, Allavena P.
   Cancer Cell. 2013 Feb 11;23(2):249-62. doi: 10.1016/j.ccr.2013.01.008.
   PMID:23410977

6. **The impairment of the High Mobility Group A (HMGA) protein function contributes to the anticancer activity of trabectedin.**
   D'Angelo D, Borbone E, Palmieri D, **Uboldi S**, Esposito F, Frapolli R, Pacelli R, D'Incalci M, Fusco A.
   Eur J Cancer. 2013 Mar;49(5):1142-51. doi: 10.1016/j.ejca.2012.10.014. Epub 2012 Nov 10.
   PMID:23149213

7. **A systems biology approach to characterize the regulatory networks leading to trabectedin resistance in an in vitro model of myxoid liposarcoma.**
Uboldi S, Calura E, Beltrame L, Fuso Nerini I, Marchini S, Cavalieri D, Erba E, Chiorino G, Ostano P, D'Angelo D, D'Incalci M, Romualdi C.
PLoS One. 2012;7(4):e35423. doi: 10.1371/journal.pone.0035423. Epub 2012 Apr 16.
PMID:22523595

8. **Characterization of a new trabectedin-resistant myxoid liposarcoma cell line that shows collateral sensitivity to methylating agents.**
Uboldi S, Bernasconi S, Romano M, Marchini S, Fuso Nerini I, Damia G, Ganzinelli M, Marangon E, Sala F, Clivio L, Chiorino G, Di Giandomenico S, Rocchi M, Capozzi O, Margison GP, Watson AJ, Caccuri AM, Pastore A, Fossati A, Mantovani R, Grosso F, Tercero JC, Erba E, D'Incalci M.
Int J Cancer. 2012 Jul 1;131(1):59-69. doi: 10.1002/ijc.26340. Epub 2011 Aug 30.
PMID:21805478

2. *LIST OF ABBREVIATIONS*

ABL1	Abelson Murine Leukemia Viral Oncogene Homolog 1
ALK	Anaplastic Lymphoma Kinase
AS	alternative splicing
ATM	Ataxia Telangiectasia mutated
ATR	Ataxia Telangiectasia and Rad3 Related gene
BCR	Breakpoint Cluster Regio
BRAF	Murine Sarcoma Viral (V-Raf) Oncogene Homolog B1
BRCA1	Breast and Ovarian Cancer Susceptibility Protein 1
BRCA2	Breast and Ovarian Cancer Susceptibility Protein 2
BSA	Bovine serum albumine
CCL	C-C Motif Chemokine Ligand
CDK1	Cyclin-dependent kinase 1
ChIP	Chromatin immunoprecipitation
ChK1	Checkpoint kinase 1
ChK2	Checkpoint kinase 2
CML	Chronic myelogenous leukemia
CPT	Camptothecin
CS	Cockayne syndrome
CXCL	C-X-C Motif Chemokine Ligand
DDR	DNA-damage response
DSB	Double strand breaks
dsDNA	double stranded DNA
dsRNA	double stranded RNA
ECM	Extracellular matrix
EGF	Epidhermal growth factor
ERBB2/HER2	Erb-B2 Receptor Tyrosine Kinase 2
ERCC	Excision repair cross-complementing gene
ERG	ETS-related gene
ES	Ewing's Sarcoma
ESFT	Ewing's Sarcoma family of tumours
esiRNA	endonuclease-siRNA
ET	Trabectedin
ETS	erythroblast transformation-specific or E twenty-six family of transcription factor
ETV1	ETS variant gene 1
ETV4	ETS variant gene 4
EWSR1	Ewing sarcoma breakpoint region 1
FANC	Fanconi's anemia proteins
FBS	fetal bovine serum
FDA	Food and Drug Administration
FEV	fifth Ewing variant
FLI1	Friend leukemia integration 1 transcription factor

H2B	histone H2B
HMG	high-mobility group proteins
HR	homologous recombination
ICL	interstrand crosslinks
IL	Interleukin
IMDM	Iscove's Dulbecco's Medium
IR	ionizing radiations
M1 or M2	Macrophages
MDSCs	myeloid-derived suppressor cells
miRNA	MicroRNA
MLS	myxoid liposarcoma tumors
MMPS	matrix metalloproteases
MMS	Methyl methanesulfonate
MSCs	Mesenchymal stem cells
NER	Nucleotide excision repair
NF-KB	Nuclear factor K-light-chain-enhancer of activated B cells
p53	tumor protein P53
PBS	Phosphate-buffered saline
PCNA	Proliferating cell nuclear antigen
PI	Propidium iodide
PlGF	Placental growth factor
PS	penicillin-streptomycin
PTX3	Pentraxin 3
RGG boxes	arginine – glycine – glycine repeats
RNA Pol II	RNA polimerase II
RNAi	RNA interference
RPA	replication protein A
RRM	RNA-recognition motif
SDS	Sodium Dodecyl Sulfate
Ser	Serine
shRNA	short hairpin RNA
siRNA	small interfering RNA
SSBs	single-strand breaks
ssRNA	single stranded RNA
STAT3	Signal Transducer and Activator Of Transcription 3
STS	soft tissue sarcoma
SYGQ	serine-tyrosine-glycine-glutamine sequence
TAM	tumor associated macrophages
TATA	also named Goldberg-Hogness box is a DNA sequence: 5'-TATAAA-3
TET	ten-eleven translocation family of proteins
TFIID	transcription factor IID
TME	tumor microenvironment
TNBC	triple-negative breast cancers

TTD	photosensitive form of trichotiodystrophy
UV	UV radiations
VEGF	Vascular endothelial growth factor
	WEE1 G2 Checkpoint Kinase
WRN	Werner RecQ helicase
XP	Xeroderam pigmentosum
XRCC	X-Ray Repair Cross Complementing 1
Y	Tyrosine

BIBLIOGRAPHY

Aarts M, Sharpe R, Garcia-Murillas I, Gevensleben H, Hurd MS, Shumway SD, Toniatti C, Ashworth A, Turner NC (2012) Forced mitotic entry of S-phase cells as a therapeutic strategy induced by inhibition of WEE1. *Cancer Discov* **2**(6)**:** 524-39

Aihara H, Ito Y, Kurumizaka H, Yokoyama S, Shibata T (1999) The N-terminal domain of the human Rad51 protein binds DNA: structure and a DNA binding surface as revealed by NMR. *J Mol Biol* **290**(2)**:** 495-504

Allavena P, Signorelli M, Chieppa M, Erba E, Bianchi G, Marchesi F, Olimpio CO, Bonardi C, Garbi A, Lissoni A, de Braud F, Jimeno J, D'Incalci M (2005) Anti-inflammatory properties of the novel antitumor agent yondelis (trabectedin): inhibition of macrophage differentiation and cytokine production. *Cancer Res* **65**(7)**:** 2964-71

Anand A, Chada K (2000) In vivo modulation of Hmgic reduces obesity. *Nat Genet* **24**(4)**:** 377-80

Arcamone F, Cassinelli G, Fantini G, Grein A, Orezzi P, Pol C, Spalla C (1969) Adriamycin, 14-hydroxydaunomycin, a new antitumor antibiotic from S. peucetius var. caesius. *Biotechnol Bioeng* **11**(6)**:** 1101-10

Arteaga CL, Engelman JA (2014) ERBB receptors: from oncogene discovery to basic science to mechanism-based cancer therapeutics. *Cancer Cell* **25**(3)**:** 282-303

Arvand A, Denny CT (2001) Biology of EWS/ETS fusions in Ewing's family tumors. *Oncogene* **20**(40)**:** 5747-54

Bai Y, Li J, Fang B, Edwards A, Zhang G, Bui M, Eschrich S, Altiok S, Koomen J, Haura EB (2012) Phosphoproteomics identifies driver tyrosine kinases in sarcoma cell lines and tumors. *Cancer Res* **72**(10)**:** 2501-11

Bailly RA, Bosselut R, Zucman J, Cormier F, Delattre O, Roussel M, Thomas G, Ghysdael J (1994) DNA-binding and transcriptional activation properties of the EWS-FLI-1 fusion protein resulting from the t(11;22) translocation in Ewing sarcoma. *Mol Cell Biol* **14**(5)**:** 3230-41

Balamuth NJ, Womer RB (2010) Ewing's sarcoma. *Lancet Oncol* **11**(2)**:** 184-92

Balkwill F, Coussens LM (2004) Cancer: an inflammatory link. *Nature* **431**(7007)**:** 405-6

Balkwill F, Mantovani A (2001) Inflammation and cancer: back to Virchow? *Lancet* **357**(9255)**:** 539-45

Bandiera A, Bonifacio D, Manfioletti G, Mantovani F, Rustighi A, Zanconati F, Fusco A, Di Bonito L, Giancotti V (1998) Expression of HMGI(Y) proteins in squamous intraepithelial and invasive lesions of the uterine cervix. *Cancer Res* **58**(3)**:** 426-31

Barker HE, Cox TR, Erler JT (2012) The rationale for targeting the LOX family in cancer. *Nat Rev Cancer* **12**(8)**:** 540-52

Bartz SR, Zhang Z, Burchard J, Imakura M, Martin M, Palmieri A, Needham R, Guo J, Gordon M, Chung N, Warrener P, Jackson AL, Carleton M, Oatley M, Locco L, Santini F, Smith T, Kunapuli P, Ferrer M, Strulovici B, Friend SH, Linsley PS (2006) Small interfering RNA screens reveal enhanced cisplatin cytotoxicity in tumor cells having both BRCA network and TP53 disruptions. *Mol Cell Biol* **26**(24)**:** 9377-86

Baruchel S, Pappo A, Krailo M, Baker KS, Wu B, Villaluna D, Lee-Scott M, Adamson PC, Blaney SM (2012) A phase 2 trial of trabectedin in children with recurrent rhabdomyosarcoma, Ewing sarcoma and non-rhabdomyosarcoma soft tissue sarcomas: a report from the Children's Oncology Group. *Eur J Cancer* **48**(4)**:** 579-85

Bearss DJ, Lee RJ, Troyer DA, Pestell RG, Windle JJ (2002) Differential effects of p21(WAF1/CIP1) deficiency on MMTV-ras and MMTV-myc mammary tumor properties. *Cancer Res* **62**(7)**:** 2077-84

Beck H, Nahse V, Larsen MS, Groth P, Clancy T, Lees M, Jorgensen M, Helleday T, Syljuasen RG, Sorensen CS (2010) Regulators of cyclin-dependent kinases are crucial for maintaining genome integrity in S phase. *J Cell Biol* **188**(5)**:** 629-38

Beljanski V, Marzilli LG, Doetsch PW (2004) DNA damage-processing pathways involved in the eukaryotic cellular response to anticancer DNA cross-linking drugs. *Mol Pharmacol* **65**(6)**:** 1496-506

Ben-David Y, Giddens EB, Bernstein A (1990) Identification and mapping of a common proviral integration site Fli-1 in erythroleukemia cells induced by Friend murine leukemia virus. *Proc Natl Acad Sci U S A* **87**(4)**:** 1332-6

Ben-David Y, Giddens EB, Letwin K, Bernstein A (1991) Erythroleukemia induction by Friend murine leukemia virus: insertional activation of a new member of the ets gene family, Fli-1, closely linked to c-ets-1. *Genes Dev* **5**(6)**:** 908-18

Benada J, Macurek L (2015) Targeting the Checkpoint to Kill Cancer Cells. *Biomolecules* **5**(3)**:** 1912-37

Beumer JH, Rademaker-Lakhai JM, Rosing H, Lopez-Lazaro L, Beijnen JH, Schellens JH (2005) Trabectedin (Yondelis, formerly ET-743), a mass balance study in patients with advanced cancer. *Invest New Drugs* **23**(5)**:** 429-36

Bianchi ME, Beltrame M, Paonessa G (1989) Specific recognition of cruciform DNA by nuclear protein HMG1. *Science* **243**(4894 Pt 1)**:** 1056-9

Birger Y, Ito Y, West KL, Landsman D, Bustin M (2001) HMGN4, a newly discovered nucleosome-binding protein encoded by an intronless gene. *DNA Cell Biol* **20**(5)**:** 257-64

Bonfanti M, La Valle E, Fernandez Sousa Faro JM, Faircloth G, Caretti G, Mantovani R, D'Incalci M (1999) Effect of ecteinascidin-743 on the interaction between DNA binding proteins and DNA. *Anticancer Drug Des* **14**(3)**:** 179-86

Bradford MM (1976) A rapid and sensitive method for the quantitation of microgram quantities of protein utilizing the principle of protein-dye binding. *Anal Biochem* **72:** 248-54

Brandon EF, Sparidans RW, Guijt KJ, Lowenthal S, Meijerman I, Beijnen JH, Schellens JH (2006) In vitro characterization of the human biotransformation and CYP reaction phenotype of ET-743 (Yondelis, Trabectidin), a novel marine anti-cancer drug. *Invest New Drugs* **24**(1)**:** 3-14

Brenner JC, Ateeq B, Li Y, Yocum AK, Cao Q, Asangani IA, Patel S, Wang X, Liang H, Yu J, Palanisamy N, Siddiqui J, Yan W, Cao X, Mehra R, Sabolch A, Basrur V, Lonigro RJ, Yang J, Tomlins SA, Maher CA, Elenitoba-Johnson KS, Hussain M, Navone NM, Pienta KJ, Varambally S, Feng FY, Chinnaiyan AM (2011) Mechanistic rationale for inhibition of poly(ADP-ribose) polymerase in ETS gene fusion-positive prostate cancer. *Cancer Cell* **19**(5)**:** 664-78

Broggini M, Coley HM, Mongelli N, Pesenti E, Wyatt MD, Hartley JA, D'Incalci M (1995) DNA sequence-specific adenine alkylation by the novel antitumor drug tallimustine (FCE 24517), a benzoyl nitrogen mustard derivative of distamycin. *Nucleic Acids Res* **23**(1)**:** 81-7

Broggini M, Erba E, Ponti M, Ballinari D, Geroni C, Spreafico F, D'Incalci M (1991) Selective DNA interaction of the novel distamycin derivative FCE 24517. *Cancer Res* **51**(1)**:** 199-204

Bryant C, Rawlinson R, Massey AJ (2014) Chk1 inhibition as a novel therapeutic strategy for treating triple-negative breast and ovarian cancers. *BMC Cancer* **14:** 570

Bustin M (2001) Revised nomenclature for high mobility group (HMG) chromosomal proteins. *Trends Biochem Sci* **26**(3)**:** 152-3

Carpenter AJ, Porter AC (2004) Construction, characterization, and complementation of a conditional-lethal DNA topoisomerase IIalpha mutant human cell line. *Mol Biol Cell* **15**(12)**:** 5700-11

Carrassa L, Chila R, Lupi M, Ricci F, Celenza C, Mazzoletti M, Broggini M, Damia G (2012) Combined inhibition of Chk1 and Wee1: in vitro synergistic effect translates to tumor growth inhibition in vivo. *Cell Cycle* **11**(13)**:** 2507-17

Castillero-Trejo Y, Eliazer S, Xiang L, Richardson JA, Ilaria RL, Jr. (2005) Expression of the EWS/FLI-1 oncogene in murine primary bone-derived cells Results in EWS/FLI-1-dependent, ewing sarcoma-like tumors. *Cancer Res* **65**(19)**:** 8698-705

Cavazzana AO, Magnani JL, Ross RA, Miser J, Triche TJ (1988) Ewing's sarcoma is an undifferentiated neuroectodermal tumor. *Prog Clin Biol Res* **271:** 487-98

Chan DA, Giaccia AJ (2011) Harnessing synthetic lethal interactions in anticancer drug discovery. *Nat Rev Drug Discov* **10**(5)**:** 351-64

Chapman PB, Hauschild A, Robert C, Haanen JB, Ascierto P, Larkin J, Dummer R, Garbe C, Testori A, Maio M, Hogg D, Lorigan P, Lebbe C, Jouary T, Schadendorf D, Ribas A, O'Day SJ, Sosman JA, Kirkwood JM, Eggermont AM, Dreno B, Nolop K, Li J, Nelson B, Hou J, Lee RJ, Flaherty KT, McArthur GA, Group B-S (2011) Improved survival with vemurafenib in melanoma with BRAF V600E mutation. *N Engl J Med* **364**(26)**:** 2507-16

Chen F, Zhuang X, Lin L, Yu P, Wang Y, Shi Y, Hu G, Sun Y (2015) New horizons in tumor microenvironment biology: challenges and opportunities. *BMC Med* **13:** 45

Chen Z, Xiao Z, Chen J, Ng SC, Sowin T, Sham H, Rosenberg S, Fesik S, Zhang H (2003) Human Chk1 expression is dispensable for somatic cell death and critical for sustaining G2 DNA damage checkpoint. *Mol Cancer Ther* **2**(6)**:** 543-8

Chen Z, Xiao Z, Gu WZ, Xue J, Bui MH, Kovar P, Li G, Wang G, Tao ZF, Tong Y, Lin NH, Sham HL, Wang JY, Sowin TJ, Rosenberg SH, Zhang H (2006) Selective Chk1 inhibitors differentially sensitize p53-deficient cancer cells to cancer therapeutics. *Int J Cancer* **119**(12)**:** 2784-94

Cheung MC, Jones RL, Judson I (2011) Acute liver toxicity with ifosfamide in the treatment of sarcoma: a case report. *J Med Case Rep* **5:** 180

Chugh R, Wagner T, Griffith KA, Taylor JM, Thomas DG, Worden FP, Leu KM, Zalupski MM, Baker LH (2007) Assessment of ifosfamide pharmacokinetics, toxicity, and relation to CYP3A4 activity as measured by the erythromycin breath test in patients with sarcoma. *Cancer* **109**(11)**:** 2315-22

Cohen P (2002) Protein kinases--the major drug targets of the twenty-first century? *Nat Rev Drug Discov* **1**(4)**:** 309-15

Colella G, Bonfanti M, D'Incalci M, Broggini M (1996) Characterization of a protein recognizing minor groove binders-damaged DNA. *Nucleic Acids Res* **24**(21)**:** 4227-33

Colmegna B, Uboldi S, Frapolli R, Licandro SA, Panini N, Galmarini CM, Badri N, Spanswick VJ, Bingham JP, Kiakos K, Erba E, Hartley JA, D'Incalci M (2015) Increased sensitivity to platinum drugs of cancer cells with acquired resistance to trabectedin. *Br J Cancer* **113**(12)**:** 1687-93

Cragg GM, Newman DJ, Weiss RB (1997) Coral reefs, forests, and thermal vents: the worldwide exploration of nature for novel antitumor agents. *Semin Oncol* **24**(2)**:** 156-63

Creemers GJ, Lund B, Verweij J (1994) Topoisomerase I inhibitors: topotecan and irenotecan. *Cancer Treat Rev* **20**(1)**:** 73-96

Cui JW, Vecchiarelli-Federico LM, Li YJ, Wang GJ, Ben-David Y (2009) Continuous Fli-1 expression plays an essential role in the proliferation and survival of F-MuLV-induced erythroleukemia and human erythroleukemia. *Leukemia* **23**(7)**:** 1311-9

D'Angelo D, Borbone E, Palmieri D, Uboldi S, Esposito F, Frapolli R, Pacelli R, D'Incalci M, Fusco A (2013) The impairment of the High Mobility Group A (HMGA) protein function contributes to the anticancer activity of trabectedin. *Eur J Cancer* **49**(5)**:** 1142-51

D'Incalci M (1998) Some hope from marine natural products. *Ann Oncol* **9**(9)**:** 937-8

D'Incalci M, Colombo T, Ubezio P, Nicoletti I, Giavazzi R, Erba E, Ferrarese L, Meco D, Riccardi R, Sessa C, Cavallini E, Jimeno J, Faircloth GT (2003) The combination of yondelis and cisplatin is synergistic against human tumor xenografts. *Eur J Cancer* **39**(13)**:** 1920-6

da Rocha AB, Lopes RM, Schwartsmann G (2001) Natural products in anticancer therapy. *Curr Opin Pharmacol* **1**(4)**:** 364-9

Damia G, Silvestri S, Carrassa L, Filiberti L, Faircloth GT, Liberi G, Foiani M, D'Incalci M (2001) Unique pattern of ET-743 activity in different cellular systems with defined deficiencies in DNA-repair pathways. *Int J Cancer* **92**(4)**:** 583-8

David-Cordonnier MH, Gajate C, Olmea O, Laine W, de la Iglesia-Vicente J, Perez C, Cuevas C, Otero G, Manzanares I, Bailly C, Mollinedo F (2005) DNA and non-DNA targets in the mechanism of action of the antitumor drug trabectedin. *Chem Biol* **12**(11)**:** 1201-10

Davies KD, Cable PL, Garrus JE, Sullivan FX, von Carlowitz I, Huerou YL, Wallace E, Woessner RD, Gross S (2011) Chk1 inhibition and Wee1 inhibition combine synergistically to impede cellular proliferation. *Cancer Biol Ther* **12**(9)**:** 788-96

de Jonge ME, Huitema AD, Rodenhuis S, Beijnen JH (2005) Clinical pharmacokinetics of cyclophosphamide. *Clin Pharmacokinet* **44**(11)**:** 1135-64

Delaloge S, Yovine A, Taamma A, Riofrio M, Brain E, Raymond E, Cottu P, Goldwasser F, Jimeno J, Misset JL, Marty M, Cvitkovic E (2001) Ecteinascidin-743: a marine-derived compound in advanced, pretreated sarcoma patients--preliminary evidence of activity. *J Clin Oncol* **19**(5)**:** 1248-55

Delattre O, Zucman J, Plougastel B, Desmaze C, Melot T, Peter M, Kovar H, Joubert I, de Jong P, Rouleau G, et al. (1992) Gene fusion with an ETS DNA-binding domain caused by chromosome translocation in human tumours. *Nature* **359**(6391)**:** 162-5

Demetri GD, Chawla SP, von Mehren M, Ritch P, Baker LH, Blay JY, Hande KR, Keohan ML, Samuels BL, Schuetze S, Lebedinsky C, Elsayed YA, Izquierdo MA, Gomez J, Park YC, Le Cesne A (2009) Efficacy and safety of trabectedin in patients with advanced or metastatic liposarcoma or leiomyosarcoma after failure of prior anthracyclines and ifosfamide: results of a randomized phase II study of two different schedules. *J Clin Oncol* **27**(25)**:** 4188-96

Detry B, Erpicum C, Paupert J, Blacher S, Maillard C, Bruyere F, Pendeville H, Remacle T, Lambert V, Balsat C, Ormenese S, Lamaye F, Janssens E, Moons L, Cataldo D,

Kridelka F, Carmeliet P, Thiry M, Foidart JM, Struman I, Noel A (2012) Matrix metalloproteinase-2 governs lymphatic vessel formation as an interstitial collagenase. *Blood* **119**(21)**:** 5048-56

Di Giandomenico S, Frapolli R, Bello E, Uboldi S, Licandro SA, Marchini S, Beltrame L, Brich S, Mauro V, Tamborini E, Pilotti S, Casali PG, Grosso F, Sanfilippo R, Gronchi A, Mantovani R, Gatta R, Galmarini CM, Sousa-Faro JM, D'Incalci M (2014) Mode of action of trabectedin in myxoid liposarcomas. *Oncogene* **33**(44)**:** 5201-10

Di Marco A, Gaetani M, Scarpinato B (1969) Adriamycin (NSC-123,127): a new antibiotic with antitumor activity. *Cancer Chemother Rep* **53**(1)**:** 33-7

Dickman PS, Liotta LA, Triche TJ (1982) Ewing's sarcoma. Characterization in established cultures and evidence of its histogenesis. *Lab Invest* **47**(4)**:** 375-82

Ebos JM, Kerbel RS (2011) Antiangiogenic therapy: impact on invasion, disease progression, and metastasis. *Nat Rev Clin Oncol* **8**(4)**:** 210-21

Erba E, Bergamaschi D, Bassano L, Damia G, Ronzoni S, Faircloth GT, D'Incalci M (2001) Ecteinascidin-743 (ET-743), a natural marine compound, with a unique mechanism of action. *Eur J Cancer* **37**(1)**:** 97-105

Ewing J (1921) Diffuse endothelioma of bone. *Proc New York Path Soc* **21:** 17-24

Fasulo B, Koyama C, Yu KR, Homola EM, Hsieh TS, Campbell SD, Sullivan W (2012) Chk1 and Wee1 kinases coordinate DNA replication, chromosome condensation, and anaphase entry. *Mol Biol Cell* **23**(6)**:** 1047-57

Featherstone C, Russell P (1991) Fission yeast p107wee1 mitotic inhibitor is a tyrosine/serine kinase. *Nature* **349**(6312)**:** 808-11

Feuerhahn S, Giraudon C, Martinez-Diez M, Bueren-Calabuig JA, Galmarini CM, Gago F, Egly JM (2011) XPF-dependent DNA breaks and RNA polymerase II arrest induced by antitumor DNA interstrand crosslinking-mimetic alkaloids. *Chem Biol* **18**(8)**:** 988-99

Forni C, Minuzzo M, Virdis E, Tamborini E, Simone M, Tavecchio M, Erba E, Grosso F, Gronchi A, Aman P, Casali P, D'Incalci M, Pilotti S, Mantovani R (2009) Trabectedin (ET-743) promotes differentiation in myxoid liposarcoma tumors. *Mol Cancer Ther* **8**(2)**:** 449-57

Foti D, Chiefari E, Fedele M, Iuliano R, Brunetti L, Paonessa F, Manfioletti G, Barbetti F, Brunetti A, Croce CM, Fusco A, Brunetti A (2005) Lack of the architectural factor HMGA1 causes insulin resistance and diabetes in humans and mice. *Nat Med* **11**(7)**:** 765-73

Frapolli R, Tamborini E, Virdis E, Bello E, Tarantino E, Marchini S, Grosso F, Sanfilippo R, Gronchi A, Tercero JC, Peloso G, Casali P, Pilotti S, D'Incalci M (2010) Novel models of myxoid liposarcoma xenografts mimicking the biological and pharmacologic features of human tumors. *Clin Cancer Res* **16**(20)**:** 4958-67

Friedman D, Hu Z, Kolb EA, Gorfajn B, Scotto KW (2002) Ecteinascidin-743 inhibits activated but not constitutive transcription. *Cancer Res* **62**(12)**:** 3377-81

Galmarini CM, D'Incalci M, Allavena P (2014) Trabectedin and plitidepsin: drugs from the sea that strike the tumor microenvironment. *Mar Drugs* **12**(2)**:** 719-33

Ganapathy V, Thangaraju M, Prasad PD (2009) Nutrient transporters in cancer: relevance to Warburg hypothesis and beyond. *Pharmacol Ther* **121**(1)**:** 29-40

Garcia-Carbonero R, Supko JG, Manola J, Seiden MV, Harmon D, Ryan DP, Quigley MT, Merriam P, Canniff J, Goss G, Matulonis U, Maki RG, Lopez T, Puchalski TA, Sancho MA, Gomez J, Guzman C, Jimeno J, Demetri GD (2004) Phase II and pharmacokinetic study of ecteinascidin 743 in patients with progressive sarcomas of soft tissues refractory to chemotherapy. *J Clin Oncol* **22**(8)**:** 1480-90

Garnett MJ, Edelman EJ, Heidorn SJ, Greenman CD, Dastur A, Lau KW, Greninger P, Thompson IR, Luo X, Soares J, Liu Q, Iorio F, Surdez D, Chen L, Milano RJ, Bignell GR, Tam AT, Davies H, Stevenson JA, Barthorpe S, Lutz SR, Kogera F, Lawrence K, McLaren-Douglas A, Mitropoulos X, Mironenko T, Thi H, Richardson L, Zhou W, Jewitt F, Zhang T, O'Brien P, Boisvert JL, Price S, Hur W, Yang W, Deng X, Butler A, Choi HG, Chang JW, Baselga J, Stamenkovic I, Engelman JA, Sharma SV, Delattre O, Saez-Rodriguez J, Gray NS, Settleman J, Futreal PA, Haber DA, Stratton MR, Ramaswamy S, McDermott U, Benes CH (2012) Systematic identification of genomic markers of drug sensitivity in cancer cells. *Nature* **483**(7391)**:** 570-5

Germano G, Frapolli R, Belgiovine C, Anselmo A, Pesce S, Liguori M, Erba E, Uboldi S, Zucchetti M, Pasqualini F, Nebuloni M, van Rooijen N, Mortarini R, Beltrame L, Marchini S, Fuso Nerini I, Sanfilippo R, Casali PG, Pilotti S, Galmarini CM, Anichini A, Mantovani A, D'Incalci M, Allavena P (2013) Role of macrophage targeting in the antitumor activity of trabectedin. *Cancer Cell* **23**(2)**:** 249-62

Germano G, Frapolli R, Simone M, Tavecchio M, Erba E, Pesce S, Pasqualini F, Grosso F, Sanfilippo R, Casali PG, Gronchi A, Virdis E, Tarantino E, Pilotti S, Greco A, Nebuloni M, Galmarini CM, Tercero JC, Mantovani A, D'Incalci M, Allavena P (2010) Antitumor and anti-inflammatory effects of trabectedin on human myxoid liposarcoma cells. *Cancer Res* **70**(6)**:** 2235-44

Gewirtz DA (1999) A critical evaluation of the mechanisms of action proposed for the antitumor effects of the anthracycline antibiotics adriamycin and daunorubicin. *Biochem Pharmacol* **57**(7)**:** 727-41

Giroux V, Iovanna J, Dagorn JC (2006) Probing the human kinome for kinases involved in pancreatic cancer cell survival and gemcitabine resistance. *FASEB J* **20**(12)**:** 1982-91

Goodwin GH, Johns EW (1973) Isolation and characterisation of two calf-thymus chromatin non-histone proteins with high contents of acidic and basic amino acids. *Eur J Biochem* **40**(1)**:** 215-9

Goto H, Kariya R, Shimamoto M, Kudo E, Taura M, Katano H, Okada S (2012) Antitumor effect of berberine against primary effusion lymphoma via inhibition of NF-kappaB pathway. *Cancer Sci* **103**(4)**:** 775-81

Goto H, Kasahara K, Inagaki M (2015) Novel insights into Chk1 regulation by phosphorylation. *Cell Struct Funct* **40**(1)**:** 43-50

Gould KL, Nurse P (1989) Tyrosine phosphorylation of the fission yeast cdc2+ protein kinase regulates entry into mitosis. *Nature* **342**(6245)**:** 39-45

Grabauskiene S, Bergeron EJ, Chen G, Thomas DG, Giordano TJ, Beer DG, Morgan MA, Reddy RM (2014) Checkpoint kinase 1 protein expression indicates sensitization to therapy by checkpoint kinase 1 inhibition in non-small cell lung cancer. *J Surg Res* **187**(1)**:** 6-13

Greten FR, Arkan MC, Bollrath J, Hsu LC, Goode J, Miething C, Goktuna SI, Neuenhahn M, Fierer J, Paxian S, Van Rooijen N, Xu Y, O'Cain T, Jaffee BB, Busch DH, Duyster J, Schmid RM, Eckmann L, Karin M (2007) NF-kappaB is a negative regulator of IL-1beta secretion as revealed by genetic and pharmacological inhibition of IKKbeta. *Cell* **130**(5)**:** 918-31

Grier HE (1997) The Ewing family of tumors. Ewing's sarcoma and primitive neuroectodermal tumors. *Pediatr Clin North Am* **44**(4)**:** 991-1004

Grohar PJ, Griffin LB, Yeung C, Chen QR, Pommier Y, Khanna C, Khan J, Helman LJ (2011) Ecteinascidin 743 interferes with the activity of EWS-FLI1 in Ewing sarcoma cells. *Neoplasia* **13**(2)**:** 145-53

Grohar PJ, Segars LE, Yeung C, Pommier Y, D'Incalci M, Mendoza A, Helman LJ (2014) Dual targeting of EWS-FLI1 activity and the associated DNA damage response with trabectedin and SN38 synergistically inhibits Ewing sarcoma cell growth. *Clin Cancer Res* **20**(5)**:** 1190-203

Gronchi A, Bui BN, Bonvalot S, Pilotti S, Ferrari S, Hohenberger P, Hohl RJ, Demetri GD, Le Cesne A, Lardelli P, Perez I, Nieto A, Tercero JC, Alfaro V, Tamborini E, Blay JY (2012) Phase II clinical trial of neoadjuvant trabectedin in patients with advanced localized myxoid liposarcoma. *Ann Oncol* **23**(3)**:** 771-6

Grosso F, Dileo P, Sanfilippo R, Stacchiotti S, Bertulli R, Piovesan C, Jimeno J, D'Incalci M, Gescher A, Casali PG (2006) Steroid premedication markedly reduces liver and bone marrow toxicity of trabectedin in advanced sarcoma. *Eur J Cancer* **42**(10)**:** 1484-90

Grosso F, Jones RL, Demetri GD, Judson IR, Blay JY, Le Cesne A, Sanfilippo R, Casieri P, Collini P, Dileo P, Spreafico C, Stacchiotti S, Tamborini E, Tercero JC, Jimeno J, D'Incalci M, Gronchi A, Fletcher JA, Pilotti S, Casali PG (2007) Efficacy of trabectedin (ecteinascidin-743) in advanced pretreated myxoid liposarcomas: a retrospective study. *Lancet Oncol* **8**(7)**:** 595-602

Guarente L (1993) Synthetic enhancement in gene interaction: a genetic tool come of age. *Trends Genet* **9**(10)**:** 362-6

Guertin AD, Martin MM, Roberts B, Hurd M, Qu X, Miselis NR, Liu Y, Li J, Feldman I, Benita Y, Bloecher A, Toniatti C, Shumway SD (2012) Unique functions of CHK1 and WEE1 underlie synergistic anti-tumor activity upon pharmacologic inhibition. *Cancer Cell Int* **12**(1)**:** 45

Hahm KB, Cho K, Lee C, Im YH, Chang J, Choi SG, Sorensen PH, Thiele CJ, Kim SJ (1999) Repression of the gene encoding the TGF-beta type II receptor is a major target of the EWS-FLI1 oncoprotein. *Nat Genet* **23**(2)**:** 222-7

Hanahan D, Coussens LM (2012) Accessories to the crime: functions of cells recruited to the tumor microenvironment. *Cancer Cell* **21**(3)**:** 309-22

Hanahan D, Weinberg RA (2011) Hallmarks of cancer: the next generation. *Cell* **144**(5)**:** 646-74

Hartwell LH, Szankasi P, Roberts CJ, Murray AW, Friend SH (1997) Integrating genetic approaches into the discovery of anticancer drugs. *Science* **278**(5340)**:** 1064-8

Hendriks HR, Fiebig HH, Giavazzi R, Langdon SP, Jimeno JM, Faircloth GT (1999) High antitumour activity of ET743 against human tumour xenografts from melanoma, non-small-cell lung and ovarian cancer. *Ann Oncol* **10**(10)**:** 1233-40

Herrero AB, Martin-Castellanos C, Marco E, Gago F, Moreno S (2006) Cross-talk between nucleotide excision and homologous recombination DNA repair pathways in the mechanism of action of antitumor trabectedin. *Cancer Res* **66**(16)**:** 8155-62

Hewett PW, Nishi K, Daft EL, Clifford Murray J (2001) Selective expression of erg isoforms in human endothelial cells. *Int J Biochem Cell Biol* **33**(4)**:** 347-55

Hirai H, Iwasawa Y, Okada M, Arai T, Nishibata T, Kobayashi M, Kimura T, Kaneko N, Ohtani J, Yamanaka K, Itadani H, Takahashi-Suzuki I, Fukasawa K, Oki H, Nambu T, Jiang J, Sakai T, Arakawa H, Sakamoto T, Sagara T, Yoshizumi T, Mizuarai S, Kotani H (2009) Small-molecule inhibition of Wee1 kinase by MK-1775 selectively sensitizes p53-deficient tumor cells to DNA-damaging agents. *Mol Cancer Ther* **8**(11)**:** 2992-3000

Hoeijmakers JH, Bootsma D (1994) DNA repair. Incisions for excision. *Nature* **371**(6499)**:** 654-5

Hu-Lieskovan S, Zhang J, Wu L, Shimada H, Schofield DE, Triche TJ (2005) EWS-FLI1 fusion protein up-regulates critical genes in neural crest development and is responsible for the observed phenotype of Ewing's family of tumors. *Cancer Res* **65**(11)**:** 4633-44

Hughes EN, Engelsberg BN, Billings PC (1992) Purification of nuclear proteins that bind to cisplatin-damaged DNA. Identity with high mobility group proteins 1 and 2. *J Biol Chem* **267**(19)**:** 13520-7

Hurov KE, Cotta-Ramusino C, Elledge SJ (2010) A genetic screen identifies the Triple T complex required for DNA damage signaling and ATM and ATR stability. *Genes Dev* **24**(17)**:** 1939-50

Iorns E, Lord CJ, Grigoriadis A, McDonald S, Fenwick K, Mackay A, Mein CA, Natrajan R, Savage K, Tamber N, Reis-Filho JS, Turner NC, Ashworth A (2009) Integrated functional, gene expression and genomic analysis for the identification of cancer targets. *PLoS One* **4**(4)**:** e5120

Iorns E, Lord CJ, Turner N, Ashworth A (2007) Utilizing RNA interference to enhance cancer drug discovery. *Nat Rev Drug Discov* **6**(7)**:** 556-68

Izbicka E, Lawrence R, Raymond E, Eckhardt G, Faircloth G, Jimeno J, Clark G, Von Hoff DD (1998) In vitro antitumor activity of the novel marine agent, ecteinascidin-743 (ET-743, NSC-648766) against human tumors explanted from patients. *Ann Oncol* **9**(9)**:** 981-7

Jasin M (2002) Homologous repair of DNA damage and tumorigenesis: the BRCA connection. *Oncogene* **21**(58)**:** 8981-93

Jeon IS, Davis JN, Braun BS, Sublett JE, Roussel MF, Denny CT, Shapiro DN (1995) A variant Ewing's sarcoma translocation (7;22) fuses the EWS gene to the ETS gene ETV1. *Oncogene* **10**(6)**:** 1229-34

Ji D, Deeds SL, Weinstein EJ (2007) A screen of shRNAs targeting tumor suppressor genes to identify factors involved in A549 paclitaxel sensitivity. *Oncol Rep* **18**(6)**:** 1499-505

Johnson KR, Lehn DA, Elton TS, Barr PJ, Reeves R (1988) Complete murine cDNA sequence, genomic structure, and tissue expression of the high mobility group protein HMG-I(Y). *J Biol Chem* **263**(34)**:** 18338-42

Johnson KR, Lehn DA, Reeves R (1989) Alternative processing of mRNAs encoding mammalian chromosomal high-mobility-group proteins HMG-I and HMG-Y. *Mol Cell Biol* **9**(5)**:** 2114-23

Junttila MR, de Sauvage FJ (2013) Influence of tumour micro-environment heterogeneity on therapeutic response. *Nature* **501**(7467)**:** 346-54

Kadin ME, Bensch KG (1971) On the origin of Ewing's tumor. *Cancer* **27**(2)**:** 257-73

Kaelin WG, Jr. (2005) The concept of synthetic lethality in the context of anticancer therapy. *Nat Rev Cancer* **5**(9)**:** 689-98

Kaelin WG, Jr. (2009) Synthetic lethality: a framework for the development of wiser cancer therapeutics. *Genome Med* **1**(10)**:** 99

Kang JH, Song KH, Jeong KC, Kim S, Choi C, Lee CH, Oh SH (2011) Involvement of Cox-2 in the metastatic potential of chemotherapy-resistant breast cancer cells. *BMC Cancer* **11:** 334

Kantarjian H, Sawyers C, Hochhaus A, Guilhot F, Schiffer C, Gambacorti-Passerini C, Niederwieser D, Resta D, Capdeville R, Zoellner U, Talpaz M, Druker B, Goldman J, O'Brien SG, Russell N, Fischer T, Ottmann O, Cony-Makhoul P, Facon T, Stone R, Miller C, Tallman M, Brown R, Schuster M, Loughran T, Gratwohl A, Mandelli F, Saglio G, Lazzarino M, Russo D, Baccarani M, Morra E, International STICMLSG (2002) Hematologic and cytogenetic responses to imatinib mesylate in chronic myelogenous leukemia. *N Engl J Med* **346**(9)**:** 645-52

Kessenbrock K, Plaks V, Werb Z (2010) Matrix metalloproteinases: regulators of the tumor microenvironment. *Cell* **141**(1)**:** 52-67

Khoury GA, Baliban RC, Floudas CA (2011) Proteome-wide post-translational modification statistics: frequency analysis and curation of the swiss-prot database. *Sci Rep* **1**

Kim C, Gao YT, Xiang YB, Barone-Adesi F, Zhang Y, Hosgood HD, Ma S, Shu XO, Ji BT, Chow WH, Seow WJ, Bassig B, Cai Q, Zheng W, Rothman N, Lan Q (2015) Home kitchen ventilation, cooking fuels, and lung cancer risk in a prospective cohort of never smoking women in Shanghai, China. *Int J Cancer* **136**(3)**:** 632-8

Koniaras K, Cuddihy AR, Christopoulos H, Hogg A, O'Connell MJ (2001) Inhibition of Chk1-dependent G2 DNA damage checkpoint radiosensitizes p53 mutant human cells. *Oncogene* **20**(51)**:** 7453-63

Kovar H (1998) Ewing's sarcoma and peripheral primitive neuroectodermal tumors after their genetic union. *Curr Opin Oncol* **10**(4)**:** 334-42

Kroll ES, Hyland KM, Hieter P, Li JJ (1996) Establishing genetic interactions by a synthetic dosage lethality phenotype. *Genetics* **143**(1)**:** 95-102

Ladenstein R PU, Le Deley MC, Whelan J, Paulussen M , U P, MC LD, J W, M P (2010) Primary disseminated multifocal Ewing sarcoma: results of the Euro-EWING 99 trial. *J Clin Oncol* **28:** 3284-91

Lau L, Supko JG, Blaney S, Hershon L, Seibel N, Krailo M, Qu W, Malkin D, Jimeno J, Bernstein M, Baruchel S (2005) A phase I and pharmacokinetic study of ecteinascidin-743 (Yondelis) in children with refractory solid tumors. A Children's Oncology Group study. *Clin Cancer Res* **11**(2 Pt 1)**:** 672-7

Le Cesne A, Cresta S, Maki RG, Blay JY, Verweij J, Poveda A, Casali PG, Balana C, Schoffski P, Grosso F, Lardelli P, Nieto A, Alfaro V, Demetri GD (2012) A retrospective analysis of antitumour activity with trabectedin in translocation-related sarcomas. *Eur J Cancer* **48**(16)**:** 3036-44

Lessnick SL, Braun BS, Denny CT, May WA (1995) Multiple domains mediate transformation by the Ewing's sarcoma EWS/FLI-1 fusion gene. *Oncogene* **10**(3)**:** 423-31

Lessnick SL, Dacwag CS, Golub TR (2002) The Ewing's sarcoma oncoprotein EWS/FLI induces a p53-dependent growth arrest in primary human fibroblasts. *Cancer Cell* **1**(4)**:** 393-401

Lessnick SL, Ladanyi M (2012) Molecular pathogenesis of Ewing sarcoma: new therapeutic and transcriptional targets. *Annu Rev Pathol* **7:** 145-59

LH H, VL R, DH S, GL P, TA. S (1984) Reaction of the antitumor antibiotic CC-1065 with DNA: structure of a DNA adduct with DNA sequence specificity. *science* **16:** 843-4

Li H, Watford W, Li C, Parmelee A, Bryant MA, Deng C, O'Shea J, Lee SB (2007) Ewing sarcoma gene EWS is essential for meiosis and B lymphocyte development. *J Clin Invest* **117**(5)**:** 1314-23

Liang D, Burkhart SL, Singh RK, Kabbaj MH, Gunjan A (2012) Histone dosage regulates DNA damage sensitivity in a checkpoint-independent manner by the homologous recombination pathway. *Nucleic Acids Res* **40**(19)**:** 9604-20

Lindqvist A, Rodriguez-Bravo V, Medema RH (2009) The decision to enter mitosis: feedback and redundancy in the mitotic entry network. *J Cell Biol* **185**(2)**:** 193-202

Liu F, Walmsley M, Rodaway A, Patient R (2008) Fli1 acts at the top of the transcriptional network driving blood and endothelial development. *Curr Biol* **18**(16)**:** 1234-40

Liu LF, Desai SD, Li TK, Mao Y, Sun M, Sim SP (2000) Mechanism of action of camptothecin. *Ann N Y Acad Sci* **922:** 1-10

Luo Y, Rockow-Magnone SK, Joseph MK, Bradner J, Butler CC, Tahir SK, Han EK, Ng SC, Severin JM, Gubbins EJ, Reilly RM, Rueter A, Simmer RL, Holzman TF, Giranda VL (2001) Abrogation of G2 checkpoint specifically sensitize p53 defective cells to cancer chemotherapeutic agents. *Anticancer Res* **21**(1A)**:** 23-8

Lust JA, Lacy MQ, Zeldenrust SR, Dispenzieri A, Gertz MA, Witzig TE, Kumar S, Hayman SR, Russell SJ, Buadi FK, Geyer SM, Campbell ME, Kyle RA, Rajkumar SV, Greipp PR, Kline MP, Xiong Y, Moon-Tasson LL, Donovan KA (2009) Induction of a chronic disease state in patients with smoldering or indolent multiple myeloma by targeting interleukin 1{beta}-induced interleukin 6 production and the myeloma proliferative component. *Mayo Clin Proc* **84**(2)**:** 114-22

MacKeigan JP, Murphy LO, Blenis J (2005) Sensitized RNAi screen of human kinases and phosphatases identifies new regulators of apoptosis and chemoresistance. *Nat Cell Biol* **7**(6)**:** 591-600

Mackenzie IR, Rademakers R, Neumann M (2010) TDP-43 and FUS in amyotrophic lateral sclerosis and frontotemporal dementia. *Lancet Neurol* **9**(10)**:** 995-1007

Madoz-Gurpide J (2009) Targeting sarcomas by proteomic approaches. *Proteomics Clin Appl* **3**(7)**:** 758-73

Magnussen GI, Holm R, Emilsen E, Rosnes AK, Slipicevic A, Florenes VA (2012) High expression of Wee1 is associated with poor disease-free survival in malignant melanoma: potential for targeted therapy. *PLoS One* **7**(6)**:** e38254

Mahajan K, Fang B, Koomen JM, Mahajan NP (2012) H2B Tyr37 phosphorylation suppresses expression of replication-dependent core histone genes. *Nat Struct Mol Biol* **19**(9)**:** 930-7

Manfioletti G, Giancotti V, Bandiera A, Buratti E, Sautiere P, Cary P, Crane-Robinson C, Coles B, Goodwin GH (1991) cDNA cloning of the HMGI-C phosphoprotein, a nuclear protein associated with neoplastic and undifferentiated phenotypes. *Nucleic Acids Res* **19**(24)**:** 6793-7

Manning G, Whyte DB, Martinez R, Hunter T, Sudarsanam S (2002) The protein kinase complement of the human genome. *Science* **298**(5600)**:** 1912-34

Marco E, David-Cordonnier MH, Bailly C, Cuevas C, Gago F (2006) Further insight into the DNA recognition mechanism of trabectedin from the differential affinity of its demethylated analogue ecteinascidin ET729 for the triplet DNA binding site CGA. *J Med Chem* **49**(23)**:** 6925-9

Martinez N, Sanchez-Beato M, Carnero A, Moneo V, Tercero JC, Fernandez I, Navarrete M, Jimeno J, Piris MA (2005) Transcriptional signature of Ecteinascidin 743 (Yondelis, Trabectedin) in human sarcoma cells explanted from chemo-naive patients. *Mol Cancer Ther* **4**(5)**:** 814-23

May WA, Gishizky ML, Lessnick SL, Lunsford LB, Lewis BC, Delattre O, Zucman J, Thomas G, Denny CT (1993a) Ewing sarcoma 11;22 translocation produces a chimeric transcription factor that requires the DNA-binding domain encoded by FLI1 for transformation. *Proc Natl Acad Sci U S A* **90**(12)**:** 5752-6

May WA, Lessnick SL, Braun BS, Klemsz M, Lewis BC, Lunsford LB, Hromas R, Denny CT (1993b) The Ewing's sarcoma EWS/FLI-1 fusion gene encodes a more potent transcriptional activator and is a more powerful transforming gene than FLI-1. *Mol Cell Biol* **13**(12)**:** 7393-8

McGowan CH, Russell P (1995) Cell cycle regulation of human WEE1. *EMBO J* **14**(10)**:** 2166-75

Meco D, Colombo T, Ubezio P, Zucchetti M, Zaffaroni M, Riccardi A, Faircloth G, Jose J, D'Incalci M, Riccardi R (2003) Effective combination of ET-743 and doxorubicin in sarcoma: preclinical studies. *Cancer Chemother Pharmacol* **52**(2)**:** 131-8

Meeks-Wagner D, Hartwell LH (1986) Normal stoichiometry of histone dimer sets is necessary for high fidelity of mitotic chromosome transmission. *Cell* **44**(1)**:** 43-52

Melet F, Motro B, Rossi DJ, Zhang L, Bernstein A (1996) Generation of a novel Fli-1 protein by gene targeting leads to a defect in thymus development and a delay in Friend virus-induced erythroleukemia. *Mol Cell Biol* **16**(6)**:** 2708-18

Merry C, Fu K, Wang J, Yeh IJ, Zhang Y (2010) Targeting the checkpoint kinase Chk1 in cancer therapy. *Cell Cycle* **9**(2)**:** 279-83

Michel B, Grompone G, Flores MJ, Bidnenko V (2004) Multiple pathways process stalled replication forks. *Proc Natl Acad Sci U S A* **101**(35)**:** 12783-8

Minuzzo M, Ceribelli M, Pitarque-Marti M, Borrelli S, Erba E, DiSilvio A, D'Incalci M, Mantovani R (2005) Selective effects of the anticancer drug Yondelis (ET-743) on cell-cycle promoters. *Mol Pharmacol* **68**(5)**:** 1496-503

Minuzzo M, Marchini S, Broggini M, Faircloth G, D'Incalci M, Mantovani R (2000) Interference of transcriptional activation by the antineoplastic drug ecteinascidin-743. *Proc Natl Acad Sci U S A* **97**(12)**:** 6780-4

Mir SE, De Witt Hamer PC, Krawczyk PM, Balaj L, Claes A, Niers JM, Van Tilborg AA, Zwinderman AH, Geerts D, Kaspers GJ, Peter Vandertop W, Cloos J, Tannous BA, Wesseling P, Aten JA, Noske DP, Van Noorden CJ, Wurdinger T (2010) In silico analysis of kinase expression identifies WEE1 as a gatekeeper against mitotic catastrophe in glioblastoma. *Cancer Cell* **18**(3)**:** 244-57

Mitchell JB, Choudhuri R, Fabre K, Sowers AL, Citrin D, Zabludoff SD, Cook JA (2010) In vitro and in vivo radiation sensitization of human tumor cells by a novel checkpoint kinase inhibitor, AZD7762. *Clin Cancer Res* **16**(7)**:** 2076-84

Miyagawa Y, Okita H, Nakaijima H, Horiuchi Y, Sato B, Taguchi T, Toyoda M, Katagiri YU, Fujimoto J, Hata J, Umezawa A, Kiyokawa N (2008) Inducible expression of chimeric EWS/ETS proteins confers Ewing's family tumor-like phenotypes to human mesenchymal progenitor cells. *Mol Cell Biol* **28**(7)**:** 2125-37

Monk B, Ghatage P, Parekh T, Henitz E, Knoblauch R, Matos-Pita A, Nieto A, Park Y, Cheng P, Li W, Favis R, Ricci D, Poveda A (2015) Effect of BRCA1 and XPG mutations on treatment response to trabectedin and pegylated liposomal doxorubicin in patients with advanced ovarian cancer: exploratory analysis of the phase 3 OVA-301 study. *Ann Oncol* **26**(5)**:** 914-20

Monk BJ, Blessing JA, Street DG, Muller CY, Burke JJ, Hensley ML (2012a) A phase II evaluation of trabectedin in the treatment of advanced, persistent, or recurrent uterine leiomyosarcoma: a gynecologic oncology group study. *Gynecol Oncol* **124**(1)**:** 48-52

Monk BJ, Herzog TJ, Kaye SB, Krasner CN, Vermorken JB, Muggia FM, Pujade-Lauraine E, Park YC, Parekh TV, Poveda AM (2012b) Trabectedin plus pegylated liposomal doxorubicin (PLD) versus PLD in recurrent ovarian cancer: overall survival analysis. *Eur J Cancer* **48**(15)**:** 2361-8

Monti P, Leone BE, Marchesi F, Balzano G, Zerbi A, Scaltrini F, Pasquali C, Calori G, Pessi F, Sperti C, Di Carlo V, Allavena P, Piemonti L (2003) The CC chemokine MCP-1/CCL2 in pancreatic cancer progression: regulation of expression and potential mechanisms of antimalignant activity. *Cancer Res* **63**(21)**:** 7451-61

Moore RJ, Owens DM, Stamp G, Arnott C, Burke F, East N, Holdsworth H, Turner L, Rollins B, Pasparakis M, Kollias G, Balkwill F (1999) Mice deficient in tumor necrosis factor-alpha are resistant to skin carcinogenesis. *Nat Med* **5**(7)**:** 828-31

Morgan MA, Parsels LA, Zhao L, Parsels JD, Davis MA, Hassan MC, Arumugarajah S, Hylander-Gans L, Morosini D, Simeone DM, Canman CE, Normolle DP, Zabludoff SD, Maybaum J, Lawrence TS (2010) Mechanism of radiosensitization by the Chk1/2 inhibitor AZD7762 involves abrogation of the G2 checkpoint and inhibition of homologous recombinational DNA repair. *Cancer Res* **70**(12)**:** 4972-81

Morohoshi F, Ootsuka Y, Arai K, Ichikawa H, Mitani S, Munakata N, Ohki M (1998) Genomic structure of the human RBP56/hTAFII68 and FUS/TLS genes. *Gene* **221**(2)**:** 191-8

Moynahan ME (2002) The cancer connection: BRCA1 and BRCA2 tumor suppression in mice and humans. *Oncogene* **21**(58)**:** 8994-9007

Mullenders J, Bernards R (2009) Loss-of-function genetic screens as a tool to improve the diagnosis and treatment of cancer. *Oncogene* **28**(50)**:** 4409-20

Murrow LM, Garimella SV, Jones TL, Caplen NJ, Lipkowitz S (2010) Identification of WEE1 as a potential molecular target in cancer cells by RNAi screening of the human tyrosine kinome. *Breast Cancer Res Treat* **122**(2)**:** 347-57

Nakatani F, Tanaka K, Sakimura R, Matsumoto Y, Matsunobu T, Li X, Hanada M, Okada T, Iwamoto Y (2003) Identification of p21WAF1/CIP1 as a direct target of EWS-Fli1 oncogenic fusion protein. *J Biol Chem* **278**(17)**:** 15105-15

Natarajan S, Hombach-Klonisch S, Droge P, Klonisch T (2013) HMGA2 inhibits apoptosis through interaction with ATR-CHK1 signaling complex in human cancer cells. *Neoplasia* **15**(3)**:** 263-80

NE S, A N (2013) Targeting the tumor microenvironment for cancer therapy. *clin chem* **59**(1)**:** 85-93

Negus RP, Stamp GW, Relf MG, Burke F, Malik ST, Bernasconi S, Allavena P, Sozzani S, Mantovani A, Balkwill FR (1995) The detection and localization of monocyte chemoattractant protein-1 (MCP-1) in human ovarian cancer. *J Clin Invest* **95**(5)**:** 2391-6

Nitiss JL (2009) Targeting DNA topoisomerase II in cancer chemotherapy. *Nat Rev Cancer* **9**(5)**:** 338-50

O'Connell BC, Adamson B, Lydeard JR, Sowa ME, Ciccia A, Bredemeyer AL, Schlabach M, Gygi SP, Elledge SJ, Harper JW (2010) A genome-wide camptothecin sensitivity

screen identifies a mammalian MMS22L-NFKBIL2 complex required for genomic stability. *Mol Cell* **40**(4)**:** 645-57

O'Donovan A, Wood RD (1993) Identical defects in DNA repair in xeroderma pigmentosum group G and rodent ERCC group 5. *Nature* **363**(6425)**:** 185-8

Ordonez JL, Amaral AT, Carcaboso AM, Herrero-Martin D, del Carmen Garcia-Macias M, Sevillano V, Alonso D, Pascual-Pasto G, San-Segundo L, Vila-Ubach M, Rodrigues T, Fraile S, Teodosio C, Mayo-Iscar A, Aracil M, Galmarini CM, Tirado OM, Mora J, de Alava E (2015) The PARP inhibitor olaparib enhances the sensitivity of Ewing sarcoma to trabectedin. *Oncotarget* **6**(22)**:** 18875-90

Ouchida M, Ohno T, Fujimura Y, Rao VN, Reddy ES (1995) Loss of tumorigenicity of Ewing's sarcoma cells expressing antisense RNA to EWS-fusion transcripts. *Oncogene* **11**(6)**:** 1049-54

Ozdemir BC, Pentcheva-Hoang T, Carstens JL, Zheng X, Wu CC, Simpson TR, Laklai H, Sugimoto H, Kahlert C, Novitskiy SV, De Jesus-Acosta A, Sharma P, Heidari P, Mahmood U, Chin L, Moses HL, Weaver VM, Maitra A, Allison JP, LeBleu VS, Kalluri R (2014) Depletion of carcinoma-associated fibroblasts and fibrosis induces immunosuppression and accelerates pancreas cancer with reduced survival. *Cancer Cell* **25**(6)**:** 719-34

Parkin DM, Stiller CA, Nectoux J (1993) International variations in the incidence of childhood bone tumours. *Int J Cancer* **53**(3)**:** 371-6

Paronetto MP (2013) Ewing sarcoma protein: a key player in human cancer. *Int J Cell Biol* **2013:** 642853

Passalacqua M, Zicca A, Sparatore B, Patrone M, Melloni E, Pontremoli S (1997) Secretion and binding of HMG1 protein to the external surface of the membrane are required for murine erythroleukemia cell differentiation. *FEBS Lett* **400**(3)**:** 275-9

Pil PM, Lippard SJ (1992) Specific binding of chromosomal protein HMG1 to DNA damaged by the anticancer drug cisplatin. *Science* **256**(5054)**:** 234-7

Plougastel B, Zucman J, Peter M, Thomas G, Delattre O (1993) Genomic structure of the EWS gene and its relationship to EWSR1, a site of tumor-associated chromosome translocation. *Genomics* **18**(3)**:** 609-15

Pommier Y, Kohlhagen G, Kohn KW, Leteurtre F, Wani MC, Wall ME (1995) Interaction of an alkylating camptothecin derivative with a DNA base at topoisomerase I-DNA cleavage sites. *Proc Natl Acad Sci U S A* **92**(19)**:** 8861-5

Puchalski TA, Ryan DP, Garcia-Carbonero R, Demetri GD, Butkiewicz L, Harmon D, Seiden MV, Maki RG, Lopez-Lazaro L, Jimeno J, Guzman C, Supko JG (2002) Pharmacokinetics of ecteinascidin 743 administered as a 24-h continuous intravenous infusion to adult patients with soft tissue sarcomas: associations with clinical characteristics, pathophysiological variables and toxicity. *Cancer Chemother Pharmacol* **50**(4)**:** 309-19

Pusztaszeri MP, Seelentag W, Bosman FT (2006) Immunohistochemical expression of endothelial markers CD31, CD34, von Willebrand factor, and Fli-1 in normal human tissues. *J Histochem Cytochem* **54**(4)**:** 385-95

Read CM, Cary PD, Crane-Robinson C, Driscoll PC, Norman DG (1993) Solution structure of a DNA-binding domain from HMG1. *Nucleic Acids Res* **21**(15)**:** 3427-36

Reeves R (2003) HMGA proteins: flexibility finds a nuclear niche? *Biochem Cell Biol* **81**(3)**:** 185-95

Reeves R, Beckerbauer L (2001) HMGI/Y proteins: flexible regulators of transcription and chromatin structure. *Biochim Biophys Acta* **1519**(1-2)**:** 13-29

Reeves R, Nissen MS (1990) The A.T-DNA-binding domain of mammalian high mobility group I chromosomal proteins. A novel peptide motif for recognizing DNA structure. *J Biol Chem* **265**(15)**:** 8573-82

Rhind N, Russell P (2000) Chk1 and Cds1: linchpins of the DNA damage and replication checkpoint pathways. *J Cell Sci* **113 (Pt 22):** 3889-96

Riccardi A, Meco D, Ubezio P, Mazzarella G, Marabese M, Faircloth GT, Jimeno J, D'Incalci M, Riccardi R (2005) Combination of trabectedin and irinotecan is highly effective in a human rhabdomyosarcoma xenograft. *Anticancer Drugs* **16**(8)**:** 811-5

Riggi N, Cironi L, Provero P, Suva ML, Kaloulis K, Garcia-Echeverria C, Hoffmann F, Trumpp A, Stamenkovic I (2005) Development of Ewing's sarcoma from primary bone marrow-derived mesenchymal progenitor cells. *Cancer Res* **65**(24)**:** 11459-68

Riggi N, Suva ML, Suva D, Cironi L, Provero P, Tercier S, Joseph JM, Stehle JC, Baumer K, Kindler V, Stamenkovic I (2008) EWS-FLI-1 expression triggers a Ewing's sarcoma initiation program in primary human mesenchymal stem cells. *Cancer Res* **68**(7)**:** 2176-85

Romero J, Zapata I, Cordoba S, Jimeno JM, Lopez-Martin JA, Tercero JC, De La Torre A, Vargas JA, Moleron R, Sanchez-Prieto R (2008) In vitro radiosensitisation by trabectedin in human cancer cell lines. *Eur J Cancer* **44**(12)**:** 1726-33

Rossi S, Orvieto E, Furlanetto A, Laurino L, Ninfo V, Dei Tos AP (2004) Utility of the immunohistochemical detection of FLI-1 expression in round cell and vascular neoplasm using a monoclonal antibody. *Mod Pathol* **17**(5)**:** 547-52

Rothenberg ML (2001) Irinotecan (CPT-11): recent developments and future directions--colorectal cancer and beyond. *Oncologist* **6**(1)**:** 66-80

Ruddon R.W., Cancer Biology, 2007. Oxford University Press

Russell MR, Levin K, Rader J, Belcastro L, Li Y, Martinez D, Pawel B, Shumway SD, Maris JM, Cole KA (2013) Combination therapy targeting the Chk1 and Wee1 kinases shows therapeutic efficacy in neuroblastoma. *Cancer Res* **73**(2)**:** 776-84

Russell P, Nurse P (1987) Negative regulation of mitosis by wee1+, a gene encoding a protein kinase homolog. *Cell* **49**(4)**:** 559-67

Sancar A (1996) DNA excision repair. *Annu Rev Biochem* **65:** 43-81

Sandberg AA (2004) Updates on the cytogenetics and molecular genetics of bone and soft tissue tumors: liposarcoma. *Cancer Genet Cytogenet* **155**(1)**:** 1-24

Sarcar B, Kahali S, Prabhu AH, Shumway SD, Xu Y, Demuth T, Chinnaiyan P (2011) Targeting radiation-induced G(2) checkpoint activation with the Wee-1 inhibitor MK-1775 in glioblastoma cell lines. *Mol Cancer Ther* **10**(12)**:** 2405-14

Sarmento LM, Povoa V, Nascimento R, Real G, Antunes I, Martins LR, Moita C, Alves PM, Abecasis M, Moita LF, Parkhouse RM, Meijerink JP, Barata JT (2015) CHK1 overexpression in T-cell acute lymphoblastic leukemia is essential for proliferation and survival by preventing excessive replication stress. *Oncogene* **34**(23)**:** 2978-90

Scaffidi P, Misteli T, Bianchi ME (2002) Release of chromatin protein HMGB1 by necrotic cells triggers inflammation. *Nature* **418**(6894)**:** 191-5

Schiraldi M, Raucci A, Munoz LM, Livoti E, Celona B, Venereau E, Apuzzo T, De Marchis F, Pedotti M, Bachi A, Thelen M, Varani L, Mellado M, Proudfoot A, Bianchi ME, Uguccioni M (2012) HMGB1 promotes recruitment of inflammatory cells to damaged tissues by forming a complex with CXCL12 and signaling via CXCR4. *J Exp Med* **209**(3)**:** 551-63

Schlueter C, Hauke S, Loeschke S, Wenk HH, Bullerdiek J (2005) HMGA1 proteins in human atherosclerotic plaques. *Pathol Res Pract* **201**(2)**:** 101-7

Schwartsmann G, Brondani da Rocha A, Berlinck R, Jimeno J (2001) Marine organisms as a source of new anticancer agents. *Lancet Oncol* **2**(4)**:** 221-5

Scotto KW (2002) ET-743: more than an innovative mechanism of action. *Anticancer Drugs* **13 Suppl 1:** S3-6

Sessa C, Perotti A, Noberasco C, De Braud F, Gallerani E, Cresta S, Zucchetti M, Vigano L, Locatelli A, Jimeno J, Feilchenfeldt JW, D'Incalci M, Capri G, Ielmini N, Gianni L (2009) Phase I clinical and pharmacokinetic study of trabectedin and doxorubicin in advanced soft tissue sarcoma and breast cancer. *Eur J Cancer* **45**(7)**:** 1153-61

Sgarra R, Rustighi A, Tessari MA, Di Bernardo J, Altamura S, Fusco A, Manfioletti G, Giancotti V (2004) Nuclear phosphoproteins HMGA and their relationship with chromatin structure and cancer. *FEBS Lett* **574**(1-3)**:** 1-8

Shao RG, Cao CX, Zhang H, Kohn KW, Wold MS, Pommier Y (1999) Replication-mediated DNA damage by camptothecin induces phosphorylation of RPA by DNA-dependent protein kinase and dissociates RPA:DNA-PK complexes. *EMBO J* **18**(5)**:** 1397-406

Shaw AT, Kim DW, Mehra R, Tan DS, Felip E, Chow LQ, Camidge DR, Vansteenkiste J, Sharma S, De Pas T, Riely GJ, Solomon BJ, Wolf J, Thomas M, Schuler M, Liu G, Santoro A, Lau YY, Goldwasser M, Boral AL, Engelman JA (2014) Ceritinib in ALK-rearranged non-small-cell lung cancer. *N Engl J Med* **370**(13)**:** 1189-97

Shi Y (2009) Serine/threonine phosphatases: mechanism through structure. *Cell* **139**(3)**:** 468-84

Shin YJ, Kim JY, Moon JW, You RM, Park JY, Nam JH (2011) Fatal Ifosfamide-induced metabolic encephalopathy in patients with recurrent epithelial ovarian cancer: report of two cases. *Cancer Res Treat* **43**(4)**:** 260-3

Shrivastav M, De Haro LP, Nickoloff JA (2008) Regulation of DNA double-strand break repair pathway choice. *Cell Res* **18**(1)**:** 134-47

Singh RK, Kabbaj MH, Paik J, Gunjan A (2009) Histone levels are regulated by phosphorylation and ubiquitylation-dependent proteolysis. *Nat Cell Biol* **11**(8)**:** 925-33

Smith MR, Saad F, Coleman R, Shore N, Fizazi K, Tombal B, Miller K, Sieber P, Karsh L, Damiao R, Tammela TL, Egerdie B, Van Poppel H, Chin J, Morote J, Gomez-Veiga F, Borkowski T, Ye Z, Kupic A, Dansey R, Goessl C (2012) Denosumab and bone-metastasis-free survival in men with castration-resistant prostate cancer: results of a phase 3, randomised, placebo-controlled trial. *Lancet* **379**(9810)**:** 39-46

Smits VA, Reaper PM, Jackson SP (2006) Rapid PIKK-dependent release of Chk1 from chromatin promotes the DNA-damage checkpoint response. *Curr Biol* **16**(2)**:** 150-9

Soares DG, Escargueil AE, Poindessous V, Sarasin A, de Gramont A, Bonatto D, Henriques JA, Larsen AK (2007) Replication and homologous recombination repair regulate DNA double-strand break formation by the antitumor alkylator ecteinascidin 743. *Proc Natl Acad Sci U S A* **104**(32)**:** 13062-7

Soares DG, Machado MS, Rocca CJ, Poindessous V, Ouaret D, Sarasin A, Galmarini CM, Henriques JA, Escargueil AE, Larsen AK (2011) Trabectedin and its C subunit modified analogue PM01183 attenuate nucleotide excision repair and show activity toward platinum-resistant cells. *Mol Cancer Ther* **10**(8)**:** 1481-9

Sorensen CS, Hansen LT, Dziegielewski J, Syljuasen RG, Lundin C, Bartek J, Helleday T (2005) The cell-cycle checkpoint kinase Chk1 is required for mammalian homologous recombination repair. *Nat Cell Biol* **7**(2)**:** 195-201

Sorensen CS, Syljuasen RG, Falck J, Schroeder T, Ronnstrand L, Khanna KK, Zhou BB, Bartek J, Lukas J (2003) Chk1 regulates the S phase checkpoint by coupling the

physiological turnover and ionizing radiation-induced accelerated proteolysis of Cdc25A. *Cancer Cell* **3**(3)**:** 247-58

Sorensen PH, Lessnick SL, Lopez-Terrada D, Liu XF, Triche TJ, Denny CT (1994) A second Ewing's sarcoma translocation, t(21;22), fuses the EWS gene to another ETS-family transcription factor, ERG. *Nat Genet* **6**(2)**:** 146-51

Sparatore B, Patrone M, Passalacqua M, Pedrazzi M, Ledda S, Pontremoli S, Melloni E (2005) Activation of A431 human carcinoma cell motility by extracellular high-mobility group box 1 protein and epidermal growth factor stimuli. *Biochem J* **389**(Pt 1)**:** 215-21

Spyropoulos DD, Pharr PN, Lavenburg KR, Jackers P, Papas TS, Ogawa M, Watson DK (2000) Hemorrhage, impaired hematopoiesis, and lethality in mouse embryos carrying a targeted disruption of the Fli1 transcription factor. *Mol Cell Biol* **20**(15)**:** 5643-52

Staege MS, Hutter C, Neumann I, Foja S, Hattenhorst UE, Hansen G, Afar D, Burdach SE (2004) DNA microarrays reveal relationship of Ewing family tumors to both endothelial and fetal neural crest-derived cells and define novel targets. *Cancer Res* **64**(22)**:** 8213-21

Stevenson M (2003) Dissecting HIV-1 through RNA interference. *Nat Rev Immunol* **3**(11)**:** 851-8

Stewart E, Goshorn R, Bradley C, Griffiths LM, Benavente C, Twarog NR, Miller GM, Caufield W, Freeman BB, 3rd, Bahrami A, Pappo A, Wu J, Loh A, Karlstrom A, Calabrese C, Gordon B, Tsurkan L, Hatfield MJ, Potter PM, Snyder SE, Thiagarajan S, Shirinifard A, Sablauer A, Shelat AA, Dyer MA (2014) Targeting the DNA repair pathway in Ewing sarcoma. *Cell Rep* **9**(3)**:** 829-41

Strathern JN, Shafer BK, McGill CB (1995) DNA synthesis errors associated with double-strand-break repair. *Genetics* **140**(3)**:** 965-72

Stros M, Launholt D, Grasser KD (2007) The HMG-box: a versatile protein domain occurring in a wide variety of DNA-binding proteins. *Cell Mol Life Sci* **64**(19-20)**:** 2590-606

Svejstrup JQ (2007) Contending with transcriptional arrest during RNAPII transcript elongation. *Trends Biochem Sci* **32**(4)**:** 165-71

Swanton C, Marani M, Pardo O, Warne PH, Kelly G, Sahai E, Elustondo F, Chang J, Temple J, Ahmed AA, Brenton JD, Downward J, Nicke B (2007) Regulators of mitotic arrest and ceramide metabolism are determinants of sensitivity to paclitaxel and other chemotherapeutic drugs. *Cancer Cell* **11**(6)**:** 498-512

Symington LS (2002) Role of RAD52 epistasis group genes in homologous recombination and double-strand break repair. *Microbiol Mol Biol Rev* **66**(4)**:** 630-70, table of contents

Taamma A, Misset JL, Riofrio M, Guzman C, Brain E, Lopez Lazaro L, Rosing H, Jimeno JM, Cvitkovic E (2001) Phase I and pharmacokinetic study of ecteinascidin-743, a new marine compound, administered as a 24-hour continuous infusion in patients with solid tumors. *J Clin Oncol* **19**(5)**:** 1256-65

Takahashi N, Li W, Banerjee D, Guan Y, Wada-Takahashi Y, Brennan MF, Chou TC, Scotto KW, Bertino JR (2002) Sequence-dependent synergistic cytotoxicity of ecteinascidin-743 and paclitaxel in human breast cancer cell lines in vitro and in vivo. *Cancer Res* **62**(23)**:** 6909-15

Takahashi N, Li WW, Banerjee D, Scotto KW, Bertino JR (2001) Sequence-dependent enhancement of cytotoxicity produced by ecteinascidin 743 (ET-743) with doxorubicin or paclitaxel in soft tissue sarcoma cells. *Clin Cancer Res* **7**(10)**:** 3251-7

Takata M, Sasaki MS, Sonoda E, Morrison C, Hashimoto M, Utsumi H, Yamaguchi-Iwai Y, Shinohara A, Takeda S (1998) Homologous recombination and non-homologous end-joining pathways of DNA double-strand break repair have overlapping roles in the maintenance of chromosomal integrity in vertebrate cells. *EMBO J* **17**(18)**:** 5497-508

Takebayashi Y, Pourquier P, Zimonjic DB, Nakayama K, Emmert S, Ueda T, Urasaki Y, Kanzaki A, Akiyama SI, Popescu N, Kraemer KH, Pommier Y (2001) Antiproliferative activity of ecteinascidin 743 is dependent upon transcription-coupled nucleotide-excision repair. *Nat Med* **7**(8)**:** 961-6

Tamir A, Howard J, Higgins RR, Li YJ, Berger L, Zacksenhaus E, Reis M, Ben-David Y (1999) Fli-1, an Ets-related transcription factor, regulates erythropoietin-induced erythroid proliferation and differentiation: evidence for direct transcriptional repression of the Rb gene during differentiation. *Mol Cell Biol* **19**(6)**:** 4452-64

Tavecchio M, Natoli C, Ubezio P, Erba E, D'Incalci M (2007) Dynamics of cell cycle phase perturbations by trabectedin (ET-743) in nucleotide excision repair (NER)-deficient and NER-proficient cells, unravelled by a novel mathematical simulation approach. *Cell Prolif* **40**(6)**:** 885-904

Tavecchio M, Simone M, Erba E, Chiolo I, Liberi G, Foiani M, D'Incalci M, Damia G (2008) Role of homologous recombination in trabectedin-induced DNA damage. *Eur J Cancer* **44**(4)**:** 609-18

Thorn CF, Oshiro C, Marsh S, Hernandez-Boussard T, McLeod H, Klein TE, Altman RB (2011) Doxorubicin pathways: pharmacodynamics and adverse effects. *Pharmacogenet Genomics* **21**(7)**:** 440-6

Tirode F, Laud-Duval K, Prieur A, Delorme B, Charbord P, Delattre O (2007) Mesenchymal stem cell features of Ewing tumors. *Cancer Cell* **11**(5)**:** 421-9

Tominaga Y, Li C, Wang RH, Deng CX (2006) Murine Wee1 plays a critical role in cell cycle regulation and pre-implantation stages of embryonic development. *Int J Biol Sci* **2**(4)**:** 161-70

Torchia EC, Jaishankar S, Baker SJ (2003) Ewing tumor fusion proteins block the differentiation of pluripotent marrow stromal cells. *Cancer Res* **63**(13)**:** 3464-8

Truong AH, Ben-David Y (2000) The role of Fli-1 in normal cell function and malignant transformation. *Oncogene* **19**(55)**:** 6482-9

Uboldi S, Calura E, Beltrame L, Fuso Nerini I, Marchini S, Cavalieri D, Erba E, Chiorino G, Ostano P, D'Angelo D, D'Incalci M, Romualdi C (2012) A systems biology approach to characterize the regulatory networks leading to trabectedin resistance in an in vitro model of myxoid liposarcoma. *PLoS One* **7**(4)**:** e35423

Uziel T, Lerenthal Y, Moyal L, Andegeko Y, Mittelman L, Shiloh Y (2003) Requirement of the MRN complex for ATM activation by DNA damage. *EMBO J* **22**(20)**:** 5612-21

Valoti G, Nicoletti MI, Pellegrino A, Jimeno J, Hendriks H, D'Incalci M, Faircloth G, Giavazzi R (1998) Ecteinascidin-743, a new marine natural product with potent antitumor activity on human ovarian carcinoma xenografts. *Clin Cancer Res* **4**(8)**:** 1977-83

van Beijnum JR, Dings RP, van der Linden E, Zwaans BM, Ramaekers FC, Mayo KH, Griffioen AW (2006) Gene expression of tumor angiogenesis dissected: specific targeting of colon cancer angiogenic vasculature. *Blood* **108**(7)**:** 2339-48

van Kesteren C, Cvitkovic E, Taamma A, Lopez-Lazaro L, Jimeno JM, Guzman C, Math t RA, Schellens JH, Misset JL, Brain E, Hillebrand MJ, Rosing H, Beijnen JH (2000) Pharmacokinetics and pharmacodynamics of the novel marine-derived anticancer agent ecteinascidin 743 in a phase I dose-finding study. *Clin Cancer Res* **6**(12)**:** 4725-32

Vance C, Rogelj B, Hortobagyi T, De Vos KJ, Nishimura AL, Sreedharan J, Hu X, Smith B, Ruddy D, Wright P, Ganesalingam J, Williams KL, Tripathi V, Al-Saraj S, Al-Chalabi A, Leigh PN, Blair IP, Nicholson G, de Belleroche J, Gallo JM, Miller CC, Shaw CE (2009) Mutations in FUS, an RNA processing protein, cause familial amyotrophic lateral sclerosis type 6. *Science* **323**(5918)**:** 1208-11

Villalona-Calero MA, Eckhardt SG, Weiss G, Hidalgo M, Beijnen JH, van Kesteren C, Rosing H, Campbell E, Kraynak M, Lopez-Lazaro L, Guzman C, Von Hoff DD, Jimeno J, Rowinsky EK (2002) A phase I and pharmacokinetic study of ecteinascidin-743 on a daily x 5 schedule in patients with solid malignancies. *Clin Cancer Res* **8**(1)**:** 75-85

Wahamaa H, Vallerskog T, Qin S, Lunderius C, LaRosa G, Andersson U, Harris HE (2007) HMGB1-secreting capacity of multiple cell lineages revealed by a novel HMGB1 ELISPOT assay. *J Leukoc Biol* **81**(1)**:** 129-36

Walker M, Black EJ, Oehler V, Gillespie DA, Scott MT (2009) Chk1 C-terminal regulatory phosphorylation mediates checkpoint activation by de-repression of Chk1 catalytic activity. *Oncogene* **28**(24)**:** 2314-23

Wang-Gillam A, Li CP, Bodoky G, Dean A, Shan YS, Jameson G, Macarulla T, Lee KH, Cunningham D, Blanc JF, Hubner RA, Chiu CF, Schwartsmann G, Siveke JT, Braiteh F, Moyo V, Belanger B, Dhindsa N, Bayever E, Von Hoff DD, Chen LT (2016) Nanoliposomal irinotecan with fluorouracil and folinic acid in metastatic pancreatic cancer after previous gemcitabine-based therapy (NAPOLI-1): a global, randomised, open-label, phase 3 trial. *Lancet* **387**(10018)**:** 545-57

Wang JC (1985) DNA topoisomerases. *Annu Rev Biochem* **54:** 665-97

Wei Y, Yu L, Bowen J, Gorovsky MA, Allis CD (1999) Phosphorylation of histone H3 is required for proper chromosome condensation and segregation. *Cell* **97**(1)**:** 99-109

Weir HM, Kraulis PJ, Hill CS, Raine AR, Laue ED, Thomas JO (1993) Structure of the HMG box motif in the B-domain of HMG1. *EMBO J* **12**(4)**:** 1311-9

Whang-Peng J, Triche TJ, Knutsen T, Miser J, Douglass EC, Israel MA (1984) Chromosome translocation in peripheral neuroepithelioma. *N Engl J Med* **311**(9)**:** 584-5

Whitehurst AW, Bodemann BO, Cardenas J, Ferguson D, Girard L, Peyton M, Minna JD, Michnoff C, Hao W, Roth MG, Xie XJ, White MA (2007) Synthetic lethal screen identification of chemosensitizer loci in cancer cells. *Nature* **446**(7137)**:** 815-9

Wood RD (1996) DNA repair in eukaryotes. *Annu Rev Biochem* **65:** 135-67

Wu CC, Li TK, Farh L, Lin LY, Lin TS, Yu YJ, Yen TJ, Chiang CW, Chan NL (2011) Structural basis of type II topoisomerase inhibition by the anticancer drug etoposide. *Science* **333**(6041)**:** 459-62

Xu N, Libertini S, Black EJ, Lao Y, Hegarat N, Walker M, Gillespie DA (2012) Cdk-mediated phosphorylation of Chk1 is required for efficient activation and full checkpoint proficiency in response to DNA damage. *Oncogene* **31**(9)**:** 1086-94

Zaki EL, Springate JE, Taub M (2003) Comparative toxicity of ifosfamide metabolites and protective effect of mesna and amifostine in cultured renal tubule cells. *Toxicol In Vitro* **17**(4)**:** 397-402

Zewail-Foote M, Hurley LH (1999) Ecteinascidin 743: a minor groove alkylator that bends DNA toward the major groove. *J Med Chem* **42**(14)**:** 2493-7

Zhang Y, Hunter T (2014) Roles of Chk1 in cell biology and cancer therapy. *Int J Cancer* **134**(5)**:** 1013-23

Zhao J, Kennedy BK, Lawrence BD, Barbie DA, Matera AG, Fletcher JA, Harlow E (2000) NPAT links cyclin E-Cdk2 to the regulation of replication-dependent histone gene transcription. *Genes Dev* **14**(18)**:** 2283-97

Zochodne B, Truong AH, Stetler K, Higgins RR, Howard J, Dumont D, Berger SA, Ben-David Y (2000) Epo regulates erythroid proliferation and differentiation through distinct signaling pathways: implication for erythropoiesis and Friend virus-induced erythroleukemia. *Oncogene* **19**(19)**:** 2296-304